The Cell Biology of Rad54: Implications for homologous recombination

Sheba Agarwal

The Cell Biology of Rad54: Implications for homologous recombination

Sheba Agarwal

Erasmus MC
Universitair Medisch Centrum Rotterdam

ERASMUS UNIVERSITEIT ROTTERDAM

Cover
"Methodical Invasion" by Sheba Agarwal

ISBN 978-90-9022870-9

The printing of this thesis was subsidized by the Dutch Cancer Society (KWF).

The research described in this thesis was performed at the Department of Cell Biology and Genetics within the Erasmus Medical Center, Rotterdam, The Netherlands.

The research has been supported by the Dutch Cancer Society (KWF).

Cover design & layout: Sheba Agarwal & Jasper Jans
Printing: Dienst Facilitaire Zaken (Repografie), Vrije Universiteit, Amsterdam

The Cell Biology of Rad54: Implications for homologous recombination

De cel biologie van Rad54:
De gevolgen voor homologe recombinatie

Proefschrift

ter verkrijging van de graad van doctor aan de
Erasmus Universiteit Rotterdam
op gezag van de

rector magnificus Prof.dr. S.W.J. Lamberts

en volgens besluit van het College voor Promoties.

De openbare verdediging zal plaatsvinden op

woensdag 2 april 2008 om 11:45 uur

door

Sheba Agarwal

geboren te Tiruchirapalli, Tamil Nadu, India

Promotiecommissie

Promotoren:	Prof.dr. R. Kanaar Prof.dr. J.H.J. Hoeijmakers
Overige leden:	Prof.dr. J.A. Grootegoed Dr. A. Houtsmuller Prof.dr. H. Joenje
Copromoter:	Dr. J. Essers

For my family,
near and far.

ॐ भूर्भुवः स्वः
तत्सवितुर्वरेण्यं ।
भर्गो देवस्य धीमहि
धियो यो नः प्रचोदयात् ।।

There is one thing even more vital to science than intelligent methods; and that is, the sincere desire to find out the truth, whatever it may be.

~ *Charles Pierce*

Contents

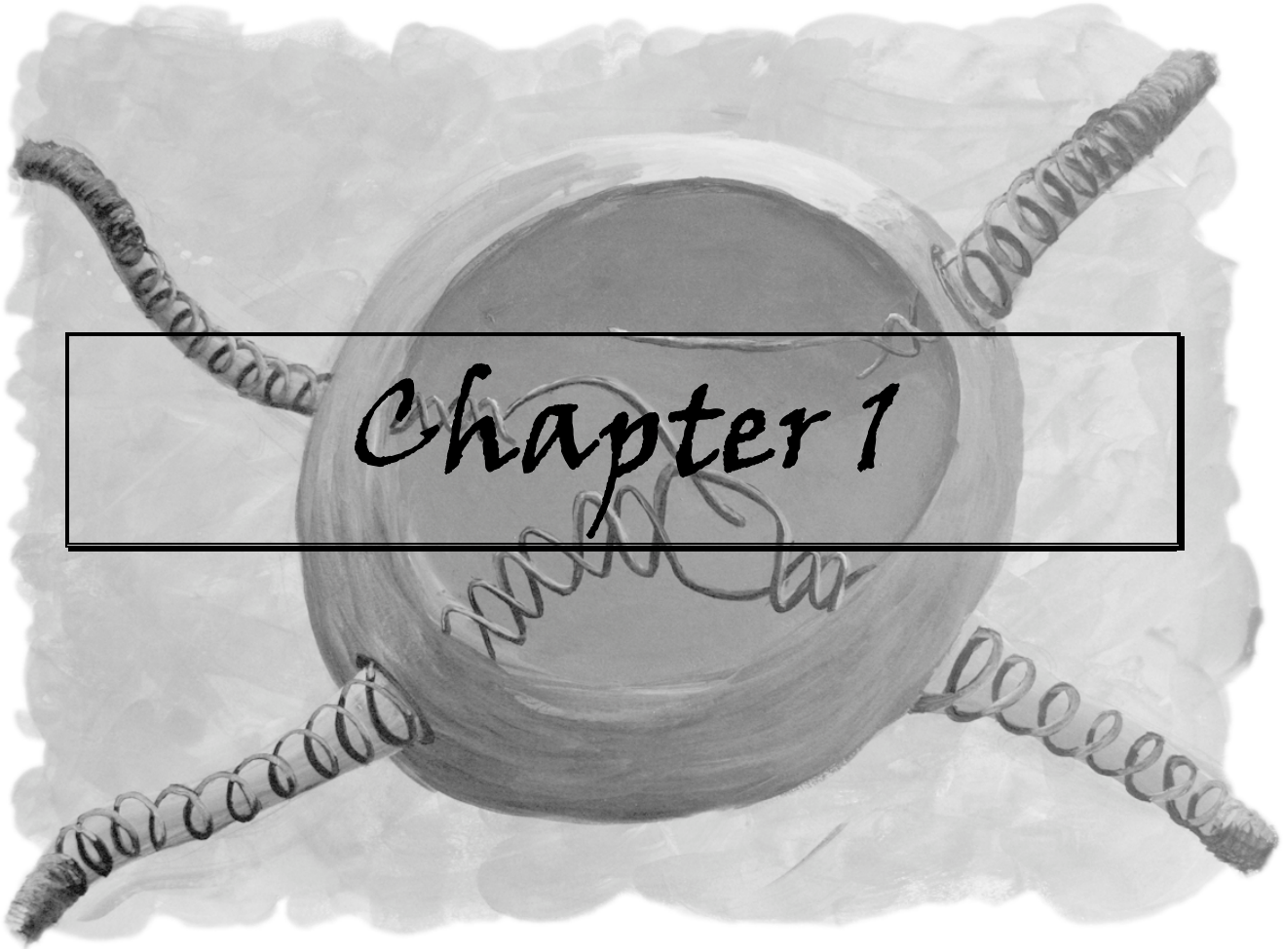

Chapter 1

General Introduction & Outline of Thesis

If real is what you can feel, smell, taste and see,
then 'real' is simply electrical signals interpreted by your brain.

~ Morpheus (The Matrix)

The survival of species is guaranteed by maintenance of genome stability, specifically the protection of DNA integrity. DNA is a chemically reactive molecule, which is continuously threatened by DNA-damaging agents, both exogenous (environmental, including ionizing radiation and mutagenic chemicals) and endogenous (byproducts of cellular metabolism, such as oxygen radicals). The continuous onslaught by such physical and chemical agents result in about 100,000 modifications per cell per day [1], and this calls for the existence of diverse DNA repair systems within the cell. The many different types of lesions that can occur in DNA have necessitated the evolution of multiple pathways to repair specific subsets of lesions. Therefore, an intricate web of repair pathways counteracts damage to free DNA from modifications that would lead to mutations, thus ensuring its error-free transcription and replication.

The lethal effects of ionizing radiation have been attributed to the formation of DNA double-strand breaks (DSBs), which, if misrepaired, can lead to chromosomal aberrations including rearrangements, deletions and translocations, cell death and, in higher organisms, cancer (see Chapter 6). Because unrepaired DSBs result in genomic fragmentation, it is of critical importance that the DSBs are repaired precisely and in a timely fashion. Homologous recombination is a high fidelity pathway that ensures the accurate repair of the broken DNA by using the information present on the undamaged template DNA, usually the sister chromatid. The process is carried out by the conserved *RAD52* epistasis group proteins, identified by the genetic analyses of ionizing radiation sensitive *Saccharomyces cerevisiae* mutants [1, 2]. In mammals, this group includes the MRN (RAD50/MRE11/NBS1) complex, RAD51, the RAD51 paralogs (RAD51B, RAD51C, RAD51D, XRCC2, XRCC3), RAD54 and RAD54B [3]. In addition, mammalian homologous recombination is also modulated by the products of the breast cancer susceptibility genes, BRCA1 and BRCA2 [4], and perhaps also genes involved in Fanconi anemia.

According to a model based on current knowledge, when a DSB occurs in the genome, it is initially detected by the MRN complex, which has been implicated in the recognition of DSBs in the context of chromatin (see Figure 3, Chapter 2). The MRN complex binds and tethers the broken DNA ends. The next step involves the endonucleolytic processing of the DSB to produce 3' tailed single-stranded DNA. Currently, the molecular details of this step are not well defined and therefore, the mechanism by which the DNA intermediate bound by MRN is handed over to the next step of recombination is still ambiguous. RAD51, the core protein of recombination,

oligomerizes on the 3' single-stranded tails giving rise to a nucleoprotein filament. This filament then recognizes homologous duplex DNA in the genome, mediates joint molecule (D-loop) formation between the broken and intact template DNA and promotes strand exchange between the recombining partner DNA molecules. However, RAD51 is unable to carry this processs out by itself. RAD51 requires the presence and function of accessory proteins to carry out its function properly, namely RPA, RAD52 (in *S. cerevisiae*), RAD51 paralogs, BRCA2 (in vertebrates) and RAD54. After DNA strand exchange, the subsequent disassembly of the nucleoprotein filament by Rad54 might be important in the promotion of the next step, where the information that was lost by the processing of the DSB is restored by DNA polymerases. The remaining single-strand nicks are sealed by DNA ligase. At this stage the two DNA strands can be physically joined in a structure referred to as a Holliday junction, which needs resolution in order for recombination to be complete. In mammals, the proteins involved in the resolution activity are not known, but several possible candidates exist, including RAD54 and a multi-protein complex containing at least some RAD51 paralogs. Once resolution is complete, partner DNA molecules are separated, and the ligation of the resolvase-induced single-strand nicks result in two intact DNA molecules.

RAD54 is an important accessory protein of RAD51. *In vitro* studies have shown that RAD54 greatly stimulates the production of D-loops by RAD51. The biochemical properties of RAD54, including ATPase activity, as well as the ability to remodel DNA-protein complexes, are thought to be important in its role in recombination. RAD54 can be involved in almost every stage of recombination. Under different circumstances, RAD54 can both stabilize nucleoprotein filaments, as well as disassemble them. RAD54 can also perturb nucleosomes on the target template DNA and promotes branch migration, thereby affecting Holliday junction processing. Most of the data that has led to the definition of RAD54 function mentioned above has been collected using biochemical assays involving purified proteins and various structures of single-stranded and double-stranded DNA. The next step is to relate the biochemical functions as elucidated by such studies to the *in vivo* function of this protein and its activity in living cells.

In this thesis, the *in vivo* role of Rad54 has been examined in mouse embryonic stem (ES) cells, a model system to study homologous recombination. **Chapter 2** describes in detail the various tools and techniques that are used in visualization and analysis of protein behavior within cells. These are used throughout the thesis in order to

investigate the cellular behavior of Rad54. Chapter 2 also defines the process of homologous recombination, and discusses the cell biology of various proteins that are known to be involved to date, including the ability of some recombination proteins to form subnuclear structures (foci). The possible structure and function of damage-induced foci are discussed, since studies and quantification of foci forms an important part of this thesis.

Chapter 3 describes in detail the making of targeted ES cells that have been used to study Rad54 at the cellular level. The endogenous *Rad54* gene in ES cells is targeted and replaced with a (wild type) cDNA, fused with a DNA sequence encoding green fluorescent protein (GFP). The result is the production of GFP-tagged Rad54 protein under the control of its own promoter. The fusion protein is expressed at endogenous levels, which eliminates the disadvantages posed by over-expression systems. The knock-in cell line shows similar sensitivity to DNA damaging agents in survival assays as wild type, untargeted cells. Using these cells, a mouse strain expressing GFP-tagged Rad54 was made, and the pattern of Rad54 expression was documented using GFP fluorescence during the various stages of embryonic development. To investigate the expression of Rad54-GFP in blood cells, 12.5 dpc mouse embryo livers were cultured in medium that allowed the enrichment of proerythroblasts, which are actively cycling progenitor cells from which red blood cells are derived. These cells expressed Rad54-GFP, and in addition, showed DNA damage-induced foci formation similar to ES cells. Using cells derived from the bone marrow, it was found that pro- and pre-B cells show Rad54-GFP expression only when they are cycling. Furthermore, immature B cells, which do not cycle but are carrying out V(D)J recombination via nonhomologous end joining, do not show Rad54-GFP expression. This preliminary evidence underscores the idea that Rad54 is expressed only in cycling cells, where recombination is thought to be the primary method of faithfully repairing DSBs. To distinguish whether Rad54 is restricted to cycling progenitor cells, or is expressed in all cycling cells regardless of differentiation status, Rad54 expression was investigated in mouse dermal fibroblasts (MDFs) and chondrocytes subjected to culture conditions where they regained cycling ability. Rad54 mRNA is present in MDFs and chondrocytes, albeit at a lower level than in progenitor cells. In addition, only a subpopulation of cells shows nuclear localization of Rad54-GFP, which correlates with low mRNA levels. While the reason for the lower expression level in a population of cycling MEFs, MDFs and chondrocytes is not understood, we conclude that rapidly dividing progenitor cells express Rad54-GFP, reinforcing the idea

that these progenitor cells use homologous recombination to repair their genome, where fidelity is vital.

The *in vivo* function of Rad54 has been studied upto this point by investigating the phenotype presented by cells that are deficient in the protein, but what happens when the protein is physically present in the cell but is functionally defective? To answer this question, further characterization of Rad54 cellular function, this time in terms of its ATPase activity, was carried out in ES cells as documented in **Chapter 4**. It is known from *in vitro* studies that Rad54 has ATPase activity that is triggered by double-stranded DNA, and is essential for most of its biochemical functions. To investigate the phenotype of cells devoid of Rad54 ATPase activity, two different cell lines were made where the endogenous gene was replaced by one of two different cDNA constructs bearing a point mutation in the ATPase domain (*Rad54*$^{K189A\text{-}GFP/-}$ and *Rad54*$^{K189R\text{-}GFP/-}$). The behavior of the ATPase defective cell lines was similar to knockout *Rad54* ES cells (*Rad54*$^{-/-}$) in survival and recombination efficiency assays, showing that the mutant cells also exhibit hypersensitivity to DNA-damaging agents and a reduced efficiency of recombination. In contrast, the ATPase mutant cells display a significantly higher number of both Rad54 and Rad51 spontaneous, uninduced nuclear foci than *Rad54*$^{GFP/-}$ cells, which was used as the control cell line in these experiments. Interestingly, the number of spontaneous Rad51 foci in ATPase mutants is also significantly higher than in *Rad54*$^{-/-}$ cells. The experiments described here provide the first evidence that the ATPase activity of Rad54 influences the cell biological behavior of Rad51. Protein mobility studies established that while Rad54 moves at the same rate through the cell nucleus regardless of whether it is wild type or ATPase-defective, the turnover of Rad54 protein in spontaneous foci is significantly delayed for the ATPase-compromised protein compared to wild type protein. In addition, using time-lapse movies, the rate of foci disappearance in *Rad54*$^{K189R\text{-}GFP/-}$ cells was slower than in wild type after induction by irradiation. These data establish the contribution and influence of Rad54 ATPase activity on the proper functioning of both Rad54 and Rad51 in living cells.

In *S. cerevisiae*, *RAD54* paralogs, *RAD54* and *RDH54*, contribute to DNA damage repair activity in mitotic as well as meiotic cells respectively. In mammals a *Rad54* paralog, *Rad54B*, has also been identified. Rad54B shares 30% amino acid sequence identity to yeast *RDH54*, and on this basis it was proposed by others to be the functional counterpart of *RDH54* in mammals. Experiments described in **Chapter 5** dispel this idea, based on biochemical, genetic and cell biology assays which show that *Rad54B* is

unlikely to be the true *S. cerevisiae RDH54* homologue because the genes are not functionally equivalent. Using purified proteins and DNA substrates, Rad54B was shown to display physical and functional interactions with Rad51 that are similar to that of Rad54. Survival assays using *Rad54*$^{-/-}$ and *Rad54B*$^{-/-}$ ES cells showed that Rad54B deficient cells are hypersensitive to ionizing radiation and mitomycin C (MMC), but display no effect on recombination efficiency. Interestingly, while there is no additive or synergistic hypersensitivity to MMC in ES cells lacking both *Rad54* and *Rad54B*, animals lacking both *Rad54* paralogs are dramatically sensitized to MMC compared to either single mutant. Finally, it was shown that Rad54, but not Rad54B, is necessary for a normal distribution of Rad51 on meiotic chromosomes, further dismissing the notion that Rad54B might be the meiotic counterpart of Rad54 in mammals. Hence, it was shown that while the paralogs have overlapping biochemical properties, genetic analyses in mouse uncovered their nonoverlapping roles. The paralogs could therefore have redundant functions in DNA damage repair, or could provide similar functions but in a tissue-specific manner.

Lastly, the importance of accurate and proper repair of DSBs is underscored by their involvement in chromosome translocations, as described in **Chapter 6**. Several types of leukemias, lymphomas and solid tumors have been documented where translocations play an important role in the development, diagnosis as well as the prognosis of the cancer. Translocations and other genomic rearrangements have been hypothesized to result from incorrect functioning of, and inappropriate rejoining of DNA ends by, DSB repair mechanisms, specifically homologous recombination and nonhomologous end joining. Mistakes in homologous recombination can occur due to the presence of highly repetitive sequences in the human genome. The process of V(D)J recombination, a physiological and strictly timed process that is normally used to create antibody diversity in lymphocytes, could accidentally join a proto-oncogene locus with the elements of the antigen receptor locus, bringing the normally quiescent proto-oncogene under an active promoter, thereby creating an oncogenic phenotype. Finally, the propensity of certain aberrant DNA structures within the genome to suffer an increased frequency of breakage is also discussed, which suggests a role of DNA stability, rather than exogenous damage, in the occurrence of translocations.

References

1. Friedberg, E.C., G.C. Walker, and W. Siede, *DNA repair and Mutagenesis.* ASM Press Washington D.C., 1995.
2. Krogh, B.O. and L.S. Symington, *Recombination proteins in yeast.* Annu Rev Genet, 2004. **38**: p. 233-71.
3. Wyman, C. and R. Kanaar, *DNA double-strand break repair: All's well that ends well.* Annu Rev Genet, 2006.
4. Turner, N., A. Tutt, and A. Ashworth, *Hallmarks of 'BRCAness' in sporadic cancers.* Nat Rev Cancer, 2004. **4**(10): p. 814-9.

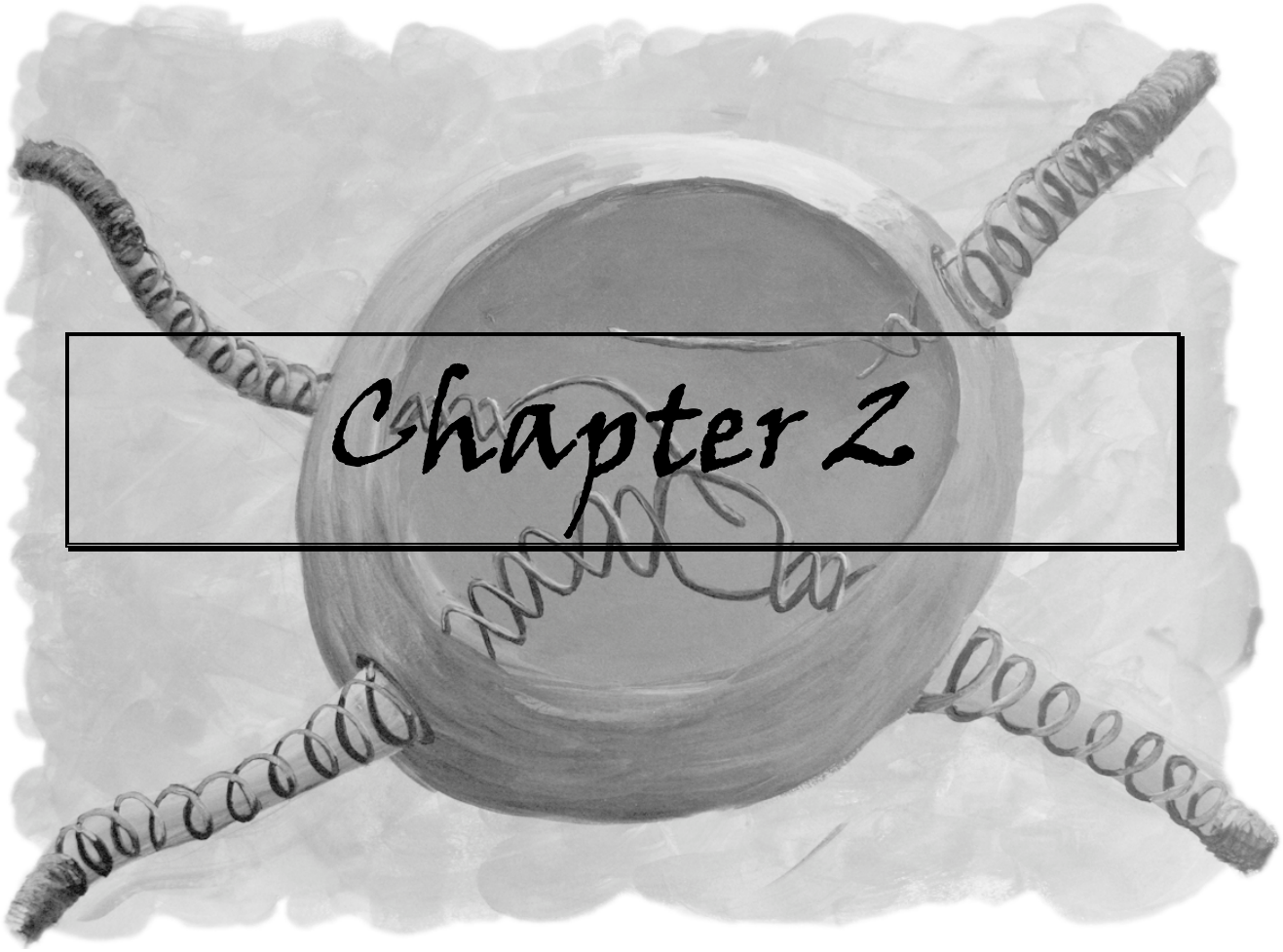

Chapter 2

The cell biology of homologous recombination

Expanded from
The cell biology of double-strand break repair.
Published in: *Molecular Genetics of Recombination* (2007), A. Aguilera & R. Rothstein (Eds.)
Topics in Current Genetics *(Springer Verlag)*: 335 – 362

Like the furtive collectors of stolen art, cell biologists are forced to be lonely admirers of spectacular architecture, exquisite symmetry, dramas of violence and death, mobility, self-sacrifice and, yes, rococo sex.

~ Lorraine Lee Cudmore

The cell biology of homologous recombination

Sheba Agarwal[1], Roland Kanaar [1,2] and Jeroen Essers[1, 2]

[1] Department of Cell Biology and Genetics, [2] Department of Radiation Oncology
Erasmus MC, PO Box 2040, 3000 CA Rotterdam, The Netherlands

Abstract

Discontinuities in double-stranded DNA, such as DNA double-strand breaks (DSBs), pose a threat to genome stability. Homologous recombination is a process that not only effectively repairs DSBs, but also promotes preservation of genome integrity by repairing DNA discontinuities arising during DNA replication. Genetic analyses identified many genes involved in DSB repair and placed them in different pathways. Biochemical analyses have aided in placing the protein products in a mechanistic framework for the pathways, while molecular biological approaches, such as chromatin immuno-precipitation, have allowed the monitoring of protein composition near DSBs in populations of fixed cells. Progress in cell biological techniques has now made it possible to analyze proteins in their physiological environment of the living cell. Here, we describe how homologous recombination proteins have been characterized using the methods of cell biology. The current challenge is to integrate insights gained on the spatio-temporal behavior of DSB repair proteins using chromatin immuno-precipitation and live cell imaging in the established genetic and biochemical frameworks for mechanisms of DSB repair.

1 Introduction

Double-strand breaks (DSBs) are detrimental lesions that disrupt the integrity of DNA in the cell. Pathological DSBs can be induced by exogenous factors, for example, ionizing radiation and a wide range of chemical compounds. Certain byproducts of cellular metabolism, such as oxygen free radicals, can also create DSBs in DNA. In contrast, DSBs can also be physiologically relevant intermediates. For example, nuclease-induced DSBs in germ cells trigger meiotic recombination that results in creation of genetic diversity. Another example is the programmed DSB formation during the assembly of active immunoglobulin and T cell receptor genes, as well as in class switch recombination to produce antibodies of different isotypes (Friedberg et al. 2004).

Whether pathological or physiological, the timely and accurate repair of DSBs is critical to the well-being of the cell. Inaccuracies in repair can result in mutations and gross chromosomal rearrangements, which can disrupt the normal functioning of the cell

and might ultimately lead to cancer. If breaks are left unrepaired, the cell can undergo genomic fragmentation, loss of chromosomes and cell death. To counteract this, mechanistically diverse methods that differ in their dependence on sequence homology have evolved to rejoin DNA ends: homology-directed repair, including homologous recombination, and non-homologous DNA end joining (Kanaar et al. 1998).

The dissection of the molecular mechanisms of DSB repair has its foundation in genetic experiments, which has revealed several pathways through which DSBs can be processed and repaired. The initial studies focused on bacteriophages, bacteria and fungi, including *Saccharomyces cerevisiae* (Shu et al. 1999; Symington 2002; Krogh and Symington 2004). Since then, it has become apparent that DSB repair pathways are conserved throughout evolution, which together with the advent of reverse genetics, has facilitated their analyses in a variety of other organisms, including mammals such as mice. The genetic approaches have been complemented and extended by biochemical analyses leading to placement of DSB repair proteins at specific steps in the pathways. More recently, molecular biological approaches, such as chromatin immuno-precipitation, have allowed the monitoring of protein composition near DSBs in populations of fixed cells. Advances in cell biology have now made it possible to analyze the behavior of DSB repair proteins and their response to DNA damage at the level of the single living cell. In this review, we describe how homologous recombination proteins have been characterized using cell biological techniques. The ultimate goal of these studies is to extend the knowledge of the individual activities of the proteins to their coordinated action within the entire homologous recombination pathway in the context of the living cell.

2 Tools and techniques of the trade

In order for a molecule to be visualized, first of all, it has to be labeled in some way. Second, a method of visualization is necessary. A labeled molecule within a cell can be detected with microscopes that are specifically designed for this purpose. These microscopes are optimized for the best possible image capture using high performance optical components and digital image acquisition, all of which is computerized. With rapid advances in techniques of microscopy, it is now possible to acquire information even at low levels of illumination or at wavelengths that cannot be detected by the human eye. In addition, it is critical that only the specific molecule that has been labeled be observed, and with minimal interference.

2.1 Fluorescence microscope

Fluorescence microscopy is based on the basic principle of fluorescence, which is observed as an emission of light in the visible spectrum after the fluorophores are excited by light of another, specific wavelength. The microscope utilizes filters which explicitly allow only certain wavelengths to activate the specimen. The activated fluorophore then emits a signal at a much lower intensity which is separated from the excitation light by using a second filter, ensuring that only emitted light reaches the eye piece or camera port of the microscope. The system ensures a high contrast between fluorescing and non-fluorescing areas. The widespread growth in the utilization of fluorescence microscopy is closely linked to the development of new synthetic and naturally occurring fluorophores with known profiles of excitation and emission wavelengths (see below).

2.2 Confocal / laser scanning microscope

Laser scanning confocal microscopy is a unique and versatile technique which enables visualization deep within living and fixed cells, as well as tissues. The method by which images are taken using a confocal microscope is fundamentally different from traditional microscopes. Instead of being bathed in light, the specimen is illuminated by one or more focused beams of light, usually from a laser. The point of illumination is brought to focus within the specimen by the objective lens, and laterally scanned using some form of scanning device under computer control. An image is assembled from the pixel information obtained by scanning the sample sequentially point by point and line by line. In this way, a series of optical sections can be collected from within the specimen, with the elimination of out-of-focus information, which results in sharper and more detailed images. Using the same principle, a sharp image can be taken not only in x and y, but also in the z plane. By moving the focus plane and scanning through serial optical slices, the single images can be put together to build up a three dimensional picture of the sample. The best horizontal resolution of the microscope is 0.2 microns, and the best vertical resolution is 0.5 microns.

2.3 Fluorescent tags

The power of fluorescence microscopy is in the plethora of different molecular fluorescent probes that are catalogued according to their absorption and fluorescent properties. The key requirement for a fluorescent molecule is that it must be sufficiently

bright and persistent for the instrument to obtain images. Classical fluorescent probes include fluorescein isothiocyanate, Lossamine, rhodamine and Texas red. Many flourophores are designed to bind to certain proteins or structures within the cell; for example, the nucleus of fixed cells is visualized by treatment with 4',6-diamidino-2-penylindole (DAPI), which stains DNA. Other DNA binding dyes include propidium iodide and Hoechst. The Alexa Fluor dyes (introduced by Molecular Probes) introduce a number of advantages and improvements over the traditional fluorophores. These include enhanced photostability, absorption spectra matched to common laser frequencies, pH insensitivity and a high degree of water solubility. In particular, these dyes can be conjugated to a series of molecules, including a broad variety of secondary antibodies which are used widely in immunostaining experiments. Alexa Fluor dyes are available in a wide range of fluorescence excitation and emission wavelength maxima, ranging from ultraviolet and deep blue to near infrared regions. Other colored probes used for the same purpose are the popular Cyanine dyes (Cy2, Cy3, Cy5, Cy7 and their derivatives).

2.4 Immunofluorescence

Immunostaining is a simple and effective way to detect a specific protein and document its behavior and localization in the cell, in snapshots over time. The technique requires chemical fixation of cells, which are then treated with an antibody that has been raised specifically against the protein in question. The signal is amplified using a secondary antibody that has been tagged with a fluorophore (such as Alexa fluors), which can be visualized when activated with a laser of its excitation wavelength. This is a relatively straightforward method and can be carried out on many cell types. In the context of repair, studies have shown that several repair proteins accumulate into punctuate nuclear foci, visible at 40x magnification, assumed to be the sites of DNA damage.

In order to investigate the temporal and spatial relationship of two or more proteins, cells may be treated with two or more primary antibodies. It is important that these antibodies have been generated in different animals. In order to distinguish the two proteins, they are visualized using secondary antibodies with fluorophores with different excitation and emission spectra. In this way, the foci forming capabilities of 2 repair proteins can be investigated for example, and also if these foci colocalize. Colocalization

of foci can strengthen the argument that two proteins work together on the repair of a DSB and therefore may complement biochemical data.

The disadvantage of using primary or tagged secondary antibodies is the possible danger of cross reaction with other proteins in the cell. In addition, the signal is never quantitative as this is dependent on extent of blocking and washing of the sample. There are also several other methodology related problems such as the masking of epitopes by fixing procedure, washing out of proteins and suboptimal penetration of the antibody.

2.5 Tagged proteins

Tracking of proteins in live cells has become a reality due to the discovery of naturally occurring fluorescent molecules, specifically, the Green Fluorescent Protein (GFP) in the North Atlantic jellyfish, *Aequorea victoria*. (Lippincott-Schwartz and Patterson 2003; Giepmans et al. 2006). Because GFP forms its chromophore within the protein core, it can be expressed in other organisms without interference or adverse biological effects. Mutagenesis of the gene sequence has resulted in variations of the GFP gene, including an improved version of GFP (enhanced GFP, eGFP), as well as proteins with a variety of absorption and emission characteristics across the entire visible spectrum, including yellow fluorescent protein, blue fluorescent protein and cyan fluorescent protein. Another commonly used fluorophore is the red fluorescent protein, isolated from the sea anemone *Discosoma striata*.

Standard recombinant DNA technology can be used to label the protein of interest in living cells. Specifically the GFP gene sequence is added in frame just before the stop codon or just after the start codon of the gene encoding the protein. The fusion protein produced as a result must be checked for functionality in order to make sure that protein carries out its cellular function properly in spite of the presence of the tag. In the context of repair proteins, these experiments include the ability of transfected cells to demonstrate wild type levels of survival against induced damage. Once physiological functionality has been established, the establishment of real time behavior can begin. Two types of experiments can be done with such cell lines. The behavior of the tagged protein can be studied by chemically fixing the cells with or without stimulus. The function and localization of the tagged protein with respect to another can be investigated by immunostaining against the other protein; this is a variation on the co-immunostaining protocol as outlined above.

The real power of using cells that have stable expressing fluorescent proteins is the direct observation of the dynamic behavior of the protein in real time. For example, we can document the behavior of a repair protein before and after DSB induction, as well as the localization of protein before and after cell division. In 4D microscopy, images are taken in x, y and z planes of the specimen, over time, creating movies which can be assembled and interpreted. The lifetimes and paths of nuclear structures, for example foci, can be tracked. Mobility studies and kinetics of proteins can be carried out by photobleaching studies.

Several caveats still exist. Some proteins cannot be tagged in this way, especially when it has been established that both N and C termini have specific roles which are necessary for the proper functioning of the protein. In addition, the ramifications of an overexpressed, tagged protein in a cell cannot be absolutely determined. For example, while the tagged repair protein is competent in its repair function, the presence of the tag might interfere in or disrupt other pathways, and this cannot be easily quantified. A technical advancement and improvement on the overexpression problem involves the targeted replacement of the gene of interest with a construct that recreates the protein, with the addition of an in-frame fluorescent tag as a reporter (*i.e.* the knock-in system). This way, the protein is tagged and produced under endogenous levels, and this is as close to the physiological situation as possible.

2.6 Fluorescence recovery after photobleaching (FRAP)

Besides the simple monitoring of the GFP-fusion protein, the photobleaching property of GFP can be exploited to obtain additional information on the protein of interest. Photobleaching is a phenomenon where a fluorophore loses its fluorescence due to photon-induced chemical damage. While this is a serious drawback of using fluorescent probes for direct observation, the local loss of fluorescence after exposure to excessive excitation light can be used to obtain information on protein mobility by fluorescence recovery after photobleaching (FRAP) experiments (Houtsmuller and Vermeulen 2001, Figure 1). These studies are done in live cells where the protein has been tagged with a fluorophore, preferably eGFP, and is expressed either stably or transiently.

During a FRAP experiment, a localized and very short high-intensity laser pulse is given to quench the fluorescence in a small area within a larger volume containing

fluorescent molecules, for example the nucleus. Bleaching of the fluorescence does not cause significant changes in protein functionality and cells retain their viability after long periods of FRAP experiments (Nakata et al. 1998; White and Stelzer 1999). Immediately after the high-intensity laser pulse, the recovery of fluorescence in the bleached region of interest is monitored as the molecules redistribute throughout the cell. Quantification of the rate of fluorescence recovery can yield information on protein diffusion rates and mobile versus immobile fractions, either spontaneously or in response to stimuli such as DNA damage. If the protein is highly mobile, it will be replenished quickly. However if it is completely immobile, then there will be no recovery. A FRAP curve consists of three phases: the prebleach period, the bleach pulse, and postbleach (recovery) period. The percentage recovery within the region of interest is a measure of the fraction of molecules that is mobile as well as the amount of permanently bleached molecules.

A variation of FRAP is fluorescence loss in photobleaching (FLIP). Molecules in one compartment are bleached, and the fluorescence in the unbleached area is monitored. The velocity of redistribution of molecules is a measure of exchange of molecules between bleached and unbleached sections. FLIP can also be coupled with FRAP, for example, to determine how long a protein stays in subnuclear bodies, like foci. In these experiments, the cell is visually divided into half, each half containing an equal number of foci. One half is bleached, and the recovery of fluorescence in the foci is monitored, while in the other half, the loss of fluorescence in the foci is monitored. In this way, protein turnover in foci can be determined. Another method to determine the protein turnover in foci is by bleaching the focus itself and monitoring the recovery of fluorescence within the area; in this case it is critical to track the movement of the focus by eye and to make sure that it remains within the region of interest while monitoring.
Several parameters can be determined by photobleaching experiments, namely, diffusion coefficient (D_{eff}), percentage immobile fraction and the duration of transient immobilization. The mobile fraction can be estimated by quantifying the fluorescence in the bleached fraction after a long recovery time and comparing it with the pre-bleach fluorescence intensity, correcting for total fluorescence removed by the bleach. An accurate effective diffusion coefficient ($\mu m^2 s^{-1}$) can be calculated from redistribution of fluorescence as a function of time. This can be calculated in several ways. One is to fit the recovery curves to a mathematically derived function. However, these mathematical models often do not reflect a true value of D_{eff} as it does not take into consideration

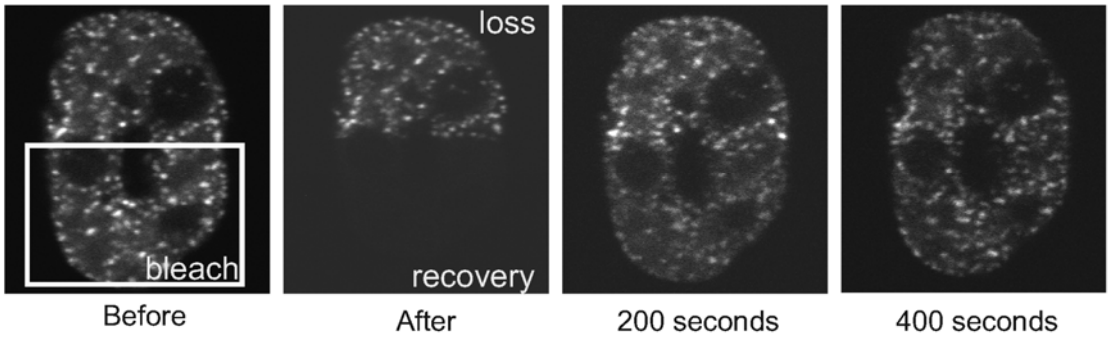

Figure 1. Example of a photobleaching procedure to determine the mobility of GFP-tagged proteins in living cells.
A region, indicated by the rectangle, of a cell containing PCNA-GFP replication foci was photobleached and fluorescence loss and recovery were monitored over time. The cell was imaged at the indicated times after bleaching. Fluorescence loss in photobleaching (FLIP) was measured in foci in the unbleached half of the cell, while fluorescence recovery after photobleaching (FRAP) was measured in foci in the bleached half of the same cell.

some parameters like the topology of the cell nucleus. Therefore the use of computer simulation might be a solution to avoid creating new mathematical models for each type of experiment and cell type.

A number of reviews are available that present in-depth discussions of a large variety of FRAP-based protocols that have been developed for specific purposes (Houtsmuller and Vermeulen 2001; Haraguchi 2002; Carrero et al. 2003; Houtsmuller 2005; Sprague and McNally 2005; Essers et al. 2006).

3 Controlled induction of DNA damage

The study of the cell biology of DSB repair mechanisms involves the investigation of difference in the behavior of repair proteins in the absence and presence of induced DNA damages. Thus, it is crucial to be able to do so conveniently and quantitatively. A number of methods have been developed, which can be classified into various categories, namely global versus local deposition of DNA damage, as well as in the induction of a specific lesion versus a spectrum of different lesions. Each method has its advantages and disadvantages.

In the context of DSB repair, DNA breaks can be introduced in a global manner by irradiating cells with ionizing radiation, for example, by using an X-ray machine or a

^{137}Cs source. These irradiation methods induce DNA damage that is dispersed over the whole nucleus. In response to global DSB induction, a number of DSB repair proteins accumulate into nuclear foci, which are high concentrations of the proteins located at the sites of DNA damage (Figure 2). However, this method also introduces other, although less genotoxic, types of DNA lesions in addition to DSBs. For example, for every DSB made, hundreds of single-strand breaks are introduced. In addition to damage to the phospho-diester backbone of the DNA, base damage also occurs (Friedberg et al. 2006).

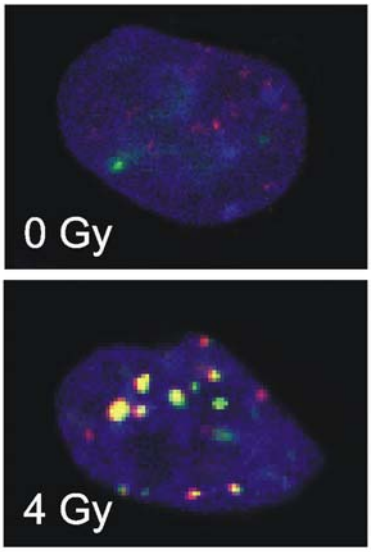

Figure 2. DNA damage induced local accumulations of DNA damage response proteins into foci.
Top panel: Nucleus of a cell before treatment with ionizing radiation. A cell, expressing the DNA repair protein Rad54 as a GFP fusion (in green), was fixed with paraformaldehyde and stained with antibodies against the DNA damage response protein 53BP1 (in red) and DAPI to detect DNA (in blue). Bottom panel: Nucleus of a cell 2 hours after treatment with 4 Gy of ionizing radiation and processed as described above.

The accumulation of repair proteins in response to global damage into nuclear structures visible by light microscopy is a remarkable phenomenon and can be exploited to characterize the dynamics of the repair response. However, such experiments require the creation of breaks in a more controlled fashion, both spatially and temporally. While global DNA damage induction methods introduce damage that is randomly distributed in the nucleus, it is possible to locally induce DNA damage by partially shielding the nucleus from the radiation source. In this way, it can be verified that the accumulation of repair proteins are indeed at sites of DNA damage and the accumulation can be analyzed in time. Also, foci at sites of induced DNA damage can be distinguished from foci that arise 'spontaneously', for example, during S phase (Tashiro et al. 1996). One method of local DSB induction involves the use of synchrotron-generated ultra-soft X-rays that are filtered through a metal grid containing micrometer spaced slits (Nelms et al. 1998). However, the method is not routinely used because first, facilities to generate ultra soft X-rays are not widely available, second, the time between irradiation and analysis of the

cells is relatively long, and third, the amount of DSBs introduced is large and difficult to control. An alternative method uses α-particle irradiation. This method has been developed recently and has number of advantages (Aten et al. 2004). Exposing cells to α-particles that travel almost horizontally relative to the cells leaves a straight track of DSBs in the nucleus. Proteins accumulating at the breaks can be visualized immediately after irradiation and deviation from the originally linear pattern can yield information on movement of chromosomal domains containing DNA breaks. Similar methods have been developed that use heavy ions instead of α-particles (Jakob et al. 2003; Lukas et al. 2005).

Alternative methods that introduce DNA damage in a spatially controlled manner have been developed with the use of lasers (Cremer et al. 1980). These methods make use of compounds that bind to or are incorporated into DNA. When these compounds are excited by the laser, they transmit energy to induce DNA lesions. For example, halogenated thymidine analogs, when incorporated in DNA, can induce single-strand breaks and DSBs in living cells when excited by a UV-A laser (Tashiro et al. 2000; Lukas et al. 2003; Lukas et al. 2005). Variations of this method use DNA intercalating Hoechst dyes either in the absence or presence of thymidine analogs (Rogakou et al. 1999; Walter et al. 2003; Bradshaw et al. 2005). In addition, there are laser-based micro-irradiation methods available that do not require exogenously added compounds. One such method makes use of the second harmonic of a pulsed neodymium-doped yttrium aluminium garnet laser that will result in DSBs (Kim et al. 2002; Kim et al. 2005). In addition, pulsed multiphoton laser technology can be used to introduce local DNA damage (Meldrum et al. 2003).

A drawback of the techniques described above is that first, the damage induced is not specific, that is, each method does not produce a single type of DNA lesion but a variety of them. Second, the spectrum of the actual induced DNA lesions is not known; an analysis of the types of damage induced by three of the above mentioned methods has revealed a wide variety of induced DNA damage (Dinant et al. 2007). Furthermore, for most laser-based methods, the local DNA damage load is unknown and will most likely be higher than at sites of DNA damage resulting from global DNA damage induction. Thus, when analyzing DSB repair proteins at the sites of locally induced DNA damage, it should be noted that repair proteins from pathways other than DSB repair might influence the results, as might the artificially high local DNA damage load.

In order to avoid the problem of introducing a large spectrum of lesions, a site-specific DSB can be created using a rare-cutting endonuclease (Haber 1995; Jasin 1996; Porteus and Carroll 2005). An example of a widely used enzyme is I-Sce I, which recognizes an 18-bp nonpalindronic sequence. Cleavage of the site is induced by transfecting cells with an I-Sce I expressing plasmid (Richardson et al. 1999). Expression of the enzyme in mammalian cells appears not to be toxic, presumably because its large recognition site provides sufficient specificity (Rouet et al. 1994a; Rouet et al. 1994b). A similar approach has been developed in the yeast *S. cerevisiae*, where the DSB-inducing enzyme of choice is most often the HO endonuclease, which normally initiates mating switch recombination. Because highly regulated promoters are available in *S. cerevisiae*, events at the induced break can be followed in time (Haber 2000). A disadvantage using these enzymes is that their recognition sequence has to be engineered in the genome. Also, they generate DSBs with complementary single-strand overhangs that can be easily ligated and might therefore not always be processed similarly to ionizing radiation-induced DSBs. To overcome some of these limitations, chimeric nucleases are being developed that couple the nuclease domain of the type II restriction enzyme Fok I to Zn-finger DNA binding domains. By combining different Zn-finger DNA binding domains, DSBs at predetermined sites in the genome can be introduced (Durai et al. 2005).

4 Homologous recombination pathways

Homologous recombination is generally an error-free pathway by which DSBs are repaired using the information on an undamaged homologous DNA molecule, usually the sister chromatid. The process is carried out by the proteins of the *RAD52* epistasis group that were originally identified by the genetic analysis of ionizing radiation hypersensitive *S. cerevisiae* mutants (Game and Mortimer 1974; Symington 2002). Many of the *RAD52* group proteins are conserved in mammals. They include the MRN (Rad50/Mre11/NBS1) complex, Rad51, the Rad51 paralogs (Rad51B, Rad51C, Rad51D XRCC2, XRCC3), Rad54 and Rad54B (Dudas and Chovanec 2004). In mammals, homologous recombination is also modulated by the products of the breast cancer susceptibility genes, BRCA1 and BRCA2 (Shivji and Venkitaraman 2004).

The process of DSB repair by homologous recombination can be divided in a number of steps, including DSB detection and processing, joint molecule formation between the broken DNA and the repair template through homologous pairing and

strand invasion, and resolution of the recombination partners (Figure 3). After DSB detection, the DNA ends go through nucleolytic processing resulting in 3' single-stranded DNA tails, which are used for the nucleation of recombination proteins on the DNA. This nucleoprotein complex is capable of pairing with intact homologous duplex DNA resulting in a joint molecule between the two recombining DNA molecules. The joint molecule is used as a template for DNA polymerases such that the information that was lost by processing is restored. The reaction is concluded by ligation of ends and the resolution of the joint molecule to yield two intact DNA copies. For simplicity, only one possibly outcome of the resolution process is shown. Nonetheless, it should be noted that multiple other outcomes exist, including one that results in crossover.

4.1 Detection and processing of DSBs

Once a DSB has occurred in the genome, the global response to its formation starts with the actual detection of the break in the context of the chromosome. A combination of biochemical and cell biological experiments has implicated the highly conserved MRN complex as an initial recognition factor of DSBs (Symington 2002). At the DSB MRN activates the ATM kinase resulting in a signaling cascade leading to cell cycle arrest (Shiloh 2003). The MRN complex is also involved in other cellular functions such as telomere maintenance, cell cycle checkpoint response and nonhomologous DNA end-joining (D'Amours and Jackson 2002). This wide range of MRN complex functions is carried out by a kaleidoscope of activities that exist within the complex, including hydrolysis of ATP, exo- and endo-nuclease, single-strand annealing, DNA end binding, tethering of broken DNA, protein interaction with, among others, the damage checkpoint kinase ATM and the signaling mediator protein MDC1 (Maser et al. 1997; Carney et al. 1998; Paull and Gellert 1998; Paull and Gellert 1999; Stewart et al. 1999; Yamaguchi-Iwai et al. 1999; de Jager et al. 2001a; de Jager et al. 2001b; de Jager et al. 2002; Hopfner et al. 2002; Kim et al. 2002; Goldberg et al. 2003; Mirzoeva and Petrini 2003; Costanzo et al. 2004; Lukas et al. 2004; Moreno-Herrero et al. 2005; Wiltzius et al. 2005).

The importance of the MRN complex for mammalian cells is underscored by the finding that all three genes that make up the MRN complex are essential for viability (Xiao and Weaver 1997; Luo et al. 1999; Yamaguchi-Iwai et al. 1999; Zhu et al. 2001). The loss of Mre11 in a conditional knockout DT40 cell line results in radiosensitivity,

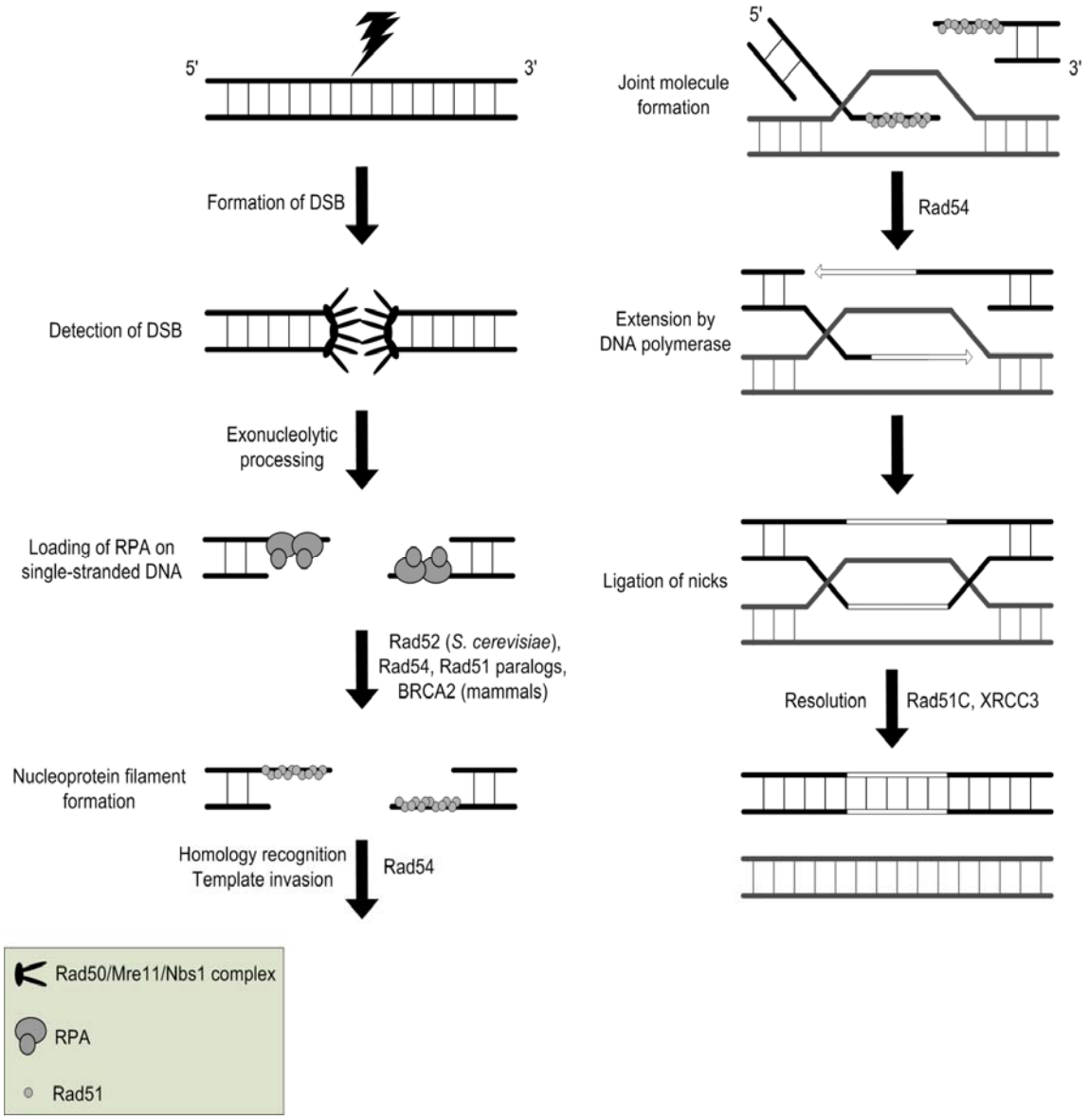

Figure 3. A model for DSB repair through homologous recombination.
The double-stranded DNA, depicted as a black ladder, suffers a DNA damage-induced DSB. Oligomers of the MRN complex tether the broken ends and initiate their processing, resulting in RPA-bound single-stranded DNA overhangs with a 3' polarity. The Rad51 recombinase is loaded on the single-stranded DNA with the assistance of mediators including Rad52 (*S. cerevisiae*), Rad51 paralogs, and BRCA2 (mammalian cells). The gray ladder represents a homologous duplex DNA (sister chromatid). The Rad51 nucleoprotein filament mediates homology recognition, joint molecule formation and strand exchange with the intact homologous duplex repair template. Steps that can be stimulated by the Rad54 protein are indicated. In this model the second DNA end of the DSB is captured by the displaced strand from the D-loop intermediate. DNA polymerization will restore missing nucleotides (indicated in white) and ligation will covalently lock the recombining partner DNA molecules into a structure joined through Holliday junctions. Resolution of the junctions by a resolvase activity that requires the Rad51 paralogs Rad51C and XRCC3 will separate the repaired DNA duplexes.

increased levels of chromosome breaks, arrest in G2 and eventual cell death (Yamaguchi-Iwai et al. 1999). In humans, hypomorphic mutations in NBS1 are associated with Nijmegen breakage syndrome (NBS) (Varon et al. 1998) and mutations in Rad50 and Mre11 cause Ataxia telangiectasia-like disease (ATLD) (Stewart et al. 1999; Taylor et al. 2004). NBS and ATLD patients are cancer-prone and their cells are radiosensitive.

The MRN complex relocalizes in response to DNA damage. In primary human fibroblasts, Mre11 and Rad50 are distributed homogeneously throughout the nuclei, but they accumulate in a high local concentration to form colocalizing foci after the global treatment of the cells with ionizing radiation (Maser et al. 1997). The physical association of these proteins is important for their accumulation into foci, since its components do not form DNA damage-induced foci in cells from NBS and ATLD patients (Carney et al. 1998; Stewart et al. 1999). In addition, the subnuclear localization of the complex also changes in response to DNA replication; it associates with chromatin in S phase and colocalizes with proliferating cell nuclear antigen (PCNA) throughout S phase (Mirzoeva and Petrini 2003).

A number of local DNA damage induction methods have demonstrated that the DNA damage-induced foci of the MRN complex colocalize with DSBs. These methods include exposure of cells to ultra-soft X-rays through an irradiation mask combined with the labeling of the generated DNA ends (Nelms et al. 1998), dye-dependent laser micro-irradiation (Paull et al. 2000; Lukas et al. 2003), and irradiation with α-particles (Aten et al. 2004). At DSBs, including those created by the local irradiation methods, the histone variant H2AX is modified by phosphorylation (Sedelnikova et al. 2003). This modified version of H2AX, γH2AX, colocalizes with the MRN complex (Paull et al. 2000). Interestingly, chromatin immunoprecipitation studies using *S. cerevisiae* showed that the phosphorylation of H2A in response to a nuclease-induced DSB can be detected up to 50 kb away from the break, but very little of it is found within 1 – 2 kb of the break. On the other hand, almost all Mre11 is concentrated within this region, in close vicinity to the break (Shroff et al. 2004). Results such as these emphasize the necessity of different techniques to address one problem, as each provides information at various levels of specificity. For example, while live cell imaging provides the advantage of real time observation of proteins in single cells, it lacks the spatial resolution provided by chromatin immunoprecipitation.

Once the DSB is detected, it is processed as the next step to its repair through homologous recombination (Figure 3). In *S. cerevisiae*, the MRX (Mre11/Rad50/Xrs2)

complex has been implicated in nucleolytic processing of the DSBs to produce the 3' tailed single-stranded DNA, which is the substrate for Rad51 binding (Lee et al. 1998). The mechanistic details of how the mammalian MRN complex participates in this reaction are not clear, since its intrinsic exonuclease activity is 3' to 5' (Paull and Gellert 1998). Thus, how the DNA intermediate is handed over from the MRN bound and processed DNA end to Rad51 is still an open question.

4.2 Nucleoprotein filament formation

Rad51 is a critical and central protein in the process of homologous recombination. *S. cerevisiae* cells deleted for *RAD51* display reduced recombination and as a result are sensitive to a range of DNA-damaging agents, including ionizing radiation, but they are still viable. In vertebrate cells, Rad51 deficiency has dire consequences; Rad51 depletion in chicken DT40 cells leads to G2/M cell cycle arrest, genomic fragmentation and cell death (Sonoda et al. 1998), while targeted disruption of *Rad51* in mouse cells results in embryonic lethality (Lim and Hasty 1996; Tsuzuki et al. 1996). Thus, Rad51 is a critical protein for high fidelity DNA damage repair during proliferation of vertebrate cells.

The function and involvement of Rad51 has been characterized extensively by biochemical studies (Figure 3). After a DSB has been detected and the DNA ends resected to produce 3' single-strand tails, it becomes the substrate for the Rad51 recombinase. Rad51 oligomerizes on the single-stranded DNA giving rise to a nucleoprotein filament, which then recognizes homologous duplex DNA in the genome, mediates joint molecule formation between the broken and intact template DNA, and promotes strand exchange between the recombining partner DNA molecules. Rad51 is aided in its function by accessory proteins, including the single-strand DNA binding protein RPA, Rad52 (in *S. cerevisiae*), the Rad51 paralogs, BRCA2 (in vertebrates) and Rad54.

At the cellular level, immunofluorescence experiments revealed that Rad51 occasionally forms nuclear accumulations referred to as foci (Haaf et al. 1995). Such spontaneous Rad51 foci are restricted to S phase (Tashiro et al. 1996), suggesting a role for Rad51 in supporting DNA replication, presumably through its involvement in recombination. In response to various global DNA-damaging agents, most cells demonstrate an accumulation of Rad51 into foci, marking presumably the sites of damage. Similar patterns of Rad51 accumulation are also observed when cells are hit by a

number of local DNA damage induction techniques, such as UV-A light micro-irradiation on nuclear DNA sensitized by incorporation of halogenated thymidine analogues, or irradiation of cells with α-particles or heavy ions (Tashiro et al. 2000; Aten et al. 2004; Hauptner et al. 2004). Although it is attractive to equate Rad51 foci formation with Rad51 nucleoprotein filament formation, there is no evidence that support this assumption. Indeed, other proteins involved in homologous recombination which show no biochemical evidence of nucleoprotein filament formation, such as BRCA2, ATM and the MRN complex, have also been shown to form foci. Instead, foci formation might be related to the fact that DNA damage, even when present only locally, induces signals that can spread out into the surrounding chromosomal domains (Shiloh 2003; Fernandez-Capetillo et al. 2004; Lukas et al. 2005).

To form nucleoprotein filaments on single-stranded DNA, Rad51 has to negotiate with RPA. *In vitro*, RPA stimulates Rad51 nucleoprotein filament formation, most likely by removing inhibitory secondary structures in the single-stranded DNA (Alani et al. 1992; Sugiyama et al. 1997; Sugiyama et al. 1998). However, order-of-addition experiments using the *S. cerevisiae* proteins have shown that if RPA is added to single-stranded DNA prior to Rad51, the displacement of RPA does not occur unless the Rad52 mediator protein is also present (Sung 1997; New et al. 1998; Shinohara et al. 1998; Sugiyama et al. 1998; Song and Sung 2000; Sugiyama and Kowalczykowski 2002; Symington 2002). In mammalian cells, colocalization of RPA, Rad51 and single-stranded DNA has been observed in ionizing radiation-induced foci (Golub et al. 1998; Raderschall et al. 1999).

RAD52 has been shown to be a very important gene for DSB repair in *S. cerevisiae*: Rad52 mutants display a more severe repair phenotype than *rad51* mutants. This contrasts sharply with the role of *Rad52* in vertebrate cells, where *Rad51* is an essential gene, but *Rad52* null mutants hardly display any phenotype. The absence of Rad52 does not affect viability or ionizing radiation sensitivity, and efficiency of gene targeting is only moderately reduced (two-fold) in mouse and chicken cells (Rijkers et al. 1998; Yamaguchi-Iwai et al. 1998). Furthermore, a systematic cell biological study analyzing foci formation by numerous homologous recombination and checkpoint proteins in living *S. cerevisiae* cells showed that Rad52 is required for Rad51 and Rad54 foci formation (Lisby et al. 2001; Lisby et al. 2004). By contrast, in mammalian cells, Rad52 is not required for foci formation of Rad51 and Rad54 (van Veelen et al. 2005b). Thus, while Rad52 in *S. cerevisiae* is placed early in the homologous recombination reaction, its role in

vertebrate cells does not appear to be of central significance. A possible reason for the difference in *rad52* mutant phenotypes in yeast and vertebrates could be functional redundancy of Rad52 in the latter. It has been shown that Rad52 deficient chicken cells in which the Rad51 paralog XRCC3 has also been deleted through a conditional knockout approach are unable to proliferate (Fujimori et al. 2001). In this respect, it is interesting to note that biochemical experiments support a role for a complex between the Rad51 paralogs Rad51B and Rad51C in Rad51 filament formation analogous to the activity of *S. cerevisiae* Rad52 (Sigurdsson et al. 2001).

In vertebrate cells, a total of five Rad51 paralogs have been identified, namely XRCC2, XRCC3, Rad51B, Rad51C and Rad51D (Thompson and Schild 2001; Thacker 2005). These proteins have 20 to 30% amino acid sequence identity to Rad51, and appear to function in complexes with each other. Two-hybrid and biochemical assays reveal the existence of a number of Rad51 paralog complexes, including complexes containing XRCC3/Rad51C and XRCC2/Rad51B/Rad51C/Rad51D (Schild et al. 2000; Masson et al. 2001a; Liu et al. 2002; Miller et al. 2002; Wiese et al. 2002). They display various biochemical activities, including DNA binding (including synthetic Holliday junctions), ATPase activity, DNA strand exchange activity and Holliday junction processing (Kurumizaka et al. 2002; Lio et al. 2003; Liu et al. 2004; Yamada et al. 2004; Yokoyama et al. 2004). The Rad51 paralogs are required for cell viability because all Rad51 paralog mouse knockouts that have been generated are lethal at the embryonic stage (Shu et al. 1999; Deans et al. 2000; Pittman and Schimenti 2000; Smiraldo et al. 2005; Thacker 2005). In contrast, chicken DT40 cells deleted for the Rad51 paralogs are viable, but this might be due to their additional inactivation of p53 (Takata et al. 2000; Takata et al. 2001). Rad51 paralog deficiency results in reduced homologous recombination efficiency, genome instability and DNA damage sensitivity, including ionizing radiation sensitivity (Johnson et al. 1999; Pierce et al. 1999; Godthelp et al. 2002; Lio et al. 2004), which is partially suppressed by the overexpression of Rad51 (Takata et al. 2001). DNA damage-induced Rad51 foci formation depends on the paralogs (Bishop et al. 1998; Takata et al. 2000; Takata et al. 2001) and the purified Rad51 paralog complex Rad51B/Rad51C stimulated Rad51 mediated strand exchange (Sigurdsson et al. 2001). Thus, the intimate relationship between Rad51 and the Rad51 paralogs is manifested at the genetic, the cell biological and biochemical levels.

Another important mediator protein in homologous recombination is the breast cancer susceptibility gene product, BRCA2. Carriers of mutations in the *BRCA2* gene are

predisposed to breast, ovarian, prostate and pancreatic cancer (Venkitaraman 2002). Rad51 and BRCA2 have many common features. For example, *BRCA2* is also an essential gene (Gowen et al. 1996; Hakem et al. 1996; Liu et al. 1996; Ludwig et al. 1997; Sharan et al. 1997; Suzuki et al. 1997); both mouse and human hypomorphic mutant cell lines display chromosomal instability and sensitivity to DNA-damaging agents (Tutt et al. 1999; Scully et al. 2000; Yu et al. 2000), as well as reduced recombination efficiency (Moynahan et al. 2001). Like the Rad51 paralogs, BRCA2 is required for DNA damage-induced Rad51 foci formation (Yuan et al. 1999; Yu et al. 2000). These similar features suggest that the direct protein-protein interaction between BRCA2 and Rad51 is of functional importance (Scully et al. 1997; Wong et al. 1997; Marmorstein et al. 1998; Davies et al. 2001; Pellegrini et al. 2002; Venkitaraman 2002).

Recently, a mechanistic basis for the mediator function of BRCA2 with respect to Rad51 nucleoprotein filaments formation was suggested. A BRCA2 family member, Brh2, has been discovered in *Ustilago maydis*, which is required for repair and recombination proficiency (Kojic et al. 2002). An ortholog of Dss1, a protein that interacts with BRCA2, has also been found to interact with Brh2, and is important in genome stability and recombination (Kojic et al. 2003; Kojic et al. 2005). Brh2 functions to recruit Rad51 to DNA and aids in the nucleation of the Rad51 filament, establishing a function for BRCA2 protein in Rad51 mediated repair of DSBs (Yang et al. 2005). A similar activity has been established for a minimal version of human BRCA2, containing some of its Rad51 interaction domains and the DNA binding domain (San Filippo et al. 2006).

At the cell biological level, BRCA2 also forms DNA damage-induced foci, which colocalize with Rad51 foci (Chen et al. 1998; Chen et al. 1999). In living cells, the interplay between BRCA2 and Rad51 has been investigated using GFP-tagged Rad51. FRAP experiments revealed the existence of two different nuclear pools of Rad51 with respect its mobility; a mobile fraction and a relatively immobile fraction (Essers et al. 2002). The relatively immobile fraction of Rad51 molecules is bound to BRCA2 and this fraction is reduced upon replication arrest with hydroxyurea (Yu et al. 2003). This behavior is lost for Rad51 mutants that no longer interact with BRCA2, suggesting a role for BRCA2 in the Rad51 DNA damage response at the cellular level. Given the behavior of BRCA2 at the biochemical and cellular level and the fact that *S. cerevisiae* does not contain a BRCA2 homolog, BRCA2 is, in addition to or in combination with the Rad51 paralogs, also a candidate for the mammalian equivalent of *S. cerevisiase* Rad52 activity.

Once the nucleoprotein filament is formed and has found the target duplex, the next step is the joint molecule formation. This is a critical step in homologous recombination, in which Rad51 is aided by Rad54. Rad54 is a member of the SWI2/SNF2 family of DNA-dependent ATPases, which have been implicated in modulating protein-DNA interactions. Mouse and chicken Rad54 deficient cells show sensitivity to DSB inducing agents, and a reduced level of homologous recombination (Bezzubova et al. 1997; Essers et al. 1997; Dronkert et al. 2000). The absence of Rad54 is compatible with mouse development, in spite of the fact that *Rad54* knockout mice as well as *Rad54* knockout ES cells are sensitive to mitomycin C. By contrast, unlike ES cells, adult *Rad54* knockout mice are not sensitive to ionizing radiation (Essers et al. 2000). However, the phenotypes related to DNA damage sensitivity and genome instability of the DNA end joining (DNA-Pk_{cs}, Ku70, or DNA Ligase IV) defective mice are dramatically enhanced when Rad54 is absent (Essers et al. 2000; Couedel et al. 2004; Mills et al. 2004). Therefore the contribution of Rad54 to repair of ionizing radiation induced DNA damage in adult mice is clearly evident when the *Rad54* knockout mutation is combined with a defect in the DNA end-joining pathway.

Biochemical experiments have revealed that the important substrate of Rad54 in recombination is double-stranded template DNA: only double-stranded DNA activates its ATPase activity (Swagemakers et al. 1998; Petukhova et al. 1999). Rad54 has been shown to be a motor protein on DNA, whose translocation can lead to supercoiling of DNA domains thereby lowering the energy required to separate the strands of the double helix (Petukhova et al. 1999; Tan et al. 1999; Mazin et al. 2000; Van Komen et al. 2000; Ristic et al. 2001). This activity is important during the strand invasion step of the Rad51 coated single-stranded DNA into the template duplex. Indeed, the Rad54 protein interacts with Rad51 (Clever et al. 1997; Golub et al. 1997; Tan et al. 1999; Van Komen et al.; Raschle et al. 2004) and this interaction has functional consequences, for example the stimulation of Rad51 mediated joint molecule formation by Rad54 (Petukhova et al. 1998; Mazin et al. 2000). In addition to this early role, biochemical experiments have also suggested a late role for Rad54 in recombination. Rad54 can remove Rad51 filaments from double-stranded DNA (Solinger and Heyer 2001; Solinger et al. 2002). Evidence for the importance of this role of Rad54 at the cellular level is provided by experiments showing that homologously paired molecules in *S. cerevisiae* cells could not be extended by a DNA polymerase in the absence of Rad54 (Sugawara et al. 2003). In addition, during

meiosis in *Rad54* knockout mice, Rad51 protein appears to remain associated with chromatin loops of synapsed chromosomes (Wesoly et al. 2006).

The finding that Rad51 and Rad54 interact closely in biochemical assays is further confirmed by cell biology analysis. Like Rad51, Rad54 forms DNA damaged-induced foci and these foci colocalize (Tan et al. 1999). Under conditions in which Rad51 DNA damage-induced foci do not form, such as in the Rad51 paralog mutants, Rad54 also fails to form foci (van Veelen et al. 2005b). In the absence of Rad54, Rad51 foci appear to be destabilized (Tan et al. 1999; van Veelen et al. 2005a). The reduced stability of Rad51 aggregation in cells lacking Rad54 is consistent with the biochemical demonstration that Rad54 can stabilize Rad51 nucleoprotein filaments (Mazin et al. 2003).

The Rad54 protein has also been analyzed in living cells. The first study to analyze DNA damage-induced foci in live cells revealed similar aggregations of recombination proteins at sites of DNA damage as seen in fixed cells (Essers et al. 2002). FRAP experiments demonstrated that these foci are highly dynamic; Rad51 and Rad54 proteins actively sample these foci through an equilibrium of association and dissociation, but they display different residence times. Furthermore, even though both recombination proteins work together in recombination, they are not present in the cell as a holo-complex in the absence of DNA damage because they diffuse through the cell at different rates. Executing DNA transactions through dynamic multi-protein complexes, rather than stable holo-complexes, allows flexibility. For example, it will facilitate cross-talk between different DNA repair pathways and coupling to other DNA transactions, such as replication.

4.3 Resolution

Once the joint molecule between the nucleoprotein filament and target duplex is formed, the information lost during end processing can be restored by DNA polymerases (Figure 3). Recently, the translesion DNA polymerase eta has been implicated in this step (Rattray and Strathern 2005). DNA polymerase eta relocalizes into foci upon UV irradiation and those foci colocalize with Rad51 (Kannouche et al. 2001). A chicken B cell derived cell line deficient in DNA polymerase eta displays defects in DSB-induced homologous recombination (Kawamoto et al. 2005). In addition, DNA polymerase eta interacts with Rad51 and can extend DNA synthesis from joint molecule recombination intermediates (McLlwraith et al. 2005). Chromatin immunoprecipitation experiments indicate that the *S. cerevisiae* Rad54 protein is important in promoting the

transition from pairing of homologous DNA strands by Rad51 to extension of the invading strand by DNA polymerases (Sugawara et al. 2003). Possibly, Rad54's potential to remove Rad51 nucleoprotein filaments from double-stranded DNA might be important in promoting this step in homologous recombination (Solinger and Heyer 2001; Solinger et al. 2002).

After all sequences are restored, remaining single-strand nicks are sealed by DNA ligase. At this stage the recombined DNA molecules can be physically joined in a structure often referred to as a Holliday junction (Figure 3). To complete recombination this junction needs to be resolved; for simplicity, one possible outcome of resolution is shown in Figure 3. In *E. coli*, this reaction is carried out by the RuvABC complex. The RuvA and RuvB proteins promote ATP-dependent branch migration of the Holliday junction, while RuvC introduces nicks in two of the four DNA strands of the Holliday junction allowing resolution of the junction into recombinant DNA molecules (West 1997). In mammalian cells, less is known about the proteins involved in resolution of Holliday junctions; however, some initial studies have found clues in elucidating this activity (Waldman and Liskay 1988; Hyde et al. 1994; Constantinou et al. 2001; Constantinou et al. 2002).

As described above, several biochemical and cellular studies have resulted in the suggestion that the Rad51 paralogs have an early function in loading Rad51 onto single-stranded DNA during the assembly of the nucleoprotein filament (Masson et al. 2001b; Sigurdsson et al. 2001; Yonetani et al. 2005). Interestingly, the identification of Rad51C and XRCC3 as components of an activity that promotes Holliday junction resolution suggest that at least some Rad51 paralogs can also have a late role in homologous recombination (Liu et al. 2004). Further evidence for this notion comes from studies showing that Rad51B can bind preferentially to synthetic Holliday junctions (Yokoyama et al. 2003). Support at the cellular level for a late function of Rad51 paralogs associated with resolution of recombination intermediates comes from studies on XRCC3 mutant hamster cells showing that gene conversion tract lengths are increased in the absence of XRCC3 (Brenneman et al. 2000). Once the Holliday junction has been cleaved by the resolvase, the partner DNA molecules are separated and ligation of the resolvase-induced single-strand nicks will produce two completely restored duplex DNA recombinants (Figure 3).

5 Recombination and replication

Above we focused on homologous recombination in the context of the repair of a pre-existing DSB. Joint molecule formation between the broken DNA and the intact repair duplex catalyzed by Rad51 and accessory factors sets up the substrate for DNA polymerases such that DNA replication can restore information lost by processing of the DSB. Conversely, homologous recombination also plays an important role in supporting DNA replication when the replication fork encounters DNA damage in its template, for example thymidine intra-strand dimers induced by UV-light (Michel et al. 2004). Depending on the type of DNA damage, processing might or might not result in a DSB. In either case, homologous recombination proteins are involved in helping the replication machinery pass the damage (Cox et al. 2000). The presence of unrepaired DNA damage serves as a block to the passage of the replication machinery. The bypass or repair of these blocks and the subsequent fidelity of DNA replication requires several coordinated processes, including chromatin remodeling, DNA repair and DNA synthesis, which has to occur in an ordered manner to achieve proper cell division. The synthesis of DNA past lesions requires the use of specialized DNA polymerases that bypass them, such as DNA polymerase eta, since the highly stringent replicative DNA polymerases cannot accommodate damaged bases in its active site (Prakash et al. 2005). It is for this reason that DNA synthesis during S phase of cells is blocked in the presence of unrepaired lesions and as a consequence, replication stalls, the replisome dissociates and the fork collapses. The resulting structures that emerge are substrates for homologous recombination.

The central protein in DNA replication and several forms of DNA repair, including nucleotide excision repair (NER) is the DNA polymerase processivity factor proliferating cell nuclear antigen (PCNA), which localizes proteins such as polymerases to DNA (Ellison and Stillman 2003). Recently, the coordination between DNA repair and replication has been studied by determining the behavior of GFP-tagged PCNA in living cells using photobleaching. While PCNA molecules move rapidly through the nucleus during the G1, S, and G2 phases of the cell cycle, they reside for 10-20 minutes in replication foci during S phase (Sporbert et al. 2002; Solomon et al. 2004; Essers et al. 2005; Solovjeva et al. 2005). To simultaneously monitor PCNA action in DNA replication and repair, local irradiation has shown an accumulation of PCNA at sites of UV-light induced DNA damage in brightly fluorescent regions, on top of the typical replication pattern. Photobleaching experiments have revealed that PCNA also binds

transiently to these local UV-damaged areas although residence times are considerably longer compared to replication foci (Solomon et al. 2004; Essers et al. 2006). This difference is not found in a PCNA mutant that can no longer be ubiquitinated (PCNA K164R), showing that one function of mono-ubiquitination of PCNA is to modulate the residence time of PCNA at sites of DNA damage (Essers et al. 2006). Similar analysis also revealed the residence time of other replication factors, such as Fen1, DNA ligase I, and RPA, which showed significant faster turnover rates at replication foci compared to PCNA, (Sporbert et al. 2002; Chapados et al. 2004; Solovjeva et al. 2005). This is reminiscent of what has been found for the IR-induced foci of the homologous recombination proteins Rad51 and Rad54 (Essers et al. 2002). Rad51, like PCNA, is a more stable component of the DNA damage-induced foci, while Rad54 reversibly interacts with these structures. The differential mobility of these proteins likely reflects their functional status *in vivo* and can therefore be used as an analytical tool to explore their function.

6 The function of DNA damage-induced foci

The formation of foci containing proteins involved in homologous recombination and checkpoint activation at sites of DNA damage is a remarkable phenomenon (Figure 2). Clearly, many molecules of each protein must accumulate at those sites. In order for a focus to be detected by immunofluoresence or by GFP signal, the number of molecules present must be in the order of 100. To gain insight into the function of foci, important questions to be answered include: (1) What is the composition of these foci? (2) Why do they contain such high numbers of molecules of proteins? (3) How do they form and how are they disassembled?

To determine the identity of all proteins in a focus is not a straightforward problem. Methods that have been successful in the analysis of the proteome of other subnuclear organelles such as nucleoli are not easily adapted to analyze foci (Andersen et al. 2002). Because biochemically isolated nucleoli can be tested for a particular activity, it may be assumed that mass spectrometric analysis will reveal the proteome of the active subnuclear organelle. Methods to isolate foci containing homologous recombination proteins are yet to be developed. The most promising approach might be to perform *in vivo* crosslinking experiments of complexes near site-specific DSBs and fishing for a specific sequence near the DSB. However, in the absence of an *in vitro* activity assay for foci activity, the interpretation of subsequent proteome analysis will be ambiguous.

Besides its composition, it would be interesting to determine why so many molecules of the homologous recombination proteins accumulate at the sites of DNA damage. It is clear from biochemical experiments that the actual number of proteins required to take the DNA strands through recombination are much lower than the sheer numbers that appear to accumulate into foci. Therefore it is conceivable that in order to do their job, a large number of homologous recombination proteins accumulate at the site of damage, while only a small subset is actually involved in damage repair. In addition, the requirement for high local concentrations of DNA repair proteins at damage sites is not a general prerequisite for repair, as shown by the fact that global UV-light irradiation of cells does not result in the formation of foci of NER proteins, for example (Houtsmuller and Vermeulen 2001). Therefore the necessity for microscopically visible foci in the repair of damage by recombination is still an open question. It is possible that such an accumulation could synchronize the presence and function of the various protein components of recombination both spatially and temporally, since it has been shown that the enzymes of homologous recombination have to work together in a timely and highly coordinated manner.

Foci of homologous recombination proteins near sites of DNA damage might simply form because the proteins could have a higher affinity for damaged compared to undamaged chromosomal domains. This would require a mechanism that distinguishes between damaged and undamaged chromosomal domains. One possible marker for chromosomal domains containing DNA damage is γH2AX. The increased local concentration of γH2AX can be rationalized as a marker of the location of a DSB, since this modification is present in the megabase chromosomal domain that contains the damage (Rogakou et al. 1999). However, the mild phenotype of *H2AX* knockout cells and mice argues that there must be alternative or additional distinctions.

Thus, once a DSB arises, modification of the chromosomal domain it is contained in might create a site with a slightly increased affinity for the recombination proteins compared to intact chromosomal domains. The difference in affinity ensures that the proteins will be concentrated and partially immobilized for a longer time at the damage-containing chromosomal domain, resulting in an accumulation of homologous recombination proteins at the DSB site. Moreover, the homogeneous distribution of freely mobile DNA repair proteins (Essers et al. 2002) ensures that all required factors are always present in the vicinity of DNA lesions wherever they occur, allowing rapid and efficient detection and subsequent repair.

New insight into the mechanism of homologous recombination repair in living cells will come from analyzing the behavior of proteins with biochemically characterized mutations to see how these affect their *in vivo* behavior. It is clear that the technology is available to sort through the mechanistic possibilities suggested from genetic and biochemical studies of homologous recombination.

References

Alani E, Thresher R, Griffith JD, Kolodner RD (1992) Characterization of DNA-binding and strand-exchange stimulation properties of y-RPA, a yeast single-strand-DNA-binding protein. J Mol Biol 227:54-71

Andersen JS, Lyon CE, Fox AH, Leung AK, Lam YW, Steen H, Mann M, Lamond AI (2002) Directed proteomic analysis of the human nucleolus. Curr Biol 12:1-11

Aten JA, Stap J, Krawczyk PM, van Oven CH, Hoebe RA, Essers J, Kanaar R (2004) Dynamics of DNA double-strand breaks revealed by clustering of damaged chromosome domains. Science 303:92-95

Bezzubova O, Silbergleit A, Yamaguchi-Iwai Y, Takeda S, Buerstedde JM (1997) Reduced X-ray resistance and homologous recombination frequencies in a RAD54-/- mutant of the chicken DT40 cell line. Cell 89:185-193

Bishop DK, Ear U, Bhattacharyya A, Calderone C, Beckett M, Weichselbaum RR, Shinohara A (1998) Xrcc3 is required for assembly of Rad51 complexes *in vivo*. J Biol Chem 273:21482-21488

Bradshaw PS, Stavropoulos DJ, Meyn MS (2005) Human telomeric protein TRF2 associates with genomic double-strand breaks as an early response to DNA damage. Nat Genet 37:193-197

Brenneman MA, Weiss AE, Nickoloff JA, Chen DJ (2000) XRCC3 is required for efficient repair of chromosome breaks by homologous recombination. Mutat Res 459:89-97

Carney JP, Maser RS, Olivares H, Davis EM, Le Beau M, Yates JR, 3rd, Hays L, Morgan WF, Petrini JH (1998) The hMre11/hRad50 protein complex and Nijmegen breakage syndrome: linkage of double-strand break repair to the cellular DNA damage response. Cell 93:477-486

Carrero G, McDonald D, Crawford E, de Vries G, Hendzel MJ (2003) Using FRAP and mathematical modeling to determine the *in vivo* kinetics of nuclear proteins. Methods 29:14-28

Chapados BR, Hosfield DJ, Han S, Qiu J, Yelent B, Shen B, Tainer JA (2004) Structural basis for FEN-1 substrate specificity and PCNA-mediated activation in DNA replication and repair. Cell 116:39-50.

Chen JJ, Silver D, Cantor S, Livingston DM, Scully R (1999) BRCA1, BRCA2, and Rad51 operate in a common DNA damage response pathway. Cancer Res 59:1752s-1756s

Chen PL, Chen CF, Chen Y, Xiao J, Sharp ZD, Lee WH (1998) The BRC repeats in BRCA2 are critical for RAD51 binding and resistance to methyl methanesulfonate treatment. Proc Natl Acad Sci U S A 95:5287-5292

Clever B, Interthal H, Schmuckli-Maurer J, King J, Sigrist M, Heyer WD (1997) Recombinational repair in yeast: functional interactions between Rad51 and Rad54 proteins. Embo J 16:2535-2544

Constantinou A, Chen XB, McGowan CH, West SC (2002) Holliday junction resolution in human cells: two junction endonucleases with distinct substrate specificities. Embo J 21:5577-5585

Constantinou A, Davies AA, West SC (2001) Branch migration and Holliday junction resolution catalyzed by activities from mammalian cells. Cell 104:259-268

Costanzo V, Paull T, Gottesman M, Gautier J (2004) Mre11 assembles linear DNA fragments into DNA damage signaling complexes. PLoS Biol 2:E110

Couedel C, Mills KD, Barchi M, Shen L, Olshen A, Johnson RD, Nussenzweig A, Essers J, Kanaar R, Li GC, Alt FW, Jasin M (2004) Collaboration of homologous recombination and nonhomologous end-joining factors for the survival and integrity of mice and cells. Genes Dev 18:1293-1304

Cox MM, Goodman MF, Kreuzer KN, Sherratt DJ, Sandler SJ, Marians KJ (2000) The importance of repairing stalled replication forks. Nature 404:37-41

Cremer C, Cremer T, Fukuda M, Nakanishi K (1980) Detection of laser--UV microirradiation-induced DNA photolesions by immunofluorescent staining. Hum Genet 54:107-110

D'Amours D, Jackson SP (2002) The Mre11 complex: at the crossroads of dna repair and checkpoint signalling. Nat Rev Mol Cell Biol 3:317-327

Davies AA, Masson JY, McIlwraith MJ, Stasiak AZ, Stasiak A, Venkitaraman AR, West SC (2001) Role of BRCA2 in control of the RAD51 recombination and DNA repair protein. Mol Cell 7:273-282

de Jager M, Dronkert ML, Modesti M, Beerens CE, Kanaar R, van Gent DC (2001a) DNA-binding and strand-annealing activities of human Mre11: implications for its roles in DNA double-strand break repair pathways. Nucleic Acids Res 29:1317-1325

de Jager M, van Noort J, van Gent DC, Dekker C, Kanaar R, Wyman C (2001b) Human Rad50/Mre11 is a flexible complex that can tether DNA ends. Mol Cell 8:1129-1135

de Jager M, Wyman C, van Gent DC, Kanaar R (2002) DNA end-binding specificity of human Rad50/Mre11 is influenced by ATP. Nucleic Acids Res 30:4425-4431

Deans B, Griffin CS, Maconochie M, Thacker J (2000) Xrcc2 is required for genetic stability, embryonic neurogenesis and viability in mice. Embo J 19:6675-6685

Dinant C, de Jager M, Essers J, van Cappellen WA, Kanaar R, Houtsmuller A, Vermeulen W (2007) Activation of multiple DNA repair pathways by sub-nuclear damage induction methods. J Cell Sci 120:2731-2740

Dronkert ML, Beverloo HB, Johnson RD, Hoeijmakers JH, Jasin M, Kanaar R (2000) Mouse RAD54 affects DNA double-strand break repair and sister chromatid exchange. Mol Cell Biol 20:3147-3156

Dudas A, Chovanec M (2004) DNA double-strand break repair by homologous recombination. Mutat Res 566:131-167

Durai S, Mani M, Kandavelou K, Wu J, Porteus MH, Chandrasegaran S (2005) Zinc finger nucleases: custom-designed molecular scissors for genome engineering of plant and mammalian cells. Nucleic Acids Res 33:5978-5990

Ellison V, Stillman B (2003) Biochemical characterization of DNA damage checkpoint complexes: clamp loader and clamp complexes with specificity for 5' recessed DNA. PLoS Biol 1:E33.

Essers J, Hendriks RW, Swagemakers SM, Troelstra C, de Wit J, Bootsma D, Hoeijmakers JH, Kanaar R (1997) Disruption of mouse RAD54 reduces ionizing radiation resistance and homologous recombination. Cell 89:195-204

Essers J, Houtsmuller AB, Kanaar R (2006) Analysis of DNA recombination and repair proteins in living cells by photobleaching microscopy. Methods Enzymology

Essers J, Houtsmuller AB, van Veelen L, Paulusma C, Nigg AL, Pastink A, Vermeulen W, Hoeijmakers JH, Kanaar R (2002) Nuclear dynamics of RAD52 group homologous recombination proteins in response to DNA damage. Embo J 21:2030-2037

Essers J, Theil AF, Baldeyron C, van Cappellen WA, Houtsmuller AB, Kanaar R, Vermeulen W (2005) Nuclear dynamics of PCNA in DNA replication and repair. Mol Cell Biol 25:9350-9359

Essers J, van Steeg H, de Wit J, Swagemakers SM, Vermeij M, Hoeijmakers JH, Kanaar R (2000) Homologous and non-homologous recombination differentially affect DNA damage repair in mice. Embo J 19:1703-1710

Fernandez-Capetillo O, Lee A, Nussenzweig M, Nussenzweig A (2004) H2AX: the histone guardian of the genome. DNA Repair (Amst) 3:959-967

Friedberg EC, McDaniel LD, Schultz RA (2004) The role of endogenous and exogenous DNA damage and mutagenesis. Curr Opin Genet Dev 14:5-10

Friedberg EC, Walker GC, Siede W, Wood RD, Schultz RA, Ellenberger T (2006) DNA Repair And Mutagenesis. ASM Press, Washington, D.C.

Fujimori A, Tachiiri S, Sonoda E, Thompson LH, Dhar PK, Hiraoka M, Takeda S, Zhang Y, Reth M, Takata M (2001) Rad52 partially substitutes for the Rad51 paralog XRCC3 in maintaining chromosomal integrity in vertebrate cells. Embo J 20:5513-5520

Game JC, Mortimer RK (1974) A genetic study of x-ray sensitive mutants in yeast. Mutat Res 24:281-292

Giepmans BN, Adams SR, Ellisman MH, Tsien RY (2006) The fluorescent toolbox for assessing protein location and function. Science 312:217-224

Godthelp BC, Wiegant WW, van Duijn-Goedhart A, Scharer OD, van Buul PP, Kanaar R, Zdzienicka MZ (2002) Mammalian Rad51C contributes to DNA cross-link resistance, sister chromatid cohesion and genomic stability. Nucleic Acids Res 30:2172-2182

Goldberg M, Stucki M, Falck J, D'Amours D, Rahman D, Pappin D, Bartek J, Jackson SP (2003) MDC1 is required for the intra-S-phase DNA damage checkpoint. Nature 421:952-956

Golub EI, Gupta RC, Haaf T, Wold MS, Radding CM (1998) Interaction of human rad51 recombination protein with single-stranded DNA binding protein, RPA. Nucleic Acids Res 26:5388-5393

Golub EI, Kovalenko OV, Gupta RC, Ward DC, Radding CM (1997) Interaction of human recombination proteins Rad51 and Rad54. Nucleic Acids Res 25:4106-4110

Gowen LC, Johnson BL, Latour AM, Sulik KK, Koller BH (1996) Brca1 deficiency results in early embryonic lethality characterized by neuroepithelial abnormalities. Nat Genet 12:191-194

Haaf T, Golub EI, Reddy G, Radding CM, Ward DC (1995) Nuclear foci of mammalian Rad51 recombination protein in somatic cells after DNA damage and its localization in synaptonemal complexes. Proc Natl Acad Sci U S A 92:2298-2302

Haber JE (1995) *In vivo* biochemistry: physical monitoring of recombination induced by site-specific endonucleases. Bioessays 17:609-620

Haber JE (2000) Lucky breaks: analysis of recombination in Saccharomyces. Mutat Res 451:53-69

Hakem R, de la Pompa JL, Sirard C, Mo R, Woo M, Hakem A, Wakeham A, Potter J, Reitmair A, Billia F, Firpo E, Hui CC, Roberts J, Rossant J, Mak TW (1996) The tumor suppressor gene Brca1 is required for embryonic cellular proliferation in the mouse. Cell 85:1009-1023

Haraguchi T (2002) Live cell imaging: approaches for studying protein dynamics in living cells. Cell Struct Funct 27:333-334

Hauptner A, Dietzel S, Drexler GA, Reichart P, Krucken R, Cremer T, Friedl AA, Dollinger G (2004) Microirradiation of cells with energetic heavy ions. Radiat Environ Biophys 42:237-245

Hopfner KP, Craig L, Moncalian G, Zinkel RA, Usui T, Owen BA, Karcher A, Henderson B, Bodmer JL, McMurray CT, Carney JP, Petrini JH, Tainer JA (2002) The Rad50 zinc-hook is a structure joining Mre11 complexes in DNA recombination and repair. Nature 418:562-566

Houtsmuller AB (2005) Fluorescence recovery after photobleaching: application to nuclear proteins. Adv Biochem Eng Biotechnol 95:177-199

Houtsmuller AB, Vermeulen W (2001) Macromolecular dynamics in living cell nuclei revealed by fluorescence redistribution after photobleaching. Histochem Cell Biol 115:13-21

Hyde H, Davies AA, Benson FE, West SC (1994) Resolution of recombination intermediates by a mammalian activity functionally analogous to Escherichia coli RuvC resolvase. J Biol Chem 269:5202-5209

Jakob B, Scholz M, Taucher-Scholz G (2003) Biological imaging of heavy charged-particle tracks. Radiat Res 159:676-684

Jasin M (1996) Genetic manipulation of genomes with rare-cutting endonucleases. Trends Genet 12:224-228

Johnson RD, Liu N, Jasin M (1999) Mammalian XRCC2 promotes the repair of DNA double-strand breaks by homologous recombination. Nature 401:397-399

Kanaar R, Hoeijmakers JH, van Gent DC (1998) Molecular mechanisms of DNA double-strand break repair. Trends Cell Biol 8:483-489

Kannouche P, Broughton BC, Volker M, Hanaoka F, Mullenders LH, Lehmann AR (2001) Domain structure, localization, and function of DNA polymerase eta, defective in xeroderma pigmentosum variant cells. Genes Dev 15:158-172

Kawamoto T, Araki K, Sonoda E, Yamashita YM, Harada K, Kikuchi K, Masutani C, Hanaoka F, Nozaki K, Hashimoto N, Takeda S (2005) Dual roles for DNA polymerase eta in homologous DNA recombination and translesion DNA synthesis. Mol Cell 20:793-799

Kim JS, Krasieva TB, Kurumizaka H, Chen DJ, Taylor AM, Yokomori K (2005) Independent and sequential recruitment of NHEJ and HR factors to DNA damage sites in mammalian cells. J Cell Biol 170:341-347

Kim JS, Krasieva TB, LaMorte V, Taylor AM, Yokomori K (2002) Specific recruitment of human cohesin to laser-induced DNA damage. J Biol Chem 277:45149-45153

Kojic M, Kostrub CF, Buchman AR, Holloman WK (2002) BRCA2 homolog required for proficiency in DNA repair, recombination, and genome stability in Ustilago maydis. Mol Cell 10:683-691

Kojic M, Yang H, Kostrub CF, Pavletich NP, Holloman WK (2003) The BRCA2-interacting protein DSS1 is vital for DNA repair, recombination, and genome stability in Ustilago maydis. Mol Cell 12:1043-1049

Kojic M, Zhou Q, Lisby M, Holloman WK (2005) Brh2-Dss1 interplay enables properly controlled recombination in Ustilago maydis. Mol Cell Biol 25:2547-2557

Krogh BO, Symington LS (2004) Recombination proteins in yeast. Annu Rev Genet 38:233-271

Kurumizaka H, Ikawa S, Nakada M, Enomoto R, Kagawa W, Kinebuchi T, Yamazoe M, Yokoyama S, Shibata T (2002) Homologous pairing and ring and filament structure formation activities of the human Xrcc2*Rad51D complex. J Biol Chem 277:14315-14320

Lee SE, Moore JK, Holmes A, Umezu K, Kolodner RD, Haber JE (1998) Saccharomyces Ku70, mre11/rad50 and RPA proteins regulate adaptation to G2/M arrest after DNA damage. Cell 94:399-409

Lim DS, Hasty P (1996) A mutation in mouse rad51 results in an early embryonic lethal that is suppressed by a mutation in p53. Mol Cell Biol 16:7133-7143

Lio YC, Mazin AV, Kowalczykowski SC, Chen DJ (2003) Complex formation by the human Rad51B and Rad51C DNA repair proteins and their activities *in vitro*. J Biol Chem 278:2469-2478

Lio YC, Schild D, Brenneman MA, Redpath JL, Chen DJ (2004) Human Rad51C deficiency destabilizes XRCC3, impairs recombination, and radiosensitizes S/G2-phase cells. J Biol Chem 279:42313-42320

Lippincott-Schwartz J, Patterson GH (2003) Development and use of fluorescent protein markers in living cells. Science 300:87-91

Lisby M, Barlow JH, Burgess RC, Rothstein R (2004) Choreography of the DNA damage response: spatiotemporal relationships among checkpoint and repair proteins. Cell 118:699-713

Lisby M, Rothstein R, Mortensen UH (2001) Rad52 forms DNA repair and recombination centers during S phase. Proc Natl Acad Sci U S A 98:8276-8282

Liu CY, Flesken-Nikitin A, Li S, Zeng Y, Lee WH (1996) Inactivation of the mouse Brca1 gene leads to failure in the morphogenesis of the egg cylinder in early postimplantation development. Genes Dev 10:1835-1843

Liu N, Schild D, Thelen MP, Thompson LH (2002) Involvement of Rad51C in two distinct protein complexes of Rad51 paralogs in human cells. Nucleic Acids Res 30:1009-1015

Liu Y, Masson JY, Shah R, O'Regan P, West SC (2004) RAD51C is required for Holliday junction processing in mammalian cells. Science 303:243-246

Ludwig T, Chapman DL, Papaioannou VE, Efstratiadis A (1997) Targeted mutations of breast cancer susceptibility gene homologs in mice: lethal phenotypes of Brca1, Brca2, Brca1/Brca2, Brca1/p53, and Brca2/p53 nullizygous embryos. Genes Dev 11:1226-1241

Lukas C, Bartek J, Lukas J (2005) Imaging of protein movement induced by chromosomal breakage: tiny 'local' lesions pose great 'global' challenges. Chromosoma 114:146-154

Lukas C, Falck J, Bartkova J, Bartek J, Lukas J (2003) Distinct spatiotemporal dynamics of mammalian checkpoint regulators induced by DNA damage. Nat Cell Biol 5:255-260

Lukas C, Melander F, Stucki M, Falck J, Bekker-Jensen S, Goldberg M, Lerenthal Y, Jackson SP, Bartek J, Lukas J (2004) Mdc1 couples DNA double-strand break recognition by Nbs1 with its H2AX-dependent chromatin retention. Embo J 23:2674-2683

Luo G, Yao MS, Bender CF, Mills M, Bladl AR, Bradley A, Petrini JH (1999) Disruption of mRad50 causes embryonic stem cell lethality, abnormal embryonic

development, and sensitivity to ionizing radiation. Proc Natl Acad Sci U S A 96:7376-7381

Marmorstein LY, Ouchi T, Aaronson SA (1998) The BRCA2 gene product functionally interacts with p53 and RAD51. Proc Natl Acad Sci U S A 95:13869-13874

Maser RS, Monsen KJ, Nelms BE, Petrini JH (1997) hMre11 and hRad50 nuclear foci are induced during the normal cellular response to DNA double-strand breaks. Mol Cell Biol 17:6087-6096

Masson JY, Stasiak AZ, Stasiak A, Benson FE, West SC (2001a) Complex formation by the human RAD51C and XRCC3 recombination repair proteins. Proc Natl Acad Sci U S A 98:8440-8446

Masson JY, Tarsounas MC, Stasiak AZ, Stasiak A, Shah R, McIlwraith MJ, Benson FE, West SC (2001b) Identification and purification of two distinct complexes containing the five RAD51 paralogs. Genes Dev 15:3296-3307

Mazin AV, Alexeev AA, Kowalczykowski SC (2003) A novel function of Rad54 protein. Stabilization of the Rad51 nucleoprotein filament. J Biol Chem 278:14029-14036

Mazin AV, Bornarth CJ, Solinger JA, Heyer WD, Kowalczykowski SC (2000) Rad54 protein is targeted to pairing loci by the Rad51 nucleoprotein filament. Mol Cell 6:583-592

McLlwraith MJ, Vaisman A, Liu Y, Fanning E, Woodgate R, West SC (2005) Human DNA polymerase eta promotes DNA synthesis from strand invasion intermediates of homologous recombination. Mol Cell 20:783-792

Meldrum RA, Botchway SW, Wharton CW, Hirst GJ (2003) Nanoscale spatial induction of ultraviolet photoproducts in cellular DNA by three-photon near-infrared absorption. EMBO Rep 4:1144-1149

Michel B, Grompone G, Flores MJ, Bidnenko V (2004) Multiple pathways process stalled replication forks. Proc Natl Acad Sci U S A 101:12783-12788

Miller KA, Yoshikawa DM, McConnell IR, Clark R, Schild D, Albala JS (2002) RAD51C interacts with RAD51B and is central to a larger protein complex *in vivo* exclusive of RAD51. J Biol Chem 277:8406-8411

Mills KD, Ferguson DO, Essers J, Eckersdorff M, Kanaar R, Alt FW (2004) Rad54 and DNA Ligase IV cooperate to maintain mammalian chromatid stability. Genes Dev 18:1283-1292

Mirzoeva OK, Petrini JH (2003) DNA replication-dependent nuclear dynamics of the Mre11 complex. Mol Cancer Res 1:207-218

Moreno-Herrero F, de Jager M, Dekker NH, Kanaar R, Wyman C, Dekker C (2005) Mesoscale conformational changes in the DNA-repair complex Rad50/Mre11/Nbs1 upon binding DNA. Nature 437:440-443

Moynahan ME, Pierce AJ, Jasin M (2001) BRCA2 is required for homology-directed repair of chromosomal breaks. Mol Cell 7:263-272

Nakata T, Terada S, Hirokawa N (1998) Visualization of the dynamics of synaptic vesicle and plasma membrane proteins in living axons. J Cell Biol 140:659-674

Nelms BE, Maser RS, MacKay JF, Lagally MG, Petrini JH (1998) In situ visualization of DNA double-strand break repair in human fibroblasts. Science 280:590-592

New JH, Sugiyama T, Zaitseva E, Kowalczykowski SC (1998) Rad52 protein stimulates DNA strand exchange by Rad51 and replication protein A. Nature 391:407-410

Paull TT, Gellert M (1998) The 3' to 5' exonuclease activity of Mre 11 facilitates repair of DNA double-strand breaks. Mol Cell 1:969-979

Paull TT, Gellert M (1999) Nbs1 potentiates ATP-driven DNA unwinding and endonuclease cleavage by the Mre11/Rad50 complex. Genes Dev 13:1276-1288

Paull TT, Rogakou EP, Yamazaki V, Kirchgessner CU, Gellert M, Bonner WM (2000) A critical role for histone H2AX in recruitment of repair factors to nuclear foci after DNA damage. Curr Biol 10:886-895

Pellegrini L, Yu DS, Lo T, Anand S, Lee M, Blundell TL, Venkitaraman AR (2002) Insights into DNA recombination from the structure of a RAD51-BRCA2 complex. Nature 420:287-293

Petukhova G, Stratton S, Sung P (1998) Catalysis of homologous DNA pairing by yeast Rad51 and Rad54 proteins. Nature 393:91-94

Petukhova G, Van Komen S, Vergano S, Klein H, Sung P (1999) Yeast Rad54 promotes Rad51-dependent homologous DNA pairing via ATP hydrolysis-driven change in DNA double helix conformation. J Biol Chem 274:29453-29462

Pierce AJ, Johnson RD, Thompson LH, Jasin M (1999) XRCC3 promotes homology-directed repair of DNA damage in mammalian cells. Genes Dev 13:2633-2638

Pittman DL, Schimenti JC (2000) Midgestation lethality in mice deficient for the RecA-related gene, Rad51d/Rad51l3. Genesis 26:167-173

Porteus MH, Carroll D (2005) Gene targeting using zinc finger nucleases. Nat Biotechnol 23:967-973

Prakash S, Johnson RE, Prakash L (2005) Eukaryotic translesion synthesis DNA polymerases: specificity of structure and function. Annu Rev Biochem 74:317-353

Raderschall E, Golub EI, Haaf T (1999) Nuclear foci of mammalian recombination proteins are located at single-stranded DNA regions formed after DNA damage. Proc Natl Acad Sci U S A 96:1921-1926

Raschle M, Van Komen S, Chi P, Ellenberger T, Sung P (2004) Multiple interactions with the Rad51 recombinase govern the homologous recombination function of Rad54. J Biol Chem 279:51973-51980

Rattray AJ, Strathern JN (2005) Homologous recombination is promoted by translesion polymerase poleta. Mol Cell 20:658-659

Richardson C, Elliott B, Jasin M (1999) Chromosomal double-strand breaks introduced in mammalian cells by expression of I-Sce I endonuclease. Methods Mol Biol 113:453-463

Rijkers T, Van Den Ouweland J, Morolli B, Rolink AG, Baarends WM, Van Sloun PP, Lohman PH, Pastink A (1998) Targeted inactivation of mouse RAD52 reduces homologous recombination but not resistance to ionizing radiation. Mol Cell Biol 18:6423-6429

Ristic D, Wyman C, Paulusma C, Kanaar R (2001) The architecture of the human Rad54-DNA complex provides evidence for protein translocation along DNA. Proc Natl Acad Sci U S A 98:8454-8460

Rogakou EP, Boon C, Redon C, Bonner WM (1999) Megabase chromatin domains involved in DNA double-strand breaks *in vivo*. J Cell Biol 146:905-916

Rouet P, Smih F, Jasin M (1994a) Expression of a site-specific endonuclease stimulates homologous recombination in mammalian cells. Proc Natl Acad Sci U S A 91:6064-6068

Rouet P, Smih F, Jasin M (1994b) Introduction of double-strand breaks into the genome of mouse cells by expression of a rare-cutting endonuclease. Mol Cell Biol 14:8096-8106

San Filippo J, Chi P, Sehorn MG, Etchin J, Krejci L, Sung P (2006) Recombination mediator and RAD51 targeting activities of a human BRCA2 polypeptide. J Biol Chem

Schild D, Lio YC, Collins DW, Tsomondo T, Chen DJ (2000) Evidence for simultaneous protein interactions between human Rad51 paralogs. J Biol Chem 275:16443-16449

Scully R, Chen J, Plug A, Xiao Y, Weaver D, Feunteun J, Ashley T, Livingston DM (1997) Association of BRCA1 with Rad51 in mitotic and meiotic cells. Cell 88:265-275

Scully R, Puget N, Vlasakova K (2000) DNA polymerase stalling, sister chromatid recombination and the BRCA genes. Oncogene 19:6176-6183

Sedelnikova OA, Pilch DR, Redon C, Bonner WM (2003) Histone H2AX in DNA damage and repair. Cancer Biol Ther 2:233-235

Sharan SK, Morimatsu M, Albrecht U, Lim DS, Regel E, Dinh C, Sands A, Eichele G, Hasty P, Bradley A (1997) Embryonic lethality and radiation hypersensitivity mediated by Rad51 in mice lacking Brca2. Nature 386:804-810

Shiloh Y (2003) ATM and related protein kinases: safeguarding genome integrity. Nat Rev Cancer 3:155-168

Shinohara A, Shinohara M, Ohta T, Matsuda S, Ogawa T (1998) Rad52 forms ring structures and co-operates with RPA in single-strand DNA annealing. Genes Cells 3:145-156

Shivji MK, Venkitaraman AR (2004) DNA recombination, chromosomal stability and carcinogenesis: insights into the role of BRCA2. DNA Repair (Amst) 3:835-843

Shroff R, Arbel-Eden A, Pilch D, Ira G, Bonner WM, Petrini JH, Haber JE, Lichten M (2004) Distribution and dynamics of chromatin modification induced by a defined DNA double-strand break. Curr Biol 14:1703-1711

Shu Z, Smith S, Wang L, Rice MC, Kmiec EB (1999) Disruption of muREC2/RAD51L1 in mice results in early embryonic lethality which can Be partially rescued in a p53(-/-) background. Mol Cell Biol 19:8686-8693

Sigurdsson S, Van Komen S, Bussen W, Schild D, Albala JS, Sung P (2001) Mediator function of the human Rad51B-Rad51C complex in Rad51/RPA-catalyzed DNA strand exchange. Genes Dev 15:3308-3318

Smiraldo PG, Gruver AM, Osborn JC, Pittman DL (2005) Extensive chromosomal instability in Rad51d-deficient mouse cells. Cancer Res 65:2089-2096

Solinger JA, Heyer WD (2001) Rad54 protein stimulates the postsynaptic phase of Rad51 protein-mediated DNA strand exchange. Proc Natl Acad Sci U S A 98:8447-8453

Solinger JA, Kiianitsa K, Heyer WD (2002) Rad54, a Swi2/Snf2-like recombinational repair protein, disassembles Rad51:dsDNA filaments. Mol Cell 10:1175-1188

Solomon DA, Cardoso MC, Knudsen ES (2004) Dynamic targeting of the replication machinery to sites of DNA damage. J Cell Biol 166:455-463.

Solovjeva L, Svetlova M, Sasina L, Tanaka K, Saijo M, Nazarov I, Bradbury M, Tomilin N (2005) High mobility of flap endonuclease 1 and DNA polymerase eta associated with replication foci in mammalian S-phase nucleus. Mol Biol Cell 16:2518-2528

Song B, Sung P (2000) Functional interactions among yeast Rad51 recombinase, Rad52 mediator, and replication protein A in DNA strand exchange. J Biol Chem 275:15895-15904

Sonoda E, Sasaki MS, Buerstedde JM, Bezzubova O, Shinohara A, Ogawa H, Takata M, Yamaguchi-Iwai Y, Takeda S (1998) Rad51-deficient vertebrate cells accumulate chromosomal breaks prior to cell death. Embo J 17:598-608

Sporbert A, Gahl A, Ankerhold R, Leonhardt H, Cardoso MC (2002) DNA polymerase clamp shows little turnover at established replication sites but sequential de novo assembly at adjacent origin clusters. Mol Cell 10:1355-1365.

Sprague BL, McNally JG (2005) FRAP analysis of binding: proper and fitting. Trends Cell Biol 15:84-91

Stewart GS, Maser RS, Stankovic T, Bressan DA, Kaplan MI, Jaspers NG, Raams A, Byrd PJ, Petrini JH, Taylor AM (1999) The DNA double-strand break repair gene hMRE11 is mutated in individuals with an ataxia-telangiectasia-like disorder. Cell 99:577-587

Sugawara N, Wang X, Haber JE (2003) *In vivo* roles of Rad52, Rad54, and Rad55 proteins in Rad51-mediated recombination. Mol Cell 12:209-219

Sugiyama T, Kowalczykowski SC (2002) Rad52 protein associates with replication protein A (RPA)-single-stranded DNA to accelerate Rad51-mediated displacement of RPA and presynaptic complex formation. J Biol Chem 277:31663-31672

Sugiyama T, New JH, Kowalczykowski SC (1998) DNA annealing by RAD52 protein is stimulated by specific interaction with the complex of replication protein A and single-stranded DNA. Proc Natl Acad Sci U S A 95:6049-6054

Sugiyama T, Zaitseva EM, Kowalczykowski SC (1997) A single-stranded DNA-binding protein is needed for efficient presynaptic complex formation by the Saccharomyces cerevisiae Rad51 protein. J Biol Chem 272:7940-7945

Sung P (1997) Function of yeast Rad52 protein as a mediator between replication protein A and the Rad51 recombinase. J Biol Chem 272:28194-28197

Suzuki A, de la Pompa JL, Hakem R, Elia A, Yoshida R, Mo R, Nishina H, Chuang T, Wakeham A, Itie A, Koo W, Billia P, Ho A, Fukumoto M, Hui CC, Mak TW (1997) Brca2 is required for embryonic cellular proliferation in the mouse. Genes Dev 11:1242-1252

Swagemakers SM, Essers J, de Wit J, Hoeijmakers JH, Kanaar R (1998) The human RAD54 recombinational DNA repair protein is a double-stranded DNA-dependent ATPase. J Biol Chem 273:28292-28297

Symington LS (2002) Role of RAD52 epistasis group genes in homologous recombination and double-strand break repair. Microbiol Mol Biol Rev 66:630-670, table of contents

Takata M, Sasaki MS, Sonoda E, Fukushima T, Morrison C, Albala JS, Swagemakers SM, Kanaar R, Thompson LH, Takeda S (2000) The Rad51 paralog Rad51B promotes homologous recombinational repair. Mol Cell Biol 20:6476-6482

Takata M, Sasaki MS, Tachiiri S, Fukushima T, Sonoda E, Schild D, Thompson LH, Takeda S (2001) Chromosome instability and defective recombinational repair in knockout mutants of the five Rad51 paralogs. Mol Cell Biol 21:2858-2866

Tan TL, Essers J, Citterio E, Swagemakers SM, de Wit J, Benson FE, Hoeijmakers JH, Kanaar R (1999) Mouse Rad54 affects DNA conformation and DNA-damage-induced Rad51 foci formation. Curr Biol 9:325-328

Tashiro S, Kotomura N, Shinohara A, Tanaka K, Ueda K, Kamada N (1996) S phase specific formation of the human Rad51 protein nuclear foci in lymphocytes. Oncogene 12:2165-2170

Tashiro S, Walter J, Shinohara A, Kamada N, Cremer T (2000) Rad51 accumulation at sites of DNA damage and in postreplicative chromatin. J Cell Biol 150:283-291

Taylor AM, Groom A, Byrd PJ (2004) Ataxia-telangiectasia-like disorder (ATLD)-its clinical presentation and molecular basis. DNA Repair (Amst) 3:1219-1225

Thacker J (2005) The RAD51 gene family, genetic instability and cancer. Cancer Lett 219:125-135

Thompson LH, Schild D (2001) Homologous recombinational repair of DNA ensures mammalian chromosome stability. Mutat Res 477:131-153

Tsuzuki T, Fujii Y, Sakumi K, Tominaga Y, Nakao K, Sekiguchi M, Matsushiro A, Yoshimura Y, MoritaT (1996) Targeted disruption of the Rad51 gene leads to lethality in embryonic mice. Proc Natl Acad Sci U S A 93:6236-6240

Tutt A, Gabriel A, Bertwistle D, Connor F, Paterson H, Peacock J, Ross G, Ashworth A (1999) Absence of Brca2 causes genome instability by chromosome breakage and loss associated with centrosome amplification. Curr Biol 9:1107-1110

Van Komen S, Petukhova G, Sigurdsson S, Stratton S, Sung P (2000) Superhelicity-driven homologous DNA pairing by yeast recombination factors Rad51 and Rad54. Mol Cell 6:563-572

Van Komen S, Petukhova G, Sigurdsson S, Sung P (2002) Functional cross-talk among Rad51, Rad54, and replication protein A in heteroduplex DNA joint formation. J Biol Chem 277:43578-43587

van Veelen LR, Cervelli T, van de Rakt MW, Theil AF, Essers J, Kanaar R (2005a) Analysis of ionizing radiation-induced foci of DNA damage repair proteins. Mutat Res 574:22-33

van Veelen LR, Essers J, van de Rakt MW, Odijk H, Pastink A, Zdzienicka MZ, Paulusma CC, Kanaar R (2005b) Ionizing radiation-induced foci formation of mammalian Rad51 and Rad54 depends on the Rad51 paralogs, but not on Rad52. Mutat Res 574:34-49

Varon R, Vissinga C, Platzer M, Cerosaletti KM, Chrzanowska KH, Saar K, Beckmann G, Seemanova E, Cooper PR, Nowak NJ, Stumm M, Weemaes CM, Gatti RA, Wilson RK, Digweed M, Rosenthal A, Sperling K, Concannon P, Reis A (1998) Nibrin, a novel DNA double-strand break repair protein, is mutated in Nijmegen breakage syndrome. Cell 93:467-476

Venkitaraman AR (2002) Cancer susceptibility and the functions of BRCA1 and BRCA2. Cell 108:171-182

Waldman AS, Liskay RM (1988) Resolution of synthetic Holliday structures by an extract of human cells. Nucleic Acids Res 16:10249-10266

Walter J, Cremer T, Miyagawa K, Tashiro S (2003) A new system for laser-UVA-microirradiation of living cells. J Microsc 209:71-75

Wesoly J, Agarwal S, Sigurdsson S, Bussen W, Van Komen S, Qin J, van Steeg H, van Benthem J, Wassenaar E, Baarends WM, Ghazvini M, Tafel AA, Heath H,

Galjart N, Essers J, Grootegoed JA, Arnheim N, Bezzubova O, Buerstedde JM, Sung P, Kanaar R (2006) Differential contributions of mammalian Rad54 paralogs to recombination, DNA damage repair, and meiosis. Mol Cell Biol 26:976-989

West SC (1997) Processing of recombination intermediates by the RuvABC proteins. Annu Rev Genet 31:213-244

White J, Stelzer E (1999) Photobleaching GFP reveals protein dynamics inside live cells. Trends Cell Biol 9:61-65.

Wiese C, Collins DW, Albala JS, Thompson LH, Kronenberg A, Schild D (2002) Interactions involving the Rad51 paralogs Rad51C and XRCC3 in human cells. Nucleic Acids Res 30:1001-1008

Wiltzius JJ, Hohl M, Fleming JC, Petrini JH (2005) The Rad50 hook domain is a critical determinant of Mre11 complex functions. Nat Struct Mol Biol 12:403-407

Wong AK, Pero R, Ormonde PA, Tavtigian SV, Bartel PL (1997) RAD51 interacts with the evolutionarily conserved BRC motifs in the human breast cancer susceptibility gene brca2. J Biol Chem 272:31941-31944

Xiao Y, Weaver DT (1997) Conditional gene targeted deletion by Cre recombinase demonstrates the requirement for the double-strand break repair Mre11 protein in murine embryonic stem cells. Nucleic Acids Res 25:2985-2991

Yamada NA, Hinz JM, Kopf VL, Segalle KD, Thompson LH (2004) XRCC3 ATPase activity is required for normal XRCC3-Rad51C complex dynamics and homologous recombination. J Biol Chem 279:23250-23254

Yamaguchi-Iwai Y, Sonoda E, Buerstedde JM, Bezzubova O, Morrison C, Takata M, Shinohara A, Takeda S (1998) Homologous recombination, but not DNA repair, is reduced in vertebrate cells deficient in RAD52. Mol Cell Biol 18:6430-6435

Yamaguchi-Iwai Y, Sonoda E, Sasaki MS, Morrison C, Haraguchi T, Hiraoka Y, Yamashita YM, Yagi T, Takata M, Price C, Kakazu N, Takeda S (1999) Mre11 is essential for the maintenance of chromosomal DNA in vertebrate cells. Embo J 18:6619-6629

Yang H, Li Q, Fan J, Holloman WK, Pavletich NP (2005) The BRCA2 homologue Brh2 nucleates RAD51 filament formation at a dsDNA-ssDNA junction. Nature 433:653-657

Yokoyama H, Kurumizaka H, Ikawa S, Yokoyama S, Shibata T (2003) Holliday junction binding activity of the human Rad51B protein. J Biol Chem 278:2767-2772

Yokoyama H, Sarai N, Kagawa W, Enomoto R, Shibata T, Kurumizaka H, Yokoyama S (2004) Preferential binding to branched DNA strands and strand-annealing activity of the human Rad51B, Rad51C, Rad51D and Xrcc2 protein complex. Nucleic Acids Res 32:2556-2565

Yonetani Y, Hochegger H, Sonoda E, Shinya S, Yoshikawa H, Takeda S, Yamazoe M (2005) Differential and collaborative actions of Rad51 paralog proteins in cellular response to DNA damage. Nucleic Acids Res 33:4544-4552

Yu DS, Sonoda E, Takeda S, Huang CL, Pellegrini L, Blundell TL, Venkitaraman AR (2003) Dynamic control of Rad51 recombinase by self-association and interaction with BRCA2. Mol Cell 12:1029-1041

Yu VP, Koehler M, Steinlein C, Schmid M, Hanakahi LA, van Gool AJ, West SC, Venkitaraman AR (2000) Gross chromosomal rearrangements and genetic exchange between nonhomologous chromosomes following BRCA2 inactivation. Genes Dev 14:1400-1406

Yuan SS, Lee SY, Chen G, Song M, Tomlinson GE, Lee EY (1999) BRCA2 is required for ionizing radiation-induced assembly of Rad51 complex *in vivo*. Cancer Res 59:3547-3551

Zhu J, Petersen S, Tessarollo L, Nussenzweig A (2001) Targeted disruption of the Nijmegen breakage syndrome gene NBS1 leads to early embryonic lethality in mice. Curr Biol 11:105-109

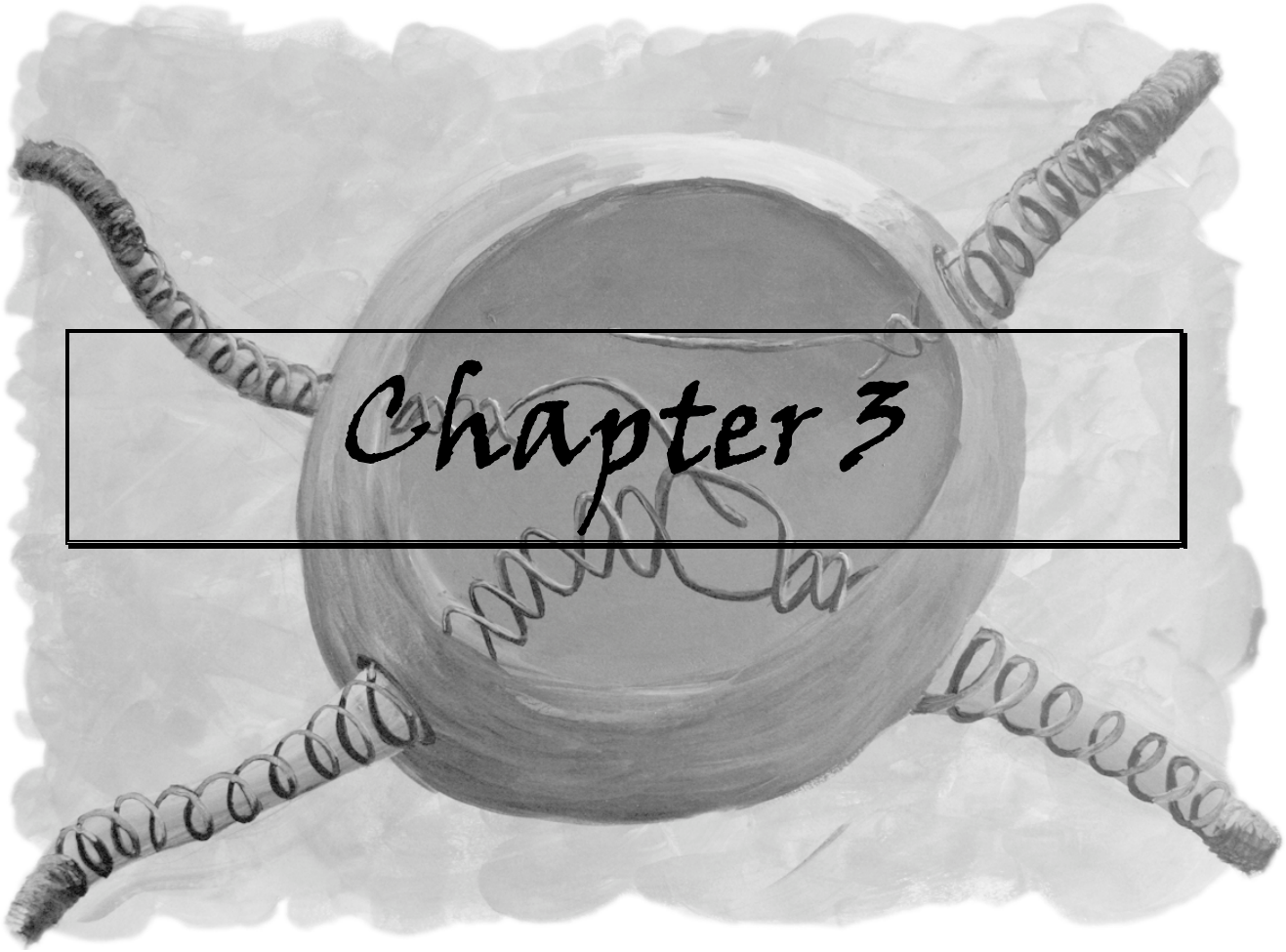

Chapter 3

Analysis of mouse fluorescence-tagged Rad54 expression *in vivo*

Manuscript in preparation

Green is the prime color of the world, and that from which its loveliness arises.

~ Pedro Calderon de la Barca

Analysis of mouse fluorescence-tagged Rad54 expression *in vivo*

Sheba Agarwal [1], Rudolph W. Hendriks [3], Javier Lopez [1], Marianne Peeters [1], Alex Maas [1], Roland Kanaar [1, 2], Jeroen Essers [1, 2]

[1] Department of Cell Biology and Genetics, [2] Department of Radiation Oncology, [3] Department of Immunology,
Erasmus Medical Center, Rotterdam, The Netherlands

Abstract

Rad54 is an important participant in homologous recombination, a high fidelity pathway of double-strand break (DSB) repair. The role of Rad54 in the precise repair of DSBs has been elucidated via the characterization of Rad54 deficient cells and mice. To further analyze the behavior of Rad54 in cells and animals, we generated a mouse model carrying a Rad54-GFP knock-in allele. The expressed fusion protein is biologically active, and thus the Rad54-GFP knock-in mouse provides a valid and useful tool to analyze spatial and temporal expression of Rad54. We analyzed the cellular distribution of Rad54 during mouse development as well as in a specific subset of cells in the adult. We have found that Rad54-GFP is expressed in 3.5, 8.5 and 13.5 days post coitum embryos. At the cellular level, Rad54-GFP is expressed in proerythroblasts until they stop proliferating. Mouse embryonic fibroblasts, dermal fibroblasts and chondrocytes only show expression in a small subpopulation of cells. In adult mice, we focused on the hematopoeitic system, where we found that Rad54-GFP expression was restricted to the proliferating stages of B and T cell development. These data show that Rad54-GFP is present in cycling cells.

Introduction

An important metabolic process that involves DNA is the repair of damage that is constantly induced by exogenous or endogenous sources [1]. In order to ensure proper DNA replication, transcription and cell survival, specialized repair pathways are used to deal with specific types of damage and rid DNA of these injuries. The double-strand break (DSB) is one of the most detrimental of DNA injuries as the continuity of both strands of DNA is affected. If not repaired properly and in a timely fashion, DSBs can lead to genomic rearrangements that can result in development of cancer [2-4].

Two major pathways are involved in the repair of DSBs: homologous recombination and nonhomologous DNA end-joining. Homologous recombination is a

high-fidelity DSB repair pathway that ensures the integrity of genetic information by using an undamaged, homologous DNA molecule, usually the sister chromatid, to repair the break [5]. The central proteins of homologous recombination and the corresponding core mechanism is conserved from yeast to mammals [6]. A DSB in the genome is detected and processed to single-stranded 3' DNA tails, the nucleation point for recombination factors. Rad51, an essential player in recombination, assembles on 3' tails to produce a nucleoprotein filament, which then mediates the critical step of homologous pairing between the broken DNA molecule and the intact template. Rad51 is assisted at various stages of recombination by mediator and accessory proteins [7], one of which is Rad54. Nonhomologous end-joining involves the simple religation of DNA ends without the need for a template. This process is not necessarily error-free [5]. DSB ends are bound and hypothetically aligned by KU70/80, thus allowing for ligation by the DNA ligase IV-XRCC4 complex [8]. The need for two mechanistically different pathways (and their corresponding proteins) for the healing of DSBs has been under investigation for a number of years [9-11]. Several theories that have been put forward to distinguish the spatial and temporal involvement of recombination and end-joining in mammalian development, and their possible overlapping roles [12].

Clues to answering this question have come from phenotypes of knockout mice. Unchallenged *Rad54*$^{-/-}$ mice display no gross abnormalities and have a normal life expectancy [13], thus making them an excellent model to study the relevance of DNA damaged-induced recombination. While *Rad54*$^{-/-}$ adult mice do not seem to be affected by ionizing radiation, *Rad54* knockout embryos and embryonic stem (ES) cells show a hypersensitivity [13], indicating a possible role of homologous recombination in early development. The involvement of recombination in DSB repair lessens as the animal matures. On the other hand, mice bearing mutations in DNA-PK or Ku80, two components of end joining, display ionizing radiation sensitivity, designating end joining as the dominant pathway of radiation-induced DSB repair in adults [10]. In addition, mice defective in both homologous recombination and end joining display higher level of irradiation sensitivity than single mutants [9, 10]. Therefore, not only is the choice of DSB repair pathway temporally regulated during development, it also has overlapping functions which enables the possibility of one repair pathway taking over the function of the other when the latter is deficient.

As has been suggested by double knockout mouse studies, the dominance of end joining in the adult mouse results in a global resistance to ionizing radiation in the

Rad54$^{-/-}$ mouse [12]. However, the analysis of Rad54 expression in different mouse tissues, as investigated by Northern blot analysis, suggests that tissue-specific homologous recombination may still exist in the adult mouse [14]. Specifically, while hardly any transcript was detected in most tissues, Rad54 transcripts are present in the thymus and spleen, which are organs of lymphoid development [14]. This implies one of two possibilities. First, the presence of Rad54 in these organs suggests that it might have a function in V(D)J recombination. Second, since both these organs have cells that rapidly divide, it is conceivable that Rad54 is expressed in highly proliferating cells. Indeed, cycling cells present the opportunity for recombination since the sister chromatid is available as a template for repair to occur. Rad54 expression has also been documented in the testis, specifically in spermatocytes in meiotic prophase, suggesting a role of Rad54 in meiotic recombination [15, 16]. Consequently, the expression of Rad54 in the adult animal is spatially regulated, indicating an active but tissue-specific role of Rad54 dependent recombination in the adult animal.

The function of Rad54 *in vivo* has been primarily deduced from cells and animals that lack the protein. Hence it is equally important to track the protein itself in cells and animals, preferably under conditions compatible with life. Using a knock-in approach, we have constructed mouse ES cells that express functional GFP-tagged Rad54 from the endogenous genomic locus. Mice generated from these cells allowed visualization and characterization of the Rad54 protein in different cell types and tissues, and through the stages of mouse development.

Materials and Methods

Generation of Rad54-GFP knock-in cells and mice

A *Rad54-GFP* knock-in construct was made by fusing genomic *Rad54* sequences containing exons I – III in frame to the cDNA consisting of exon IV to XVIII of *Rad54*. The coding sequence of eGFP (Clontech) was inserted at the C-terminus 3' site of *Rad54*, followed by a puromycin selectable marker (Figure 1A). The construct was made such that the homologous integration of the construct in the genome results in the production of GFP-tagged Rad54 from the endogenous promoter. After linearization, the *Rad54-GFP* construct was purified using electro-elution, phenol extraction and ethanol precipitation. The construct was electroporated into ES cells using a 2 mm cuvette (BTX), at 117 V, 1200 μF and for 10 ms in an ECM 830 electroporator (BTX). After puromycin selection (1 μg/ml), clones were isolated and homologous integration of the

construct was verified. The genomic DNA was analyzed by DNA blot analysis using StuI as a diagnostic site, and a probe that recognized exons VII and VIII. The production of GFP tagged Rad54 was confirmed by immunoblot analysis using whole cell extracts from correctly targeted clones which were analyzed with anti-GFP (mouse monoclonal, Roche Applied Science) and anti-Rad54 [13]. DNA damage sensitivities of ES cells were performed using clonogenic survival assay as described [13]. ES cells that contained the correctly targeted event were injected into blastocysts. Male chimeric mice were crossed with females to obtain *Rad54*$^{GFP/+}$ mice, which were then intercrossed to obtain *Rad54*$^{GFP/GFP}$ mice.

Isolation of embryos, proerythroblasts and MEFs

Timed pregnancies were obtained by crossing heterozygous *Rad54*$^{GFP/+}$ mice and the plugged females were sacrificed at a specified time point. Embryos were isolated and genotyped by PCR. 3.5, 8.5 and 13.5 days post coitum (dpc) embryos were collected, placed on glass cover slips and observed using a 40X objective using a Zeiss LSM510 confocal microscope.

To isolate proerythroblasts, timed pregnancies were sacrificed at 12.5 dpc. *Rad54*$^{+/+}$ and *Rad54*$^{GFP/GFP}$ embryos were obtained and their livers were isolated and washed in sterile PBS. After making a single cell suspension by pipetting the liver up and down, the cells were seeded in 24 well dishes in proerythroblast expansion medium for 24 hours. This medium serves to halt differentiation of the proerythroblasts and maintain them as rapidly cycling precursors [17].The presence of proerythroblasts was checked by electronic cell counter (CASY-1, Counter and Analyser system, Scharfe-System, Reutlingen, Germany). The cells were pelleted and fixed with 2% paraformaldehyde before being subjected to fluorescence-activated cell sorting/flow cytometry (FACS). In addition, to visualize individual cells, proerythroblasts were irradiated with 8 Gy ionizing radiation (using a ^{137}Cs source), attached to polylysine coated glass slides (Poly-prep slides, Sigma), fixed with 2% paraformaldehyde for 15 minutes and then mounted with DAPI/DAPCO/Vectashield (Vector Labs).

Rad54$^{+/+}$ and *Rad54*$^{GFP/GFP}$ mouse embryonic fibroblasts (MEFs) were isolated by removing the liver, heart and head of the 12.5 dpc embryo. The rest of the embryo was minced in PBS and plated in MEF medium (50% DMEM, 50% Ham's F10, 10% FCS, 1% pen/strep). After a few days, explants were observed to grow out from the tissue pieces, and the cells were passaged when the dish was full. In preparation for FACS, low

passage MEFs were trypsinized, washed and then fixed with 2% paraformaldehyde. MEFs were grown on glass slides for live cell imaging. Cells were also observed after being fixed, mounted, and sealed as mentioned above.

Analysis of Rad54-GFP in B- and T- cells

Six week old mice were sacrificed and femurs were cleaned of muscle and ligaments, and crushed. Thymus and bone marrow cell suspensions were prepared using a 100 μm cell strainer. In order to generate the cell populations of large cycling expanding pre B-cells, bone marrow samples were cultured in the presence of IL-7 (100U/ml) for a period of 5 days [18].

Total bone marrow and thymus cell suspensions were incubated with one of the following: (a) monoclonal antibodies specific for the B-cell surface markers B220, CD43 and IgM (Becton Dickinson), (b) various hematopoietic lineage markers (Ter 119, ER-MP20), or (c) markers that signify the individual stages of T cell development (CD4, CD8, CD3, CD25, CD44). After treatment with the antibodies, the cells were subjected to flow cytometry (Calibur, Becton Dickinson) and analyzed with CellQuest (Becton Dickinson) software.

Isolation of mouse ear chondrocytes and dermal fibroblasts

Adult *Rad54*$^{GFP/GFP}$ and *Rad54*$^{+/+}$ mice were sacrificed and the auricular cartilage was isolated from the inner ear of the mice. The tissues was sterilized with 70% ethanol and cut into small pieces with a scalpel. The tissue pieces were then treated overnight with 1.6 mg/ml of collagenase type II (Gibco/BRL, Carlsbad, CA) in chondrocyte medium (50% DMEM, 50% Ham's F10, 10% FCS, 1% pen/strep). Chondrocytes attach and expand over the period of a week. During this time period, the medium was changed every other day and cells were passaged when confluent. For analysis, cells were fixed with 2% (v/v) paraformaldehyde before flow cytometry. In addition, chondrocytes were grown on glass slides, fixed and mounted with DAPI/DAPCO/Vectashield.

For dermal fibroblasts, a small piece of tail of *Rad54*$^{GFP/GFP}$ and *Rad54*$^{+/+}$ adult mice was cut and the skin was isolated. The tissue was sterilized with 70% ethanol, cut into small pieces and treated with collagenase type II described as above. Cells were grown in fibroblast medium (50% DMEM, 50% Ham's F10, 10% FCS, 100 U/ml penicillin, 100 μg/ml streptomycin). Preparation of cells for analysis was carried out in the same way as with chondrocytes.

Visualization of Rad54-GFP in cells

Rad54$^{GFP/GFP}$ cells were visualized with a Zeiss LSM 510 microscope consisting of an Axiovert 100 inverted microscope, equipped with an Argon gas laser (visualizing Alexa 488, green). Images were taken with 63x oil immersion lens. Live cells grown on glass were observed by mounting the 24 mm circular glass coverslip on a microscope equipped with a live cell chamber. Images were analyzed in the Zeiss LSM image browser.

RT-PCR analysis

Total mRNA was purified from wild type cells using TRIzol Reagent (Invitrogen) according to manufacturer's protocol. cDNA was then made with SuperScriptII RNase H-reverse transcriptase (Invitrogen) after DNase I amplification grade (Invitrogen) treatment, also according to manufacturer's protocol. *Rad54* specific primers were designed to amplify a 108-bp product between the first and second exon. The forward and reverse primer sequences are 5' ACTGCTGGACTTGCGTTTCT 3' and 5' AGCTTAGCTCCCAGCCAGTT 3', respectively. RT-PCR was run for 30 cycles using 55 ^{o}C as annealing temperature. Primers were used to amplify the HPRT cDNA for a quantitative control of total cDNA.

Results

Generation and analysis of ES cells and mice carrying a Rad54^{GFP} *allele*

To study the cellular behavior and expression pattern of Rad54, mouse ES cells which express GFP-tagged wild type Rad54 from the endogenous locus were generated. A targeting knock-in construct consisting of exons IV to XVIII *Rad54* cDNA fused with the GFP gene sequence (Figure 1A), was electroporated into specific pathogen-free wild type ES cells. Puromycin-resistant clones, which were possible candidates for containing the homologously integrated knock-in construct, were picked and expanded. Clones were genotyped by DNA blot analysis, where a homologous targeting event by the *Rad54-GFP* knock-in construct results in the appearance of a 6.5 kb doublet. Due to limitation in resolution, an increase in intensity of the 6.5kb bands was observed compared to the other bands resulting from the Rad54 locus (Figure 1B). Therefore, a clone that gave the wild type, 9.0 kb band, as well as the 6.5 kb doublet was genotyped as *Rad54*$^{GFP/+}$. Proper

expression of Rad54 was also confirmed by immunoblot analysis. The targeted allele gives rise to a GFP fusion protein of 110 kDa, while the wild type allele gives an 85 kDa Rad54 band, which was observed in Figure 1C.

The functionality of the Rad54-GFP fusion protein was tested by carrying out clonal survival assays in response to DNA damage induction. While *Rad54*$^{-/-}$ cells are hypersensitive to increasing γ-irradiation dosage [13], *Rad54*$^{GFP/-}$ cells were found to be similarly sensitive as *Rad54*$^{+/-}$, showing wild type behavior of these cells in terms of DNA repair (Figure 1D). In addition, Rad54-GFP showed nuclear localization, and formed nuclear foci in response to ionizing radiation (Figure 1E). This behavior is characteristic for a number of homologous recombination proteins including wild type Rad54 [19]. A correctly targeted clone of genotype *Rad54*$^{GFP/+}$ was expanded and injected into wild type blastocysts. Chimeric mice obtained were backcrossed to obtain *Rad54*$^{GFP/+}$ animals, which were bred to obtain *Rad54*$^{GFP/GFP}$ animals. The mice were obtained at Mendelian inheritance ratios, indicating normal transmission of the *Rad54-GFP* allele.

Visualization of Rad54-GFP in embryos shows expression in all cells

To determine the pattern of Rad54-GFP expression at various stages of development, 3.5, 8.5 and 13.5 dpc embryos were isolated in which Rad54-GFP was visualized. GFP positive 3.5 dpc embryos indicated the presence of Rad54-GFP protein in the embryos (Figure 2A). In 8.5 dpc embryos, Rad54-GFP was noted in three discernible areas; the head, heart and somites (Figure 2B). Other organs become distinct in 13.5 dpc embryos, and Rad54-GFP was seen in most cells of the organs where rapid cell division and tissue expansion is taking place (Figure 2C).

Rad54-GFP expression in fetal and adult hematopoeic system

The hematopoietic system was chosen to follow developmental changes in Rad54-GFP expression because of its well-characterized stages of cell development and the possibility to select for progenitor cells and differentiated cells. *Rad54*$^{+/+}$ and *Rad54*$^{GFP/GFP}$ fetal livers were isolated from embryos obtained as a result of a mating between *Rad54*$^{GFP/+}$ mice and cultured for 24 hours in order to enrich the culture for the rapidly proliferating proerythroblasts. The proerythroblasts were maintained in culture as the earliest of the immature forms recognizable as the precursor of the mature erythrocyte, as previously described [17]. Flow cytometry showed that these cells from fetal livers express Rad54-GFP, as seen by a clear peak shift in the profile (Figure 3A). It was noted that there was a

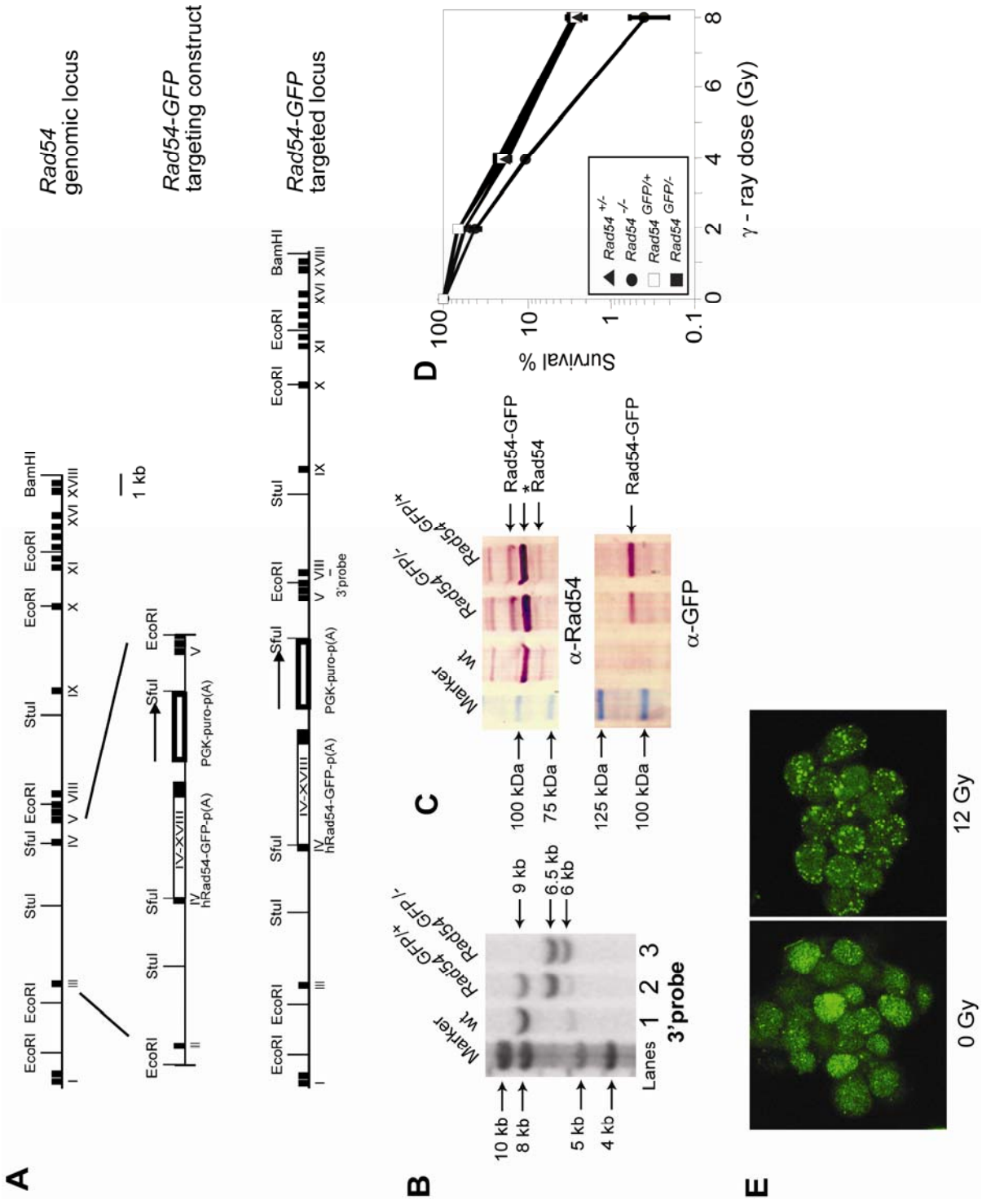
A
Rad54 genomic locus
Rad54-GFP targeting construct
Rad54-GFP targeted locus
1 kb
hRad54-GFP-p(A)
PGK-puro-p(A)
3'probe
B
3'probe
Lanes 1 2 3
9 kb
6.5 kb
6 kb
10 kb
8 kb
5 kb
4 kb
C
α-Rad54
α-GFP
Rad54-GFP
Rad54
100 kDa
75 kDa
125 kDa
D
Survival %
γ - ray dose (Gy)
E
0 Gy
12 Gy

Figure 1

Generation and analysis of mouse ES cells containing a *Rad54^{GFP}* allele

(A) Schematic representation of the mouse *Rad54* locus and the gene targeting construct. The top line represents a 30 kb portion of endogenous *Rad54* locus, where black boxes indicate exons I through XVIII. The middle line shows the linearized targeting construct, containing the human *RAD54* cDNA sequence spanning exon IV-XVIII fused to the *GFP* coding sequence. The construct contains a gene encoding for puromycin resistance as a selectable marker. As shown by the final line, the targeting construct will replace the regions between exon III and VIII when correctly integrated to generate the targeted allele. Homologous integration results in the expression of full length, GFP-tagged Rad54 from its endogenous promoter. **(B)** DNA blot analysis of ES cells carrying the knock-in contruct. DNA blot analysis was carried out using genomic DNA purified from puromycin positive clones and digested with StuI. Detection of bands was carried out using a probe that recognized exon VII/VIII, as indicated in Figure 1A. The wild type (wt) allele results in a 9.0 kb band (lane 1). The knockout allele yields a 6.0kb band (lane 3), while knock-in allele is characterized by a doublet (a band of higher intensity) around 6.5 kb (lanes 2 & 3). **(C)** Immunoblot blot analysis of proteins produced by the *Rad54-GFP* knock-in allele. Whole cells extracts of ES cells with the indicated genotype were probed with affinity purified anti-human Rad54 antibodies (top) and anti-GFP (bottom). The position of Rad54 and Rad54-GFP are indicated and an asterix marks a non-specific signal in the top blot. Wild type Rad54 is 85 kDa and was seen in both wt and *Rad54$^{GFP/+}$* lanes (top), while Rad54-GFP is 110 kDa, as shown by both the α-Rad54 and α-GFP. **(D)** Clonal survival analysis of *Rad54$^{GFP/-}$*. ES cells of the indicated genotypes for their ability to survive treatment with increasing doses of irradiation. The assays were done in triplicate and the error bars indicated the standard error of the mean. *Rad54$^{GFP/-}$* cells are not hypersensitive to irradiation, indicating that the GFP tag on Rad54 does not compromise its function and is as functionally active as wild type Rad54 in cells. **(E)** Cellular localization of *Rad54$^{GFP/GFP}$* ES cells. Confocal images of fixed *Rad54$^{GFP/GFP}$* ES cells without (left panel) and with (right panel) irradiation are shown. Rad54-GFP accumulated as foci 1 hour after treatment with 12 Gy.

small subpopulation that was not Rad54-GFP positive (arrowed "shoulder"). This is likely to be due to the fact that there were other cells, like macrophages, which were still present in a short-term culture of proerythroblasts. In addition, when these cells were attached to poly-lysine coated slides and observed under the confocal microscope, Rad54-GFP localized in the large nucleus characteristic of these cells (Figure 3B). When the cells were treated with ionizing radiation, these cells displayed accumulation of Rad54-GFP into nuclear foci (Figure 3B, right panel), a behavior that is similar to Rad54 in ES cells (Figure 1E). As noted for the FACS profile, there are other types of cells in the population that were not Rad54-GFP positive (arrowed in Figure 3B).

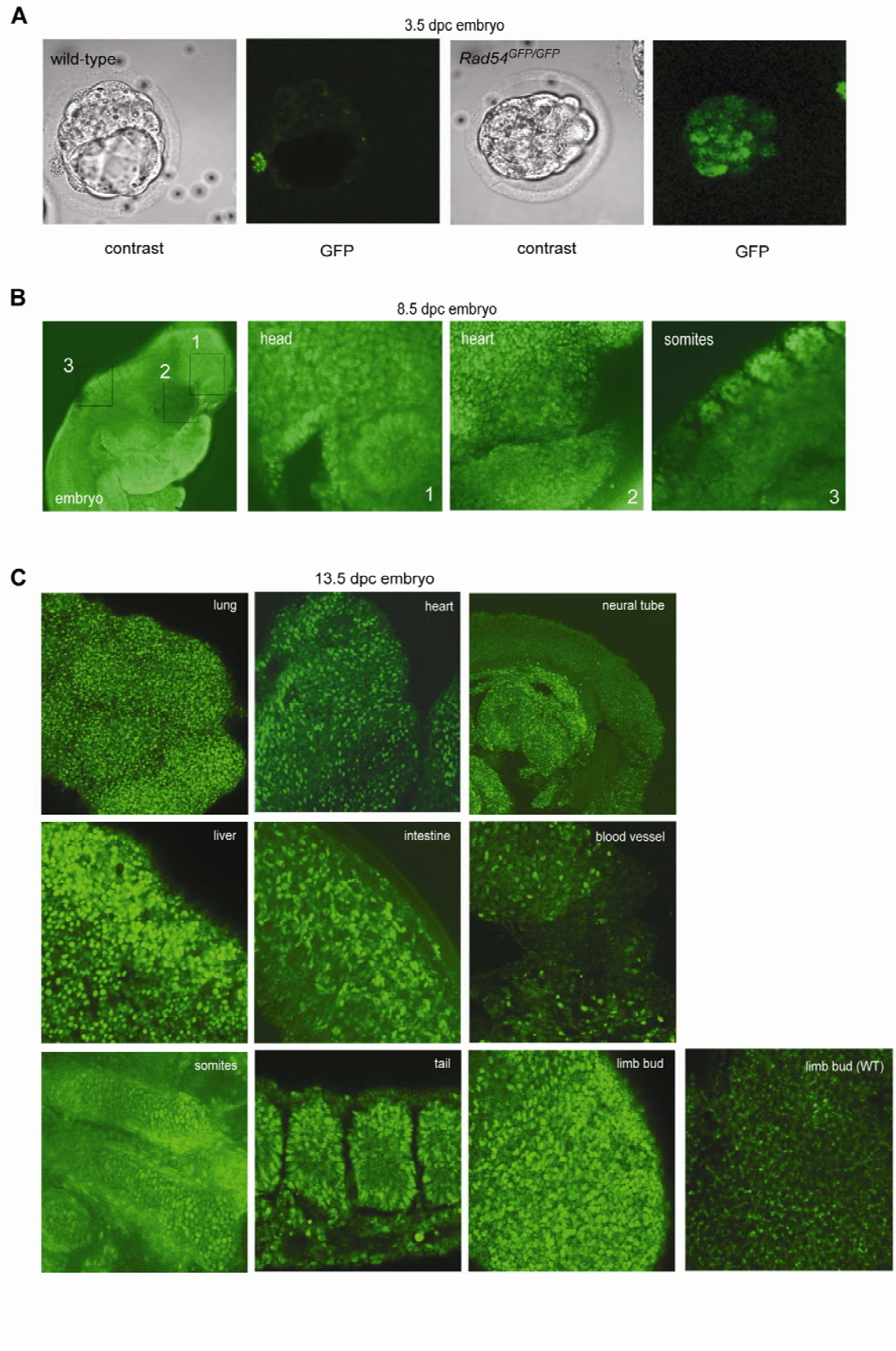
A
3.5 dpc embryo
wild-type
Rad54GFP/GFP
contrast
GFP
contrast
GFP
B
8.5 dpc embryo
1
2
3
embryo
head
1
heart
2
somites
3
C
13.5 dpc embryo
lung
heart
neural tube
liver
intestine
blood vessel
somites
tail
limb bud
limb bud (WT)

Figure 2
Rad54-GFP is expressed during embryonic development
(A) Comparison of wild type and *Rad54*$^{GFP/+}$ embryos at 3.5 dpc. Contrast and fluorescent confocal pictures of both genotypes are shown, indicating the presence of Rad54-GFP in *Rad54*$^{GFP/+}$ embryo (right), but not in the wild type (left). **(B)** Analysis of *Rad54*$^{GFP/GFP}$ embryo at 8.5 dpc. At this stage, most organs have not formed and only gross parts of the embryo are recognizable, all of which showed the presence of Rad54-GFP. **(C)** Analysis of *Rad54*$^{GFP/GFP}$ embryo at 13.5 dpc. Indicated organs were distinguishable with the confocal microscope and showed the presence of Rad54-GFP. An image of the wild type (WT) limb bud is shown for comparison.

The site of hematopoiesis switches to several different organs during embryonic and fetal development. First, the yolk sac provides the site for mainly primitive erythropoiesis in the early embryo. Then, the first hematopoeitic stem cells are found in the aorta-gonad-mesonephros (AGM) region. One day later, hematopoeitic stem cells can be found in the yolk sac, placenta and fetal liver. Finally, at birth, the bone marrow is established as the primary source of mature blood cells, and is the location of highly dividing hematopoietic stem cells [20, 21]. To study Rad54-GFP expression in adult hematopoietic site, adult bone marrow was isolated and the cells were separated according to cell surface markers, specifically B220 and Ter119. B220 is a marker specific for B-lineage cells, namely B lymphocytes and their precursors. B-lineage cells were separated from erythroid precursors by Ter119 staining. Ter119 is an antibody that reacts with mouse erythroid cells from early proerythroblast stage at the point where these cells are committed to differentiation to mature erythrocytes [22]. The larger, Ter119-positive cells from *Rad54*$^{GFP/GFP}$ mice were actively dividing and show a shift into compartment 3, indicating Rad54-GFP expression (33% of total population, right panel of Figure 3C). As cells matured and started differentiation to become mature erythrocytes, they stopped replicating and became smaller (52 – 55 % of total population, compartment 1, Figure 3C). These cells also showed loss of Rad54-GFP expression (compartment 1, right panel). These data indicate the presence of Rad54-GFP in proerythroblasts extracted from both the fetal liver as well as the adult bone marrow. In addition, as proerythroblasts mature, the Rad54-GFP expression is lost.

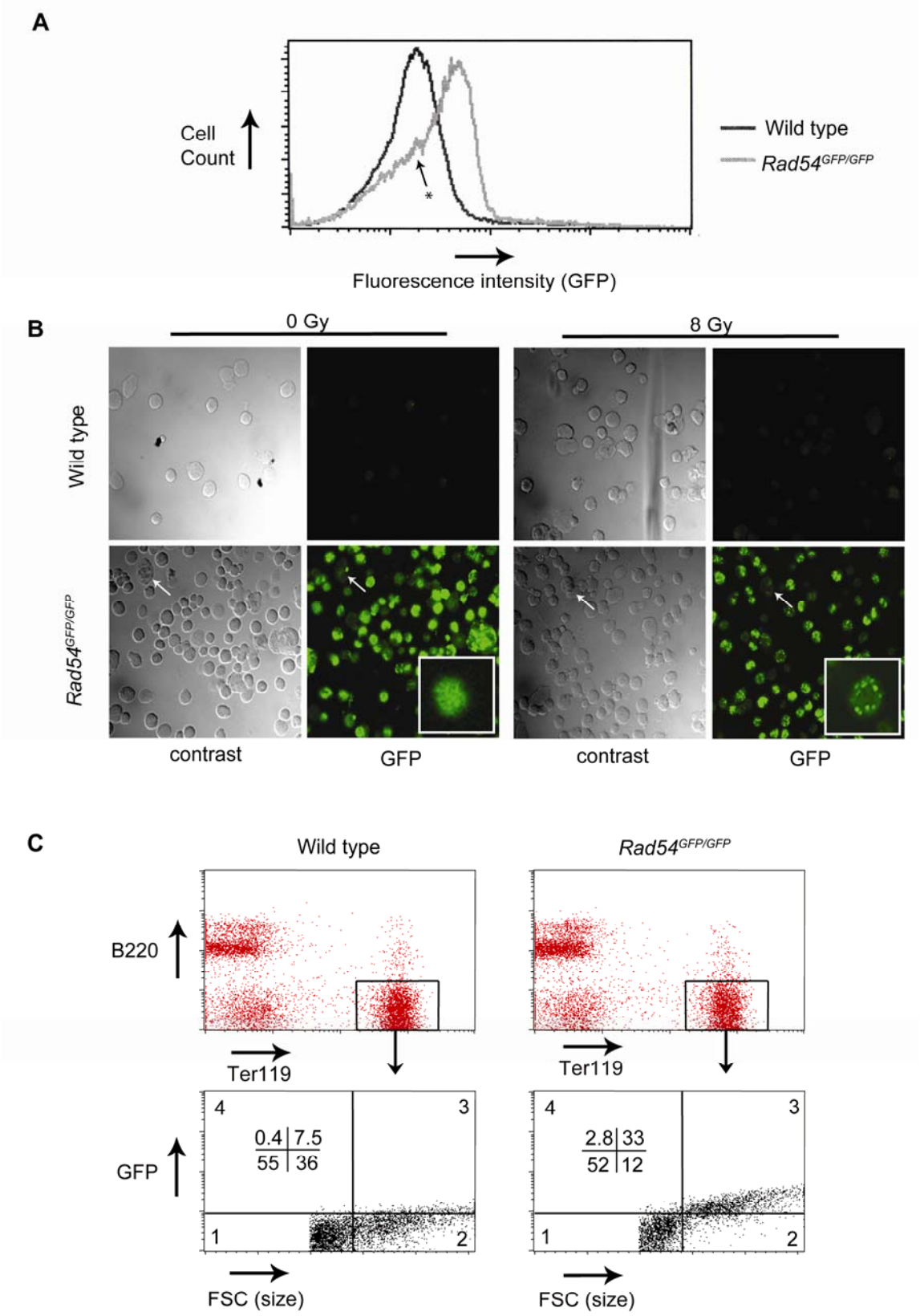
A
Cell Count
Wild type
Rad54GFP/GFP
*
Fluorescence intensity (GFP)
B
0 Gy
8 Gy
Wild type
Rad54GFP/GFP
contrast
GFP
contrast
GFP
C
Wild type
Rad54GFP/GFP
B220
Ter119
Ter119
GFP
4
3
0.4
7.5
55
36
1
2
2.8
33
52
12
FSC (size)
FSC (size)

Figure 3

Rad54-GFP is present in dividing progenitor cells during erythrocyte differentiation

(A) FACs analysis of proerythroblasts from embryonic fetal livers. Livers from 12.5 dpc embryos were harvested and grown in proerythroblast expansion medium for 24 hours, before undergoing cell sorting for GFP positive cells. Proerythroblasts extracted from *Rad54*$^{GFP/GFP}$ embryos show a marked shift in peaks as compared to wild type, indicating the expression of Rad54-GFP in almost all cells. An arrow and asterisk indicate a small "shoulder" in the profile indicating the presence of a small subpopulation of cells that are Rad54-GFP negative. **(B)** Confocal images of proerythroblasts. Fixed proerythroblasts were observed without (left) and with (right) irradiation. *Rad54*$^{GFP/GFP}$ cells show Rad54-GFP expression, which localizes into nuclear foci after 8 Gy irradiation. Image was taken 1 hour after irradiation. Morphologically distinct cells which show no Rad54-GFP are arrowed. **(C)** FACs analysis of adult bone marrow. Adult bone marrow cells from both wild type and *Rad54*$^{GFP/GFP}$ mice were extracted and according to cell surface markers (top panel), namely B220 (B-cell specific marker) and Ter119 (proerythroblast specific marker). The Ter119 positive cells were further analyzed for GFP positive cells (bottom panel). The larger, actively cycling proerythroblasts showed the production of Rad54-GFP (compartment 3, bottom right panel). Smaller, quiescent cells in compartment 1 are undergoing differentiation and were Rad54-GFP negative. The numbers in the table in the bottom panel represent the relative percentage of cells in each compartment.

Rad54-GFP in B- and T-cell development

It was previously reported by RNA blot analysis that Rad54 is highly expressed in the thymus, an organ which hosts the development of T cells [14]. Two distinct possibilities for Rad54 presence are suggested: one, that Rad54 has a role in V(D)J recombination, and two, that Rad54 is ubiquitously present in replicating cells. In order to distinguish between these possibilities for Rad54 in the development of T cells and B cells, the thymus and bone marrow were isolated from an adult mouse and analyzed.

Total bone marrow cell suspensions from *Rad54*$^{GFP/GFP}$ mice were analyzed by flow cytometry. Using surface markers B220, CD43 and Immunoglobulin M (IgM), various stages of B cell differentiation were gated and analyzed for forward scatter (as a measure for cell size) and Rad54-GFP expression (Figure 4A) [23]. Cells were defined as large and associated with active cycling if they fell beyond approximately 500 in the forward scatter compartment (FSC) (compartment 2, Figure 4A). Alternately, cells that fell below approximately 500 (compartment 1, Figure 4A) were defined as small and associated with non-cycling cells. In the pro-B cell stage, non-cycling cells are carrying out Ig heavy chain recombination, panel I [24]. In the pre-B cell stage, non-cycling cells are undergoing light chain rearrangement, panel II. GFP-positive cells were seen in compartment 3 and 4.

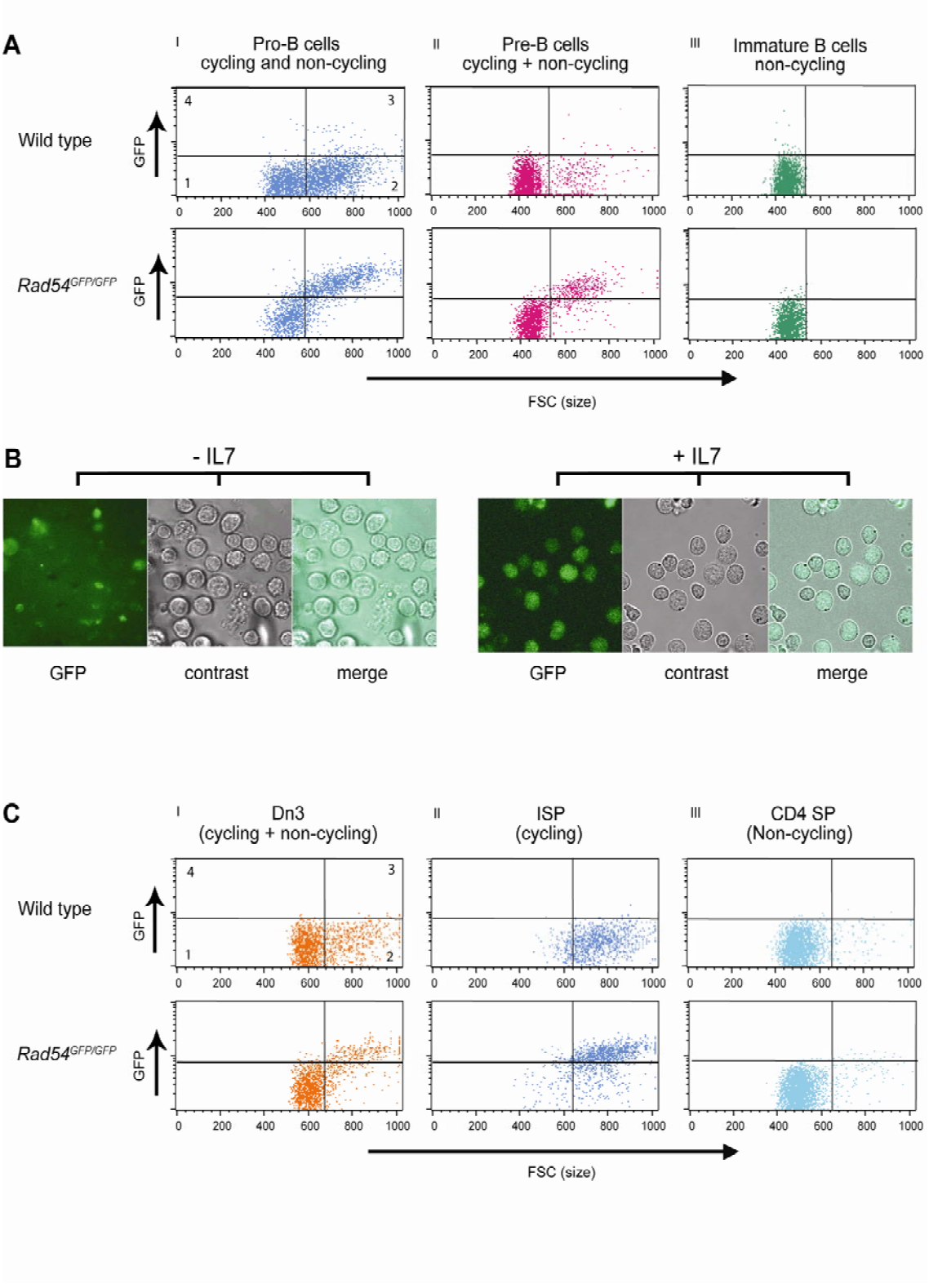
A
I
Pro-B cells
cycling and non-cycling
II
Pre-B cells
cycling + non-cycling
III
Immature B cells
non-cycling
Wild type
Rad54GFP/GFP
GFP
4
3
1
2
0
200
400
600
800
1000
FSC (size)
B
- IL7
+ IL7
GFP
contrast
merge
C
I
Dn3
(cycling + non-cycling)
II
ISP
(cycling)
III
CD4 SP
(Non-cycling)
Wild type
Rad54GFP/GFP
GFP
FSC (size)

Figure 4
Rad54-GFP is present in proliferating B and T cells in adult mice
(A) FACs profiles of cells in various stages of B cell development. Bone marrow cells were isolated from adult wild type and *Rad54*$^{GFP/GFP}$ mice. Cells representing the different stages of development (Pro B, Pre B and immature B cells) were electronically gated and analysed. Large cycling cells were GFP positive (compartment 3), while smaller, non-cycling cells which are also carrying out V(D)J recombination were not expressing Rad54-GFP (compartment 1). Wild type cells did not show any GFP positive cells. **(B)** Confocal images of pre-B cells. Bone marrow was cultured in IL7-containing media enriching for pre-B cells which have completed V(D)J recombination and are actively cycling; these cells are positive for Rad54-GFP (right). When IL7 is removed from the culture medium, pre-B cells become quiescent and Rad54-GFP expression disappears (left). **(C)** Analysis of cells undergoing T cell differentiation by FACs. T cells were isolated from adult thymus and sorted by their differentiation status by electronic gating and analysis. Cycling cells show a shift into compartment 3, showing Rad54-GFP expression, while smaller, non-cycling cells do not (compartment 1).

In the pro-B and pre-B cells that are undergoing V(D)J recombination, there was no Rad54-GFP signal detected; on the other hand, cells that are actively expanding showed a clear shift into compartment 3, indicating that Rad54-GFP appeared exclusively in cycling cells during B cell maturation. Non-cycling immature B cells did not express Rad54-GFP (panel III). Visualization of this result was carried out by culturing total bone marrow cells in IL7 for 5 days, which specifically selects for and enriches the culture for pre B-cells which have completed Ig heavy chain V(D)J recombination [25], and are cycling (Figure 4B). The homogenous population of pre B-cells displayed nuclear localization of Rad54-GFP (right panel). However, when these cells were cultured for 2 days in the absence of IL7, small resting pre-B cells that are involved in rearrangement of the IgL chain genes resulted, and in these cells Rad54-GFP was not detectable, except for some aspecific staining (left panel).

Similarly, developing T cells were isolated from thymus and followed through the various stages of maturation [26]. Again, cycling cells were seen in compartment 2, non-cycling cells were in compartment 1, and GFP-positive cells were seen in compartments 3 and 4 (Figure 4C). Non-cycling T cells in panel I also carry out V(D)J recombination, which did not show the presence of Rad54-GFP. Cycling T cells at the same stage however, displayed Rad54-GFP expression. T cells that are cycling and expanding (panel II) were positive for Rad54-GFP, but once they stop (panel III), they lost expression. These data show that Rad54-GFP is expressed in cells that are actively cycling and expanding, but is not detectable in non-cycling cells, suggesting that Rad54 does not

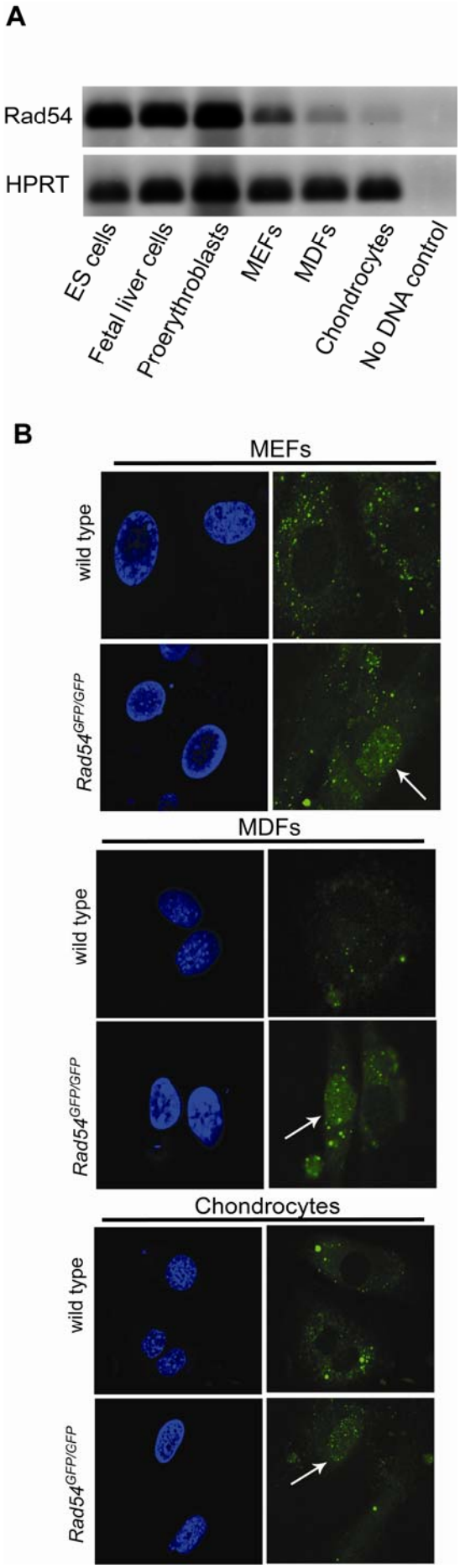

Figure 5

Rad54 is present in proliferating cells

(A) PCR on cDNA isolated from different cell types. Results show PCR products obtained from cDNA with HPRT primers (bottom panel) or Rad54 primers (top panel). Expression is present in all these cell types, although at different levels.

(B) Confocal images of MEFs, MDFs and chondrocytes. Dividing cells from each type were fixed on slides, stained with DAPI and observed for Rad54-GFP expression. In each case there is a small percentage of cells that show nuclear staining of Rad54-GFP (arrowed).

appear to have a prominent role in V(D)J recombination, as previously predicted by studies using Rad54 knockout mice [13].

Rad54-GFP expression in other cell types

So far we have established that Rad54-GFP is present in actively cycling cells early in development, as well as in hematopoietic progenitors. To investigate the relationship between the expression of Rad54 and differentiation status of cells, we isolated three kinds of cells from *Rad54*$^{GFP/GFP}$ embryos and mice - mouse embryonic fibroblasts (MEFs), mouse dermal fibroblasts (MDFs) and cells from the mouse ear (chondrocytes). All these cells resumed cycling when put into culture. Quantitative PCR was performed on cDNA isolated from wild type cells, and *Rad54* mRNA was found to be present in all cell types (Figure 5A). However, the levels were different: ES cells showed the highest level of Rad54 expression, while MEFs, MDFs and chondrocytes display a low level of Rad54 message. Q-PCR analysis revealed that relative to ES cells, MEFs contain 5-fold less Rad54 mRNA. No reliable quantitative data could be obtained for MDFs and chondrocytes (data not shown). In addition, when observed under the confocal microscope, all cells showed considerable cytoplasmic auto-fluorescence, but only a small subset displayed a distinct and uniform nuclear staining (Figure 5B). Preliminary quantification resulted in approximately 10% MEFs showing nuclear localization of Rad54-GFP in a subconfluent culture. This was noticeably absent from the *Rad54*$^{+/+}$ cells. Furthermore, on top of the nuclear localization, Rad54-GFP foci could be observed, which is indicative for cells in S phase [27].

Discussion

The Rad54^{GFP} *knock-in system*

The intimate connection of Rad54 to homologous recombination has been extrapolated from biochemical evidence as well as from the characterization of cells which lack Rad54. Here, the behavior of Rad54 in living cells is investigated where its spatial and temporal localization has been studied using *Rad54*^{GFP} knock-in cells and mice at various stages of development, an approach that bypasses the difficulties posed by overexpression and transient systems. The advantage of using a knock-in strategy, where the Rad54-GFP fusion construct is integrated into the genome at the endogenous *Rad54* locus (Figure 1A and B), is that the level of GFP-tagged Rad54 expression is comparable to the wild type protein (Figure 1C). The localization and cellular behavior of the tagged

protein may therefore be expected to mimic that of the wild type protein in embryos and cells derived from *Rad54*$^{GFP/GFP}$ mice. Functionality of the GFP-tagged protein was determined using the survival behavior of *Rad54*$^{GFP/-}$ ES cells with increasing doses of irradiation (Figure 1D), as well as the ability of Rad54 to form foci after treatment with irradiation (Figure 1E, [19, 28]). This shows that the Rad54GFP knock-in mouse provides a valid and useful tool to analyze spatial and temporal expression of Rad54 *in vivo*.

Rad54-GFP is confined to dividing cells during differentiation of the hematopoeic system

Correctly targeted ES cells were used to make *Rad54*$^{GFP/GFP}$ mice used in further experiments, including the study of Rad54-GFP expression during various stages of embryonic development (Figure 2). Rad54-GFP is present at least up to 13.5 dpc and in various organs. In particular, the hematopoietic system was chosen to track the expression of Rad54-GFP particularly due to its well-defined cellular differentiation program that can be followed in detail using appropriate cell surface markers. Proerythroblasts derived from 12.5 dpc embryos show an active production of Rad54-GFP (Figure 3A), the foci forming behavior of which was similar to ES cells (Figure 3B). Since Rad54 is an important player in homologous recombination, it is conceivable that in proerythroblasts, like in ES cells [13] , this pathway is used to repair DSBs, ensuring the faithful transmission of the genome during the rapid expansion of these cells.

Rad54-GFP expression is not confined to cells derived from embryos. Rad54-GFP is highly expressed not only in proerythroblasts from fetal livers but also those derived from adult bone marrow, indicating that tissue and cell specific expression of Rad54, and therefore homologous recombination, exists in the adult mouse. This premise is underscored by the expression profiles of developing B and T cells, where cells that divide express Rad54-GFP, but non-dividing cells that are carrying out V(D)J recombination do not (Figure 4). Importantly, these data also make a distinction between the two possibilities raised in the earlier work [14] and confirms expression of Rad54-GFP in organs where cells are engaged in high rates of division, rather than showing a function in V(D)J recombination.

Rad54-GFP is also present in dividing terminally differentiated cells, but only in a small percentage of the population.

Finally, Rad54-GFP expression was investigated in dividing cell types other than ES cells or proerythroblasts (Figure 5). Cells derived from mouse skin and auricular cartilage are at the stage of terminal differentiation, and do not undergo division *in situ*. However when these tissues are isolated and forced into division using culture conditions, a small recovery of Rad54-GFP expression is observed. However, unlike ES cells and proerythroblasts where a homogenous expression of Rad54-GFP is seen throughout the population of cells, only a small percentage of the MEF, MDF and chondrocyte population express Rad54-GFP: approximately 10% of MEFs show nuclear localization within a population of cells which is not confluent and is therefore still dividing rapidly. Homologous recombination has been postulated to be a cell cycle dependent process, taking place during S and G2 phases simply due to the presence of the sister chromatid during this time [29]. The fact that Rad54 is present at a slightly higher level in S/G2 phases strengthens this argument [30]. Therefore, a possible explanation for the differences in Rad54 expression profiles between ES cell/proerythroblast populations and MEFs/MDFs/chondrocytes is that the former are continuously expanding and therefore have a larger fraction of cells in S/G2 phase compared to the latter [31], where the longer doubling time of the latter makes the different phases of the cell cycle more distinct. We have as yet not determined whether Rad54 is confined to a specific cell cycle stage in these cells, or if there is a small percentage of cells that continuously express Rad54-GFP, although previous experiments have suggested that the level of Rad54 expression is highest at S phase [30]. Cells could be stained with S phase specific antigens such as Ki67 to determine the correlation between low expression of Rad54-GFP in these cells and S phase. We have also not excluded the possibility that the knock-in locus is silenced selectively in most primary MEFs/MDFs/chondrocytes, and this can be examined by methylation-specific multiplex ligation dependent probe amplification (MLPA). In addition, MDFs and chondrocytes are terminally differentiated cells, and this might be the cause of a low Rad54-GFP expression. This option also needs to be investigated.

Interestingly, it has been found that *Rad54*$^{-/-}$ MEFs display wild type resistance to ionizing radiation, in sharp contrast to the hypersensitivity of *Rad54*$^{-/-}$ ES cells [32]. This might be correlated to the small percentage of cells that express Rad54-GFP in MEFs compared to ES cells, demonstrating a functional link between the presence of Rad54

and its involvement of homologous recombination. Indeed, since Rad54 has been shown to be only present in specific tissues and even only in certain cellular subsets ([14] and this work), the adult animal relies on other pathways (such as nonhomologous end joining) for the repair of DSBs. This premise is further underscored by the finding that while *Rad54*$^{-/-}$ animals are not sensitive to irradiation, if the core proteins of nonhomologous end joining are knocked out, a hypersensitivity compared to nonhomologous end joining mutants only is noted [9-11].

Expression profiles of Rad54-GFP in mitotic and meiotic cells.

Using an in-depth analysis of the Rad54-GFP knock-in mouse, we have shown in this study that Rad54-GFP expression coincides with mitotic cells and high cellular proliferation. We have established that Rad54-GFP is present, as expected, in the cells of the various organs as well as in the early developmental stages of the hematopoeitic system of the developing embryo. During embryo development, it is critical to ensure faithful replication of the genome in every cell; therefore homologous recombination is the DSB repair pathway of choice. The role of Rad54 in recombination is strengthened by the fact that *Rad54*$^{-/-}$ ES cells are sensitive to ionizing radiation, a DSB-inducing agent [13]. Since the presence of Rad54-GFP in the erythrocyte precursor cells predicts the involvement of homologous recombination in progenitor cells, it is probable that progenitor cells in other adult tissues maintain their genome in the same way. Rad54-GFP is also expressed in a small subset of MDFs and chondrocytes derived from adult mouse. The common denominator is that these cells are cycling, and they display detectable levels of Rad54-GFP expression. However, the function of Rad54 in the latter type cells is yet undetermined, since by survival analyses, *Rad54*$^{-/-}$ MEFs are not sensitive to ionizing radiation. Further studies are necessary to determine the purpose of the low level of Rad54 expression in these cells.

The subcellular localization of Rad54-GFP in meiotic cells has also been previously determined in mouse testis tubules from the Rad54-GFP mouse [14]. In that study, three-dimensional optical image analyses showed high Rad54-GFP expression in the mitotic stem cells (spermatogonia) of the male gametes up until entry into meiotic prophase. Rad54-GFP expression reappeared in the pachytene stage and was lost from diplotene onwards.

The analysis of Rad54-GFP expression illustrates the use of the Rad54-GFP knock-in mouse model to detect proliferating cells *in vivo*, since it allows the *in situ*

identification of single cells expressing Rad54 protein amidst non-expressing cells through detailed three-dimensional optical microscopy of isolated tissues. We conclude that the Rad54-GFP knock-in mouse might be valuable in the identification of yet unknown stem/progenitor cell niches in various organ systems of the intact animals. The advantage of the knock-in mouse model is that these studies can be done in live cells, without the need for staining with S phase specific antigens.

Acknowledgements

The authors would like to acknowledge the technical assistance of Gemma Dingjan (FACS experiments), Sabine Middendorp and Esther Zijlstra (for culture experiments for microscopy) and Gert van Cappellen (for confocal miscroscopy).

References

1. Friedberg, E.C., L.D. McDaniel, and R.A. Schultz, *The role of endogenous and exogenous DNA damage and mutagenesis.* Curr Opin Genet Dev, 2004. **14**(1): p. 5-10.
2. Agarwal, S., A.A. Tafel, and R. Kanaar, *DNA double-strand break repair and chromosome translocations.* DNA Repair (Amst), 2006. **5**(9-10): p. 1075-81.
3. Bassing, C.H. and F.W. Alt, *The cellular response to general and programmed DNA double strand breaks.* DNA Repair (Amst), 2004. **3**(8-9): p. 781-96.
4. Hoeijmakers, J.H., *Genome maintenance mechanisms for preventing cancer.* Nature, 2001. **411**(6835): p. 366-74.
5. Wyman, C. and R. Kanaar, *DNA Double-Strand Break Repair: All's Well That Ends Well.* Annu Rev Genet, 2006.
6. Wyman, C., D. Ristic, and R. Kanaar, *Homologous recombination-mediated double-strand break repair.* DNA Repair (Amst), 2004. **3**(8-9): p. 827-33.
7. Sung, P., et al., *Rad51 recombinase and recombination mediators.* J Biol Chem, 2003. **278**(44): p. 42729-32.
8. Feldmann, E., et al., *DNA double-strand break repair in cell-free extracts from Ku80-deficient cells: implications for Ku serving as an alignment factor in non-homologous DNA end joining.* Nucleic Acids Res, 2000. **28**(13): p. 2585-96.
9. Couedel, C., et al., *Collaboration of homologous recombination and nonhomologous end-joining factors for the survival and integrity of mice and cells.* Genes Dev, 2004. **18**(11): p. 1293-304.
10. Essers, J., et al., *Homologous and non-homologous recombination differentially affect DNA damage repair in mice.* Embo J, 2000. **19**(7): p. 1703-10.
11. Mills, K.D., et al., *Rad54 and DNA Ligase IV cooperate to maintain mammalian chromatid stability.* Genes Dev, 2004. **18**(11): p. 1283-92.

12. Brugmans, L., R. Kanaar, and J. Essers, *Analysis of DNA double-strand break repair pathways in mice.* Mutat Res, 2006.
13. Essers, J., et al., *Disruption of mouse RAD54 reduces ionizing radiation resistance and homologous recombination.* Cell, 1997. **89**(2): p. 195-204.
14. Kanaar, R., et al., *Human and mouse homologs of the Saccharomyces cerevisiae RAD54 DNA repair gene: evidence for functional conservation.* Curr Biol, 1996. **6**(7): p. 828-38.
15. Uringa, E.J., *Functions and dynamics of DNA repair proteins in mitosis and meiosis.* (PhD thesis, Erasmus MC, Rotterdam), 2005.
16. Wesoly, J., et al., *Differential contributions of mammalian Rad54 paralogs to recombination, DNA damage repair, and meiosis.* Mol Cell Biol, 2006. **26**(3): p. 976-89.
17. Dolznig, H., et al., *Establishment of normal, terminally differentiating mouse erythroid progenitors: molecular characterization by cDNA arrays.* Faseb J, 2001. **15**(8): p. 1442-4.
18. Middendorp, S., G.M. Dingjan, and R.W. Hendriks, *Impaired precursor B cell differentiation in Bruton's tyrosine kinase-deficient mice.* J Immunol, 2002. **168**(6): p. 2695-703.
19. Tan, T.L., et al., *Mouse Rad54 affects DNA conformation and DNA-damage-induced Rad51 foci formation.* Curr Biol, 1999. **9**(6): p. 325-8.
20. Morrison, S.J., N. Uchida, and I.L. Weissman, *The biology of hematopoietic stem cells.* Annu Rev Cell Dev Biol, 1995. **11**: p. 35-71.
21. Tavassoli, M., *Embryonic and fetal hemopoiesis: an overview.* Blood Cells, 1991. **17**(2): p. 269-81; discussion 282-6.
22. Kina, T., et al., *The monoclonal antibody TER-119 recognizes a molecule associated with glycophorin A and specifically marks the late stages of murine erythroid lineage.* Br J Haematol, 2000. **109**(2): p. 280-7.
23. Tsubata, T. and S. Nishikawa, *Molecular and cellular aspects of early B-cell development.* Curr Opin Immunol, 1991. **3**(2): p. 186-92.
24. Meffre, E., et al., *Circulating human B cells that express surrogate light chains and edited receptors.* Nat Immunol, 2000. **1**(3): p. 207-13.
25. Melchers, F., *B cell development and its deregulation to transformed states at the pre-B cell receptor-expressing pre-BII cell stage.* Curr Top Microbiol Immunol, 2005. **294**: p. 1-17.
26. Rothenberg, E.V. and T. Taghon, *Molecular genetics of T cell development.* Annu Rev Immunol, 2005. **23**: p. 601-49.
27. Tashiro, S., et al., *S phase specific formation of the human Rad51 protein nuclear foci in lymphocytes.* Oncogene, 1996. **12**(10): p. 2165-70.
28. van Veelen, L.R., et al., *Ionizing radiation-induced foci formation of mammalian Rad51 and Rad54 depends on the Rad51 paralogs, but not on Rad52.* Mutat Res, 2005. **574**(1-2): p. 34-49.
29. Sonoda, E., et al., *Differential usage of non-homologous end-joining and homologous recombination in double strand break repair.* DNA Repair (Amst), 2006. **5**(9-10): p. 1021-9.

30. Essers, J., et al., *Analysis of mouse Rad54 expression and its implications for homologous recombination.* DNA Repair (Amst), 2002. **1**(10): p. 779-93.
31. de Waard, H., *Genome caretaking and differentiation.* (PhD thesis, Erasmus MC, Rotterdam), 2004.
32. Brugmans, L., *Nbs1: a multifaceted protein in the DNA damage response* (PhD thesis, ErasmusMC, Rotterdam), 2008.

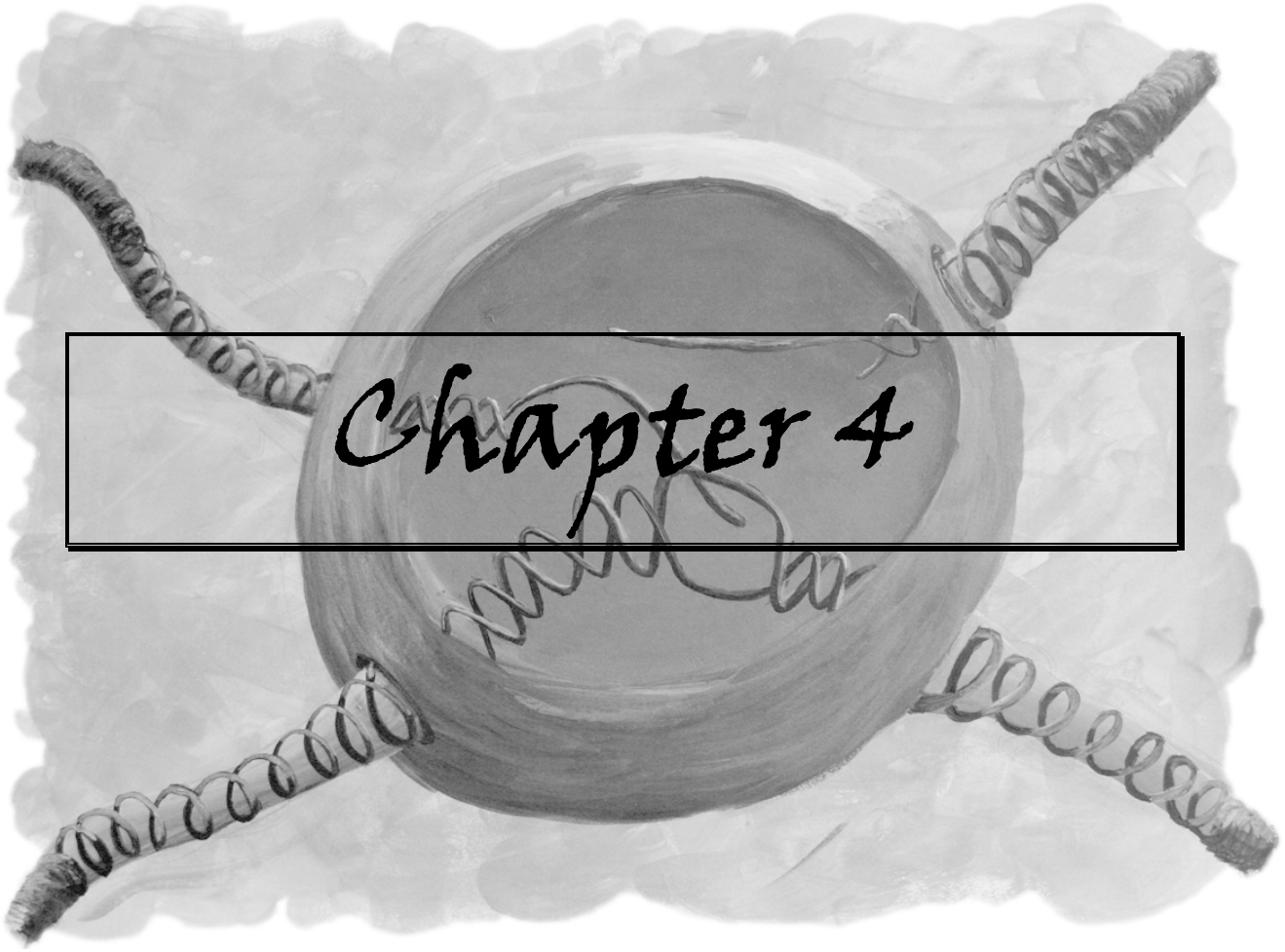

Chapter 4

ATP hydrolysis by mammalian Rad54 controls nuclear foci kinetics and is essential for DNA damage repair

Manuscript in preparation

That's the whole problem with science. You've got a bunch of empiricists trying to describe things of unimaginable wonder.

~ Calvin & Hobbes (Bill Watterson)

ATP hydrolysis by mammalian Rad54 controls nuclear foci kinetics and is essential for DNA damage repair

Sheba Agarwal [1], Aude Guénolé[1], Samuel L. Linsen[1, 5], Wiggert A. van Cappellen[3], Adriaan Houtsmuller[4], Roland Kanaar [1, 2], Jeroen Essers [1, 2]

[1] Department of Cell Biology and Genetics, [2] Department of Radiation Oncology, [3]Department of Reproduction and Development, [4]Department of Pathology, Erasmus MC, Rotterdam, The Netherlands
[5] Functional Genomics and Bioinformatics, Hubrecht Institute, Utrecht, The Netherlands (present address)

Abstract

Rad54 is a member of the SWI2/SNF2 family of DNA dependent ATPases. It is an important accessory protein that has a central role in assisting Rad51 in homologous recombination via a variety of biochemical activities. Most of these activities are dependent on RAD54's ability to hydrolyze ATP. To study the impact of the loss of this ATPase activity in mammalian cells, we have generated two knock-in mouse embryonic stem cell lines expressing GFP-tagged Rad54 protein which carry point mutations in the ATPase domain, K189R and K189A, which render Rad54 devoid of ATPase activity. Rad54 ATPase mutant cells behave similarly to Rad54 knockout cells with respect to sensitivity to DNA-damaging agents and demonstrate compromised gene targeting by homologous recombination. This shows the essential role of ATP hydrolysis by Rad54 in DNA double strand break repair. However, contrary to knockout cells, mutant cells demonstrate an elevated level of spontaneous Rad54 foci and Rad51 foci. Time-lapse imaging indicates that Rad54 mutant cells display a slower rate of damage-induced foci clearance. In addition, the residence time of the protein in is higher in the mutant cells than in wild type cells. We conclude that the presence of mutant Rad54 influences both Rad54 and Rad51 cellular behavior. This study also establishes the role of Rad54 ATPase activity in effective protein turnover in spontaneous and damage-induced foci as well as disappearance of foci after damage.

Introduction

Cells have evolved a number of pathways to deal with DNA damage in order to preserve the integrity of their genome. This damage is created by endogenous and exogenous sources. Endogenous sources include by-products of cellular metabolism like oxygen radicals, while exogenous sources include ultraviolet and ionizing radiation [1].

Among different kinds of lesions, DNA double-strand breaks (DSBs) present a special challenge to the cells because the continuity of the double helix is lost. If misrepaired, DSBs can cause genome rearrangements such as translocations and deletions that can result in the development of cancer [1-3]. Thus it is paramount that DSBs are repaired precisely and in a timely fashion.

Homologous recombination is an error free, high fidelity pathway that repairs DSBs by using an undamaged homologous DNA molecule (usually the sister chromatid present after replication) as a template to repair the broken molecule [4]. The process is carried out by the Rad52 epistasis group proteins, identified by the genetic analyses of ionizing radiation sensitive *Saccharomyces cerevisiae* mutants [5, 6]. A number of Rad52 group proteins, including Rad51 and Rad54, are conserved in mammals, as is the core mechanism of homologous recombination [7]. The central protein of homologous recombination is Rad51. It mediates the critical step of homologous pairing and DNA strand exchange between the broken DNA molecule and the homologous intact repair template. Once a DSB occurs, it is processed to single-stranded DNA tails with a 3' polarity, onto which Rad51 protomers assemble into a nucleoprotein filament. This nucleoprotein filament is the active molecular entity in recognition of homologous DNA and the subsequent exchange of DNA strands. An extensive number of mediator and/or accessory proteins are implicated in assisting Rad51 at various stages of recombination [8], one of which is Rad54.

RAD54, first identified in *S. cerevisiae*, is conserved in vertebrates [9-11]. Rad54 is a member of the SWI2/SNF2 family of double-strand DNA-stimulated ATPases that modulate protein-DNA interactions [12, 13]. *Rad54* knockout mouse embryonic stem (ES) cells are ionizing radiation sensitive, have a reduced level of homologous recombination and display defects in repair of DSBs [10, 14]. A plethora of biochemical activities of Rad54 have been uncovered that have the potential to augment the central function of Rad51 in homologous recombination [15, 16]. First, Rad54 physically interacts with Rad51, both *in vitro* and *in vivo* [17-20]. It is interesting to note that in mammalian cells the interaction between the proteins occurs only in cells that have been challenged with DNA-damaging agents. This suggests that Rad54 interacts with the Rad51 nucleoprotein filament, rather than Rad51 protomers that are not engaged in recombination [20, 21]. Second, Rad54 has a potent ATPase activity that is triggered specifically by double-stranded DNA [22, 23]. Third, the interaction between Rad54 and Rad51 is not only physical but also functional, as Rad54 stimulates Rad51-mediated D-

loop formation, which is the generation of a joint between homologous DNA molecules. This function is dependent on the ATPase activity of Rad54 [22]. Fourth, the protein uses energy gained from ATP hydrolysis to translocate along the DNA double helix [24-26]. Fifth, presumably through its DNA translocase activity, Rad54 can affect the interaction of proteins with DNA. Specifically, it can influence the position of histones on DNA and remove Rad51 nucleoprotein filaments from double-stranded DNA [27-30]. Sixth, its translocase activity also allows the protein to perturb DNA structures. Rad54 can promote branch migration thereby affecting the processing of the Holliday junction, which is a 4-way DNA junction that can arise as intermediates at sites where the recombination partners are physically joined [31]. Finally, Rad54 has been shown to dissociate intermediates of the homologous recombination reaction by its branch migration activity [32]. Many of the biochemical activities of Rad54 are affected by abrogating its ATPase activity. Hence, the proper functioning of Rad54 depends on its ability to harness the energy from ATP hydrolysis, and this in turn is responsible for augmenting the role of Rad51.

In the context of a cell, a striking characteristic of a number of proteins involved in homologous recombination, including Rad51 and Rad54, is their ability to accumulate at a high local concentration into structures termed foci [20, 33, 34]. This occurs spontaneously in a low percentage of cells in S phase in the absence of exogenously induced DNA damage [35, 36]. Upon the administration of DNA damage to cells, the majority of cells display colocalizing Rad51 and Rad54 foci at sites of DNA damage [20, 37, 38]. While the nature, composition and requirement for foci formation is not apparent from a biochemical point, it is clear that the foci (particularly of Rad51) are biologically relevant, because mutant cells that cannot form them are DNA damage sensitive and display spontaneous chromosomal aberrations [39, 40]. The nature of these foci with respect to protein composition is highly dynamic. Photobleaching experiments have shown that Rad51 and Rad54 associate and dissociate with foci, with each protein having a characteristic dwell time [21]. Thus far, the *in vivo* function of Rad54 has been studied by the characterization of cells lacking the protein. In this study, we characterize cellular behavior of Rad54 and Rad51 in cells where Rad54 is physically present, but defective in its ATPase activity.

Materials and methods

Mouse embryonic stem cell culture

The mouse embryonic stem cells used to generate ES cells expressing ATPase-defective Rad54 had the genotype *Rad54*$^{wt\text{-}HA/-}$, where one allele is disrupted, and the other expresses HA-tagged Rad54 from the endogenous Rad54 locus [20]. All ES cells were cultured in 45% DMEM, 45% Buffalo rat liver cell conditioned DMEM (filtered), 10% FCS, 0.5% non-essential amino acids, penicillin (100 U/ml), streptomycin (100 μg/ml), 0.1 mM β-mercaptoethanol, and 1000 U/ml leukemia inhibitory factor (LIF).

Antibodies

The primary antibodies used in this study were: anti-Rad51 (rabbit polyclonal, [40]), anti-Rad54 (rabbit polyclonal, [10]) and anti-γH2AX (mouse monoclonal clone JBW301, Upstate). The secondary antibodies used in this study were: goat anti-rabbit coupled with alkaline phosphatase (Roche), goat anti-mouse coupled with alkaline phosphatase (Roche) and goat anti-rabbit coupled with Alexa 543 (Molecular Probes/Invitrogen).

Generation of ES cells carrying knock-in alleles expressing ATPase-defective Rad54 protein

Targeting constructs bearing either K189A or K189R mutation (Figure 1) were purified as plasmids and linearized with PvuI, and then purified using electro-elution, phenol extraction and ethanol precipitation. These linearized constructs were then electroporated into *Rad54*$^{wt\text{-}HA/-}$ cells using a 2 mm cuvette, at 117 V, 1200 μF and for 10 ms in an ECM 830 electroporator (BTX). Replacement of the *Rad54*^{HA} locus would generate ES cells with the genotype *Rad54*$^{K189A\text{-}GFP/-}$ or *Rad54*$^{K189R\text{-}GFP/-}$. Twenty four hours after electroporation, cells were subjected to puromycin selection (1μg/ml). One hundred puromycin resistant colonies were isolated for each construct and their DNA was analyzed for homologous integration of the knock-in constructs in the *Rad54-HA* locus by DNA blotting using a probe recognizing exons VII and VIII. Genomic sequence analysis was performed to confirm the correct integration and presence of mutations in the *Rad54* locus. Protein production was analyzed by immunoblot analysis using whole cell extracts from the correctly targeted clones with anti-Rad54 antibody. DNA damage sensitivities of the cells were performed using clonogenic survival assays as described [10]. Briefly, a known number of cells at various dilutions were seeded in 6 cm dishes in triplicate. For ionizing radiation, dishes were treated right away with the

indicated dosage. For the rest, cells were allowed to attach for 12 – 16 hours before treatment. MMC was added for one hour before washing. Aphidicolin, hydroxyurea and etoposide were added to cells for 12 hours before replenishing the plates with normal medium. Colonies resulting from the experiments were counted after 5 – 7 days. Finally, as a measure of homologous recombination efficiency, the frequency of homologous versus random integration of gene targeting constructs in the *Rb* locus was determined as previously described [41].

Immunofluorescence and quantification of foci

ES cells were seeded on a feeder layer of lethally irradiated (70% - 80%) confluent mouse embryonic fibroblasts and left to attach overnight. Cells were irradiated with the indicated doses of ionizing radiation using a ^{137}Cs source and left to recover for the indicated amount of time. For immunofluorescence, the cells were washed twice with PBS and fixed with 2% paraformaldehyde for 15 minutes at room temperature. Permeabilization was carried out with a quick PBS/0.1% Triton X-100 wash, followed by two more washes for 10 minutes. Blocking was carried out with a PBS+ (PBS/0.15% glycine/0.5% BSA) wash. Cells were then treated with the primary antibody diluted in PBS+ and incubated at 37°C for 90 minutes, in a dark and humid chamber. They were washed with PBS/0.1% Triton X-100, once quickly and twice for 10 minutes. Treatment with the secondary antibody was similar as outlined above. Samples were mounted on glass slides with DAPI/DAPCO/Vectashield (Vector labs) and sealed. Immunofluorescence was documented using confocal images obtained with a Zeiss LSM 510, consisting of an Axiovert 100 inverted microscope, equipped with an Argon gas laser (visualizing Alexa 488, green) and a Helium Neon laser (visualizing Alexa 543, red). Images were taken with 63x oil immersion (N.A. 1.4) on a single plane of thickness ~ 1μm, through the middle of the cell, unless otherwise stated. Live cells grown on glass could be observed by growing ES cells on MEF feeder layers on 24 mm circular glass coverslip and then mounting the coverslip on a specially adapted chamber which allowed the cells to remain in medium and at 37°C. Images were analyzed with AIM (Carl Zeiss, Jena). Fluorescent signal in an area equal to or greater than 0.5μm x 0.5μm was considered a focus. In all cases (except for live imaging and automated foci counting, below), quantification was carried out by manual counting of foci in a single confocal plane of optimal thickness 1μm through the approximate middle of the cells' nuclei. Quantification was defined as the mean number of foci per cell per confocal plane,

where the number of foci in each image were counted and then averaged by the number of cells present. Two foci were defined as colocalizing if they were at the same spot and contained both colors. Colocalization was quantified as the number of colocalizing foci as a percentage of the sum of the colocalizing foci plus the total number of non-colocalizing foci, unless otherwise specified.

Live imaging and automated foci counting

ES cells were grown up to a monolayer of 70% confluency on lethally irradiated MEF feeder layer overnight on 24mm round coverslips. Cells were irradiated with 8Gy and were transferred 45 minutes post irradiation to a specially adapted chamber fitted to the confocal microscope where they could be maintained at 37°C with 5% CO_2 for long periods of time. Using a macro for automated time-lapse imaging, the cells were imaged every 15 minutes, taking 10 Z slices (covering 9µm), for a time period of 14 hours for the wild type cells, and 29 hours for the *Rad54*$^{K189R\text{-}GFP/-}$ cells, which corresponded to the time the cells need to re-stabilize foci numbers to the ones seen at the beginning of the experiment. Movies were analyzed in AIM (Carl Zeiss, Jena) software. The maximum projection of the stacks at the different time points was then processed in ImageJ [42] to analyze foci number, where the threshold was adjusted until the size of a single focus was determined, limiting the fluorescent signal from the range of 57 to 69, so threshold starting at a value between 57 and 69. From the resulting image, the number of particles was counted using the particles analysis function. The number of cells in each frame was counted by increasing the threshold until all cells were covered. The resulting fluorescent signal/surface of the whole field was divided by the surface of a single cell. The data thus obtained was graphed as number of foci per cell over the time during which the cells were imaged.

Fluorescent recovery after photobleaching (FRAP)

A strip of 0.5µm wide spanning the width of the nucleus (without any spontaneously occurring foci) was bleached at 80% of the Argon gas laser intensity, at a single iteration to determine the mobility of free Rad54 protein [21]. Normalization of fluorescence intensities and analysis of diffusion rates were performed as described in a previous publication [21]. Because the level of fluorescence in the ES cells was low, a number of adjustments were made. The time interval at which subsequent measurements (at 10% laser intensity) were taken was 0.1 second, and 100 measurements after the

bleach pulse were made. Wild type ES cells stably transfected with pGK-GFP-p(A) were used as a positive control for fluorescence recovery, where cells with comparable fluorescence level as the knock-in cells were chosen and treated as detailed above. The recovery of free GFP in ES cells resulted in a final post-bleach relative fluorescence intensity of 0.7, indicating that the strip-FRAP protocol led to the irreversible bleaching of approximately 30% of all fluorescent protein in the cell nucleus. To determine the protein turnover in the spontaneous as well as DNA damaged induced foci in the ES cells, an area of 0.75 x 0.75μm containing a focus was bleached at 80% intensity, and fluorescence recovery was measured in the area. Fluorescence intensity measurements were taken every 0.2 seconds, with a total of 100 such measurements after the bleach pulse. Sixty cells were monitored for each genotype in three independent experiments.

Results

Generation of Rad54 ATPase-defective knock-in ES cells

To study the effect of the ATPase activity of Rad54 at the cellular level, mouse ES cells that express ATPase-defective versions of GFP-fused Rad54 from the endogenous *Rad54* locus were generated. A targeting construct, consisting of the human *RAD54* cDNA exons IV – XVIII fused to a GFP coding sequence and containing a point mutation in the Walker A ATPase domain (Figure 1A), was electroporated into ES cells of the genotype $Rad54^{wt\text{-}HA/-}$ [20]. Two different constructs were used: the first where lysine at position 189 was replaced by arginine (indicated by K189R), and second in which the lysine is replaced by alanine, the K189A mutation. The ATPase activity of the purified $Rad54^{K189R}$ and $Rad54^{K189A}$ proteins was more than 100-fold reduced in comparison to the wild type protein ([23] and data not shown). Clones carrying a homologously integrated knock-in construct were identified by DNA blot analysis. A probe that detects exons VII and VIII was used in combination with genomic DNA digested with StuI. This yielded the expected doublet of bands around 6.5 kb for the *Rad54* knock-in allele. Meanwhile, a 6.0 kb band, which is diagnostic for the Rad54 knockout allele, was observed (Figure 1B). Proper expression of the full-length Rad54-GFP fusion proteins was confirmed by immunoblot analysis (Figure 1C). In the subsequent studies, two independent clones for $Rad54^{K189R\text{-}GFP/-}$ and a single clone for $Rad54^{K189A\text{-}GFP/-}$ were used. As a positive control for all experiments, knock-in $Rad54^{wt\text{-}GFP/-}$ ES cells were used; these cells express wild type Rad54 fused to GFP from the

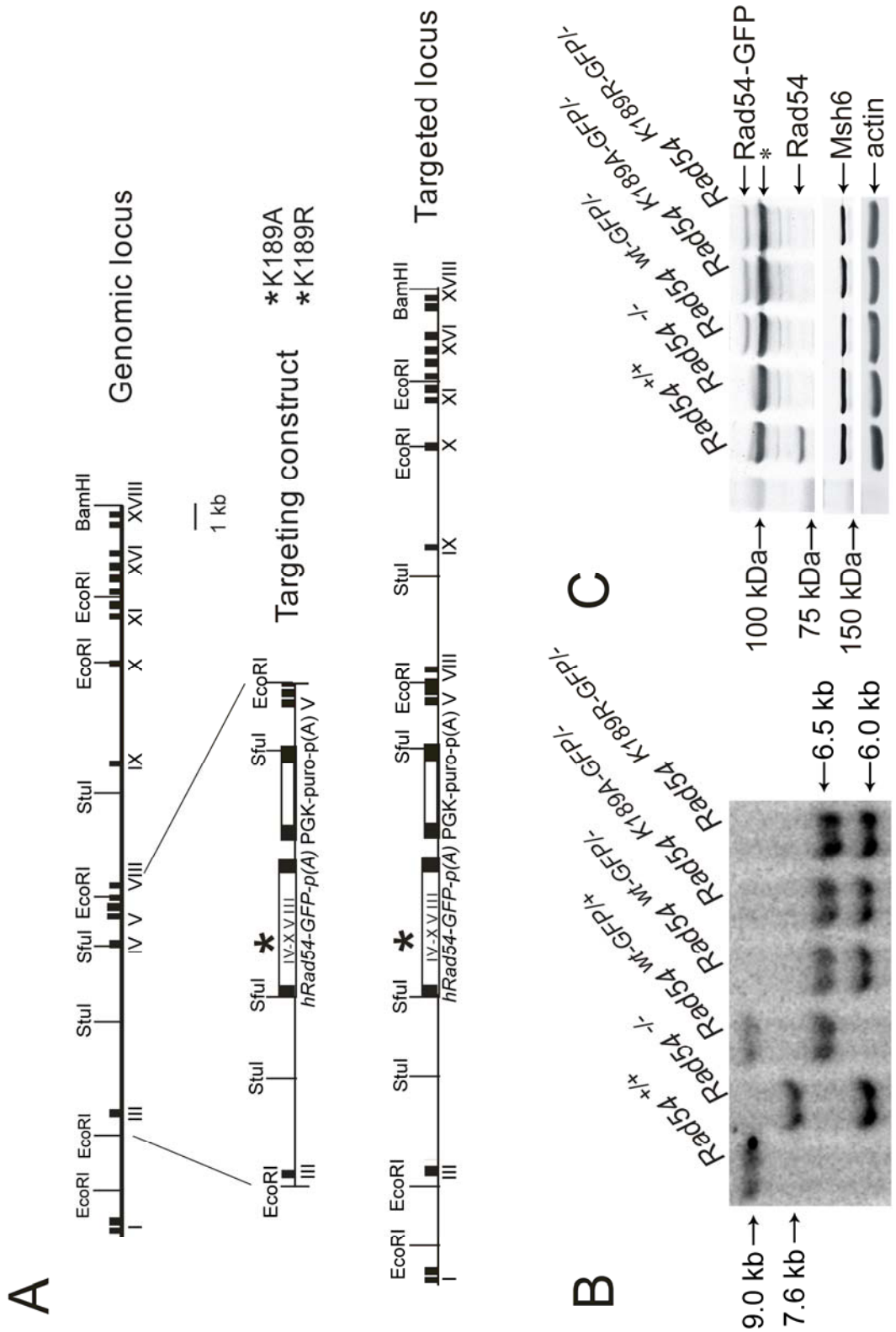
A
Genomic locus
Targeting construct
Targeted locus
1 kb
*K189A
*K189R
EcoRI
StuI
SfuI
BamHI
hRad54-GFP-p(A) PGK-puro-p(A)
B
C
Rad54 +/+
Rad54 -/-
Rad54 wt-GFP/+
Rad54 K189A-GFP/-
Rad54 K189R-GFP/-
9.0 kb
7.6 kb
6.5 kb
6.0 kb
Rad54-GFP
Rad54
Msh6
actin
100 kDa
75 kDa
150 kDa

Figure 1. Generation of mouse ES cells carrying ATPase-defective *Rad54* alleles. **(A)** Schematic representation of the mouse *Rad54* locus and the gene targeting constructs. The top line represent a 30 kb portion of endogenous *Rad54* locus, where black boxes indicate exons I through XVIII. The middle line shows the linearized targeting construct, containing the human *RAD54* cDNA sequence spanning exon IV-XVIII fused to the *GFP* coding sequence. The K189R and K189A mutations in the Walker A ATPase domain are indicated by the asterix. The construct contains a gene encoding for puromycin resistance as a selectable marker. The targeting construct will replace the regions between exon III and VIII when correctly integrated to generate the targeted allele, as shown in the targeted locus. Homologous integration results in the expression of full length, GFP-tagged Rad54 from its endogenous promoter. **(B)** DNA blot analysis of ES cells carrying the knock-in contructs. DNA blot analysis was carried out using genomic DNA purified from puromycin resistant clones and digested with StuI. Detection of bands was carried out using a probe that recognized exon VII/VIII. Restriction of the wild type allele by StuI, (indicated by "+"), yields a 9.0 kb band after hybridization with an exon VII/VIII probe. Diagnostic bands for the neomycin resistant knockout alleles, indicated by "-", are 7.6 kb for a hygromycin resistant allele and 6.0 kb for a neomycin resistant allele. Knock-in alleles are characterized by a doublet of bands around 6.5 kb. **(C)** Immunoblot analysis of proteins produced by the Rad54-GFP knock-in alleles. Whole cell extracts of ES cells with the indicated genotype were probed with affinity purified anti-human Rad54 antibody. The position of Rad54 and Rad54-GFP are indicated. The asterix indicates a non-specific signal. Antibodies against Msh6 and actin were used to confirm equal protein loading.

endogenous *Rad54* locus. The function of Rad54 is not affected by its fusion to GFP because $Rad54^{wt\text{-}GFP/-}$ cells are not DNA damage hypersensitive (Chapter 3, this thesis).

The ATPase activity of Rad54 cells contributes to DNA damage resistance and homologous recombination

Mouse $Rad54^{-/-}$ ES cells are hypersensitive to the ionizing radiation and the interstrand DNA crosslinker mitomycin C [10]. Therefore, we investigated the effect of these DNA-damaging agents on $Rad54^{K189R\text{-}GFP/-}$ and $Rad54^{K189A\text{-}GFP/-}$ ES cells. Cells expressing ATPase-defective versions of Rad54 were hypersensitive to ionizing radiation and mitomycin C compared to isogenic control cells. This hypersensitivity was similar to that demonstrated by cells lacking Rad54 protein altogether (Figure 2A). These cell lines were also tested for their sensitivities to agents that interfered with replication fork progression, namely UV, aphidicolin, hydroxyurea and etoposide (Figure 2B). There is no clear hypersensitivity of $Rad54^{-/-}$ cells or cells with ATPase point mutations to any of these agents, suggesting that Rad54 is probably not involved in the repair of stalled replication forks under the conditions tested.

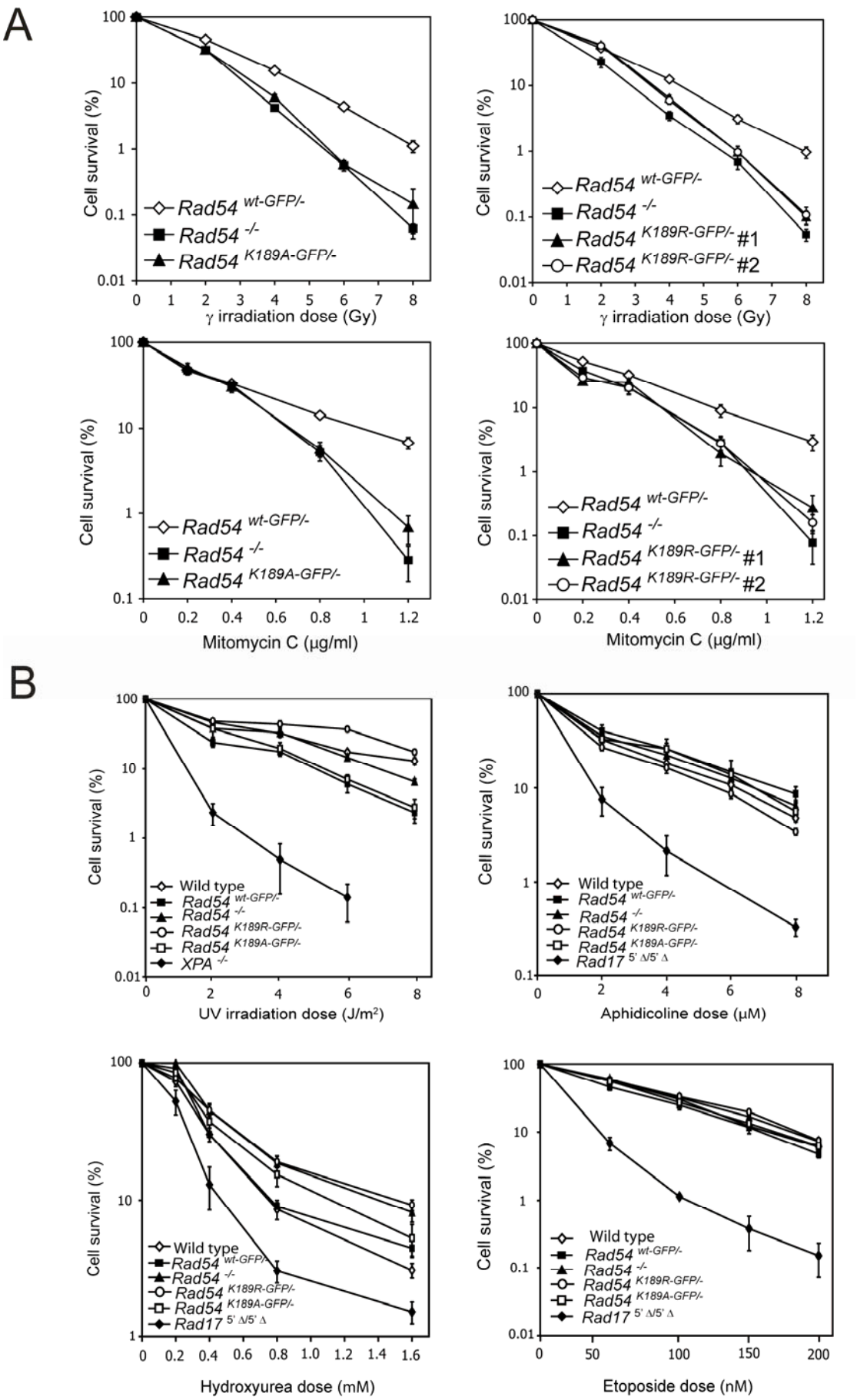
A
Cell survival (%)
γ irradiation dose (Gy)
Rad54 wt-GFP/-
Rad54 -/-
Rad54 K189A-GFP/-
Rad54 K189R-GFP/- #1
Rad54 K189R-GFP/- #2
Mitomycin C (μg/ml)
B
UV irradiation dose (J/m²)
Wild type
Rad54 wt-GFP/-
Rad54 -/-
Rad54 K189R-GFP/-
Rad54 K189A-GFP/-
XPA -/-
Aphidicoline dose (μM)
Rad17 5' Δ/5' Δ
Hydroxyurea dose (mM)
Etoposide dose (nM)

Figure 2. Effect of DNA-damaging agents on survival of Rad54 ATPase deficient cells (A) Irradiation and MMC clonogenic survival assays. ES cells of the indicated genotypes were tested for their ability to survive treatments with increasing doses of ionizing radiation (top panels) or mitomycin C (bottom panel) using clonogenic survival assays. The assays were performed in triplicate and the error bars indicated the standard error of the mean. **(B)** Clonogenic survival assays with replication stalling agents. ES cells of indicated genotypes were tested for their ability to survive treatments with increasing doses of UV, aphidicolin, hydroxyurea and etoposide as described. In each case, a hypersensitive cell line was used as a control (*XPA*$^{-/-}$ for UV, *Rad17* $^{5'\Delta/5'\Delta}$ for the others).

Next we tested the effect of the Rad54 ATPase activity on homologous recombination. As a measure of homologous recombination efficiency, we determined the efficiency of homologous gene targeting [21, 41]. ES cells of the genotypes indicated in Table 1 were electroporated with a linearized targeting construct for the Rb locus that carried a hygromycin selectable marker gene. Genomic DNA was isolated from individual clones and analyzed by DNA-blotting to discriminate between homologous and random integration events. Homologous recombination efficiency was measured as the percentage of clones containing the homologously integrated targeting construct relative to the total number of drug-resistant clones analyzed (Table 1). The homologous targeting efficiency of approximately 32% in *Rad54*$^{wt\text{-}GFP/-}$ ES cells was reduced to around 1% in *Rad54*$^{K189R\text{-}GFP/-}$ and *Rad54*$^{K189A\text{-}GFP/-}$ ES cells. A similar reduction in homologous recombination efficiency was observed in the absence of Rad54. We conclude that the ATPase activity of Rad54 is essential for its DNA repair and recombination functions *in vivo*. In these assays, the physical presence of ATPase-defective Rad54 or the complete absence of the protein results in indistinguishable phenotypes.

Defective ATP hydrolysis by Rad54 results in an increase in foci in unchallenged cells but does not show increased DNA damage

We next analyzed the Rad54 ATPase-defective mutant cells for accumulation of Rad54 foci in the absence of exogenously induced DNA damage. DNA damage repair protein foci, including Rad54, are observed in unchallenged cells are thought to be present at sites of spontaneous DNA DSBs, such as those which might occur at impaired DNA replication forks [43]. Observation of living cells using a confocal microscope revealed a significant difference in the amount of foci present in cells containing wild type Rad54 versus cells containing Rad54^{K189R} and Rad54^{K189A} (Figure 3, $p < 0.0001$). The presence of wild type Rad54 resulted in approximately 1 Rad54 focus per cell per

Genotype	Targeting Efficiency at Rb locus
Rad54$^{wt\text{-}GFP/-}$	31.9% (16 out of 46)
Rad54$^{K189R\text{-}GFP/-}$	0.95% (1 out of 105)
Rad54$^{K189A\text{-}GFP/-}$	1.2% (1 out of 81)
Rad54$^{-/-}$	<1% (0 out of 82)*

Table 1. Efficiency of homologous recombination in Rad54 ATPase-defective cells. ES cells with the indicated genotypes were electroporated with a linearized Rb-Hyg construct [41]. Hygromycin resistant clones were expanded, genomic DNA purified, and subjected to DNA blot analysis to distinguish between randomly and homologously integrated events. Values indicate the percentage of clones that contain the homologously integrated targeting construct relative to the total number of clones analyzed. Absolute numbers are indicated in parentheses. The differences in recombination efficiency between *Rad54*$^{wt\text{-}GFP/-}$ cells and cells of all other genotypes listed are significant ($p < 0.001$), while the difference between the mutant genotypes is not. *This value was previously determined [10].

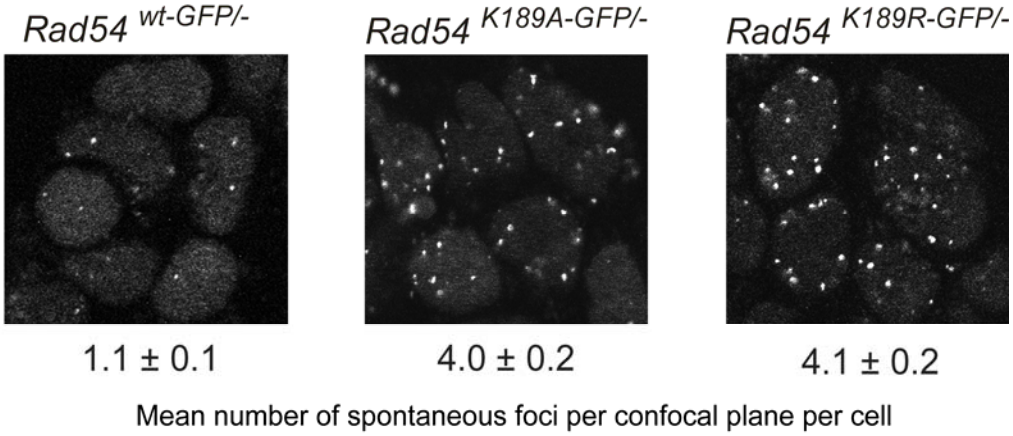

Figure 3. Cellular behavior of wild type and ATPase-defective Rad54. Confocal images of living ES cell with the indicated genotypes are shown. ES cells were grown on a MEF feeder layer and imaged live with the confocal microscope. Spontaneously occurring accumulations of wild type and ATPase-defective Rad54-GFP can be observed as nuclear foci. The mean number of spontaneous foci per cell per confocal plane as well as the standard error of the mean was determined by counting at least 250 cells per genotype. The difference in the mean number of foci in cells expressing wild type Rad54 is significant from the mean number of foci in the cells expressing either version of ATPase-defective Rad54 ($p < 0.0001$), as determined by student's t test.

confocal slice (number of cells, n = 360, mean = 1.1, standard error of mean (SEM) = 0.1), while cells in which Rad54 is ATPase-defective displayed on average approximately 4 foci (*Rad54*$^{K189A\text{-}GFP/-}$: n = 309, mean = 4.0, SEM = 0.2; *Rad54*$^{K189R\text{-}GFP/-}$: n = 293, mean = 4.1, SEM = 0.2). Also, the percentage of cells containing 5 or more Rad54 foci per confocal slice was approximately 4-fold higher in *Rad54*$^{K189R\text{-}GFP/-}$ and *Rad54*$^{K189A\text{-}GFP/-}$ compared to *Rad54*$^{wt\text{-}GFP/-}$ ES cells (data not shown). It should be noted that the increase in spontaneous foci is only observed when all Rad54 molecules in the cell are ATPase-defective, since such an increase is absent in *Rad54*$^{K189R\text{-}GFP/+}$ and *Rad54*$^{K189A\text{-}GFP/+}$ cells (data not shown).

A number of proteins involved in the cellular response to DNA damage and DNA damage repair are known to accumulate in foci at sites of DNA damage [4]. Therefore, we examined whether the increased number of 'spontaneous' foci detected in Rad54 mutant cells correlated with sites of DNA damage in these cells. First, we investigated the level of γH2AX, an early marker for DSBs, in whole cell extracts from wild type and mutant cell lines. Anti-γH2AX antibodies recognize a specific phosphorylation on the histone variant H2AX that is triggered by certain types of DNA damage, including DNA DSBs [44]. However, no increase in the basal level of H2AX phosphorylation was detected by immunoblotting in populations of unchallenged *Rad54*$^{K189R\text{-}GFP/-}$ and *Rad54*$^{K189A\text{-}GFP/-}$ compared to *Rad54*$^{wt\text{-}GFP/-}$ ES cells (Figure 4A, left panel). The cells expressing ATPase-defective Rad54 were able to increase H2AX phosphorylation upon treatment with ionizing radiation (Figure 4A, right panel). In addition, γH2AX accumulates in foci after DSB induction, which was analyzed by immunofluorescence experiments in our cells (Figure 4B and C). Since both mutant cells behave similarly in the Western analysis, only *Rad54*$^{K189R\text{-}GFP/-}$ cells were examined. Untreated *Rad54*$^{wt\text{-}GFP/-}$ and *Rad54*$^{K189R\text{-}GFP/-}$ ES cells displayed similar levels of γH2AX foci per cell per confocal slice (*Rad54*$^{wt\text{-}GFP/-}$: n = 53, mean = 9.0, SEM = 0.7; *Rad54*$^{K189R\text{-}GFP/-}$: n = 59, mean = 9.7, SEM = 0.8; p = 0.54), consistent with the immunoblotting results (Figure 4B, quantification in Figure 4C). Furthermore, qualitative analysis revealed that ES cells contain many more γH2AX foci than Rad54 foci (Figure 4B). However, most, if not all, Rad54 foci (either those made up of wild type Rad54-GFP or ATPase-defective Rad54-GFP) localize at sites of H2AX phosphorylation. Therefore, within the limitations of this technique, we conclude that the number of γH2AX foci and level of γH2AX phosphorylation are similar in the various genotypes, and this illustrates that Rad54 ATPase mutants do not contain a dramatic increase in level of DSBs compared to wild

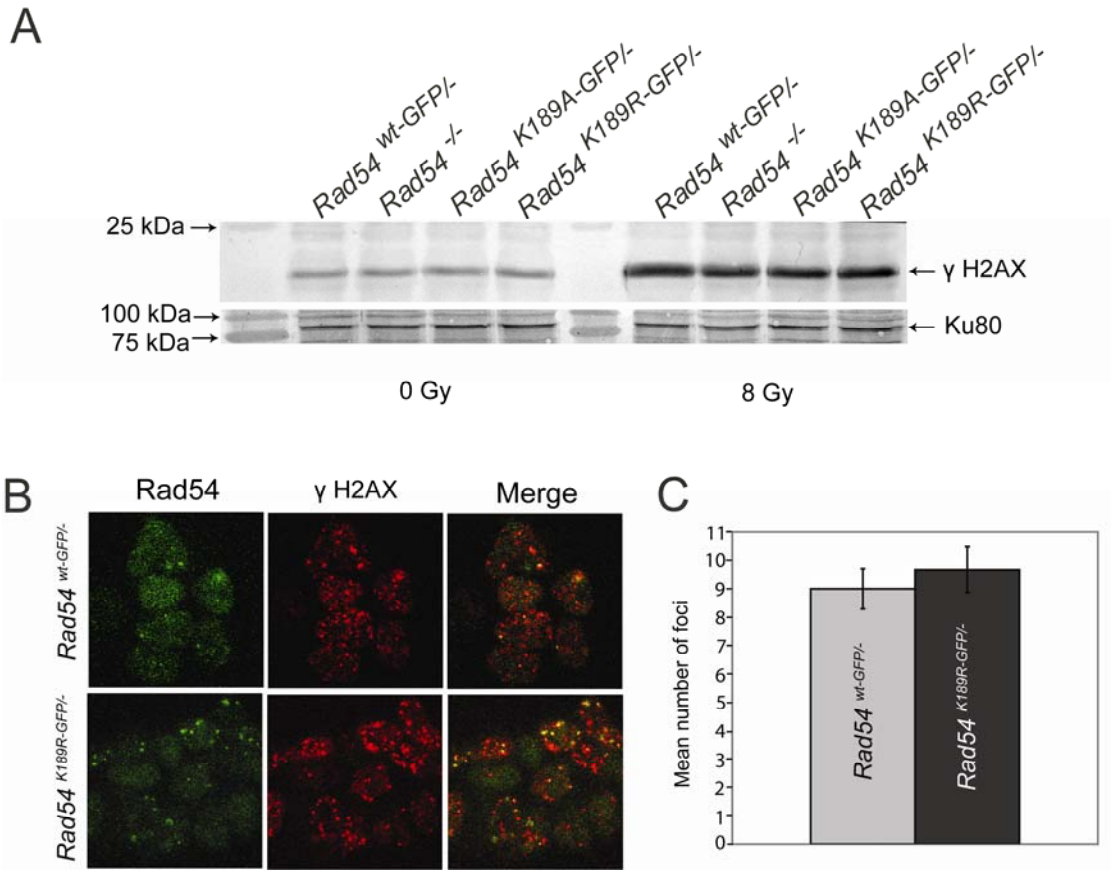

Figure 4. Analysis of DNA damage markers in Rad54 ATPase-defective ES cells. **(A)** Detection of γ-H2AX by immunoblotting. Whole cell extracts of ES cells with the indicated genotype were prepared either before (left hand panel) or 1 hour after irradiation with 8 Gy (right hand panel) and analyzed by immunoblotting using an anti-γH2AX antibody. Antibodies against Ku80 were used to confirm equal loading (lower panel). **(B)** Detection of γ-H2AX by immunofluorescence in untreated ES cells. The top panel shows Rad54-GFP, γ-H2AX staining and the merged image of *Rad54*$^{wt\text{-}GFP/-}$ ES cells, while the bottom panel shows the same in *Rad54*$^{K189R\text{-}GFP/-}$ cells. (**C**) Quantification of the average number of γH2AX foci *Rad54*$^{wt\text{-}GFP/-}$ and *Rad54*$^{K189R\text{-}GFP/-}$ ES cells. γH2AX foci were counted in one confocal plane for at least 50 cells and the mean is graphed, along with error bars representing the standard error of the mean. The means of γH2AX foci between wild type and *Rad54*$^{K189R\text{-}GFP/-}$ cells are not significantly different ($p = 0.54$), as determined by the student's t-test.

type cells. Hence, the increase in spontaneous Rad54 foci in unchallenged *Rad54*$^{K189R\text{-}GFP/-}$ and *Rad54*$^{K189A\text{-}GFP/-}$ ES cells is not due to an increased level of DSBs in these cells as identified by γH2AX.

ATP hydrolysis by Rad54 affects Rad51 foci behavior in unchallenged cells

Rad54 is an accessory protein for Rad51, which performs the core reaction of homologous recombination, homologous DNA paring and DNA strand exchange [4].

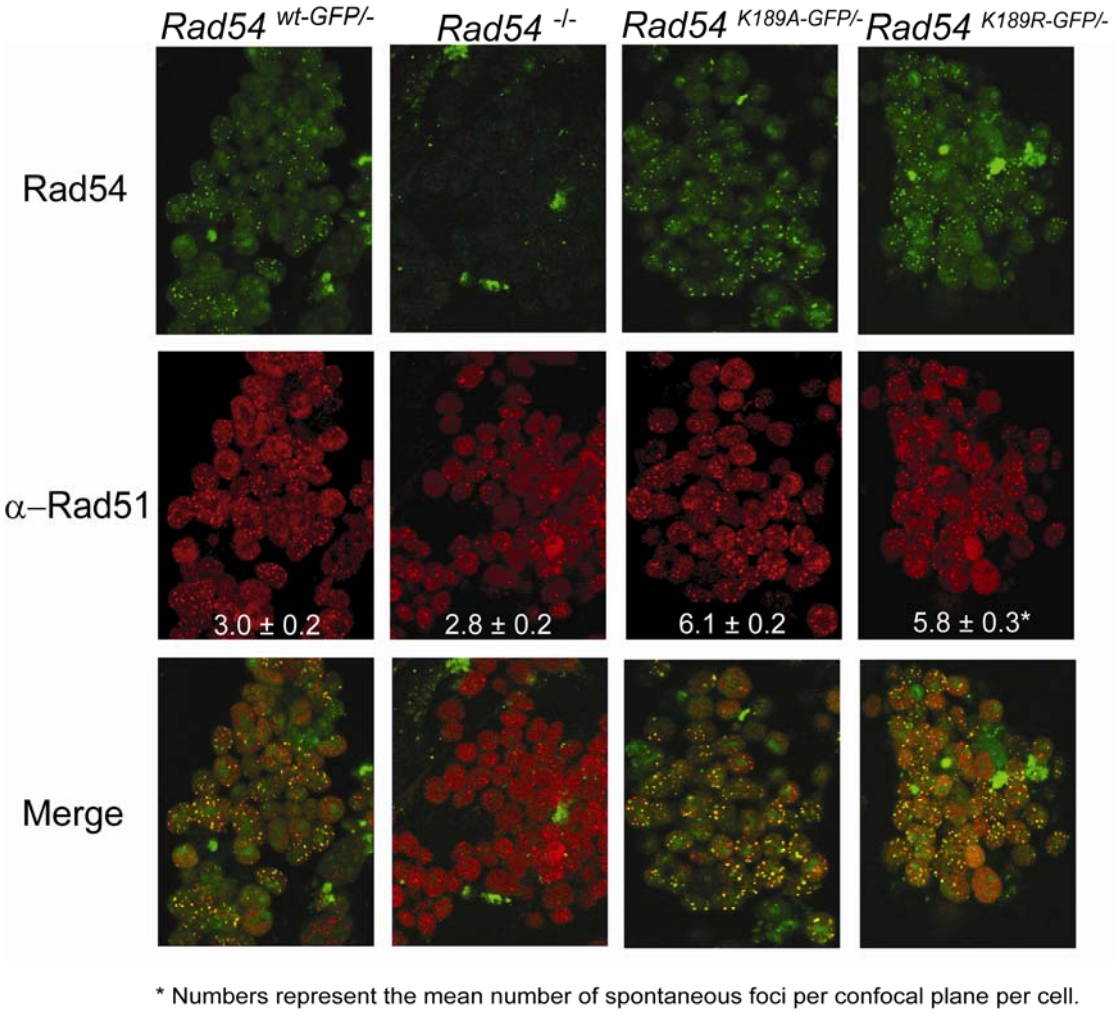

Figure 5. Effect of Rad54 ATPase activity on Rad51 foci. Rad51 immunostaining in untreated ES cells of the indicated genotypes. The top panels show confocal images of Rad54 as detected by GFP fluorescence. The middle panels show the Rad51 staining pattern as detected by anti-Rad51 antibody staining. The merged pictures are shown in the bottom panel. The mean number of Rad51 foci per cell per confocal plane, determined by counting at least 150 cells, is indicated. The difference in number of Rad51 foci per cells between *Rad54*$^{wt\text{-}GFP/-}$ and *Rad54*$^{-/-}$ ES cells and the difference between *Rad54*$^{K189R\text{-}GFP/-}$ and *Rad54*$^{K189A\text{-}GFP/-}$ ES cells is not significant ($p = 0.58$, 0.50 respectively), while the difference between these two groups is ($p < 0.0001$), as determined by student's t test.

The proteins physically interact and work together closely in a number of biochemical assays [8]. At the cellular level, both proteins colocalize in DNA damage-induced foci [20]. We analyzed Rad51 foci in the mutant cells to determine whether the ATPase activity of Rad54 impacted the behavior of Rad51 *in vivo*. Unchallenged ES cells were fixed, stained with an antibody against Rad51. Both Rad51 and Rad54-GFP were

detected by confocal microscopy (Figure 5). Compared to cells expressing wild type Rad54-GFP, cells expressing the ATPase-defective variants of Rad54-GFP displayed a statistically significant two-fold increase in the number of 'spontaneous' Rad51 foci (*Rad54*$^{wt\text{-}GFP/-}$: n = 223, mean = 3.0, SEM = 0.2; *Rad54*$^{K189A\text{-}GFP/-}$: n = 202, mean = 6.1, SEM = 0.2; *Rad54*$^{K189R\text{-}GFP/-}$: n = 168, mean = 5.8, SEM = 0.3; $p < 0.0001$ for comparison of wild type with mutants). The difference in Rad54 foci number between wild type and mutants seems to be more pronounced in live cells (Figure 3) than in fixed cells (Figure 5). This could be due to fixation of cells, which results in cell shrinkage as well as a decrease in fluorescent intensity. In either case however, the difference in foci numbers are significant. Furthermore, almost all Rad54 foci detected (>90%), including those of Rad54^{K189R} and Rad54^{K189A}, colocalized with Rad51 (Figure 5). Interestingly, while the number of Rad51 foci was elevated in cells expressing the ATPase-defective Rad54 mutants, it was not increased in cells completely lacking Rad54 (n = 187, mean = 2.8, SEM = 0.2; $p = 0.58$ for comparison between wild type and knockout, $p < 0.0001$ for comparison of knockout with mutants). This defines the only phenotypical difference between Rad54 mutant and *Rad54*$^{-/-}$ cells observed so far.

ATPase-defective Rad54 causes a delay in irradiation induced foci disappearance

It has been shown previously that the number of Rad54 foci in cells increases after DSB induction, such as with γ irradiation [20]. We wanted to investigate how the ATPase activity of Rad54 influences the induction of Rad54 foci by DNA damage. To study this, we carried out time course experiments, looking at the number of foci in cells irradiated with 8 Gy and fixed at different time points. The average number of Rad54 foci in the different ES cells was determined (Figure 6A). The number of Rad54 foci induced upon DNA damage induction peaked at 2 hours for all genotypes before decreasing over time. However, even after 24 hours, the levels of foci in mutant cells did not return to that of unchallenged cells. A matching time course was also done with Rad51 foci, and a comparable profile of foci disappearance, as of Rad54, was observed (data not shown).

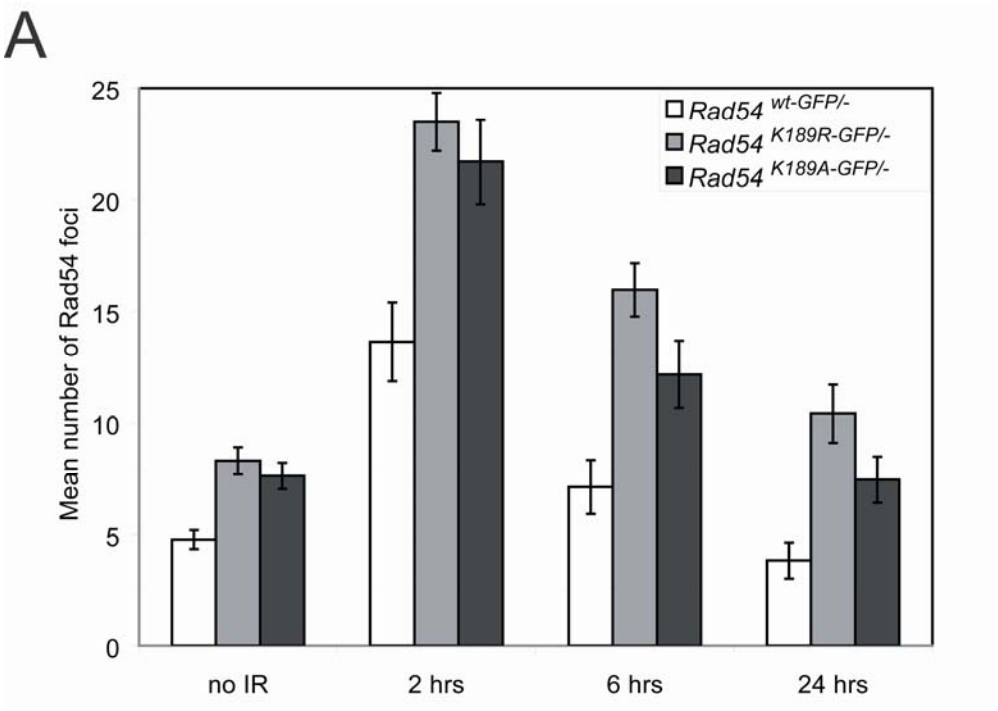

Figure 6. Quantification of Rad54 foci over time in response to irradiation.

(A) Manual quantification of the disappearance of irradiation induced Rad54 foci in fixed cells. The mean number of Rad54 foci per cell per confocal plane was determined at time points 2, 6 and 24 hours post irradiation in *Rad54*$^{wt\text{-}GFP/-}$, *Rad54*$^{K189R\text{-}GFP/-}$ and *Rad54*$^{K189R\text{-}GFP/-}$ ES cells.

In order to investigate the rate of DNA damage-induced Rad54 foci disappearance in wild type and ATPase-defective cells, a more automated system of foci analysis and counting was developed, using time lapse movies analyzed by AIM and Image J. The advantage of this approach was that live cells, rather than fixed cells, were documented. In addition, this method greatly increases the time resolution at which measurements can be made. It should be noted that the automated foci counting was done on projections of 10 confocal slices in this experiment using ImageJ, and this is different from previous quantifications which were done manually and on a single confocal slice. Since *Rad54*$^{K189A\text{-}GFP/-}$ cells behave in a similar way to *Rad54*$^{K189R\text{-}GFP/-}$ cells in terms of Rad54 foci dynamics (Figure 6A), this experiment was done only with the K189R mutant cell line. Imaging of live *Rad54*$^{wt\text{-}GFP/-}$ and *Rad54*$^{K189R\text{-}GFP/-}$ ES cells was started 45 minutes after irradiation with 8 Gy (Figure 6B).

Several observations can be made from this experiment. First, the number of foci in the *Rad54*$^{K189R\text{-}GFP/-}$ cells is always higher than the wild type and this corresponds to the result obtained with manual counting of foci per cell per confocal slice. Second, the

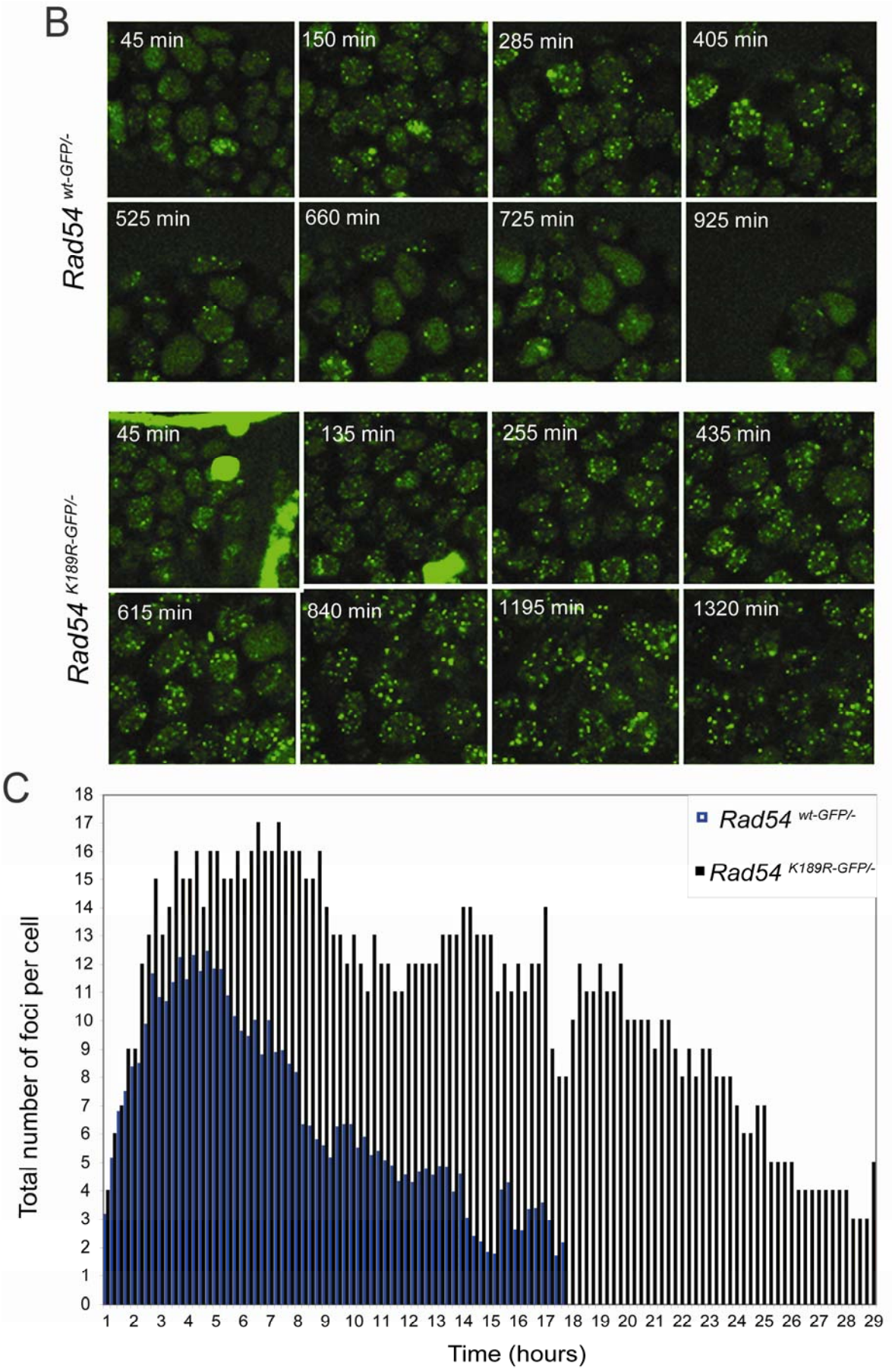
B
Rad54 wt-GFP/-
45 min
150 min
285 min
405 min
525 min
660 min
725 min
925 min
Rad54 K189R-GFP/-
45 min
135 min
255 min
435 min
615 min
840 min
1195 min
1320 min
C
Rad54 wt-GFP/-
Rad54 K189R-GFP/-
Total number of foci per cell
Time (hours)

Figure 6. Quantification of Rad54 foci over time in response to irradiation. (con't) **(B)** Stills from time-lapse movies of irradiated *Rad54*$^{wt\text{-}GFP/-}$ and *Rad54*$^{K189R\text{-}GFP/-}$ ES cells. Cells were treated with 8 Gy and imaged every 15 minutes starting 45 minutes post irradiation. Every picture represents the maximum projection image of each frame obtained from the resulting movie at the time point indicated. **(C)** Automated quantification of foci per cell over time from the movies represented in panel B. The mean foci number per cell for each genotype was obtained with ImageJ from the maximum projection image of a 10 slice Z stack through each frame and was graphed against time.

dynamics of the formation of foci after 8Gy is comparable in wild type and mutant; foci numbers peaks at around 3 to 4 hours in both cell types. Third, foci number starts to diminish faster in wild type as compared to the mutant. While the peak of foci number in wild type stays for an interval of two hours ($3 \leq t \leq 5$ hours), time interval in the mutant is increased to about six hours ($3 \leq t \leq 9$ hours). Finally, the time taken for the mutant cell line to re-stabilize irradiation induced foci to the number at the start of the experiment is longer than in the wild type (29 hours for mutant, 14 hours for wild type). Using an alternative quantification, the time required for a two fold reduction in the number of Rad54 from their peak values for *Rad54*$^{K189R\text{-}GFP/-}$ cells is approximately 18 hours, while for wild type cells, it is 5 hours. Collectively, this data indicates a delay in foci dynamics in response to irradiation in the K189R mutant cells compared to wild type cells. When the number of foci over time were compared using an ANOVA analysis, the difference was significant ($p<0.0001$).

Attenuation of ATP hydrolysis by Rad54 increases its residence time in foci

The ATPase activity of Rad54 is essential for many of its biochemical activities [16], but its effect on the dynamics of the protein is unknown. Using photobleaching experiments in living cells, we determined previously that all of the homogenously distributed Rad54-GFP in the nucleoplasm is mobile with a diffusion rate that is approximately 1.3-fold less than GFP itself [21]. In order to determine whether the ATPase activity of Rad54 influences its mobility, we performed fluorescence redistribution after photobleaching (FRAP) experiments using the wild type ($n = 60$) and ATPase-defective Rad54-GFP knock-in ES cells ($n = 60$ for both). Fluorescence in a small strip spanning the width of the nucleus was bleached by applying a 0.2s high-intensity laser pulse. Any possible spontaneous Rad54 foci were excluded. Fluorescence recovery in the strip was monitored every 0.1s for 10s in about 60 nuclei per genotype. As a control, the recovery rates of Rad54-GFP were compared with ES cells

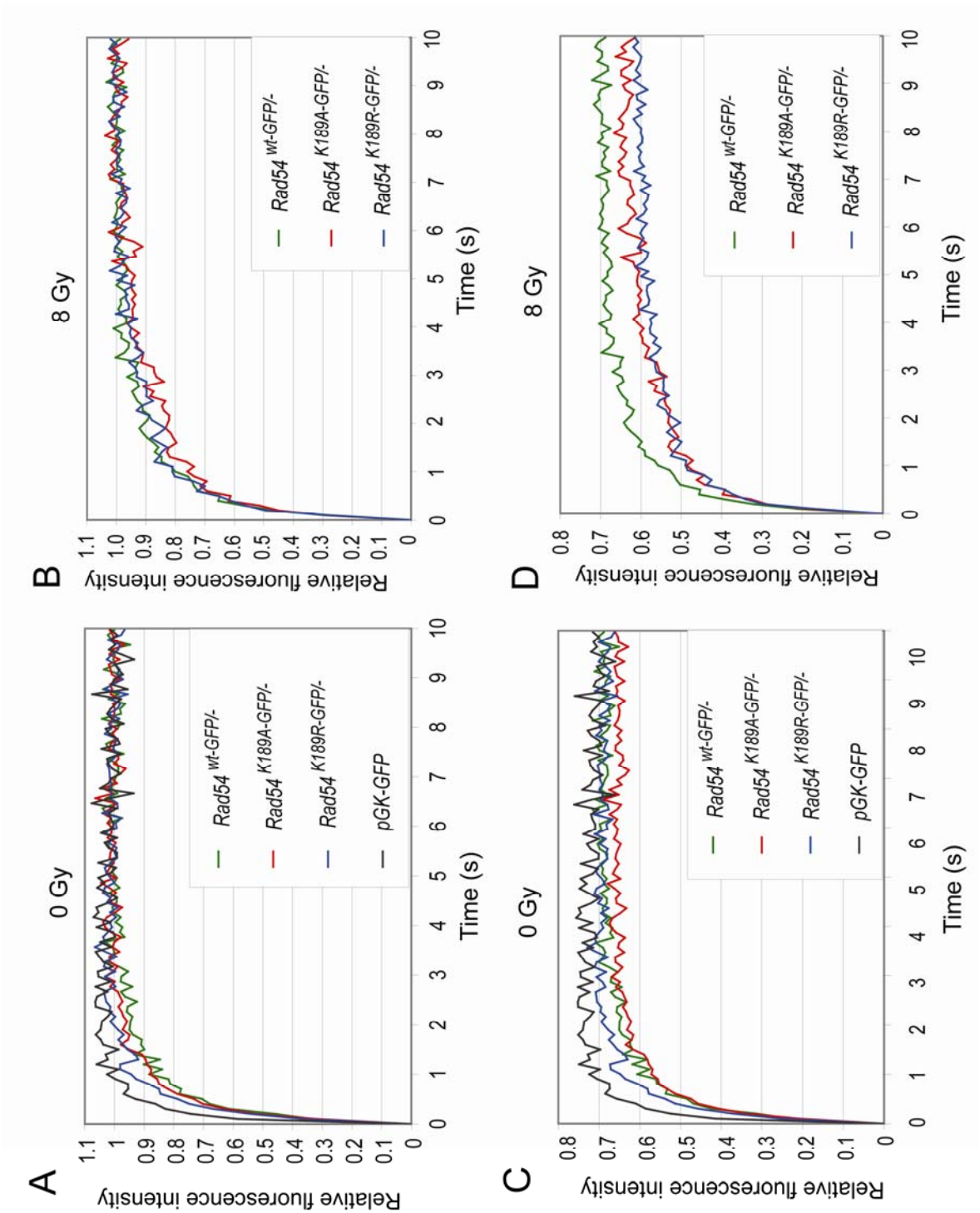
A
0 Gy
Relative fluorescence intensity
Time (s)
Rad54 wt-GFP/-
Rad54 K189A-GFP/-
Rad54 K189R-GFP/-
pGK-GFP
B
8 Gy
Relative fluorescence intensity
Time (s)
Rad54 wt-GFP/-
Rad54 K189A-GFP/-
Rad54 K189R-GFP/-
C
0 Gy
Relative fluorescence intensity
Time (s)
Rad54 wt-GFP/-
Rad54 K189A-GFP/-
Rad54 K189R-GFP/-
pGK-GFP
D
8 Gy
Relative fluorescence intensity
Time (s)
Rad54 wt-GFP/-
Rad54 K189A-GFP/-
Rad54 K189R-GFP/-

Figure 7. **Influence of the ATPase of Rad54 on its nuclear mobility.** ES cells of the indicated genotype were subjected to FRAP analyses to determine the effect of Rad54's ATPase activity on its mobility in the nucleoplasm either in the presence or absence of exogenously induced DNA damage. Strip-FRAP analysis of ATPase proficient and deficient Rad54 to determine its relative effective diffusion rate and immobile fraction in the nucleus of ES cells before **(A & C)** and 1 hour after irradiation with 8 Gy **(B & D)**. Graphs represent the mean values of relative fluorescence from a total of at least 60 cells bleached. Fluorescence in a small strip spanning the entire nucleus was bleached with a short high intensity laser pulse and its recovery was monitored over time. The average of relative fluorescence intensity was plotted as a function of time for each protein using two different normalization methods (see text). In addition to Rad54 and its variants, the mobility of GFP itself was monitored (pGK-GFP).

expressing free GFP. It is presumed that at these levels, which are comparable by eye, all GFP molecules are freely mobile through the nucleus.

FRAP recovery curves were compared for two parameters – the effective diffusion rate and the immobile protein fraction. The effective diffusion rate was determined by the rate of fluorescence recovery during the $0 \leq t \leq 3$ second time interval. The immobile protein fraction was determined by the level that is reached by relative fluorescence intensity at the end of the measurement ($t = 10$ seconds). In order to verify the first parameter, the relative fluorescence was plotted over time after normalizing the data by setting the value of the immediate post-bleach fluorescence intensity ($t = 0$ seconds) to 0, and the final post-bleach fluorescence intensity to 1 (Figure 7A). In this way we determined that in unchallenged cells, the rate of fluorescence recovery for the three genotypes was similar, indicating the similarity in diffusion behavior of GFP-tagged Rad54. The recovery of free GFP is clearly faster than the fusion proteins, which is likely to be due to differences in size. The rapid recovery of relative fluorescence is an indication of the swift rate of protein diffusion through the nucleoplasm. To elucidate the second parameter, that is, the fraction of immobilized Rad54, relative fluorescence intensity was plotted over time after normalizing the data by setting the value of the pre-bleach fluorescence intensity to 1 and the immediate post-bleach ($t = 0$ seconds) fluorescence intensity to 0 (Figure 7C). The recovery of free GFP in ES cells resulted in a final post-bleach relative fluorescence intensity of 0.7, indicating that the strip-FRAP protocol led to the irreversible bleaching of approximately 30% of all fluorescent protein in the cell nucleus. The relative fluorescence intensities of $Rad54^{GFP}$, $Rad54^{K189R\text{-}GFP}$, and $Rad54^{K189A\text{-}GFP}$ proteins recovered to the approximate levels

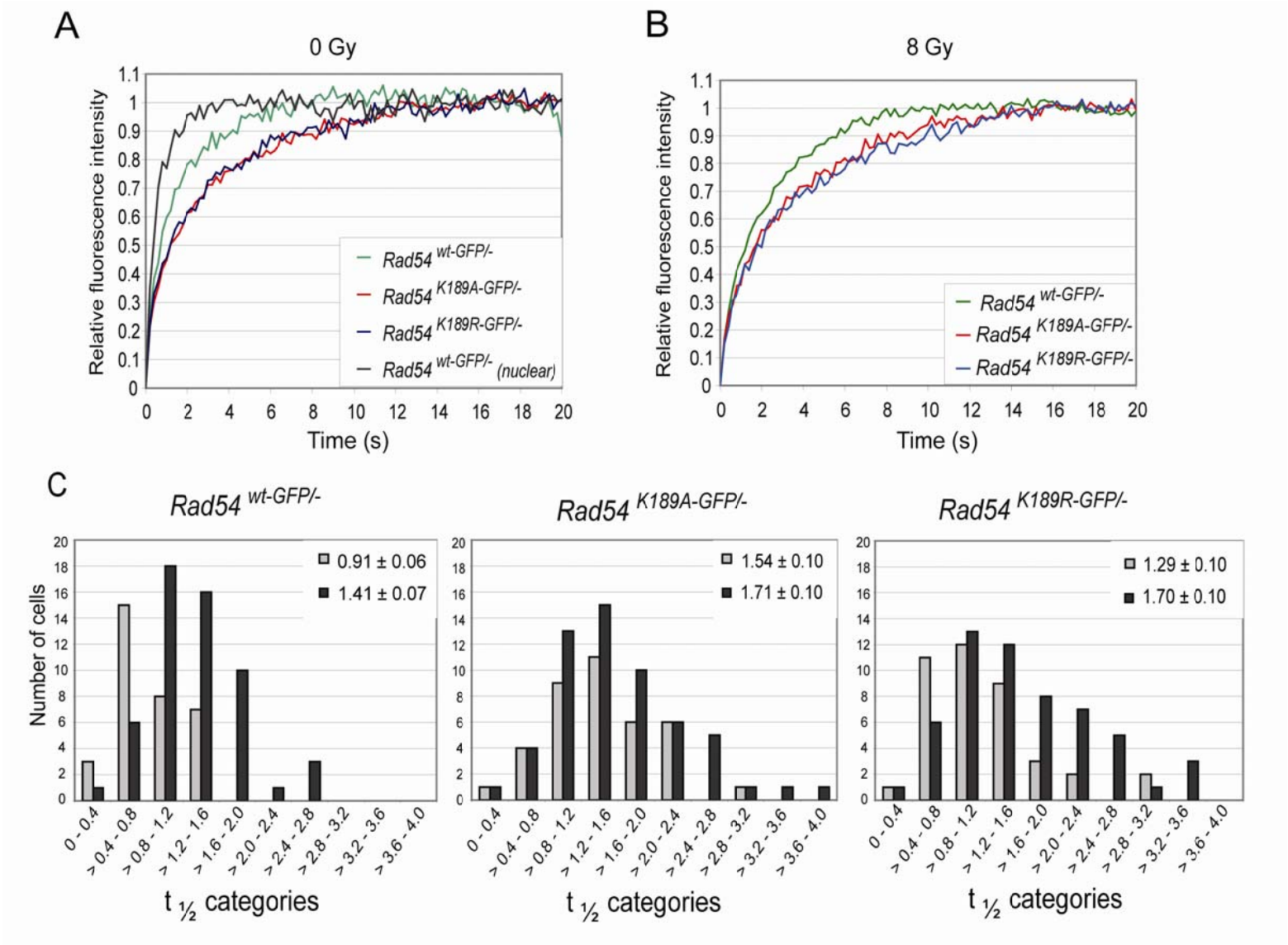
A
0 Gy
Relative fluorescence intensity
Time (s)
Rad54 wt-GFP/-
Rad54 K189A-GFP/-
Rad54 K189R-GFP/-
Rad54 wt-GFP/- (nuclear)
B
8 Gy
Relative fluorescence intensity
Time (s)
Rad54 wt-GFP/-
Rad54 K189A-GFP/-
Rad54 K189R-GFP/-
C
Rad54 wt-GFP/-
0.91 ± 0.06
1.41 ± 0.07
Rad54 K189A-GFP/-
1.54 ± 0.10
1.71 ± 0.10
Rad54 K189R-GFP/-
1.29 ± 0.10
1.70 ± 0.10
Number of cells
0 - 0.4
> 0.4 - 0.8
> 0.8 - 1.2
> 1.2 - 1.6
> 1.6 - 2.0
> 2.0 - 2.4
> 2.4 - 2.8
> 2.8 - 3.2
> 3.2 - 3.6
> 3.6 - 4.0
t ½ categories

Figure 8. Spot FRAP analysis of Rad54 in foci. (A & B) Spot-FRAP analysis of Rad54 in foci. A small square containing an individual Rad54 focus was bleached and monitored for fluorescence recovery for each indicated genotype. The average of the relative fluorescence intensities, obtained from a total of at least 35 cells bleached was plotted against time where the value immediately after the bleach is normalized to 0, and the final post-bleach intensity to 1. The left panel displays the results of experiments performed on untreated cells containing spontaneous foci **(A)**, while foci analyzed in the right panel were induced by treating cells with 8 Gy of ionizing radiation **(B)**. As a control the fluorescence recovery of non-foci associated Rad54 was quantified (black line). **(C)** Histogram of Spot-FRAP analysis. The $t_{½}$ obtained from individual fluorescence recovery curves of all three cell lines were categorized and plotted in a histogram. Light grey (▫) represents cells untreated by irradiation, and dark grey (■) represents cells treated with irradiation.

of GFP itself (Figure 7C), showing that the ATPase activity of Rad54 is not required for the nuclear mobility of its non-foci associated fraction.

The mobility of non-foci associated Rad54 protein was also investigated in irradiated cells, where it was found that the rate of fluorescence recovery during $0 \leq t \leq 3$ second interval was comparable for all cell lines as shown in Figure 7B (n = 61 for wild type, n = 56 for both mutants). In contrast to the unchallenged cells, the ATPase mutants displayed a lower level of final post-bleach fluorescence recovery when treated with irradiation (Figure 7D). This could be due to the fact that most of ATPase-defective Rad54 is associated with foci after irradiation and this results in a larger immobile fraction than in cells expressing wild type protein. The fact that the number of foci per cell in the mutants is higher than in wild type 2 hours post irradiation confirms this premise (Figure 6).

A remarkable feature of DNA damage induced foci is their highly dynamic nature. We previously showed that these accumulations of proteins are not static but that their components reversibly associate and dissociate [21]. To determine whether the ATPase activity of Rad54 influences this cell biological feature of the protein we analyzed protein turnover in the foci using photobleaching techniques. For this purpose, we used a spot-FRAP protocol in which a small square encompassing a single Rad54-containing focus was bleached and subsequently monitored (Figure 8).

In this way we quantified the fluorescence recovery of ATPase-proficient (n = 37) and defective Rad54 (n = 37 for $Rad54^{K189A\text{-}GFP/-}$, n = 43 for $Rad54^{K189R\text{-}GFP/-}$) (Figure 8A). As a control, the same protocol was applied to non-foci associated Rad54-GFP in the wild type cells (n = 49). The data was normalized by setting the post-bleach fluorescence intensity to 1, while the fluorescence intensity immediately after the bleach

pulse was set to 0 for each focus. It was interesting to note that the recovery rate of fluorescence was significantly reduced for foci formed by ATPase-defective Rad54 compared to wild type Rad54 (Figure 8A). In addition, the presence of a Rad54-GFP focus within the region of interest retards the rate of fluorescence recovery as compared to free Rad54-GFP in the wild type cells (Figure 8A, compare black line to green line). Protein turnover is normal when a wild type allele is present (*Rad54*$^{K189A\text{-}GFP/+}$ and *Rad54*$^{K189R\text{-}GFP/+}$), making this a recessive effect (data not shown). To quantify this retardation of fluorescence recovery we determined the half-life ($t_{½}$) of fluorescence recovery in the Rad54 foci formed by the different Rad54 variants; $t_{½}$ is defined as the mean of the time at which the relative fluorescence intensity reached half the final fluorescence intensity in each cell measured for each genotype. The average value of $t_{½}$ obtained for the three different Rad54 variants is shown in parentheses in the legends for Figure 8C. The $t_{½}$ of ATPase proficient foci was 0.91 ± 0.06 seconds, which represents a faster recovery compared to *Rad54*$^{K189A\text{-}GFP/-}$ (1.54 ± 0.10 seconds) and *Rad54*$^{K189R\text{-}GFP/-}$ (1.29 ± 0.10 seconds) ($p < 0.001$ for comparison between wild type and mutants). Therefore, the inability of Rad54 to hydrolyze ATP resulted in an approximately 40% – 60% slower fluorescence recovery in foci. To visualize these differences more clearly, we grouped and plotted the $t_{½}$ values obtained as outlined above in a histogram (Figure 8C). The resultant graph showed a normal distribution for the wild type Rad54 with a relatively small base, extending between t = 0 to 1.6 seconds. The peak was at >0.4 – 0.8 seconds. In contrast, the peak for $t_{½}$ was shifted for the mutants; >1.2 – 1.6 seconds for Rad54$^{K189A\text{-}GFP}$ and >0.8 – 1.2 seconds for Rad54$^{K189R\text{-}GFP}$. In addition, the base of the distribution was broader, extending between t = 0 to 3.2 seconds in both mutants.

We also compared the rates of fluorescence recovery in foci after irradiation (n = 57 for wild type, n = 58 for mutants) (Figure 8B). Residence time of Rad54 appears to be increased in all cell lines after 8 Gy irradiation, but again, the increased time of protein turnover is clear with Rad54 mutants ($p < 0.05$) (compare Figure 8A left and right panel; see quantification in Figure 8C). Furthermore, the peak of the residence time of Rad54 for wild type cells shifted (>0.8 – 1.2 seconds, Figure 8C). This was not clearly seen in the case of the ATPase mutants, although the histogram base seems to increase slightly after irradiation.

Discussion

Rad54 is a multifunctional protein that promotes the progression of homologous recombination, an accurate pathway of repairing DSBs [16]. In addition to a close functional interaction with Rad51 (the central protein of homologous recombination), Rad54 also displays potent ATPase activity. This allows the protein to translocate along DNA and change its conformation, thereby perturbing its structures and influencing histone positions [15]. In this way, Rad54 assists Rad51 to pair the template DNA with the broken DNA molecule in need of repair. In this study, we have investigated the effect of two different mutations in the ATPase domain of Rad54, both resulting in the loss of ATPase activity, on its cellular behavior.

The primary results of this study are as follows. First, there is a higher number of Rad54 spontaneous foci in unchallenged cells bearing ATPase-defective Rad54 compared to cells expressing wild type Rad54. Second, these cells also demonstrate an increase in spontaneous Rad51 foci. However, this increase of foci containing homologous recombination proteins does not correspond to an increase in DNA damage. Third, the ATPase activity of Rad54 is not essential for the initial increase in Rad54 foci in response to irradiation. In contrast, the rate of the disappearance of DNA damage-induced foci is delayed when the ATPase activity of Rad54 is attenuated. Finally, photobleaching studies showed an increased residence time of ATPase-defective Rad54 in foci compared to ATPase-proficient Rad54. These points are discussed in the next paragraphs.

The ATPase activity of Rad54 is essential for its DNA repair function in vivo

In order to address the importance of the ATPase activity of Rad54 in the cell we generated mouse embryonic stem (ES) cells that express ATPase-defective mutants fused to a carboxyterminal GFP tag from the endogenous Rad54 locus (Figure 1), ensuring physiological levels of mutant protein (Figure 1C).

The DNA damage sensitivity profiles of the ATPase-defective Rad54 mutant are comparable to Rad54 knockout cells in that they are similarly hypersensitive to MMC and irradiation (Figure 2A). In addition, Rad54 ATPase-defective and Rad54 knockout cells are equally impaired in homologous recombination efficiency as measured by homologous gene targeting efficiency (Table 1), showing that the ATPase activity is required to effectively integrate a linear piece of DNA into the homologous location in the genome. These results reveal a correlation between the biochemical importance of the Rad54 ATPase function and its *in vivo* importance for DNA repair. On the other

hand, Rad54 knockout cells as well as cells carrying the Rad54 mutants are not hypersensitive to UV, aphidicolin, hydroxyurea and etoposide (Figure 2B), showing little involvement of Rad54 or its ATPase activity in the repair of stalled replication forks in these assays.

Differential cellular behavior of ATPase-proficient and -defective Rad54

A remarkable feature of *Rad54*$^{K189R\text{-}GFP/-}$ and *Rad54*$^{K189A\text{-}GFP/-}$ cells is the presence of an elevated number of spontaneous Rad54 foci in their nuclei compared to *Rad54*$^{wt\text{-}GFP/-}$ cells (Figure 3). Interestingly, the level of γH2AX, a DNA damage marker, is similar in the Rad54 ATPase-defective and Rad54 ATPase proficient cells (Figure 4A). This indicates that the increase in the number of spontaneous foci does not correlate with an increase in spontaneous DNA damage in Rad54 ATPase-defective cells. Consistently, when analyzed by immunofluorescence, no corresponding increase in the number γH2AX foci can be detected (Figure 4C). Thus, within the limitations of these techniques, the level of DNA damage is not significantly different in mutant and wild type cells, indicating that the elevated number of spontaneous foci is not due to an increased number of unrepaired breaks. This is consistent with the absence of an overt proliferation defect, as well as unaffected genomic stability, of the cells expressing ATPase-defective Rad54 and cells lacking Rad54 (data not shown).

An interesting feature of ES cells is their high number of γH2AX foci compared to, for example, HeLa cells and fibroblasts. The reason for this could be due to the high percentage of the rapidly cycling ES cells in the S phase compared to other cell types [45, 46], where physiological DSBs are thought to occur [36]. Our results show that not all γH2AX colocalizes with Rad54. However, the reverse is true: most Rad54 foci colocalize with γH2AX (Figure 4B). While the dynamics of γH2AX foci formation and disassembly as compared to recombination proteins has not been determined, we can nonetheless conclude that the Rad54 and γH2AX foci mark the sites where DSBs are located at some point in time. Further, the recruitment of Rad54 to sites of damage marked by γH2AX is unaffected by its ATPase activity.

In addition to causing an increase in its own foci in unchallenged cells, the inability of Rad54 to hydrolyze ATP effectively also causes a corresponding increase in the foci of its partner protein, Rad51 (Figure 5). Biochemical studies have shown that Rad54 displaces Rad51 from heteroduplex DNA, and that Rad54^{KR} mutant protein

stabilizes the Rad51 filament, rather than promoting its disassembly over time [30]. This situation is exacerbated by the fact that Rad51 itself binds DNA stably and its own ATP hydrolysis is not sufficient to initiate dissociation of the nucleoprotein filaments and continuous turnover of Rad51 on heteroduplex DNA [30]. In addition it was shown by foci counting that Rad51 foci exhibit a longer half-life in the absence of Rad54 [47, 48]. Therefore it is conceivable that the overall level of ATPase activity in a system with an ATPase-deficient Rad54 is too low to properly maintain Rad51 turnover on DNA, therefore resulting in a possible stalling of the repair reaction and persistent Rad51 foci.

Yet, when Rad54 is absent, the number of spontaneous Rad51 foci is comparable to wild type, even though these foci are less stable [20, 40]. Therefore the physical presence of the mutant Rad54 protein makes a significant difference in the dynamics of Rad51 foci, in contrast to full Rad54 deletion. However, the absence of Rad54 or the presence of the ATPase defective protein is equally detrimental for cellular survival capability after exposure to certain DNA damaging agents or for the homologous targeting efficiency. With respect to the stability of Rad51 foci as well as their clearance this raises the possibility that another protein takes over Rad54's function in its absence. However the redundant protein fails to substitute for Rad54's DNA repair activity because this is still impaired in knockout cells. In mutant cells, ATPase-defective Rad54 seems to accumulate normally into foci, and thus the redundant protein might have limited access to the area, which leads to a change in Rad51 foci dynamics. An excellent candidate for this function is the Rad54 paralog Rad54B [49]. The presence of the ATPase-defective Rad54 protein would then dominantly affect this aspect of Rad54B activity and this possibility needs to be investigated.

Kinetics of assembly and disassembly of Rad54 foci

Foci are considered to be biologically relevant because mutant cell lines that cannot form them are sensitive to DNA damage and display a higher degree of spontaneous chromosomal aberrations [4]. Further, the presence and quantification of foci has been used as an indication of repair activity since foci form within a short time in response to DNA-damaging agents, and decrease in number over time. Nonetheless, the nature and purpose of a focus is ambiguous. The Rad54 focus has been characterized as a highly dynamic structure, on which Rad54 is actively and rapidly associating and disassociating ([21] and Figure 8). Further a recent study has established a role of Rad54 in the formation of DNA networks, that is, Rad54 is able to bind double-stranded DNA

in close proximity [54]. Thus, one may speculate that, at least with Rad54, a focus represents a large concentration of constantly exchanging proteins which brings together and binds double-stranded DNA for the purpose of recombinational repair.

To date the molecular processes required for the formation and clearance of recombination proteins in foci are not well understood. Foci have also been assumed to represent one or all of the various stages of recombination, but it should be emphasized that there is no direct evidence linking foci with the formation of nucleoprotein filaments. Therefore the analysis of foci assembly and disassembly is not a definitive method of distinguishing between the different stages of recombination. In spite of this the notion that formation of Rad54 damage induced foci does not require Rad54 ATPase activity (Figure 6) could possibly be a consequence of the proficiency of ATPase-defective Rad54 in Rad51 filaments stabilization [51]. This is underscored by the finding that the level of unrepaired breaks in the ATPase mutant cells is similar to wild type cells and the recruitment of Rad54 to sites of damage is unaffected by its ATPase activity (Figure 4). Further, the delay in the start of foci clearance is remininescent of synaptic malfunction, also indicated by biochemical experiments where ATPase-defective Rad54 is deficient in joint molecule formation [52]. Finally, since Rad54 and its ATPase activity has been implicated in dismantling the Rad51 nucleoprotein filament [30, 53] as well as branch migration and Holliday junction processing and disassembly [31, 32, 55], the delay in foci disappearance could be a reflection of this defect.

In this study, we have determined that first, the rate at which damage-induced foci disappear is about twice as long in the *Rad54*$^{K189R\text{-}GFP/-}$ cells than in the wild type cells (Figure 6), and second, there is retardation in protein turnover in the focus as shown by photobleaching experiments (Figure 8). The combined effect could result in the increased number of spontaneous foci seen in Rad54 ATPase mutants. We propose that when physiological breaks occur in ATPase mutant cells during S phase, the formation of foci is normal. However, they are not cleared up at the same rate as in wild type cells because of a delay in being processed and in the subsequent disassembly. This results in an accumulation of persistent foci, and the long term consequence of this might be the repair defect seen in these mutants.

Acknowledgements

The authors would like to acknowledge the technical assistance of Ellen van Drunen (chromosome spreads and counting) and Linda Brugmans (Southerns in the targeting experiment).

References

1. Agarwal, S., A.A. Tafel, and R. Kanaar, *DNA double-strand break repair and chromosome translocations.* DNA Repair (Amst), 2006. **5**(9-10): p. 1075-81.
2. Bassing, C.H. and F.W. Alt, *The cellular response to general and programmed DNA double strand breaks.* DNA Repair (Amst), 2004. **3**(8-9): p. 781-96.
3. Hoeijmakers, J.H., *Genome maintenance mechanisms for preventing cancer.* Nature, 2001. **411**(6835): p. 366-74.
4. Wyman, C. and R. Kanaar, *DNA Double-Strand Break Repair: All's Well That Ends Well.* Annu Rev Genet, 2006.
5. Game, J.C. and R.K. Mortimer, *A genetic study of x-ray sensitive mutants in yeast.* Mutat Res, 1974. **24**(3): p. 281-92.
6. Symington, L.S., *Role of RAD52 epistasis group genes in homologous recombination and double-strand break repair.* Microbiol Mol Biol Rev, 2002. **66**(4): p. 630-70, table of contents.
7. Wyman, C., D. Ristic, and R. Kanaar, *Homologous recombination-mediated double-strand break repair.* DNA Repair (Amst), 2004. **3**(8-9): p. 827-33.
8. Sung, P., et al., *Rad51 recombinase and recombination mediators.* J Biol Chem, 2003. **278**(44): p. 42729-32.
9. Bezzubova, O., et al., *Reduced X-ray resistance and homologous recombination frequencies in a RAD54-/- mutant of the chicken DT40 cell line.* Cell, 1997. **89**(2): p. 185-93.
10. Essers, J., et al., *Disruption of mouse RAD54 reduces ionizing radiation resistance and homologous recombination.* Cell, 1997. **89**(2): p. 195-204.
11. Kanaar, R., et al., *Human and mouse homologs of the Saccharomyces cerevisiae RAD54 DNA repair gene: evidence for functional conservation.* Curr Biol, 1996. **6**(7): p. 828-38.
12. Peterson, C.L. and J. Cote, *Cellular machineries for chromosomal DNA repair.* Genes Dev, 2004. **18**(6): p. 602-16.
13. Pollard, K.J. and C.L. Peterson, *Chromatin remodeling: a marriage between two families?* Bioessays, 1998. **20**(9): p. 771-80.
14. Dronkert, M.L., et al., *Mouse RAD54 affects DNA double-strand break repair and sister chromatid exchange.* Mol Cell Biol, 2000. **20**(9): p. 3147-56.
15. Heyer, W.D., et al., *Rad54: the Swiss Army knife of homologous recombination?* Nucleic Acids Res, 2006. **34**(15): p. 4115-25.
16. Tan, T.L., R. Kanaar, and C. Wyman, *Rad54, a Jack of all trades in homologous recombination.* DNA Repair (Amst), 2003. **2**(7): p. 787-94.
17. Clever, B., et al., *Recombinational repair in yeast: functional interactions between Rad51 and Rad54 proteins.* Embo J, 1997. **16**(9): p. 2535-44.
18. Golub, E.I., et al., *Interaction of human recombination proteins Rad51 and Rad54.* Nucleic Acids Res, 1997. **25**(20): p. 4106-10.
19. Jiang, H., et al., *Direct association between the yeast Rad51 and Rad54 recombination proteins.* J Biol Chem, 1996. **271**(52): p. 33181-6.
20. Tan, T.L., et al., *Mouse Rad54 affects DNA conformation and DNA-damage-induced Rad51 foci formation.* Curr Biol, 1999. **9**(6): p. 325-8.
21. Essers, J., et al., *Nuclear dynamics of RAD52 group homologous recombination proteins in response to DNA damage.* Embo J, 2002. **21**(8): p. 2030-7.

22. Petukhova, G., S. Stratton, and P. Sung, *Catalysis of homologous DNA pairing by yeast Rad51 and Rad54 proteins.* Nature, 1998. **393**(6680): p. 91-4.
23. Swagemakers, S.M., et al., *The human RAD54 recombinational DNA repair protein is a double-stranded DNA-dependent ATPase.* J Biol Chem, 1998. **273**(43): p. 28292-7.
24. Amitani, I., R.J. Baskin, and S.C. Kowalczykowski, *Visualization of Rad54, a chromatin remodeling protein, translocating on single DNA molecules.* Mol Cell, 2006. **23**(1): p. 143-8.
25. Ristic, D., et al., *The architecture of the human Rad54-DNA complex provides evidence for protein translocation along DNA.* Proc Natl Acad Sci U S A, 2001. **98**(15): p. 8454-60.
26. Van Komen, S., et al., *Superhelicity-driven homologous DNA pairing by yeast recombination factors Rad51 and Rad54.* Mol Cell, 2000. **6**(3): p. 563-72.
27. Alexeev, A., A. Mazin, and S.C. Kowalczykowski, *Rad54 protein possesses chromatin-remodeling activity stimulated by the Rad51-ssDNA nucleoprotein filament.* Nat Struct Biol, 2003. **10**(3): p. 182-6.
28. Alexiadis, V. and J.T. Kadonaga, *Strand pairing by Rad54 and Rad51 is enhanced by chromatin.* Genes Dev, 2002. **16**(21): p. 2767-71.
29. Jaskelioff, M., et al., *Rad54p is a chromatin remodeling enzyme required for heteroduplex DNA joint formation with chromatin.* J Biol Chem, 2003. **278**(11): p. 9212-8.
30. Solinger, J.A., K. Kiianitsa, and W.D. Heyer, *Rad54, a Swi2/Snf2-like recombinational repair protein, disassembles Rad51:dsDNA filaments.* Mol Cell, 2002. **10**(5): p. 1175-88.
31. Bugreev, D.V., O.M. Mazina, and A.V. Mazin, *Rad54 protein promotes branch migration of Holliday junctions.* Nature, 2006. **442**(7102): p. 590-3.
32. Bugreev, D.V., F. Hanaoka, and A.V. Mazin, *Rad54 dissociates homologous recombination intermediates by branch migration.* Nat Struct Mol Biol, 2007. **14**(8): p. 746-53.
33. Haaf, T., et al., *Nuclear foci of mammalian Rad51 recombination protein in somatic cells after DNA damage and its localization in synaptonemal complexes.* Proc Natl Acad Sci U S A, 1995. **92**(6): p. 2298-302.
34. Essers, J., A.B. Houtsmuller, and R. Kanaar, *Analysis of DNA recombination and repair proteins in living cells by photobleaching microscopy.* Methods Enzymol, 2006. **408**: p. 463-85.
35. Tarsounas, M., D. Davies, and S.C. West, *BRCA2-dependent and independent formation of RAD51 nuclear foci.* Oncogene, 2003. **22**(8): p. 1115-23.
36. Tashiro, S., et al., *S phase specific formation of the human Rad51 protein nuclear foci in lymphocytes.* Oncogene, 1996. **12**(10): p. 2165-70.
37. Aten, J.A., et al., *Dynamics of DNA double-strand breaks revealed by clustering of damaged chromosome domains.* Science, 2004. **303**(5654): p. 92-5.
38. Tashiro, S., et al., *Rad51 accumulation at sites of DNA damage and in postreplicative chromatin.* J Cell Biol, 2000. **150**(2): p. 283-91.
39. Thacker, J. and M.Z. Zdzienicka, *The XRCC genes: expanding roles in DNA double-strand break repair.* DNA Repair (Amst), 2004. **3**(8-9): p. 1081-90.
40. van Veelen, L.R., et al., *Ionizing radiation-induced foci formation of mammalian Rad51 and Rad54 depends on the Rad51 paralogs, but not on Rad52.* Mutat Res, 2005. **574**(1-2): p. 34-49.
41. Niedernhofer, L.J., et al., *The structure-specific endonuclease Ercc1-Xpf is required for targeted gene replacement in embryonic stem cells.* Embo J, 2001. **20**(22): p. 6540-9.
42. Abramoff, M.D., P.J. Magelhaes, and S.J. Ram, *Image Processing with ImageJ.* Biophotonics International, 2004. **11**(7): p. 36-42.

43. Cox, M.M., et al., *The importance of repairing stalled replication forks.* Nature, 2000. **404**(6773): p. 37-41.
44. Rogakou, E.P., et al., *DNA double-stranded breaks induce histone H2AX phosphorylation on serine 139.* J Biol Chem, 1998. **273**(10): p. 5858-68.
45. de Waard, H., *Genome caretaking and differentiation.* (PhD thesis, Erasmus MC, Rotterdam), 2004.
46. Hanada, K., et al., *The structure-specific endonuclease Mus81-Eme1 promotes conversion of interstrand DNA crosslinks into double-strands breaks.* Embo J, 2006. **25**(20): p. 4921-32.
47. Shinohara, M., et al., *Tid1/Rdh54 promotes colocalization of rad51 and dmc1 during meiotic recombination.* Proc Natl Acad Sci U S A, 2000. **97**(20): p. 10814-9.
48. Takata, M., et al., *The Rad51 paralog Rad51B promotes homologous recombinational repair.* Mol Cell Biol, 2000. **20**(17): p. 6476-82.
49. Wesoly, J., et al., *Differential contributions of mammalian Rad54 paralogs to recombination, DNA damage repair, and meiosis.* Mol Cell Biol, 2006. **26**(3): p. 976-89.
50. Lisby, M. and R. Rothstein, *DNA damage checkpoint and repair centers.* Curr Opin Cell Biol, 2004. **16**(3): p. 328-34.
51. Mazin, A.V., A.A. Alexeev, and S.C. Kowalczykowski, *A novel function of Rad54 protein. Stabilization of the Rad51 nucleoprotein filament.* J Biol Chem, 2003. **278**(16): p. 14029-36.
52. Solinger, J.A., et al., *Rad54 protein stimulates heteroduplex DNA formation in the synaptic phase of DNA strand exchange via specific interactions with the presynaptic Rad51 nucleoprotein filament.* J Mol Biol, 2001. **307**(5): p. 1207-21.
53. Solinger, J.A. and W.D. Heyer, *Rad54 protein stimulates the postsynaptic phase of Rad51 protein-mediated DNA strand exchange.* Proc Natl Acad Sci U S A, 2001. **98**(15): p. 8447-53.
54. Bianco, P.R., et al., *Rad54 oligomers translocate and cross-bridge double-stranded DNA to stimulate synapsis.* J Mol Biol, 2007. **374**(3): p. 618-40.
55. Mazina, O.M., et al., *Interactions of human rad54 protein with branched DNA molecules.* J Biol Chem, 2007. **282**(29): p. 21068-80.

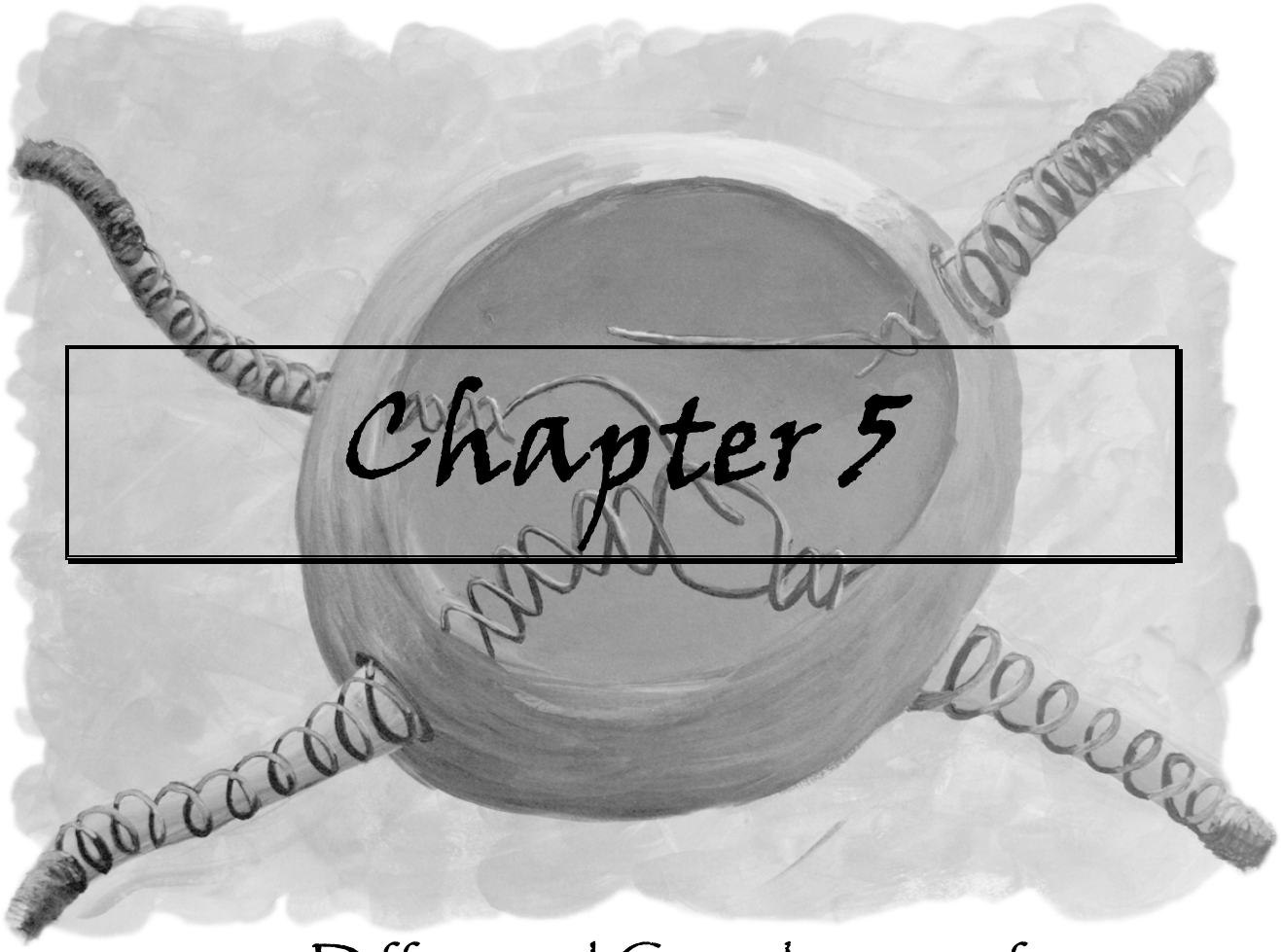

Chapter 5

Differential Contributions of Mammalian Rad54 Paralogs to Recombination, DNA Damage Repair and Meiosis

Published in:
Molecular and Cellular Biology 26 (3): 976 – 989
2006

It's déjà vu all over again.

~ Yogi Berra

Differential contributions of mammalian Rad54 paralogs to recombination, DNA damage repair and meiosis

Joanna Wesoly[1], Sheba Agarwal[1], Stefan Sigurdsson[6], Wendy Bussen[6], Stephen Van Komen[6], Jian Qin[7], Harry van Steeg[4], Jan van Benthem[4], Evelyne Wassenaar[2], Willy M. Baarends[2], Mehrnaz Ghazvini[1], Agnieszka A. Tafel[1], Helen Heath[1], Niels Galjart[1], Jeroen Essers[1], J. Anton Grootegoed[2], Normen Arnheim[7], Olga Bezzubova[8], Jean-Marie Buerstedde[8], Patrick Sung[5], and Roland Kanaar[1,3,*]

[1]Department of Cell Biology and Genetics, [2]Department of Reproduction and Development, [3]Department of Radiation Oncology, Erasmus MC, PO Box 1738, 3000 DR Rotterdam, The Netherlands
[4]Department of Toxicology, Pathology and Genetics, National Institute of Public Health and The Environment, PO Box 1, 3720 BA Bilthoven, The Netherlands
[5]Yale University School of Medicine, Molecular Biophysics and Biochemistry, New Haven, CT 06520, USA
[6]Department of Molecular Medicine and Institute of Biotechnology, University of Texas Health Science Center, San Antonio, TX 78245-3207, USA
[7]Molecular and Computational Biology Program, University of Southern California, Los Angeles, CA 90089-2910, USA
[8]GSF, Institute for Molecular Radiobiology, Neuheberg, Germany

*Corresponding author: r.kanaar@erasmusmc.nl

Abstract

Homologous recombination is a versatile DNA damage repair pathway requiring Rad51 and Rad54. Here we show that a mammalian Rad54 paralog, Rad54B, displays similar physical and functional interactions with Rad51 and DNA compared to Rad54. While ablation of Rad54 in mouse embryonic stem (ES) cells leads to a mild reduction in homologous recombination efficiency, the absence of Rad54B has little effect. However, the absence of both Rad54 and Rad54B dramatically reduces homologous recombination efficiency. Furthermore, we show that Rad54B protects ES cells from ionizing radiation and the interstrand DNA crosslinking agent mitomycin C. Interestingly, at the ES cell level the paralogs do not display an additive or synergic interaction with respect to mitomycin C sensitivity, yet animals lacking both Rad54 and Rad54B are dramatically sensitized to mitomycin C as compared to either single mutant. This suggests that the paralogs possibly function in a tissue-specific manner. Finally, we show that Rad54, but not Rad54B, is needed for a normal distribution of Rad51 on meiotic chromosomes.
Thus, even though the paralogs have similar biochemical properties, genetic analysis in mice uncovered their non-overlapping roles.

Introduction

DNA double-strand breaks (DSBs) are among a plethora of lesions that threaten the integrity of the genome. If not properly processed DSBs can lead to cell cycle arrest or illegitimate DNA rearrangements such as translocations, inversions, or deletions. These rearrangements can contribute to cell dysfunction, cell death, or carcinogenesis (22). DSBs can arise through the action of exogenous DNA damaging agents, but they also arise from endogenous sources, such as oxidative DNA damage and as a consequence of DNA replication (10, 22). Homologous recombination is a major DNA repair pathway by which DSBs are repaired. Homologous recombination is generally a precise way of resolving DSBs, because it uses homologous sequence, usually provided on the sister chromatid, as a repair template (54).

Homologous recombination is a complex process requiring a number of proteins of the *RAD52* epistasis group including Rad51 and Rad54. Rad51 is the key player in this process because it is critical for homology recognition and performs strand exchange between recombining DNA molecules. A pivotal intermediate in these reactions is the Rad51 nucleoprotein filament. This forms when Rad51 polymerizes on single-stranded DNA that results from DNA damage processing (54). Rad54 is an important accessory factor for Rad51 (56). A number of biochemical characteristics of Rad54 have been well defined for different species ranging from yeast to humans (8, 18, 24, 31, 37, 38, 42, 47, 48, 53, 55, 59). Rad54 is a double-stranded DNA-dependent ATPase that can translocate on DNA thereby affecting DNA topology. Biochemically, Rad54 has been implicated to participate in multiple steps of homologous recombination. It can stabilize the Rad51 nucleoprotein filament in an early stage of recombination (30). At a subsequent stage it can promote chromatin remodelling (1, 2, 23) and stimulate Rad51-mediated formation of a joint molecule between the broken DNA and the repair template, referred to as a D-loop (37). In later stages of the reaction it can displace Rad51 from DNA (49).

Cell biological experiments have revealed that Rad54 accumulates to form dynamic foci at sites of DNA damage (29, 55) that display rapid turn-over of Rad54 (16). In those foci Rad54 colocalizes with and stabilizes Rad51 (55, 60). Chromatin immunoprecipitation experiments using *Saccharomyces cerevisiae* cells underscore the co-operation between Rad51 and Rad54 (50, 63). In the absence of Rad54, Rad51 is still able to pair homologous sequences, but the joint molecules are qualitatively different from those formed in the presence of Rad54 (50, 62).

Genetic analysis of *RAD54* has been performed in a number of species including yeast and mice. *S. cerevisiae* cells with mutated *RAD54* are DNA damage sensitive, including ionizing radiation, are severely defective in gene conversion and exhibit increased chromosome loss (21, 26, 43, 46). Mouse *Rad54* knockout embryonic stem (ES) cells are ionizing radiation and mitomycin C sensitive, show reduced homologous recombination efficiency as measured by gene targeting and display aberrant DSB repair (14, 15). Interestingly, while *Rad54* knockout mice are sensitive to the interstrand DNA cross-linking agent mitomycin C, they are not ionizing radiation sensitive (17). The contribution of Rad54-mediated homologous recombination to repair ionizing radiation induced damage in adult animal is revealed when non-homologous DNA end joining, an alternative and mechanistically distinct DSB repair pathway, is also impaired (9, 17, 32). A possible explanation for this observation is the existence of redundancy in Rad54 function in mammalian cells.

In *S. cerevisiae*, a *RAD54* homolog, *RDH54* (also know as *TID1*), has been identified (13, 27, 45). Its biochemical properties are similar to that of Rad54, for example, Rdh54 is an ATPase and it stimulates D-loop formation by Rad51 (39). The phenotypes of *rad54* and *rdh54* mutants are distinct, but do appear to be related to defects in homologous recombination. While *rad54* mutants are sensitive to the alkylating agent methyl methanesulfonate, *rdh54* mutants are not or less so (27, 45). However, in the absence of *RAD54*, the contribution of *RDH54* to cell survival is uncovered because *rad54 rdh54* double mutants are more sensitive to methyl methanesulfonate than either single mutant. While *RAD54* affects both intra- and interchromosomal recombination, *RDH54* seems to be more important for interchromosomal recombination than for intrachromosomal recombination (3, 27, 45). An interaction between the two genes has been found in meiosis. While sporulation efficiency and spore viability are reduced in the *rad54* and *rdh54* single mutants, these parameters are synergistically reduced in *rad54 rdh54* double mutants, likely reflecting partial overlapping functions of *RAD54* and *RDH54* during meiotic recombination (44).

A *RAD54* homolog, named *RAD54B*, has also been identified in human cells (33, 57). This gene has been labeled the mammalian homolog of yeast *RDH54*. However, this classification is based on amino acid sequence similarity and not on extensive functional analysis. Here we report the biochemical and genetic characterization of mammalian *Rad54B*. We show that mammalian Rad54B has biochemical properties similar to that of Rad54. However, the results of genetic experiments using *Rad54*

knockout, *Rad54B* knockout and *Rad54 Rad54B* double knockout cells and mice, suggests that mammalian *Rad54B* is unlikely to be the true *S. cerevisiae RDH54* homolog because the genes are not functionally equivalent.

Materials and Methods

Isolation of human and mouse RAD54B DNA

The *hRAD54B* cDNA was initially cloned as two fragments from a human testis cDNA library by PCR using the following primers (fragment 1:

5'-GCAGGGCCAGTGGTTTCTGTC and

5'-GTGGTCCTGATCAACAGTAAAT;

fragment 2: 5'-ATTTACTGTTGATCAGGACCAC and

5'-GAAGAGCAATGGAATGTCAGAA).

The two PCR fragments were digested with BclI, ligated together, and used as a template for amplification of the full length *hRAD54B* cDNA with the following primers:

5'-CGGGATCC*CAT**ATG***AGACGATCTGCAGCACC and

5'-CGGGATCC**CTA**TGTGCCAGTAGCTTGAG (BamHI sites are underlined, NdeI site is italicized, and start and stop codons are in bold).

The PCR product was cloned into the BamHI site of pUC18 and sequenced. The mouse *Rad54B* cDNA was isolated using a combination of RT PCR with degenerate primers (25) and cDNA library screening. The resulting 2658 bp cDNA mouse *Rad54B* has the Genebank identification number NM009015.

Expression and purification of hRad54B

The *hRAD54B* cDNA was subcloned from pUC18 into the BamHI site of pFastBac (Invitrogen). The hRad54B-pFastBac was transformed into DH10Bac cells, and the resulting bacmid was isolated and used to generate a recombinant hRad54B baculovirus in Sf9 insect cells. The virus was amplified by infecting 100 ml of Sf9 suspension culture at an MOI of 0.1 for 48 hours. To express hRad54B, Hi-Five insect cells were infected with the hRad54B recombinant virus at an M.O.I. of 10 and harvested after 72 hours. Cells collected from 150 ml of insect cell culture were suspended in 20 ml cell breakage buffer (50 mM Tris-HCl, pH 7.5, 10% sucrose, 10 mM EDTA, 600 mM KCl, 1 mM DTT, and the following protease inhibitors: aprotinin, chymostatin,

leupeptin, and pepstatin A, each at 5 μg/ml, and 1 mM PMSF) and lysed by passage through a French Press. The lysate was clarified by centrifugation (100,000 x *g*), and the resulting supernatant was treated with ammonium sulfate (0.21 g/ml). The protein precipitate was harvested by centrifugation and re-dissolved in 20 ml K buffer (20 mM KH_2PO_4, pH 7.4, 10% glycerol, 0.5 mM EDTA, 0.01% Igepal, and 1 mM DTT). The protein solution, with conductivity equivalent to 150 mM KCl, was passed in tandem over Q-Sepharose and SP-Sepharose columns (7 ml each), with hRad54B protein passing through the Q column but being retained on the SP column. To elute hRad54B, the SP column was developed with a 60 ml, 150-700 mM KCl gradient in K buffer. The hRad54B-containing fractions (350 mM KCl) were pooled, diluted with an equal volume of K buffer, and loaded onto a 5 ml macro-hydroxyapatite column, which was developed with a 60 ml, 0-300 mM KH_2PO_4 gradient in K buffer, with hRad54B eluting at 150 mM KH_2PO_4. The peak fractions were diluted with an equal volume of T buffer (25 mM Tris-HCl, pH 7.5, 10% glycerol, 0.5 mM EDTA, 0.01% Igepal, and 1 mM DTT), and applied onto a 1 ml Mono S column, which was eluted with a 30 ml, 100-700 mM KCl gradient in K buffer, with hRad54B eluting at 350 mM KCl. Following the addition of 1/10 volume of 3 M KCl, the peak fractions were pooled and concentrated to 500 μl in a Centricon-30 microconcentrator (Millipore). The concentrated protein was loaded onto a 20 ml Sephacryl S-300 column pre-equilibrated with K buffer containing 500 mM KCl and eluted with the same buffer. The peak fractions were pooled, concentrated to 3 to 3.5 mg/ml, and stored in 3 μl portions at –80°C.

Generation of hRad54B antibodies

The portion of hRad54B encompassing amino acid residues 13-395 was fused to glutathione *S*-transferase in the vector pGEX-3X. The GST-hRad54B fusion protein was expressed in *E. coli* BL21 (DE3) cells and purified from inclusion bodies by preparative SDS-PAGE to use as antigen for raising polyclonal antibodies in rabbits (Strategic Biosolutions). The same antigen was covalently coupled to cyanogen bromide-activated Sepharose 4B to use as affinity matrix for purifying antibodies from the rabbit antisera, as described (52).

DNA substrates

Topologically relaxed ϕX174 DNA was prepared by treatment with calf thymus topoisomerase I, as described (59), and pBluescript SK DNA was made in *E. coli* DH5α

as described (38). The oligonucleotide used in the D-loop reaction is complementary to positions 1932–2022 of the pBluescript SK DNA and had the sequence: 5'-AAATCAATCTAAAGTATATATGAGTAAACTTGGTCTGACAGTTACCAATGC TTAATCAGTGAGGCACCTATCTCAGCGATCTGTCTATTT-3'.This oligonucleotide was 5' end-labeled with [γ^{32}P]ATP and T4 polynucleotide kinase to use in D-loop reactions.

Protein activity assays

Binding of hRad54B to hRad51 was assessed with the use of immobilized hRad51 protein. hRad51 protein and bovine serum albumin (BSA) were coupled to Affi-Gel 15 beads following the instructions of the manufacturer (Bio-Rad). The matrices contained 4 and 12 mg/ml of hRad51 and BSA, respectively. hRad54B (1.3 μg) was incubated with 5 μl of Affi-BSA or Affi-hRad51 at 4°C for 30 minutes in 30 μl of K buffer containing 50 mM KCl and 0.1% TritionX-100 with constant gentle tapping. This was followed by washing the beads twice with the same buffer (50 μl each time) before treating them with 30 μl of 2% SDS at 37°C for 5 minutes to elute bound hRad54B. In Fig. 1C, hRad54B (1.3 μg) was mixed with yeast extract containing 100 μg total protein in 30 μl of buffer and mixed with the hRad51 and BSA beads as above. The various fractions (10 μl each) were analyzed by SDS-PAGE and Coomassie staining or immuno-blotting for their hRad54B content. Note that in Fig. 1C, lane 5, some hRad51 protein is detected, which is probably due to the multimeric nature of hRad51. Since not all of the subunits in this multimeric structure become covalently conjugated to the Affi-gel beads, the non-covalently linked subunits will be eluted by the SDS treatment. The amount of covalently conjugated BSA to the Affi-gel beads was quantified by determining the protein coupling efficiency using SDS-PAGE.

DNA supercoiling and helix-opening activities of hRad54B were assessed as follows: The indicated amount of hRad54B was incubated with topologically relaxed ϕX174 dsDNA (5 μM base pairs) for 2 min at 23°C in 11.8 μl of reaction buffer (50 mM Tris-HCl, pH 7.8, 3 mM $MgCl_2$, 1 mM dithiothreitol, 2 mM ATP, and an ATP regenerating system consisting of 10 mM creatine phosphate and 28 μg/ml creatine kinase). Following the addition of 200 ng of *E. coli* topoisomerase I in 0.7 μl, the reactions were incubated at 37°C for 10 minutes and then deproteinized by treatment with 0.5% SDS and proteinase K (0.5 mg/ml) for 10 min at 37°C. Reaction products were separated in a 1% agarose gel in TAE buffer (40 mM Tris-acetate, pH 7.4,

containing 0.5 mM EDTA) and stained with ethidium bromide. The sensitivity of DNA to P1 nuclease was assayed in the same manner, except that *E. coli* topoisomerase I was replaced by 0.4 units of P1 nuclease (Roche) and the DNA species were resolved in a 1% agarose gel containing 10 μM ethidium bromide. In some instances, the indicated amount of hRad51 was also included in the initial incubation period.

ATP hydrolysis activity of hRad54B was determined by incubating hRad54B protein (120 nM) with ϕX174 RFI DNA (23 μM base pairs) and 1.5 mM ATP with or without 300 nM yRad51 or hRad51 K133R in 10 μl of reaction buffer (20 mM Tris-HCl, pH 7.4, 25 mM KCl, 1 mM DTT, 4 mM $MgCl_2$, 100 μg/ml BSA) at 30°C for the indicated times. The level of ATP hydrolysis was determined by thin layer chromatography, as described (37).

Reactions to measure the effect of hRad54B on hRad51-mediated D-loop formation were performed as follows: hRad51 (800 nM) was incubated with the 5'-labeled 90-mer oligonucleotide (2.5 μM nucleotides) for 4 min at 37°C in 40 μl of reaction buffer (20 mM Tris-HCl, pH 7.4, 100 μg/ml BSA, 1 mM $MgCl_2$, 2 mM ATP, and the ATP generating system described above). This was followed by the addition of hRad54B (400 nM) in 4 μl and a 2 min incubation at 23°C. The reaction was completed by adding pBluescript SK replicative form I DNA (190 μM base pairs) in 6 μl. The reaction mixtures were incubated at 30°C, and 6.3 μl aliquots were withdrawn at the indicated times, deproteinized, and run in 1% agarose gels in TAE buffer. The gels were dried, and the level of D-loop was quantified by phosphorimaging analysis. The reactions containing hRad51K133R were assembled in buffer that contained 5 mM $MgCl_2$. The percent D-loop refers to the proportion of the radiolabeled oligonucleotide that was incorporated into the pBluescript RFI DNA.

Generation of a mRad54B disruption construct and mRad54B knockout mice

A 129 mouse genomic library (Stratagene, Cat# 946308) was screened with a DNA fragment from the *mRad54B* cDNA sequence. A positive clone was picked and the DNA was subsequently subcloned into a pBluescript KS. The restriction map of the genomic DNA was determined using EcoRI, BglII, BamHI and XbaI; it was also noted that this particular stretch of genomic DNA contained 7 exons. A 1851 bp fragment between EcoRI and BglII sites in the genomic DNA was replaced with 1108 bp XhoI/HindIII fragment from pMC1neo (Stratagene). This pMC1neo fragment contained the neomycin gene under the control of tk promoter. The neomycin marker

gene was flanked by a approximately 9 kb EcoRI and a 1097 bp BglII-XbaI fragments of the *mRad54B* locus. When used in gene targeting, this construct was expected to eliminate 28 highly conserved amino acids, in effect knocking out functional *mRad54B*. The targeting construct was electroporated into E14 ES cells, which were then put under G418 selection. Positive clones were screened by DNA blot analysis using Probe A (see Fig. 5). One out of 238 clones showed a fragment of a size expected for targeted integration of the construct. This was further confirmed using several restriction enzymes and both upstream (A) and downstream (B) probes (Fig. 5B). ES cells that contained this targeted event were injected into blastocysts. This gave rise to 17 chimeric males, which were then backcrossed to BDF1 females, in order to get pure knockout mice.

Homologous targeting assays

The efficiency of homologous recombination was assessed by homologous gene targeting assays to different loci, *mRad54* and *CTCF*. The *mRad54*-puro targeting construct and experiments have been described previously (15). DNA blot analysis was carried out to distinguish between targeted events versus random integration of the *mRad54* construct. In the case of *CTCF* targeting, PCR was carried out on genomic DNA of transfected clones. The appearance of a 5 kb PCR product indicated a homologous targeting event. Mouse *Rad54B* specific PCR served as an internal control. χ^2 tests were performed to evaluate the significance of differences in homologous recombination frequencies.

DNA damage sensitivity assays

Cellular clonogenic survival assays have been described previously (15). Every measurement was performed in triplicate. For ionizing radiation survivals assays, cells were exposed to the specified dose of γ-rays. For mitomycin C survival assays, cells were incubated in medium containing the specified concentration of mitomycin C for an hour. The cells were then washed with PBS, and replenished with fresh medium. The cells were allowed to grow for 10 days, after which the colonies were stained and counted. The mitomycin C survival experiments were performed four times. Cloning efficiencies of untreated cells varied between 10-30%.

Ionizing radiation and mitomycin C sensitivity was assessed with the use of two to four month old littermates from the various genotypes (wild type, *mRad54*$^{-/-}$, *mRad54B*$^{-/-}$, *mRad54*$^{-/-}$ *mRad54B*$^{-/-}$). They were irradiated with a 7 Gy dose (^{137}Cs source)

and monitored for 21 days. Surviving animals were euthanized. Male and female mice were injected with 15, 10, 7.5, 5, 2.5 and 1 mg of mitomycin C per kg bodyweight and monitored for 14 days.

DNA damage processing was indirectly assessed by the micronucleus assay. 100 µl of peripheral blood was collected by orbital puncture, and the micronucleus assay was performed as described (19). Five hundred polychromatic erythrocytes were scored for the presence of micronuclei using an Axioplan fluorescence microscope.

Immunocytochemistry of meiotic chromosomes

Testis were isolated from 1, 2, and 5 month old 129/Bl6 mice and processed as previously described (36). Immunofluorescence was performed as described (4). Sycp3 mouse monoclonal antibody was a kind gift from C. Heyting, Wageningen, The Netherlands. The anti-hRad51 antibody was as described (16).

Measuring recombination using single sperm typing

Isolation of individual sperm, sperm lysis, single sperm multiplex PCR and statistical analysis of the frequency of crossing over were carried out as described previously (12, 28, 41). Recombination in two regions was analyzed. The 13.1 cM chromosome 2 interval was between $(CA)_n$ microsatellite markers D2Mit213 and D2Mit412, while the 24.1 cM chromosome 7 interval was between D7Mit268 and D7Mit353 (http://www.broad.mit.edu/cgi-bin/mouse/index). The primer sequences are given in Supplemental Materials Table 1.

Results

Isolation of a cDNA encoding a mammalian Rad54 paralog

DNA oligonucleotides of degenerate sequence based on conserved amino acid motifs in the SWI2/SNF2 family of proteins were used to isolate a *Rad54* paralog, which we named mouse *Rad54B (mRad54B)*, from mouse cDNA libraries. The *mRad54B* cDNA consisted of a 2658 bp open reading frame with the potential to code for an 886 amino acid protein with a predicted molecular mass of 103 kDa. Amino acid sequence comparison of mRad54 and mRad54B revealed 33% sequence identity that extends over the entire length of the proteins. The predicted amino acid sequence of mRad54B shows 80% sequence identity with human Rad54B (hRad54B) (20). Further sequence analysis indicated that human and mouse Rad54B displayed 34% sequence identity to both *S.*

cerevisiae Rad54 and Rdh54. To obtain insight in the function of mammalian Rad54B, we characterized it biochemically and genetically.

Human Rad54B forms a complex with human Rad51

The *hRAD54B* cDNA was cloned, expressed in High-five insect cells and purified (Supplemental Fig. 1). In contrast to mammalian Rad54 which can directly interact with mammalian Rad51 (18, 55), it has been suggested that hRad54B does not interact directly with hRad51. This conclusion was reached because no association between hRad51 and hRad54B was detected in either a yeast-two hybrid assay or in *in vitro* pulldown assays with purified proteins (58). Since genetic evidence implicates Rad54B in homologous recombination (33), we re-examined whether hRad51 and hRad54B form a complex. The hRad51 protein was immobilized on Affi-Gel beads and interaction of hRad54B with these beads was assessed. As shown in Fig. 1 A and B, hRad54B was retained on the Affi-hRad51 beads but did not associate with beads conjugated to BSA. To further establish the specificity of the hRad51/hRad54B interaction, a small amount of purified hRad54B was mixed with an excess of yeast extract proteins and this mixture was incubated with the Affi-hRad51 beads. As shown in Fig. 1C and D, among the many proteins that were present, only hRad54B was retained on the hRad51 affinity beads. As expected, hRad54B did not bind to the control beads that contained BSA. Taken together, these results demonstrate a direct and highly specific interaction between hRad54B and hRad51.

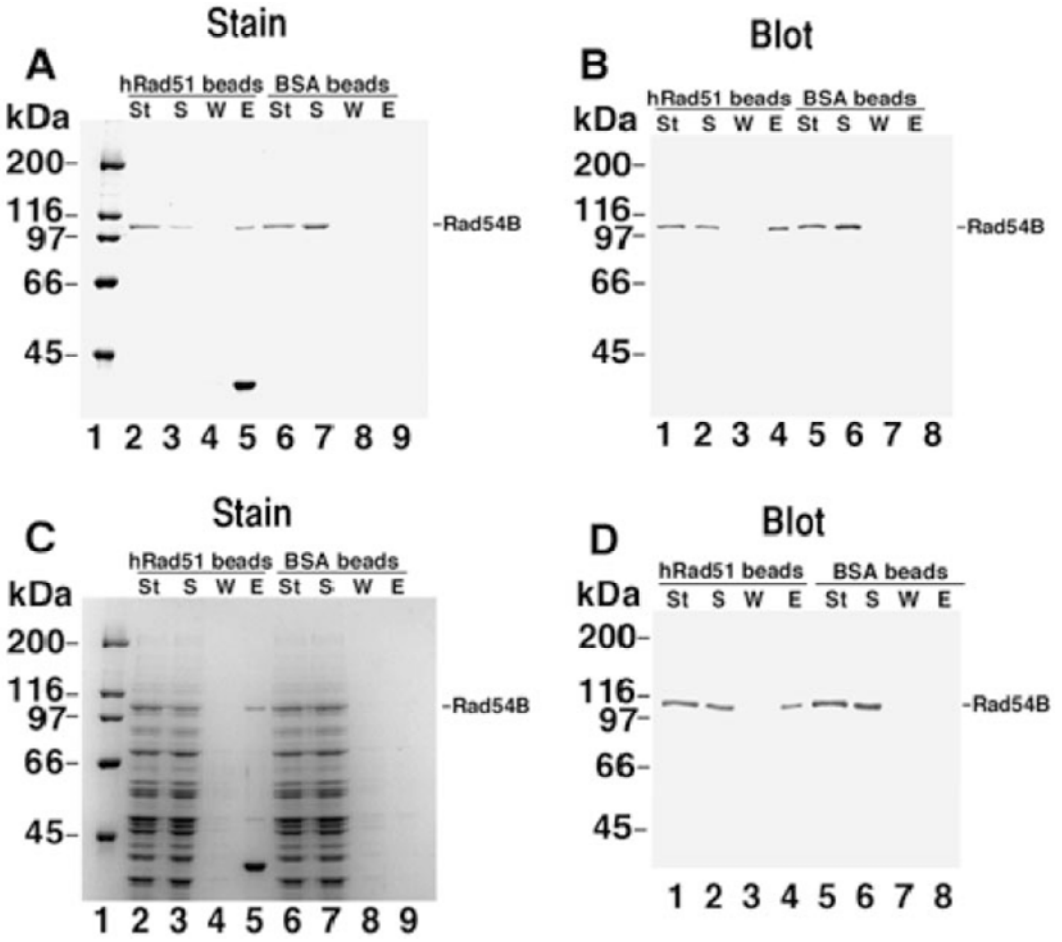

Figure 1. Direct protein-protein interactions between human Rad54B and human Rad51. hRad51 protein or BSA was coupled to Affi-Gel beads and binding of hRad54B was investigated. **(A)** The starting material (St), supernatant (S), wash (W) and eluate (E) from hRad51- and BSA-containing beads, respectively, were separated in a denaturing gel and stained with Coomassie blue. Interaction of hRad54B and hRad51 is evident from the presence of hRad54B in lane 5 compared to its absence in lane 9. **(B)** Immunoblot of a similar experiment as shown in panel A probed with anti-hRad54B antibodies. **(C)** To assess the specificity of the interaction between hRad54B and hRad51, purified hRad54B was mixed with a protein extract from *S. cerevisiae* cells and the mixture was incubated with the hRad51- or BSA-containing beads. Human Rad54B was specifically retained on the hRad51-containing beads (lane 5). **(D)** A similar experiment as shown in panel C, except the gel was probed with anti-hRad54B antibodies. Size of protein molecular mass markers is indicated in kDa.

Human Rad54B has DNA translocase activity and promotes DNA helix opening

The Rad54 and Rdh54 proteins use the energy from ATP hydrolysis to translocate along duplex DNA, inducing positive supercoils ahead of protein movement and compensatory negative supercoils behind (39, 42, 47, 59). Since, like Rad54 and Rdh54, hRad54B possesses the seven conserved helicase motifs common to SWI2/SNF2 family members (51) and double-stranded DNA-dependent ATPase

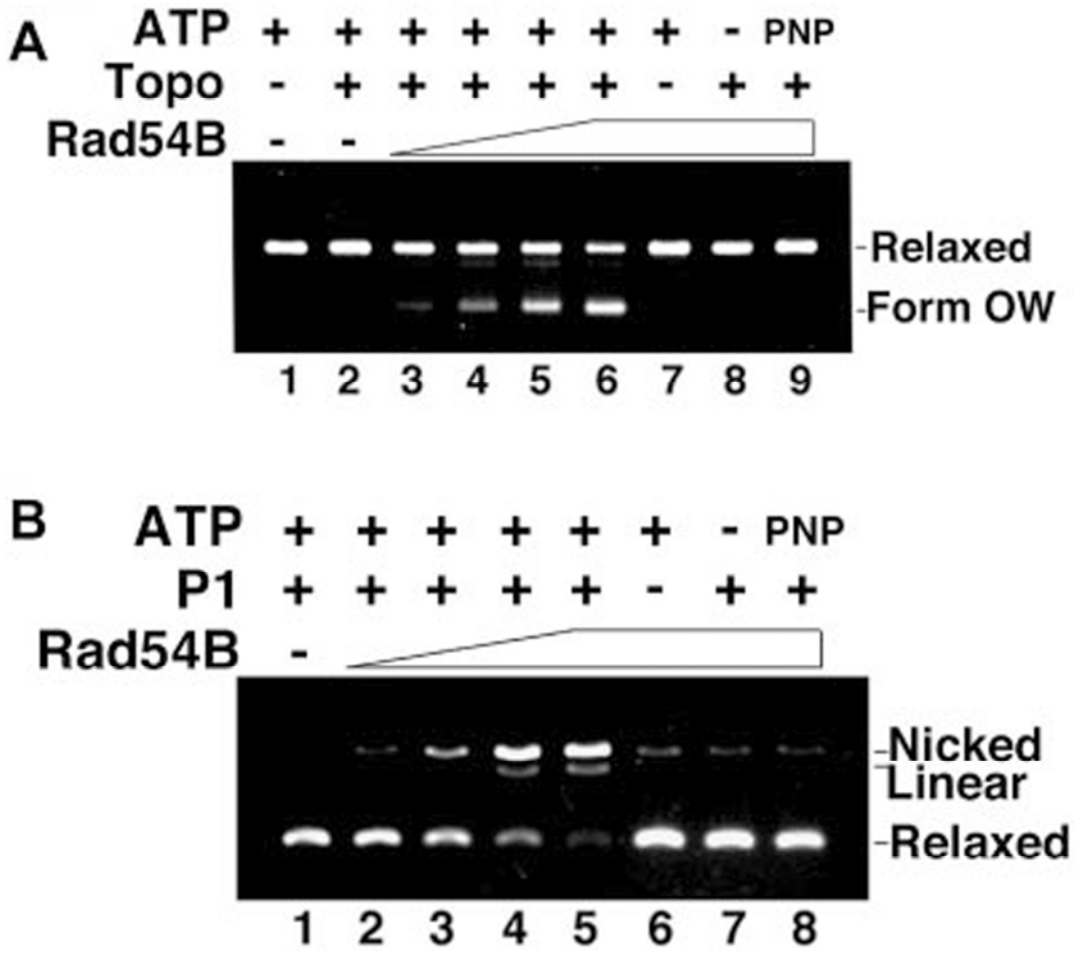

Figure 2. Human Rad54B has ATP-dependent DNA translocase activity that promotes opening of the DNA double helix. (A) A topologically relaxed plasmid substrate was incubated with hRad54B, after which *E. coli* topoisomerase I was added to remove any negative supercoils generated in the substrate. The ability to translocate along DNA will result in the formation of an overwound (Form OW) DNA species due to remaining positive supercoils in the substrate. Human Rad54B generated Form OW DNA, which increased with increasing amount of protein (lanes 3-6). The assay depended on *E. coli* Topo I (lane 7), and hRad54B translocase activity required ATP (lane 8) and its hydrolysis (lane 9, AMP-PNP). The concentrations of hRad54B used were 300, 400, and 500 nM in lanes 3-5, respectively, and 650 nM in lanes 6-9. **(B)** The presence of single-stranded DNA that results from an opening of double-stranded DNA by hRad54B translocation was probed with the use of single-strand nuclease P1. With an increasing amount of hRad54B, there was more single-stranded DNA present, resulting in P1 digestion of the single-stranded DNA and formation of the nicked form of the DNA substrate (lanes 2-5). Nicking activity was greatly diminished upon the omission of P1 nuclease (lane 6) or ATP (lane 7), or when ATP was substituted with the non-hydrolyzable ATP analogue AMP-PNP (lane 8). DNA incubated with P1 (lane 1) was included as control. The concentrations of hRad54B used were 100, 200, and 300 nM in lanes 2-4, respectively, and 400 nM in lanes 5-8.

activity (58), it was of interest to examine hRad54B protein for translocase activity. To this end we employed an assay that is based on the principle that *E. coli* topoisomerase I

removes negative supercoils from DNA, but is unable to act upon positive supercoils. For the reaction, a topologically relaxed plasmid substrate was incubated with hRad54B, and then *E. coli* topoisomerase I was added to remove any negative supercoils generated in the substrate. An ability of hRad54B to translocate on DNA will result in the formation an overwound (Form OW) DNA species (38, 42, 47, 59). Utilizing this assay system, we found that hRad54B generates Form OW DNA (Fig. 2). This supercoiling reaction was dependent on ATP hydrolysis by hRad54B, as evidenced by the lack of Form OW when ATP was omitted from the reaction or replaced with the non-hydrolyzable analogue AMP-PNP (Fig. 2A, lanes 8 and 9).

The ability of Rad54 to generate negative supercoils in duplex DNA leads to the transient opening of the DNA strands in the duplex (47, 59), as indicated by the sensitivity of a topologically relaxed DNA template to the single-strand specific nuclease P1. We used the same strategy devised for Rad54 to examine whether hRad54B renders topologically relaxed DNA sensitive to P1. As seen in Fig. 2B, the DNA substrate alone was not digested by P1 nuclease because of the lack of single-stranded character in the DNA, but with increasing amounts of hRad54B, progressively more of the DNA substrate was converted into the nicked form. These results show that the negative supercoiling induced by hRad54B translocation causes transient opening of the DNA double strand. As expected, the DNA strand opening activity of hRad54B was dependent upon ATP hydrolysis, as sensitivity to P1 nuclease was greatly attenuated when ATP was absent or substituted with AMP-PNP (Fig. 2B, lanes 7 and 8).

Stimulation of human Rad54B activities by human Rad51

Since hRad51 and hRad54B physically interact (Fig. 1), we tested whether the proteins functionally co-operate in biochemical reactions they catalyze. We examined the effect of hRad51 on hRad54B activities described above. In contrast to a previous report indicating that hRad51 had no effect on the hRad54B ATPase activity (58), we consistently detected a significant stimulation of this activity by hRad51 K133R, a mutant variant of hRad51 that is capable of ATP binding but not hydrolysis (Fig. 3A). The species specificity of hRad54B ATPase stimulation was established by showing that *S. cerevisiae* Rad51 was unable to enhance the ATP hydrolytic reaction (Fig. 3A). We next tested whether hRad51 could stimulate the ability of hRad54B to promote DNA

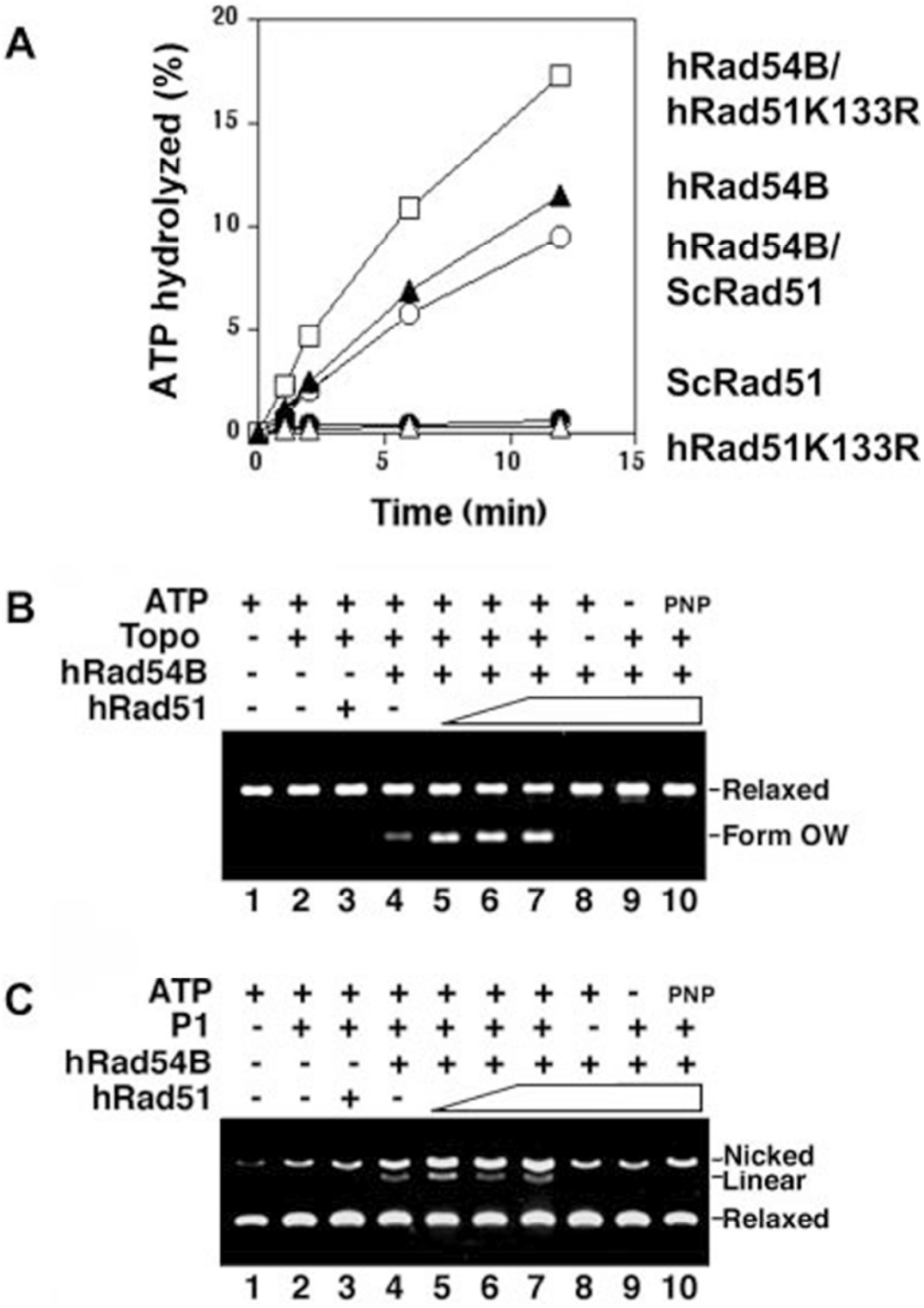
A
ATP hydrolyzed (%)
Time (min)
hRad54B/
hRad51K133R
hRad54B
hRad54B/
ScRad51
ScRad51
hRad51K133R
B
ATP
Topo
hRad54B
hRad51
PNP
Relaxed
Form OW
C
ATP
P1
hRad54B
hRad51
PNP
Nicked
Linear
Relaxed

Figure 3. Human Rad54B and human Rad51 functionally interact. (A) Human Rad51 stimulates the ATPase activity of hRad54B. Human Rad54B (120 nM) was incubated with [γ-^{32}P]-ATP and various forms of Rad51, and the percentage of ATP hydrolyzed was determined. A significant stimulation of hRad54B ATPase activity was detected with hRad51 K133R (300 nM), a mutant variant of hRad51 that can bind but not hydrolyze ATP. The effect is species specific because Rad51 from *S. cerevisiae* (ScRad51; 300 nM) did not affect the ATPase activity of hRad54B. **(B)** Human Rad51 stimulates hRad54B in the translocase assay. The formation of Form OW DNA was determined in the presence of Topo I, hRad54B (300 nM) and hRad51 (0, 200, 300, and 400 nM, respectively, in lanes 4-7). In control reactions, hRad51 (400 nM) and DNA were incubated with topoisomerase and ATP but no hRad54B (lane 3), with hRad54B and ATP but no topoisomerase (lane 8), with hRad54B and topoisomerase but no ATP (lane 9), or with hRad54B, topoisomerase, and AMP-PNP (lane 10, PNP). DNA alone (lane 1) and DNA incubated with topoisomerase (lane 2), both in the presence of ATP, were also analyzed. Form OW denotes the positively supercoiled DNA species generated. **(C)** Human Rad51 stimulates hRad54B in the P1 nuclease assay. The ability of hRad54B to open up the DNA double helix is enhanced by the presence of hRad51. hRad54B (100 nM) was incubated with topologically relaxed DNA, ATP, P1 nuclease, and hRad51 (100, 200, 300 nM in lanes 5-7, respectively) or without hRad51 (lane 4). In control reactions, hRad51 (300 nM) and DNA were incubated with P1 and ATP but no hRad54B (lane 3), with hRad54B and ATP but no P1 (lane 8), hRad54B and P1 but no ATP (lane 9), or with hRad54B, P1, and AMP-PNP (lane 10, PNP). DNA alone (lane 1) and DNA incubated with P1 (lane 2), both in the presence of ATP, were also analyzed.

supercoiling and DNA strand opening. Using the same systems described above, hRad51 indeed stimulated the supercoiling activity of hRad54B (Fig. 3B) as well as its ability to open the DNA double helix (Fig. 3C), while Rad51 alone did not possess either of these activities (Fig. 3B and C, lane 3).

D-loop formation by human Rad54B and human Rad51

During homologous recombination, homologous pairing between two recombining DNA molecules results in the formation of a D-loop (51). We showed previously that the hRad51 and hRad54 proteins functionally co-operate in D-loop formation (47). Here, we examined the influence of hRad54B on the ability of hRad51 to mediate the D-loop reaction. As reported before (7, 47), in buffer that contains Mg^{2+}, hRad51 by itself had little ability to form D-loops (Fig. 4A and B, lane 2). Importantly, in the presence of hRad54B protein, hRad51-dependent D-loop formation could be easily detected even after only 15 s of incubation (Fig. 4A). Similar to our published results on the hRad51/hRad54-mediated D-loop reaction (47), the D-loop made by hRad51 and hRad54B appeared to be unstable. The instability of the D-loop made by hRad51/hRad54 has been attributed to ATP hydrolysis by hRad51, which is expected to

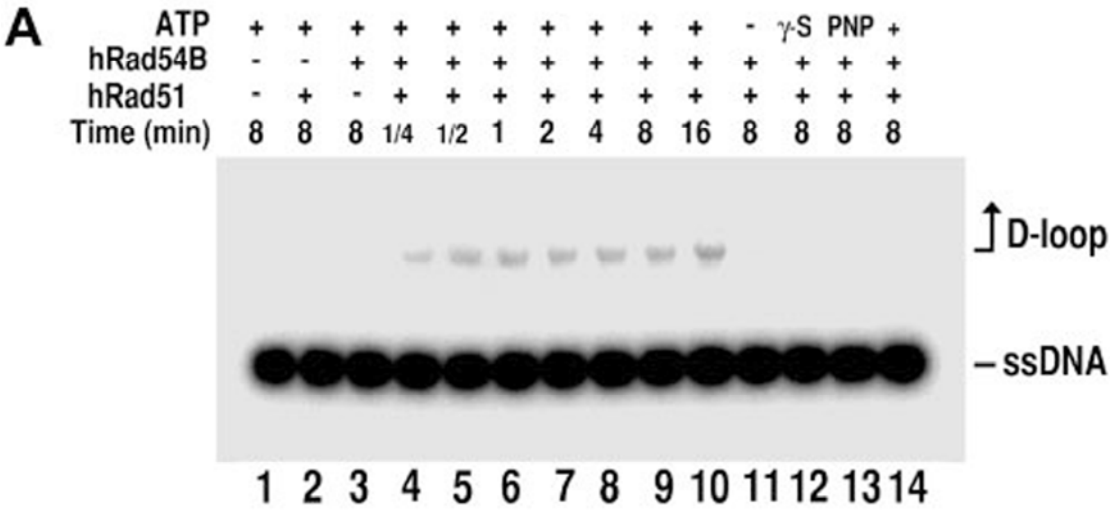
A
ATP + + + + + + + + + + - γ-S PNP +
hRad54B - - + + + + + + + + + + + +
hRad51 - + - + + + + + + + + + + +
Time (min) 8 8 8 1/4 1/2 1 2 4 8 16 8 8 8 8
D-loop
ssDNA
1 2 3 4 5 6 7 8 9 10 11 12 13 14

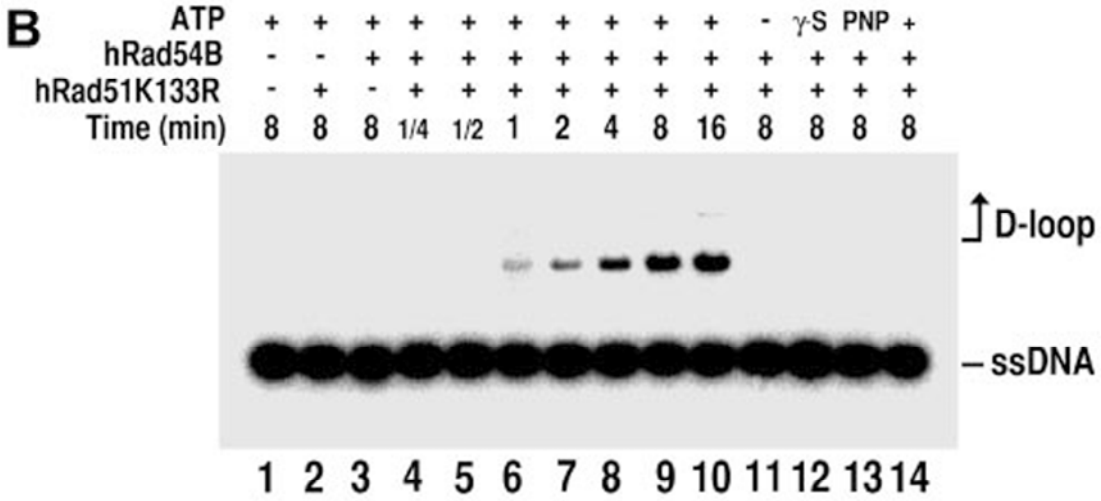
B
ATP + + + + + + + + + + - γ-S PNP +
hRad54B - - + + + + + + + + + + + +
hRad51K133R - + - + + + + + + + + + + +
Time (min) 8 8 8 1/4 1/2 1 2 4 8 16 8 8 8 8
D-loop
ssDNA
1 2 3 4 5 6 7 8 9 10 11 12 13 14

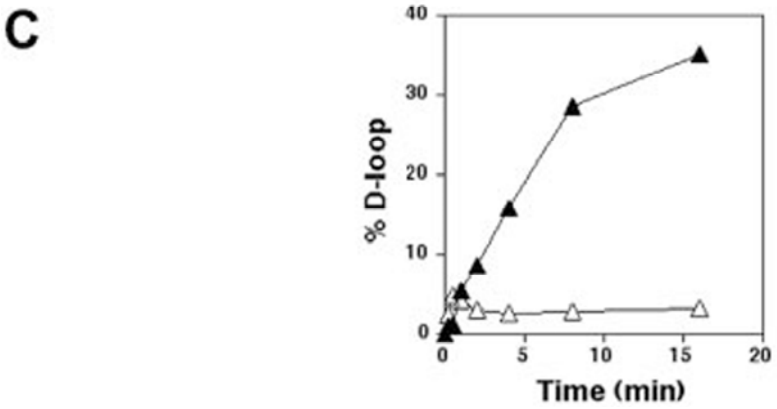
C
% D-loop
Time (min)
0
10
20
30
40
0
5
10
15
20

Figure 4. Human Rad54B stimulates D-loop formation by human Rad51. The formation and the subsequent stability of D-loops formed in the presence of hRad51 and hRad54B was studied. **(A)** The radiolabeled 90-mer oligonucleotide was incubated with hRad51 and ATP to allow filament formation, after which hRad54B and the homologous duplex target (pBluescript RFI DNA) were incorporated, and a portion of the reaction mixture was removed at the indicated times for analysis (lanes 4 to 10). The controls include: incubation of DNA substrates with ATP but no recombination protein (lane 1); incubation of DNA substrates with ATP and either Rad51 (lane 2) or hRad54B (lane 3); incubation of DNA substrates with hRad51 and hRad54B but no ATP (lane 11), or with ATP-γ-S (lane 12) or AMP-PNP (lane 13). As expected, substitution of pBluescript DNA with heterologous duplex DNA (X174) abolished D-loop formation (lane 14). **(B)** D-loop reactions were carried out as in (A) using hRad51K133R. **(C)** The results from lanes 4 to 10 of panel A (open triangles) and panel B (solid triangles) are plotted.

cause its turnover from the newly made DNA joint to initiate a second round of homologous pairing that dissociates the D-loop. In support of this premise, when hRad51 was replaced by the ATPase defective hRad51 K133R protein, the D-loop formed with hRad54B accumulated to a much higher level (Fig. 4, B and C). Regardless of whether hRad51 or hRad51 K133R was used, D-loop formation required ATP, which could not be replaced by ATPγS or AMP-PNP (Fig. 4A and B, lanes 11-13, respectively). As expected, the D-loop reaction requires homology between the single-stranded and double-stranded DNA substrates (Fig. 4A and B, lane 14).

Generation of Rad54B disrupted mouse ES cells and mice

The biochemical activities of the mammalian Rad54B protein determined above are consistent with a role for the protein in homologous recombination. To determine its role *in vivo* and to assess the biological relevance of mammalian Rad54B, we generated *Rad54B* knockout mouse ES cells and mice. A clone spanning the 3' region of *mRad54B* was isolated from a mouse genomic library and subsequently characterized by restriction analysis and intro-exon border mapping (Fig. 5A) and chromosomal localization (Supplemental Fig. 2) (40, 61). From this clone, a targeting vector was derived that upon homologous integration into the endogenous *mRad54B* locus would eliminate 28 highly conserved amino acids spanning the last conserved SWI2/SNF2 family member motif. The targeting vector was electroporated into E14 ES cells and after selection, correctly targeted clones were identified by DNA blotting using a unique probe outside the targeting sequence (Fig. 5B). A targeted clone was propagated and injected into blastocysts to generate mice carrying the disrupted *mRad54B* allele. Inactivation of the

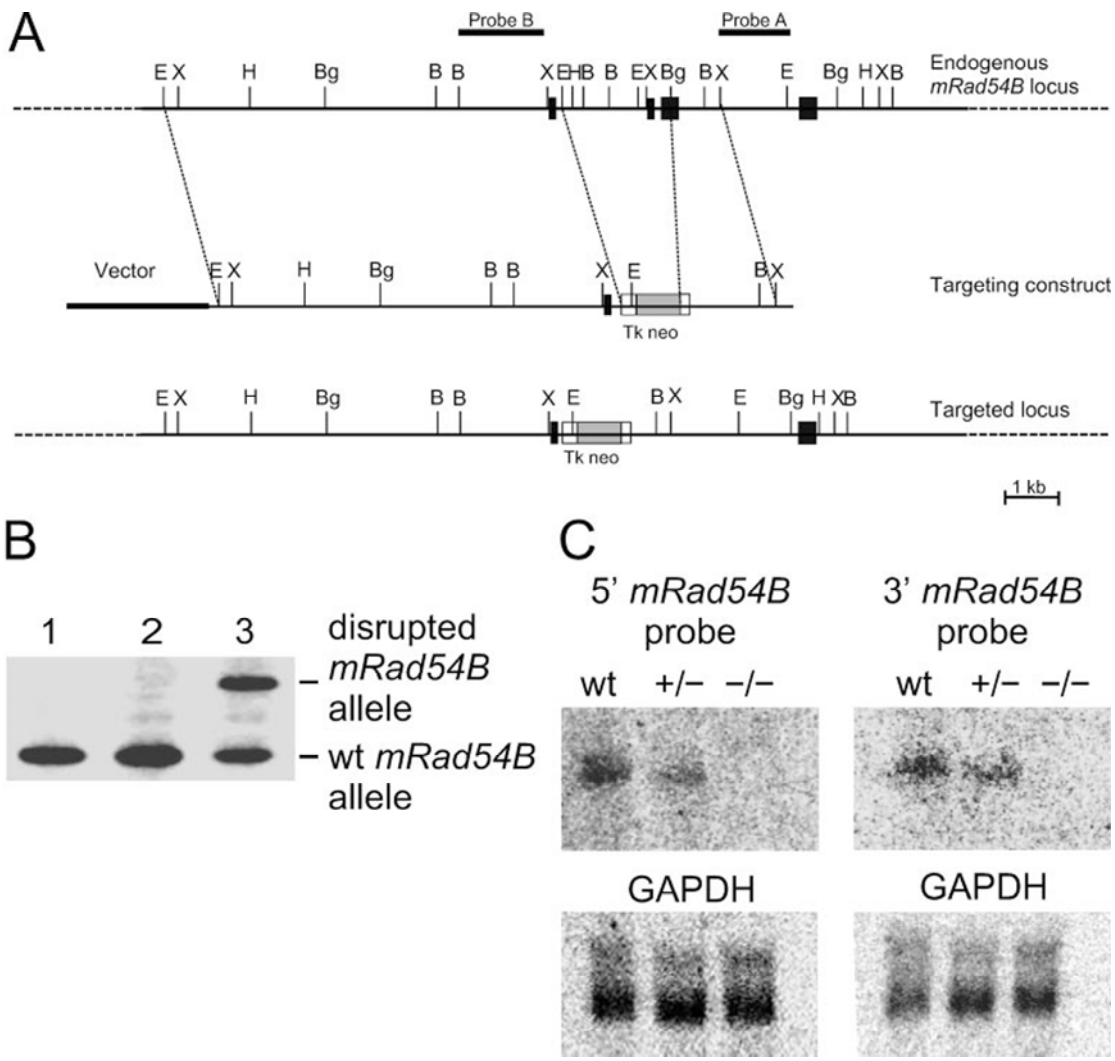

Figure 5. Characterization of part of the mouse *Rad54B* genomic locus and generation of mouse ES cells carrying a disrupted *mRad54B* allele. (A) Part of the *mRad54B* genomic locus and structure of the targeting construct. Exons 12-15 are indicated by black boxes. Shown are the locations of selected restriction sites, EcoRI (E), BamHI (B), BglII (Bg), HindIII (H), XbaI (X). The positions of two different probes, named A and B, are indicated. **(B)** DNA blot analysis of G418 resistant ES clones using probe A and EcoRI digested DNA. The wild type (wt) allele yields a 3.0 kb band while the disrupted allele results in a 3.6 kb band. (lane 1, wild type ES cell; lane 2, clone with a randomly integrated targeting construct; lane 3, clone with a homologously integrated targeting construct). **(C)** RNA blot analysis of *mRad54B* transcripts in mice carrying the disrupted allele. Total RNA (15 μg) isolated from testes of wild type, *mRad54B*$^{+/-}$ and *mRad54B*$^{-/-}$ males was probed with 5' and 3' *mRad54B* cDNA probes. A GAPDH cDNA probe served as a loading control.

mRad54B gene in *mRad54B*$^{-/-}$ mice was confirmed using RNA blot analysis (Fig. 5C). In RNA samples prepared from testis from both wild type and *mRad54B*$^{+/-}$ mice, a 2.3 kb

mRad54B transcript was observed. No transcript was detected with either a 5' or 3' probe for *mRad54B* in testes from *mRad54B*$^{-/-}$ mice.

Interbreeding of *mRad54B*$^{+/-}$ mice resulted in a Mendelian segregation of the disrupted *mRad54B* allele. Thus, mRad54B disruption did not result in embryonic or neonatal lethality. No statistically significant difference in weight was observed among *mRad54B*$^{-/-}$, *mRad54B*$^{+/-}$ and *mRad54B*$^{+/+}$ littermates. Importantly, the *mRad54B*$^{-/-}$ mice exhibited no macroscopic abnormalities up to at least six months of age. *mRad54B*$^{+/-}$ animals were crossed to obtained blastocysts, which were then used to isolate *mRad54B*$^{-/-}$ ES cells. Two independent *mRad54B*$^{-/-}$ ES cell lines were obtained, one in 129 background, and the other in 129/bl6 background. To obtain cells and animals in which both *mRad54* paralogs were disrupted *mRad54B*$^{+/-}$ mice were crossed with *mRad54*$^{+/-}$ mice. Similar to *mRad54*$^{-/-}$ and *mRad54B*$^{-/-}$ mice, *mRad54*$^{-/-}$ *mRad54B*$^{-/-}$ mice displayed no overt phenotypes and appeared normal. *mRad54*$^{-/-}$, *mRad54B*$^{-/-}$, and *mRad54*$^{-/-}$ *mRad54B*$^{-/-}$ ES cells were isolated from blastocysts obtained from intercrossing mice carrying different combinations of the *mRad54* and *mRad54B* knockout alleles.

Frequencies of targeted integration in mouse Rad54B deficient cells

Previously, we have shown the involvement of mammalian *Rad54* in homologous recombination by demonstrating that the efficiency of homologous gene targeting is reduced by 3 to10-fold in *mRad54*$^{-/-}$ ES cells (15). To test whether *mRad54B* is involved in homologous recombination as well, we examined the capacity of wild type, *mRad54B*$^{-/-}$ and *mRad54*$^{-/-}$ *mRad54B*$^{-/-}$ cells for gene targeting. Cells were transfected with linearized targeting constructs for either the *mRad54* or the *CTCF* locus. Both constructs carried puromycin resistance selectable marker flanked by regions of homology. Homologous integration events into *mRad54* and *CTCF* loci were detected by DNA blotting and PCR, respectively (Table 1 and data not shown). Interestingly, the efficiency of homologous recombination as measured by gene targeting was not reduced in *mRad54B*$^{-/-}$ cells as compared to wild type cells (Table 1). However, the involvement of *mRad54B* in homologous recombination was revealed in absence of *mRad54*. Hardly any homologous integration events were detected in *mRad54*$^{-/-}$ *mRad54B*$^{-/-}$ ES cells.

ES cell genotype	Targeted locus[b]			
	mRad54		*CTCF*	
mRad54$^{+/+}$ *mRad54B*$^{+/+}$	69.0%	(87/126)	60.0%	(54/90)
mRad54$^{+/+}$ *mRad54B*$^{-/-}$	64.7%	(178/275)	54.0%	(61/113)
mRad54$^{-/-}$ *mRad54B*$^{+/+}$	2.1%[c]	(6/284)	21.3%	(36/169)
mRad54$^{-/-}$ *mRad54B*$^{-/-}$	<0.17%	(0/560)	2.1%	(7/332)

Table 1. Efficiency of homologous recombination in wild type (m*Rad54*$^{+/+}$ m*Rad54B*$^{+/+}$), *mRad54*$^{-/-}$, *mRad54B*$^{-/-}$ and *mRad54*$^{-/-}$ *mRad54B*$^{-/-}$ ES cells as measured by homologous gene targeting. [a]

[a] ES cells of the indicated genotype were electroporated with the indicated gene targeting constructs. After selection under the appropriate conditions individual clones were isolated and expanded. Genomic DNA from the clones was isolated. For clones electroporated with *mRad54* targeting construct genomic DNA was digested with the appropriate restriction enzyme, electrophoresed through an agarose gel and transferred to a nylon membrane. Membranes were hybridized with radiolabeled probes that discriminated between homologously and randomly integrated targeting construct. For the clones electroporated with the *CTCF* targeting construct, genomic DNA was used for PCR reactions that discriminated between random and homologous integration events.

[b] The percentage of clones containing homologously integrated targeting construct relative to the total number of analyzed clones is indicated. Absolute numbers are indicated in parentheses. The differences in targeting efficiency between wild type and *mRad54*$^{-/-}$ cells, between wild type and *mRad54*$^{-/-}$ *mRad54B*$^{-/-}$ cells, between *mRad54*$^{-/-}$ and *mRad54*$^{-/-}$ *mRad54B*$^{-/-}$ cells, between *mRad54B*$^{-/-}$ and *mRad54*$^{-/-}$ cells, and between *mRad54B*$^{-/-}$ and *mRad54*$^{-/-}$ *mRad54B*$^{-/-}$ cells are statistically significant for both loci ($p<0.001$ by χ^2 analysis).

[c] Previously reported (34).

Mouse Rad54B deficiency confers hypersensitivity to ionizing radiation and mitomycin C

To determine whether the contribution of *mRad54B* to homologous recombination impinges on the ability of the cell to repair DNA damage, we examined the effect of ionizing radiation and mitomycin C on the survival of wild type, *mRad54*$^{-/-}$, *mRad54B*$^{-/-}$ and *mRad54*$^{-/-}$ *mRad54B*$^{-/-}$ ES cells. While *mRad54*$^{-/-}$ ES cells are 2- to 3-fold more sensitive to ionizing irradiation than wild type ES cells (15), *mRad54B*$^{-/-}$ cells were only 1.5-fold more sensitive than wild type ES cells (Fig. 6A). The ionizing radiation sensitivity of the double mutant *mRad54*$^{-/-}$ *mRad54B*$^{-/-}$ ES cells was similar to that of *mRad54*$^{-/-}$ ES cells. For mitomycin C, *mRad54*$^{-/-}$ and *mRad54B*$^{-/-}$ single mutant ES cells

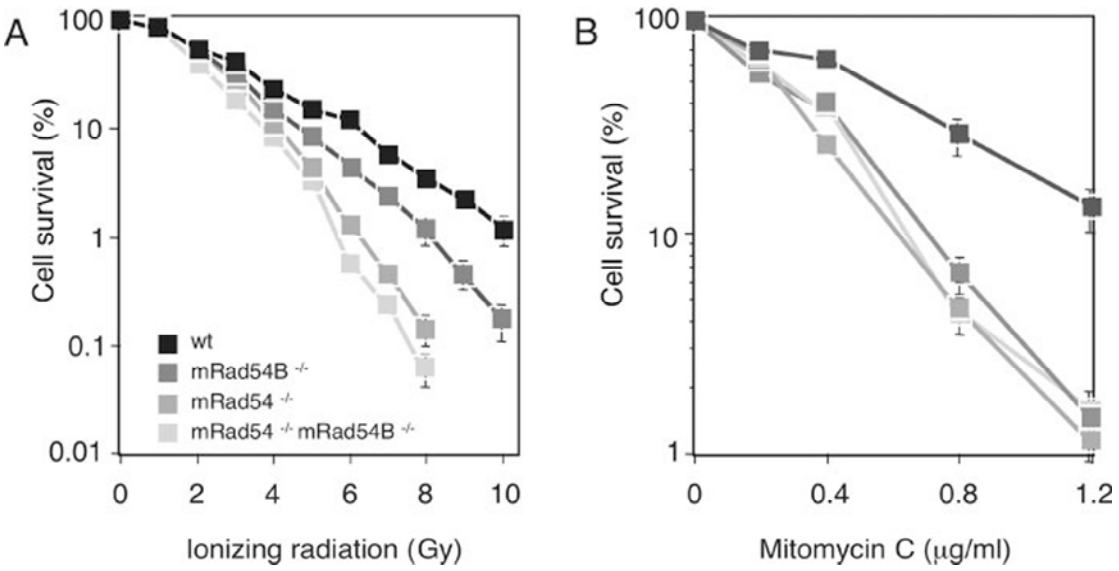

Figure 6. Effect of ionizing radiation and mitomycin C on wild type, *mRad54*$^{-/-}$, *mRad54B*$^{-/-}$ and *mRad54*$^{-/-}$ *mRad54B*$^{-/-}$ ES cells. (A) Clonogenic survival of wild type (wt) and mutant ES cells after irradiation with increasing doses of γ-rays. The percentage of surviving cells measured by their colony-forming ability is plotted as function of the γ-ray dose. **(B)** Clonogenic survival of wild type, *mRad54*$^{-/-}$, *mRad54B*$^{-/-}$ and *mRad54*$^{-/-}$ *mRad54B*$^{-/-}$ ES cells after treatment with mitomycin C. Error bars (some obscured by the symbols) represent standard error of the mean.

showed a similar hypersensitivity compared to the double mutant *mRad54*$^{-/-}$ *mRad54B*$^{-/-}$ ES cells (Fig. 6B). We conclude that, in addition to mRad54, mRad54B also contributes to repair of ionizing radiation and mitomycin C induced DNA damage.

Mice lacking both Rad54 paralogs are extremely sensitive to mitomycin C

To establish the impact of *mRad54B* on protection from the adverse effects of induced DNA damage in the adult animal wild type, *mRad54*$^{-/-}$, *mRad54B*$^{-/-}$ and *mRad54*$^{-/-}$ *mRad54B*$^{-/-}$ mice were exposed to ionizing radiation and mitomycin C. As has been found for m*Rad54*$^{-/-}$ mice neither *mRad54B*$^{-/-}$ nor *mRad54*$^{-/-}$ *mRad54B*$^{-/-}$ mice were sensitive to ionizing radiation. All the 2- to 4-months old littermates survived exposure to 7 Gy of ionizing radiation (data not shown).

Previously, we showed that *mRad54*$^{-/-}$ mice are hypersensitive to mitomycin C (17). To reveal whether *mRad54B* also contributes to protection from the mitomycin C induced DNA damage, wild type, *mRad54*$^{-/-}$, *mRad54B*$^{-/-}$ and *mRad54*$^{-/-}$ *mRad54B*$^{-/-}$ mice were injected peritoneally with different doses of mitomycin C and monitored for 14 days. As is the case for *mRad54*$^{-/-}$ mice, *mRad54B*$^{-/-}$ mice were hypersensitive to mitomycin C (Fig. 7). At a dose of 7.5 mg mitomycin C per kg of bodyweight, approximately 60%

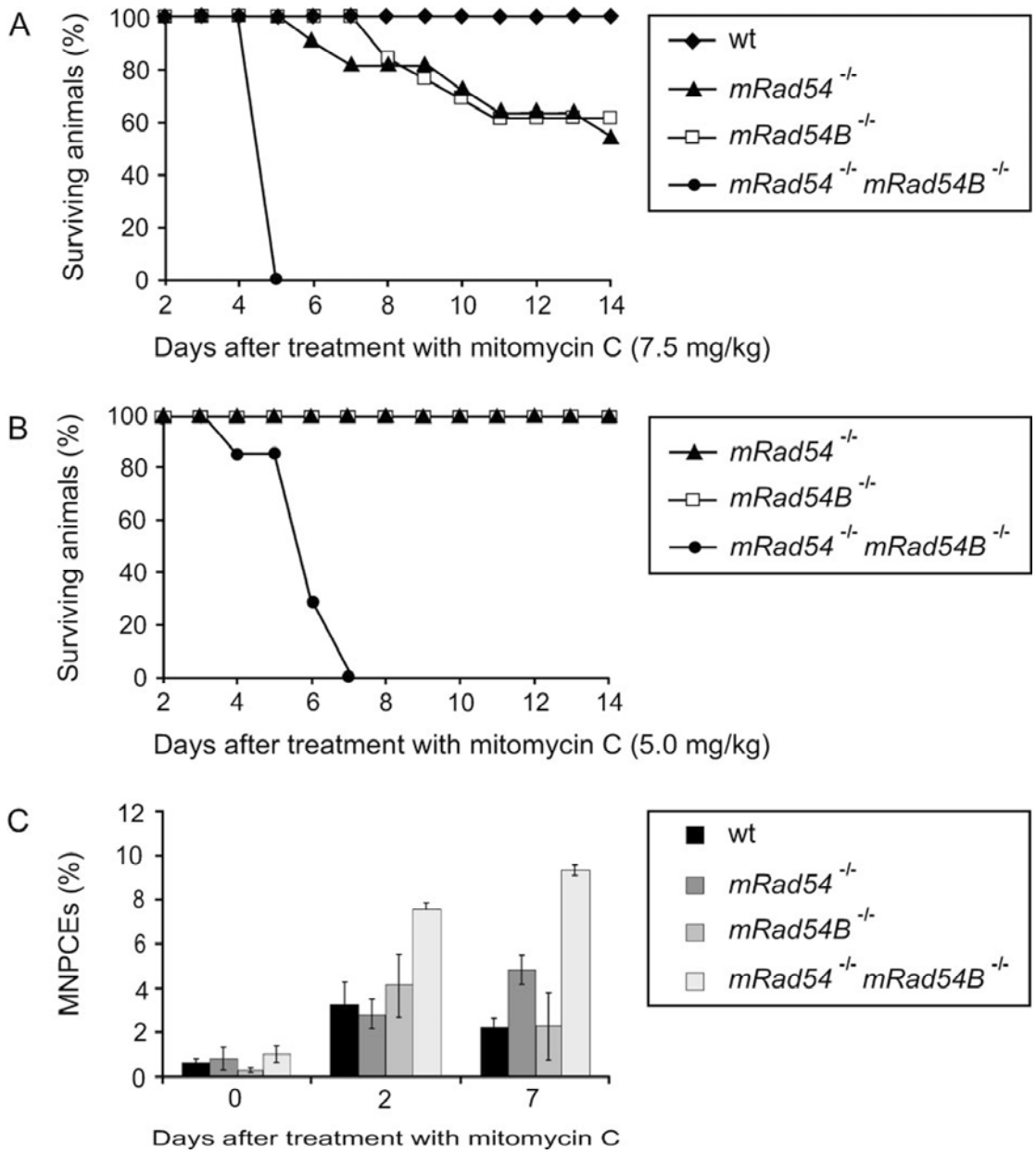

Figure 7. Impact of *mRad54B* on the mitomycin C sensitivity of mice. (A) Survival curve of wild type (n=6), *mRad54*$^{-/-}$ (n=11), *mRad54B*$^{-/-}$ (n=13) and *mRad54*$^{-/-}$ *mRad54B*$^{-/-}$ (n=4) mice after a single intraperitoneal injection of 7.5 mg of mitomycin C per kg bodyweight. **(B)** Survival curve of *mRad54*$^{-/-}$ (n=2), *mRad54B*$^{-/-}$ (n=2), and *mRad54*$^{-/-}$ *mRad54B*$^{-/-}$ (n=7) mice after treatment with 5 mg/kg mitomycin C. **(C)** Induction of micronuclei by mitomycin C in polychromatic erythrocytes. Mice of the indicated genotypes were intraperitoneally injected with 2.5 mg/kg bodyweight mitomycin C. Plotted are percentages of micronuclei-containing polychromatic erythrocytes (MNPCEs) per 500 polychromatic erythrocytes at day zero, two and seven after treatment. Data points represent average from three independently treated animals. The standard error of the mean is indicated.

of the *mRad54*$^{-/-}$ and *mRad54B*$^{-/-}$ mice survived, compared to 100% of the wild type mice. By contrast, none of the *mRad54*$^{-/-}$ *mRad54B*$^{-/-}$ mice survived the treatment. The latency period of death for *mRad54B*$^{-/-}$ mice was comparable to *mRad54*$^{-/-}$ mice. At the lower dose of 5 mg/kg mitomycin C all *mRad54*$^{-/-}$ and *mRad54B*$^{-/-}$ mice survived. In stark contrast, all of the *mRad54*$^{-/-}$ *mRad54B*$^{-/-}$ mice died within 7 days. We conclude that the mammalian Rad54 paralogs function synergistically to protect mice from the deleterious effects of mitomycin C.

The bone marrow is a major target for mitomycin C-inflicted damage *in vivo*. Therefore, we tested whether mitomycin C treatment affected cells in the blood to a different extend in *mRad54*$^{-/-}$ *mRad54B*$^{-/-}$ animals and *mRad54*$^{-/-}$ and *mRad54B*$^{-/-}$ animals using the peripheral blood micronucleus assay. The presence of micronuclei in polychromatic erythrocytes provides a measure of chromosomal aberrations. A single dose of 2.5 mg mitomycin C per kg bodyweight was administered to 6- to 8-week old animals. This treatment resulted in increases in the frequency of micronuclei-containing polychromatic erythrocytes (Fig. 7C). Before the mitomycin C treatment the percentage of micronuclei-containing polychromatic erythrocytes was similar in wild type, *mRad54*$^{-/-}$, *mRad54B*$^{-/-}$ and *mRad54*$^{-/-}$ *mRad54B*$^{-/-}$ animals. Consistent with the mitomycin C hypersensitivity of *mRad54*$^{-/-}$ *mRad54B*$^{-/-}$ mice, the crosslinking agent induced significantly higher levels of micronuclei-containing polychromatic erythrocytes in *mRad54*$^{-/-}$ *mRad54B*$^{-/-}$ mice rather than *mRad54*$^{-/-}$ and *mRad54B*$^{-/-}$ mice (Fig. 7C).

Abnormal chromosomal distribution of mouse Rad51 during meiosis in the absence of Rad54

In *S. cerevisiae*, the function of the Rad54 paralogs appears to overlap to some extend as indicated by their effects on sporulation efficiency and spore viability (27, 45). To assess the effect of the mammalian Rad54 homologs on meiosis we analyzed meiotic prophase chromosomes in spread nuclei of primary spermatocytes isolated from control, *mRad54*$^{-/-}$, *mRad54B*$^{-/-}$ and *mRad54*$^{-/-}$ *mRad54B*$^{-/-}$ mice. The chromosomes were immunostained for Sycp3 to identify the meiosis-specific synaptonemal complex that organizes the paired homologous chromosomes (Fig. 8A). Given the functional interaction between mammalian Rad54 and Rad54B in mitotic cells, we co-stained the chromosomes for mRad51. During the early stages of meiotic prophase, leptotene and zygotene, the distribution of mRad51 was similar in spread nuclei from all genotypes. However, in later stages, pachytene and diplotene, abnormal mRad51 localization was observed in spread nuclei from *mRad54*$^{-/-}$ and *mRad54*$^{-/-}$ *mRad54B*$^{-/-}$ mice. In control and

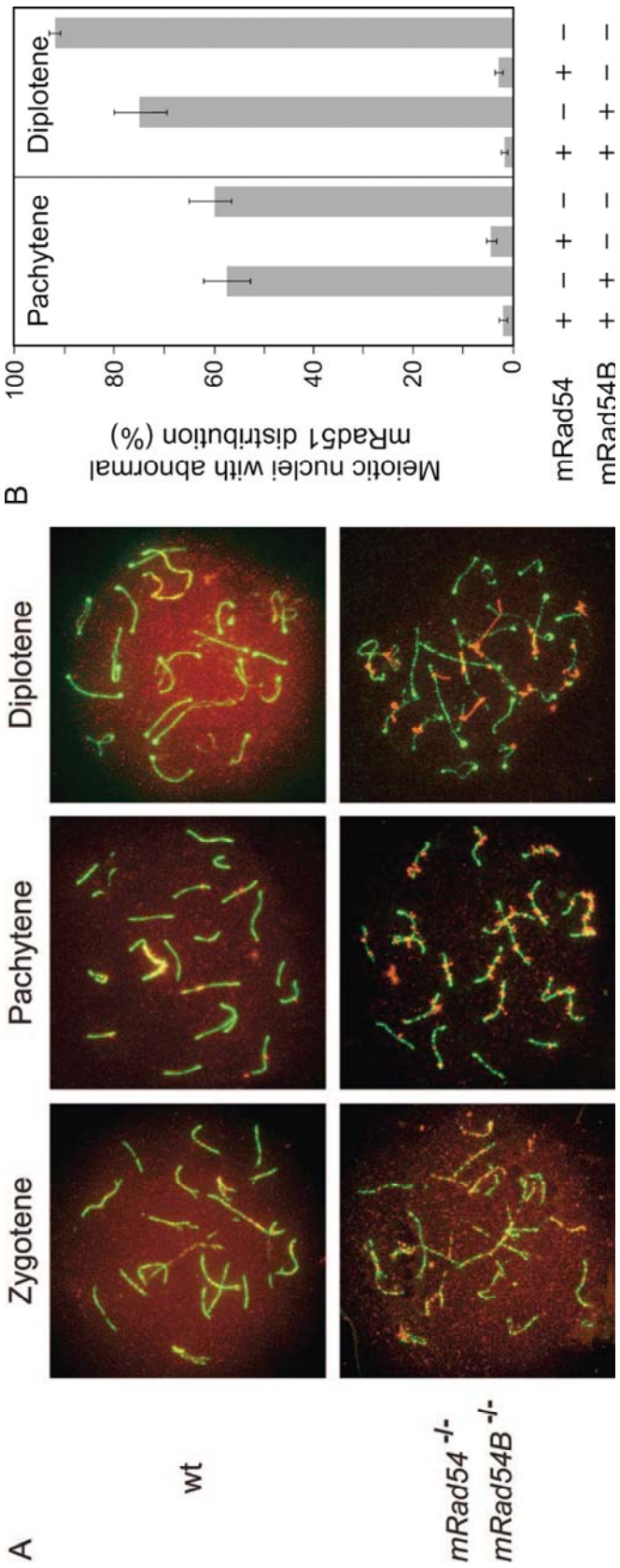
A
wt
mRad54 -/-
mRad54B -/-
Zygotene
Pachytene
Diplotene
B
Meiotic nuclei with abnormal
mRad51 distribution (%)
100
80
60
40
20
0
Pachytene
Diplotene
mRad54 + − + − + − + −
mRad54B + + − − + + − −

Figure 8. Analysis of mouse Rad51 localization on meiotic chromosomes from mRad54- and mRad54B-proficient and -deficient mice. (**A**) Localization of mRad51 (red) and Sycp3 (green) on spread nuclei of primary spermatocytes as detected by immunofluorescence. Shown are chromosome spreads from zygotene, pachytene and diplotene stages of meiosis from wild type (upper panel) and *mRad54*$^{-/-}$ *mRad54B*$^{-/-}$ (lower panel) mice. In leptotene (not shown) and zygotene no aberrant mRad51 and/or Sycp3 staining was observed irrespective of genotype. In pachytene and diplotene abnormal mRad51 distribution was detected in a high percentage of meiotic chromosome spreads derived from *mRad54*$^{-/-}$ and *mRad54*$^{-/-}$ *mRad54B*$^{-/-}$ mice. (**B**) Quantification of meiotic nuclei displaying aberrant mRad51 staining. Proficiency and deficiency of the mRad54 and mRad54B proteins in the animals from which the spermatocytes were taken is indicated by '+' and '-' signs, respectively. Spermatocytes were isolated from mRad54- and mRad54B-proficient mice (n=8), mRad54-deficient mRad54B-proficient mice (n=9), mRad54-proficient mRad54B-deficient mice (n=8) and mRad54 mRad54B-deficient mice (n=4). Percentage of meiotic nuclei with aberrant mRad51 distributions is indicated. One hundred meiotic nuclei per animal were analyzed. Error bars indicated standard error of the mean.

mRad54B$^{-/-}$ nuclei, the mRad51 signal was present on the pachytene chromosomes as well as in an overall staining of the nucleus. However, in spread nuclei derived from *mRad54*$^{-/-}$ and *mRad54*$^{-/-}$ *mRad54B*$^{-/-}$ animals, the mRad51 signal was concentrated in abnormal focus-like structures on the chromosomes only (Fig. 8A and B). The defective mRad51 distribution is even more pronounced in diplotene, where abnormally long stretches of mRad51 were observed, instead of the normal homogenous nuclear staining. Interestingly, despite the cytological abnormalities in mRad51 localization in the absence of mRad54, meiotic homologous recombination appeared to be affected only mildly. Using single sperm typing, crossing over was compared between *mRad54*$^{-/-}$ and wild type animals, each heterozygous for 129/J and C57/BL6 markers flanking the chosen regions. The recombination fraction was 0.14 (95% confidence interval [CI] = 0.09 to 0.18) in a *mRad54*$^{-/-}$ animal and 0.20 (95% CI = 0.15 to 0.25) in the wild type control for the chromosome 2 region. Using two other mice, the chromosome 7 region recombination fraction was 0.25 (95% CI = 0.21 to 0.30) in the *mRad54*$^{-/-}$ animal and 0.32 (95% CI = 0.27 to 0.37) in the wild type. The 95% confidence intervals for the *mRad54*$^{-/-}$ and wild type individuals overlapped in both regions indicating there was no statistically significant difference between the two genotypes. Note, however, that the recombination fraction for the *mRad54*$^{-/-}$ animals was reduced to about the same degree compared to wild type animals for the genetic intervals on both chromosome 2 and 7 (30% and 22%, respectively). There was no overt defect in fertility of *mRad54*$^{-/-}$, *mRad54B*$^{-/-}$ and *mRad54*$^{-/-}$ *mRad54B*$^{-/-}$ mice (data not shown).

Discussion

Homologous recombination is a versatile DNA damage repair pathway that is essential for preservation of genome integrity. Among lesions that initiate homologous recombination are single-stranded DNA gaps and DSBs. This feature makes homologous recombination ideally suited to underpin DNA replication, because single-stranded DNA gaps and DSBs occur at corrupted replication forks that arise either due to spontaneous or induced DNA damage. Homologous recombination between sister chromatids can rebuild these disabled replication forks in situ in the absence of a replication origin (10). Due to this important function homologous recombination is essential for mammalian cell viability. The requirement for homologous recombination is not limited to mitotically dividing cells; the process is also central in meiosis to generate genetic diversity by repairing meiosis-specific DSBs with the homologous chromosome as a recombination partner.

A key player in homologous recombination is Rad51, the homology recognition and DNA strand exchange protein. The essential role of homologous recombination for mammalian cell viability is underscored by the lethality of Rad51 knockout cells and mice (54). However, not all proteins involved in homologous recombination are essential, implying that either redundancy in function or the existence of subpathways of recombination that by themselves are not essential for cell viability. One example of a homologous recombination protein that is not essential for cell viability is the Rad51 accessory factor Rad54 (6, 15). To address whether there is potential redundancy in Rad54 function or recombination subpathways requiring a specialized Rad54 protein, we biochemically and genetically characterized the mammalian Rad54 paralog Rad54B.

The mammalian Rad54 paralogs have similar biochemical activities

We performed biochemical analyses of hRad54B to compare and contrast its activities with hRad54. We find that, like hRad54, hRad54B is a double-stranded DNA-dependent ATPase (Fig. 3 and (57)). However, its ATP turnover rate is about 6-fold lower than hRad54 (53, 58). In addition, we show that hRad54B has DNA translocase and DNA double helix opening activities similar to those of hRad54 (Fig. 2; (37, 39, 42, 55)). Another well-explored activity of hRad54 is its interaction with hRad51 (18, 31, 55, 59). Interestingly, it has been reported that hRad54B is different from hRad54 in this respect (58). However, using more direct assays we demonstrate that hRad54B does

interact with hRad51 and that this interaction is highly specific (Fig. 1). Furthermore, we demonstrate that this interaction is functional. Human Rad51 stimulates the ATPase activity, DNA translocase and DNA double helix opening activities of hRad54B (Fig. 3). Conversely, hRad54B stimulates the formation of D-loops, a critical intermediate in homologous recombination, generated by hRad51 (Fig. 4). We conclude hRad54B has biochemical activities similar to those of its paralog, hRad54. Therefore, hRad54 and hRad54B could provide redundant functions with respect to homologous recombination-mediated DNA damage repair or could provide similar functions but in a tissue-specific manner.

A contribution of mRad54B to homologous recombination in vivo is revealed in the absence of mRad54

The biochemical activities of the mammalian Rad54B suggest a role for the protein in homologous recombination *in vivo*. Previously, it has been reported that human Rad54B contributes to homologous recombination, because homologous gene targeting is reduced in the human colon cancer cell line HCT116 in which Rad54B had been inactivated (33). Curiously, this cell line is not sensitive to any DNA damaging agents tested, including ionizing radiation and interstrand DNA crosslinkers. The disadvantage of this cell line is its genetic instability; it is mismatch repair deficient, displays micro-satellite instability and harbors numerous chromosomal aberrations. To assess the biological impact on homologous recombination and DNA damage repair of mammalian Rad54B, we generated *Rad54B* knockout ES cells. In contrast to the HCT116 cells, these cells are non-transformed, display a stable normal karyotype and carry no additional adverse mutations that complicate the interpretation of the results. As a further advantage, the ES cells allowed us to generate double mutants that in addition to inactivated *mRad54B* alleles, also carried disrupted *mRad54* alleles.

As a reporter on homologous recombination, we measured the efficiency of homologous gene targeting in wild type ES cells and derivates in which either one or both Rad54 paralogs are inactivated. In accordance with previous results, the absence of mRad54 results in a reduced homologous recombination efficiency (15). Depending on the locus, the reduction varies between 3- to 30-fold (Table 1). In the absence of Rad54B, we consistently observe an approximately 10% reduction in recombination efficiency, but even with more than 400 events analyzed, this reduction is not statistically significant. However, cells lacking both Rad54 paralogs have a 30- to 400-fold reduced homologous recombination efficiency compared to wild type cells (Table 1). This is a

reduction of a further 10-fold compared to the absence of mRad54 alone. Thus, the involvement of mRad54B in the homologous recombination subpathway that mediates gene targeting is uncovered in the absence of mRad54.

Both mammalian Rad54 paralogs contribute to cell survival in response to DNA damage

Because homologous recombination is a versatile mechanism to repair DNA damage compared to repair mechanisms that rely on a specific DNA damage recognition protein to initiate the reaction, it is remarkable that a hRad54B-deficient cancer cell line is not hypersensitive to DNA damaging agents (33). Given the caveats mentioned above, we examined DNA damage sensitivity in mouse ES cells instead. Lack of Rad54 in ES cells results in cellular hypersensitivity to ionizing radiation and mitomycin C (15). In contrast to the hRad54B-deficient cancer line, ES cells lacking mRad54B are hypersensitive to ionizing radiation and mitomycin C (Fig. 6). At the cellular level our results reveal no strong indication for an additive or synergic interaction between the two Rad54 paralogs with respect to the repair of ionizing radiation and mitomycin C-induced DNA damage repair.

The Rad54 paralogs synergistically contribute to mitomycin C resistance in mice

The contribution of Rad54 to survival of mice in response to DNA damage differs from that in ES cells. While *mRad54*$^{-/-}$ ES are ionizing radiation and mitomycin C hypersensitive, *mRad54*$^{-/-}$ mice are mitomycin C but not ionizing radiation hypersensitive (17). We tested whether the lack of ionizing radiation hypersensitivity in mice is due to redundancy in mRad54 function provided by mRad54B. However, this is not the case because *mRad54*$^{-/-}$ *mRad54B*$^{-/-}$ mice are also not overtly ionizing radiation hypersensitive (data not shown). The contribution of homologous recombination to repair of ionizing radiation-induced DNA damage is revealed in the absence of non-homologous DNA end-joining, an alternative mechanistically distinct DSB repair pathway (17). Possibly, while homologous recombination an important DNA repair pathway for two-ended breaks, such as those induced by ionizing radiation, in rapidly dividing ES cells, non-homologous DNA end-joining is much better suited for repair of these lesions in the many non-diving cells of the adult mice. In contrast, mitomycin C-induced DNA interstrand cross-links are processed into single-ended DSBs by DNA replication (35).

Single-ended DSBs cannot be acted upon efficiently by non-homologous DNA end-joining and require homologous recombination for repair instead (11). As is the case for *mRad54*$^{-/-}$ mice, *mRad54B*$^{-/-}$ mice are mitomycin C hypersensitive (Fig. 7). Furthermore, mRad54$^{-/-}$ mRad54B$^{-/-}$ double mutant mice are extremely mitomycin C hypersensitive. This synergistic effect of the Rad54 paralogs could be due to their functions in distinct subpathways of interstrand DNA crosslink repair. However, given their biochemical similarities and the lack of a significant difference in mitomycin C hypersensitivity of *mRad54B*$^{-/-}$ versus *mRad54*$^{-/-}$ *mRad54B*$^{-/-}$ ES cells this is unlikely. Alternatively, the Rad54 paralogs might have a tissue-specific function by differentially contributing to interstrand DNA crosslink repair in different cell types of mice. This premise predicts that there should be differences in expression of the Rad54 paralogs among different tissues. Although no direct connection is currently available, the existing data does suggest that this could be the case. For example, while expression of hRAD54B is extremely low in the spleen (Supplemental Fig. 2), expression of mRad54 in the spleen is robust (25).

Mammalian Rad54 affects the distribution of Rad51 on meiotic chromosomes

Both Rad54 paralogs in *S. cerevisiae* contribute to meiosis and therefore we analyzed the effect of the mammalian Rad54 paralogs on mouse meiotic prophase chromosomes. Because both mammalian Rad54 paralogs functionally interact with Rad51, we investigated the distribution of mRad51 on meiotic prophase chromosomes. During meiosis, mRad51 is first observed in the leptotene and zygotene stages as foci distributed throughout the nucleus (5). Subsequently, mRad51 foci arrange into linear arrays that colocalize with the axial elements of the synaptonemal complex. mRad51 staining disappears during late pachytene and diplotene. Interestingly, the absence of mRad54 results in an aberrant mRad51 distribution on meiotic chromosomes in spread nuclei from primary spermatocytes, consisting of foci- and thread-like mRad51 structures localized on the chromosomal loops emanating from the synaptonemal complex that persist into the diplotene stage (Fig. 8A and B). In contrast, mRad54B deficiency does not have a dramatic impact on mRad51 localization during meiosis. Possibly, mRad54B has a minor role, because when mRad54 is also absent, the percentage of meiotic spread nuclei with abnormal mRad51 distributions increase only slightly in diplotene.

Even though the absence of the Rad54 paralogs causes an abnormal mRad51 distribution, meiosis appears not to be affected with regard to other features. *mRad54*$^{-/-}$, *mRad54B*$^{-/-}$, and *mRad54*$^{-/-}$ *mRad54B*$^{-/-}$ mice are fertile, no increase in apoptosis during

spermatogenesis is detected, and there is no difference in the number of MLH1 foci on meiotic chromosomes in spread nuclei (data not shown). Furthermore, the absence of Rad54 only slightly affects the frequency of meiotic crossing-over. Meiotic homologous recombination in mammals might depend for most of the functions provided by Rad54 paralogs on a yet unidentified, potentially meiosis-specific, Rad54 paralog. The aberrant mRad51 distribution is consistent with a role suggested for Rad54 in *S. cerevisiae*, namely its ability to remove Rad51 filaments from double-stranded DNA (49). This would be a late stage function of mRad54 during homologous recombination, at a stage when actual repair of DSBs has already taken place, or at a stage at which this can be accomplished by mechanisms that no longer require mRad54.

Comparison of the yeast and mammalian Rad54 paralogs

Taken together our data lead us to conclude that the premise that mammalian Rad54B is the functional homolog of *S. cerevisiae* Rdh54 is unlikely. While *S. cerevisiae rdh54* mutant cells display no overt DNA damage sensitivities, *mRad54B*$^{-/-}$ ES cells do. Furthermore, both *S. cerevisiae* Rad54 paralogs make significant contributions to meiotic homologous recombination. In particular, Rdh54 plays an important role in interhomolog recombination (3). In contrast, we have not detected an essential role of the mammalian Rad54 paralogs in meiosis. It is possible that a yet undiscovered meiosis-specific Rad54 paralog exists in mammals. Alternatively, rather than being strictly assigned to meiotic DSB repair, this hypothetical Rad54 paralog might overlap in DSB repair function with Rad54 and Rad54B and take over part of the function of both Rad54 and Rad54B in their absence, which would be consistent with the viability of *mRad54*$^{-/-}$ *mRad54B*$^{-/-}$ mice and the essential role of homologous recombination for mammalian cell viability. However, when challenged with exogenous DNA damaging agents such as mitomycin C, the DNA damage load might exceed the threshold of its ability to repair on its own, and this is reflected by the mitomycin C hypersensitivity of Rad54 and Rad54B deficient mice. The DNA damage threshold may also explain the apparent normal viability of the Rad54 and Rad54B deficient mice, because the level of endogenous DNA damage might be low enough to be effectively handled by a yet unidentified Rad54 paralog.

Acknowledgments

We thank Ellen van Drunen and Miranda Boeve for technical assistance. This work was supported by grants from the Dutch Cancer Society (KWF), the Netherlands Organization for Scientific Research (NWO), the European Commission, NIH (grants GM57814 and CA110415 to PS and GM36745 to NA).

References

1. **Alexeev, A., A. Mazin, and S. C. Kowalczykowski.** 2003. Rad54 protein possesses chromatin-remodeling activity stimulated by the Rad51-ssDNA nucleoprotein filament. Nat Struct Biol **10:**182-6.
2. **Alexiadis, V., A. Lusser, and J. T. Kadonaga.** 2004. A conserved N-terminal motif in Rad54 is important for chromatin remodeling and homologous strand pairing. J Biol Chem **279:**27824-9.
3. **Arbel, A., D. Zenvirth, and G. Simchen.** 1999. Sister chromatid-based DNA repair is mediated by RAD54, not by DMC1 or TID1. Embo J **18:**2648-58.
4. **Baarends, W. M., E. Wassenaar, J. W. Hoogerbrugge, G. van Cappellen, H. P. Roest, J. Vreeburg, M. Ooms, J. H. Hoeijmakers, and J. A. Grootegoed.** 2003. Loss of HR6B ubiquitin-conjugating activity results in damaged synaptonemal complex structure and increased crossing-over frequency during the male meiotic prophase. Mol Cell Biol **23:**1151-62.
5. **Barlow, A. L., F. E. Benson, S. C. West, and M. A. Hulten.** 1997. Distribution of the Rad51 recombinase in human and mouse spermatocytes. Embo J **16:**5207-15.
6. **Bezzubova, O., A. Silbergleit, Y. Yamaguchi-Iwai, S. Takeda, and J. M. Buerstedde.** 1997. Reduced X-ray resistance and homologous recombination frequencies in a RAD54-/- mutant of the chicken DT40 cell line. Cell **89:**185-93.
7. **Bugreev, D. V., and A. V. Mazin.** 2004. Ca2+ activates human homologous recombination protein Rad51 by modulating its ATPase activity. Proc Natl Acad Sci U S A **101:**9988-93.
8. **Clever, B., H. Interthal, J. Schmuckli-Maurer, J. King, M. Sigrist, and W. D. Heyer.** 1997. Recombinational repair in yeast: functional interactions between Rad51 and Rad54 proteins. Embo J **16:**2535-44.
9. **Couedel, C., K. D. Mills, M. Barchi, L. Shen, A. Olshen, R. D. Johnson, A. Nussenzweig, J. Essers, R. Kanaar, G. C. Li, F. W. Alt, and M. Jasin.** 2004. Collaboration of homologous recombination and nonhomologous end-joining factors for the survival and integrity of mice and cells. Genes Dev **18:**1293-304.
10. **Cox, M. M., M. F. Goodman, K. N. Kreuzer, D. J. Sherratt, S. J. Sandler, and K. J. Marians.** 2000. The importance of repairing stalled replication forks. Nature **404:**37-41.
11. **Cromie, G. A., J. C. Connelly, and D. R. Leach.** 2001. Recombination at double-strand breaks and DNA ends: conserved mechanisms from phage to humans. Mol Cell **8:**1163-74.
12. **Cui, X. F., H. H. Li, T. M. Goradia, K. Lange, H. H. Kazazian, Jr., D. Galas, and N. Arnheim.** 1989. Single-sperm typing: determination of genetic distance between the G gamma-globin and parathyroid hormone loci by using the polymerase chain reaction and allele-specific oligomers. Proc Natl Acad Sci U S A **86:**9389-93.

13. **Dresser, M. E., D. J. Ewing, M. N. Conrad, A. M. Dominguez, R. Barstead, H. Jiang, and T. Kodadek.** 1997. DMC1 functions in a Saccharomyces cerevisiae meiotic pathway that is largely independent of the RAD51 pathway. Genetics **147:**533-44.
14. **Dronkert, M. L., H. B. Beverloo, R. D. Johnson, J. H. Hoeijmakers, M. Jasin, and R. Kanaar.** 2000. Mouse RAD54 affects DNA double-strand break repair and sister chromatid exchange. Mol Cell Biol **20:**3147-56.
15. **Essers, J., R. W. Hendriks, S. M. Swagemakers, C. Troelstra, J. de Wit, D. Bootsma, J. H. Hoeijmakers, and R. Kanaar.** 1997. Disruption of mouse RAD54 reduces ionizing radiation resistance and homologous recombination. Cell **89:**195-204.
16. **Essers, J., R. W. Hendriks, J. Wesoly, C. E. Beerens, B. Smit, J. H. Hoeijmakers, C. Wyman, M. L. Dronkert, and R. Kanaar.** 2002. Analysis of mouse Rad54 expression and its implications for homologous recombination. DNA Repair (Amst) **1:**779-93.
17. **Essers, J., H. van Steeg, J. de Wit, S. M. Swagemakers, M. Vermeij, J. H. Hoeijmakers, and R. Kanaar.** 2000. Homologous and non-homologous recombination differentially affect DNA damage repair in mice. Embo J **19:**1703-10.
18. **Golub, E. I., O. V. Kovalenko, R. C. Gupta, D. C. Ward, and C. M. Radding.** 1997. Interaction of human recombination proteins Rad51 and Rad54. Nucleic Acids Res **25:**4106-10.
19. **Hayashi, M., T. Morita, Y. Kodama, T. Sofuni, and M. Ishidate, Jr.** 1990. The micronucleus assay with mouse peripheral blood reticulocytes using acridine orange-coated slides. Mutat Res **245:**245-9.
20. **Hiramoto, T., T. Nakanishi, T. Sumiyoshi, T. Fukuda, S. Matsuura, H. Tauchi, K. Komatsu, Y. Shibasaki, H. Inui, M. Watatani, M. Yasutomi, K. Sumii, G. Kajiyama, N. Kamada, K. Miyagawa, and K. Kamiya.** 1999. Mutations of a novel human RAD54 homologue, RAD54B, in primary cancer. Oncogene **18:**3422-6.
21. **Ho, K. S., and R. K. Mortimer.** 1975. X-ray-induced lethality and chromosome breakage and repair in a radiosensitive strain of yeast. Basic Life Sci **5B:**545-7.
22. **Hoeijmakers, J. H.** 2001. Genome maintenance mechanisms for preventing cancer. Nature **411:**366-74.
23. **Jaskelioff, M., S. Van Komen, J. E. Krebs, P. Sung, and C. L. Peterson.** 2003. Rad54p is a chromatin remodeling enzyme required for heteroduplex DNA joint formation with chromatin. J Biol Chem **278:**9212-8.
24. **Jiang, H., Y. Xie, P. Houston, K. Stemke-Hale, U. H. Mortensen, R. Rothstein, and T. Kodadek.** 1996. Direct association between the yeast Rad51 and Rad54 recombination proteins. J Biol Chem **271:**33181-6.
25. **Kanaar, R., C. Troelstra, S. M. Swagemakers, J. Essers, B. Smit, J. H. Franssen, A. Pastink, O. Y. Bezzubova, J. M. Buerstedde, B. Clever, W. D. Heyer, and J. H. Hoeijmakers.** 1996. Human and mouse homologs of the Saccharomyces cerevisiae RAD54 DNA repair gene: evidence for functional conservation. Curr Biol **6:**828-38.
26. **Kim, P. M., K. S. Paffett, J. A. Solinger, W. D. Heyer, and J. A. Nickoloff.** 2002. Spontaneous and double-strand break-induced recombination, and gene conversion tract lengths, are differentially affected by overexpression of wild-type or ATPase-defective yeast Rad54. Nucleic Acids Res **30:**2727-35.

27. **Klein, H. L.** 1997. RDH54, a RAD54 homologue in Saccharomyces cerevisiae, is required for mitotic diploid-specific recombination and repair and for meiosis. Genetics **147:**1533-43.
28. **Li, H. H., U. B. Gyllensten, X. F. Cui, R. K. Saiki, H. A. Erlich, and N. Arnheim.** 1988. Amplification and analysis of DNA sequences in single human sperm and diploid cells. Nature **335:**414-7.
29. **Lisby, M., J. H. Barlow, R. C. Burgess, and R. Rothstein.** 2004. Choreography of the DNA damage response: spatiotemporal relationships among checkpoint and repair proteins. Cell **118:**699-713.
30. **Mazin, A. V., A. A. Alexeev, and S. C. Kowalczykowski.** 2003. A novel function of Rad54 protein. Stabilization of the Rad51 nucleoprotein filament. J Biol Chem **278:**14029-36.
31. **Mazin, A. V., C. J. Bornarth, J. A. Solinger, W. D. Heyer, and S. C. Kowalczykowski.** 2000. Rad54 protein is targeted to pairing loci by the Rad51 nucleoprotein filament. Mol Cell **6:**583-92.
32. **Mills, K. D., D. O. Ferguson, J. Essers, M. Eckersdorff, R. Kanaar, and F. W. Alt.** 2004. Rad54 and DNA Ligase IV cooperate to maintain mammalian chromatid stability. Genes Dev **18:**1283-92.
33. **Miyagawa, K., T. Tsuruga, A. Kinomura, K. Usui, M. Katsura, S. Tashiro, H. Mishima, and K. Tanaka.** 2002. A role for RAD54B in homologous recombination in human cells. Embo J **21:**175-80.
34. **Niedernhofer, L. J., J. Essers, G. Weeda, B. Beverloo, J. de Wit, M. Muijtjens, H. Odijk, J. H. Hoeijmakers, and R. Kanaar.** 2001. The structure-specific endonuclease Ercc1-Xpf is required for targeted gene replacement in embryonic stem cells. Embo J **20:**6540-9.
35. **Niedernhofer, L. J., H. Odijk, M. Budzowska, E. van Drunen, A. Maas, A. F. Theil, J. de Wit, N. G. Jaspers, H. B. Beverloo, J. H. Hoeijmakers, and R. Kanaar.** 2004. The structure-specific endonuclease Ercc1-Xpf is required to resolve DNA interstrand cross-link-induced double-strand breaks. Mol Cell Biol **24:**5776-87.
36. **Peters, A. H., A. W. Plug, M. J. van Vugt, and P. de Boer.** 1997. A drying-down technique for the spreading of mammalian meiocytes from the male and female germline. Chromosome Res **5:**66-8.
37. **Petukhova, G., S. Stratton, and P. Sung.** 1998. Catalysis of homologous DNA pairing by yeast Rad51 and Rad54 proteins. Nature **393:**91-4.
38. **Petukhova, G., S. A. Stratton, and P. Sung.** 1999. Single strand DNA binding and annealing activities in the yeast recombination factor Rad59. J Biol Chem **274:**33839-42.
39. **Petukhova, G., P. Sung, and H. Klein.** 2000. Promotion of Rad51-dependent D-loop formation by yeast recombination factor Rdh54/Tid1. Genes Dev **14:**2206-15.
40. **Pinkel, D., T. Straume, and J. W. Gray.** 1986. Cytogenetic analysis using quantitative, high-sensitivity, fluorescence hybridization. Proc Natl Acad Sci U S A **83:**2934-8.
41. **Qin, J., S. Baker, H. Te Riele, R. M. Liskay, and N. Arnheim.** 2002. Evidence for the lack of mismatch-repair directed antirecombination during mouse meiosis. J Hered **93:**201-5.
42. **Ristic, D., C. Wyman, C. Paulusma, and R. Kanaar.** 2001. The architecture of the human Rad54-DNA complex provides evidence for protein translocation along DNA. Proc Natl Acad Sci U S A **98:**8454-60.

43. **Schmuckli-Maurer, J., M. Rolfsmeier, H. Nguyen, and W. D. Heyer.** 2003. Genome instability in rad54 mutants of Saccharomyces cerevisiae. Nucleic Acids Res **31:**1013-23.
44. **Shinohara, M., S. L. Gasior, D. K. Bishop, and A. Shinohara.** 2000. Tid1/Rdh54 promotes colocalization of rad51 and dmc1 during meiotic recombination. Proc Natl Acad Sci U S A **97:**10814-9.
45. **Shinohara, M., E. Shita-Yamaguchi, J. M. Buerstedde, H. Shinagawa, H. Ogawa, and A. Shinohara.** 1997. Characterization of the roles of the Saccharomyces cerevisiae RAD54 gene and a homologue of RAD54, RDH54/TID1, in mitosis and meiosis. Genetics **147:**1545-56.
46. **Signon, L., A. Malkova, M. L. Naylor, H. Klein, and J. E. Haber.** 2001. Genetic requirements for RAD51- and RAD54-independent break-induced replication repair of a chromosomal double-strand break. Mol Cell Biol **21:**2048-56.
47. **Sigurdsson, S., S. Van Komen, G. Petukhova, and P. Sung.** 2002. Homologous DNA pairing by human recombination factors Rad51 and Rad54. J Biol Chem **277:**42790-4.
48. **Solinger, J. A., and W. D. Heyer.** 2001. Rad54 protein stimulates the postsynaptic phase of Rad51 protein-mediated DNA strand exchange. Proc Natl Acad Sci U S A **98:**8447-53.
49. **Solinger, J. A., K. Kiianitsa, and W. D. Heyer.** 2002. Rad54, a Swi2/Snf2-like recombinational repair protein, disassembles Rad51:dsDNA filaments. Mol Cell **10:**1175-88.
50. **Sugawara, N., X. Wang, and J. E. Haber.** 2003. *In vivo* roles of Rad52, Rad54, and Rad55 proteins in Rad51-mediated recombination. Mol Cell **12:**209-19.
51. **Sung, P., L. Krejci, S. Van Komen, and M. G. Sehorn.** 2003. Rad51 recombinase and recombination mediators. J Biol Chem **278:**42729-32.
52. **Sung, P., L. Prakash, S. Weber, and S. Prakash.** 1987. The RAD3 gene of Saccharomyces cerevisiae encodes a DNA-dependent ATPase. Proc Natl Acad Sci U S A **84:**6045-9.
53. **Swagemakers, S. M., J. Essers, J. de Wit, J. H. Hoeijmakers, and R. Kanaar.** 1998. The human RAD54 recombinational DNA repair protein is a double-stranded DNA-dependent ATPase. J Biol Chem **273:**28292-7.
54. **Symington, L. S.** 2002. Role of RAD52 epistasis group genes in homologous recombination and double-strand break repair. Microbiol Mol Biol Rev **66:**630-70, table of contents.
55. **Tan, T. L., J. Essers, E. Citterio, S. M. Swagemakers, J. de Wit, F. E. Benson, J. H. Hoeijmakers, and R. Kanaar.** 1999. Mouse Rad54 affects DNA conformation and DNA-damage-induced Rad51 foci formation. Curr Biol **9:**325-8.
56. **Tan, T. L., R. Kanaar, and C. Wyman.** 2003. Rad54, a Jack of all trades in homologous recombination. DNA Repair (Amst) **2:**787-94.
57. **Tanaka, K., T. Hiramoto, T. Fukuda, and K. Miyagawa.** 2000. A novel human rad54 homologue, Rad54B, associates with Rad51. J Biol Chem **275:**26316-21.
58. **Tanaka, K., W. Kagawa, T. Kinebuchi, H. Kurumizaka, and K. Miyagawa.** 2002. Human Rad54B is a double-stranded DNA-dependent ATPase and has biochemical properties different from its structural homolog in yeast, Tid1/Rdh54. Nucleic Acids Res **30:**1346-53.

59. **Van Komen, S., G. Petukhova, S. Sigurdsson, S. Stratton, and P. Sung.** 2000. Superhelicity-driven homologous DNA pairing by yeast recombination factors Rad51 and Rad54. Mol Cell **6:**563-72.
60. **van Veelen, L. R., T. Cervelli, M. W. van de Rakt, A. F. Theil, J. Essers, and R. Kanaar.** 2005. Analysis of ionizing radiation-induced foci of DNA damage repair proteins. Mutat Res **574:**22-33.
61. **Weeda, G., J. Wiegant, M. van der Ploeg, A. H. Geurts van Kessel, A. J. van der Eb, and J. H. Hoeijmakers.** 1991. Localization of the xeroderma pigmentosum group B-correcting gene ERCC3 to human chromosome 2q21. Genomics **10:**1035-40.
62. **Wolner, B., and C. L. Peterson.** 2005. ATP-dependent and ATP-independent roles for the Rad54 chromatin remodeling enzyme during recombinational repair of a DNA double strand break. J Biol Chem **280:**10855-60.
63. **Wolner, B., S. van Komen, P. Sung, and C. L. Peterson.** 2003. Recruitment of the recombinational repair machinery to a DNA double-strand break in yeast. Mol Cell **12:**221-32.

Supplemental data

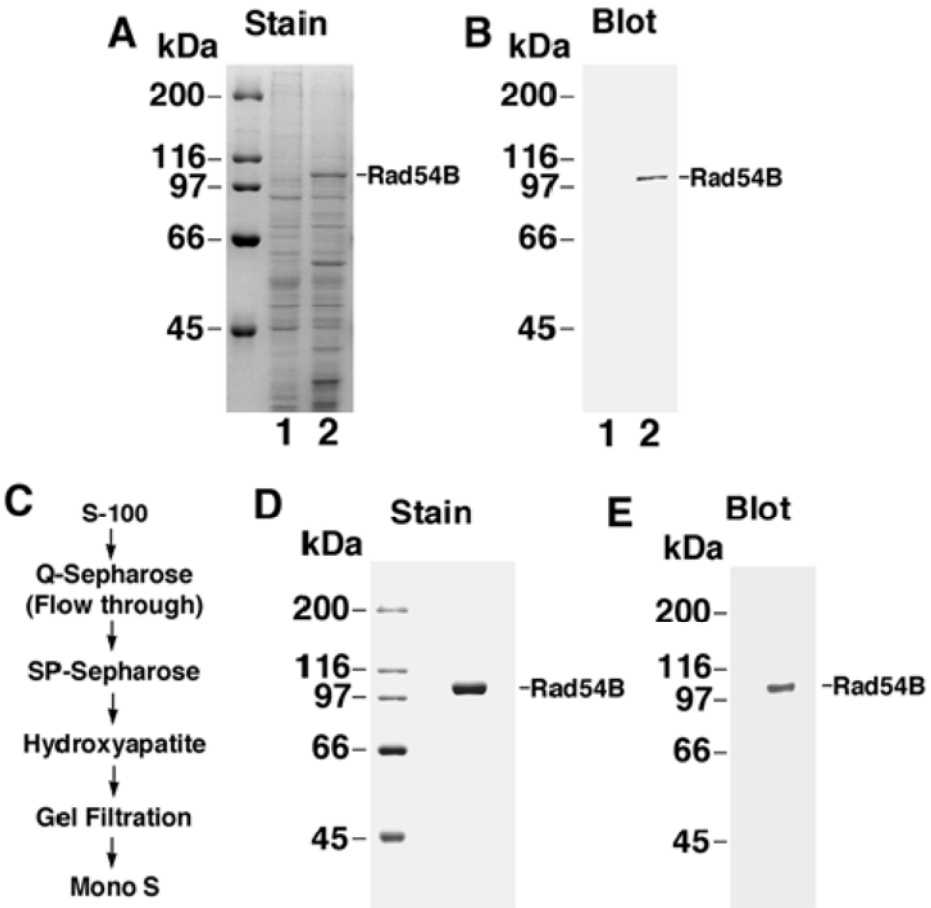

Supplementary Figure 1. **Expression and purification of human Rad54B.** The *hRAD54B* cDNA was cloned from a testis cDNA library using the polymerase chain reaction. The cDNA was sequenced and then used to generate a recombinant bacculovirus. For protein purification, High-five insect cells were infected with the hRad54B recombinant bacculovirus at an M.O.I. of 10. Cells were harvested, lysed, and fractionated in a series of chromatographic columns to obtain nearly homogeneous hRad54B. The overall yield was ~1 mg of hRad54B from 150 ml of insect cell culture. Three independent preparations of hRad54B gave similar results in all the biochemical assays described here. **(A)** Coomassie Blue-stained SDS-PAGE gel of High-five cells extracts. Lane 1, uninfected cells; lane 2, cells infected with the hRad54B producing baculovirus. **(B)** Immunoblot containing the same cell extracts as shown in (A), probed with anti-hRad54B antibodies. **(C)** Outline of the fractionation scheme used to purify the hRad54B protein. **(D)** Coomassie Blue-stained SDS-PAGE gel containing a sample of the final hRad54B preparation (1.2 μg). **(E)** Immunoblot containing the final hRad54B preparation probed with anti-hRad54B antibodies.

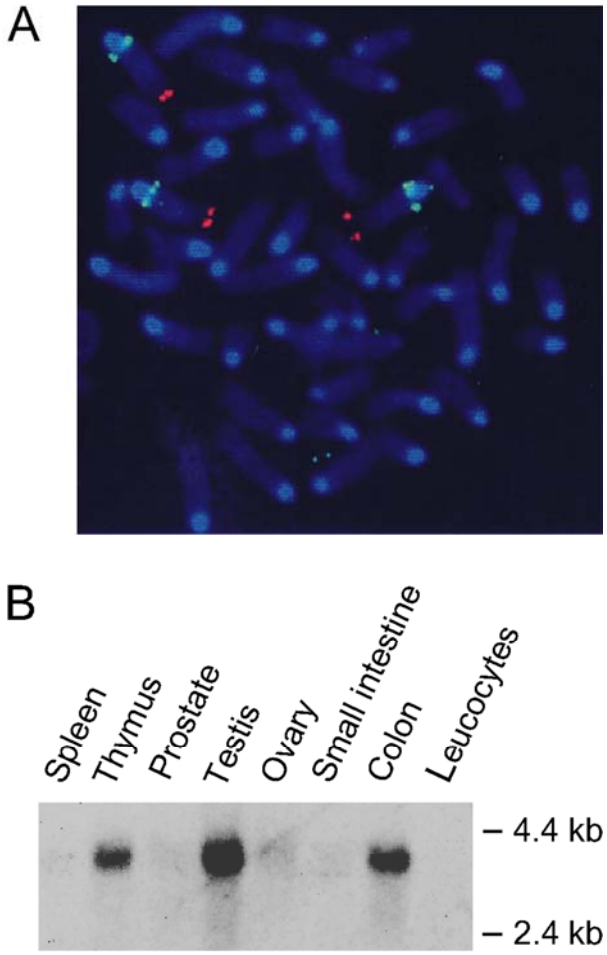

Supplementary Figure 2. Chromosomal localization and expression pattern of mammalian *Rad54B*. (A) Chromosomal localization of *mRad54B* by fluorescent *in situ* hybridization. The chromosomal localization of *mRad54B* was determined by FISH on a murine erythroid cell line containing a chromosome 4 trisomy (16). Treatment of metaphase spreads prior to hybridization was described previously (61). A PAC clone containing *mRad54B* genomic DNA fragment was labeled with digoxigenin and used in combination with chromosome 4 specific telomeric probe labeled with biotin. Together with mouse Cot-1 DNA probes were hybridized to metaphase spreads as described (40). To detect the *mRad54B* signal metaphase spreads were incubated with sheep-anti-digoxigenin-rhodamine and donkey-anti-sheep-texas-red, the telomeric probe was detected using avidin D-FITC. Slides were dehydrated with ethanol, air dried and counterstained with DAPI in antifade media. The *mRad54B* hybridization signal, in green, was detected on chromosome 4 near band A2. The chromosome 4 specific probe is in red. DAPI counterstaining of the chromosome spread revealed the chromosome banding pattern. Mouse *Rad54B* is located in a region syntenic to human chromosome 8q21, where human *Rad54B* is localized (20). **(B)** Expression of mammalian *Rad54B* in different human tissues. A RNA blot (human Multiple Tissue Northern blot, Clontech, cat # 7759-1) containing approximately 2 μg of poly $(A)^+$ RNA isolated from the indicated tissues was hybridized with a probe derived from the *hRad54B* cDNA.

Supplemental Table 1.

Primers used for single sperm PCR

Marker	First-round primers	Second-round primers	PCR product (129/J)
D2Mit213	WR, 5'CAAGATGGAGCATTTCTGACC3'	WL, WR	138 bp
D2Mit412	WL, WR	WR, 5'GTATCATCTTTCATGTGAAAAC3'	92 bp
D7Mit268	WL, WR	WR, 5'TGCCATGGCACAGGCACTCC3'	112 bp
D7Mit353	WL, 5'GAACTCAAGGCTTCACACTTTAGGC3'	WL, WR	88 bp

The primers for each locus were based on sequences found at the Whitehead Institute website http://www.broad.mit.edu/cgi-bin/mouse/index. The sizes of the C57BL6 PCR products can also be found at this site. WL, identical to left Whitehead primer; WR, identical to right Whitehead primer.

PCR reaction conditions Two rounds of PCR were used in single sperm typing. In the first round, primer pairs for two different markers on the same chromosome were used to amplify both loci flanking the interval in each sperm. A 2 μl aliquot of first-round PCR product was then used in each of two separate second-round reactions, one for each individual marker. The first round of PCR consists of an initial denaturation at 94°C for 4 min, 30 cycles at 94°C for 45 s for denaturation, and one temperature for annealing and extension for 3 min, with the final extension at 72°C for 5 min. The annealing and extension temperature was 60°C for *D7Mit268*, and *D7Mit353* and 55°C for *D2Mit213*, and *D2Mit412*. All PCRs contained 10 mM Tris-Cl (pH 8.3), 50 mM KCl, 1.5 mM $MgCl_2$, 0.01% gelatin, 50 μM each of dATP, dGTP, dCTP, and TTP, 0.2 μM of each primer and one unit of *Taq* DNA polymerase in 50 μl. The conditions for the second round were the same as for the first round except that a 90 s annealing and extension time was used. The products were resolved on 6% polyacrylamide gels, stained with ethidium bromide, and photographed under ultraviolet (UV) illumination.

Data Analysis Analysis of a large number of sperm makes it possible to determine whether any individual sperm is a recombinant or a nonrecombinant, even if the phase is not known; for linked loci, nonrecombinant sperm are more frequent than recombinant sperm. Calculating the recombination fraction by the ratio of recombinant sperm to total sperm is subject to error. Instead, the sperm-typing data were analyzed using the TWOLOC program (12) which estimates the recombination fraction and its standard error while allowing for experimental errors: inefficient single molecule PCR, more than one sperm present in a sample, and contamination.

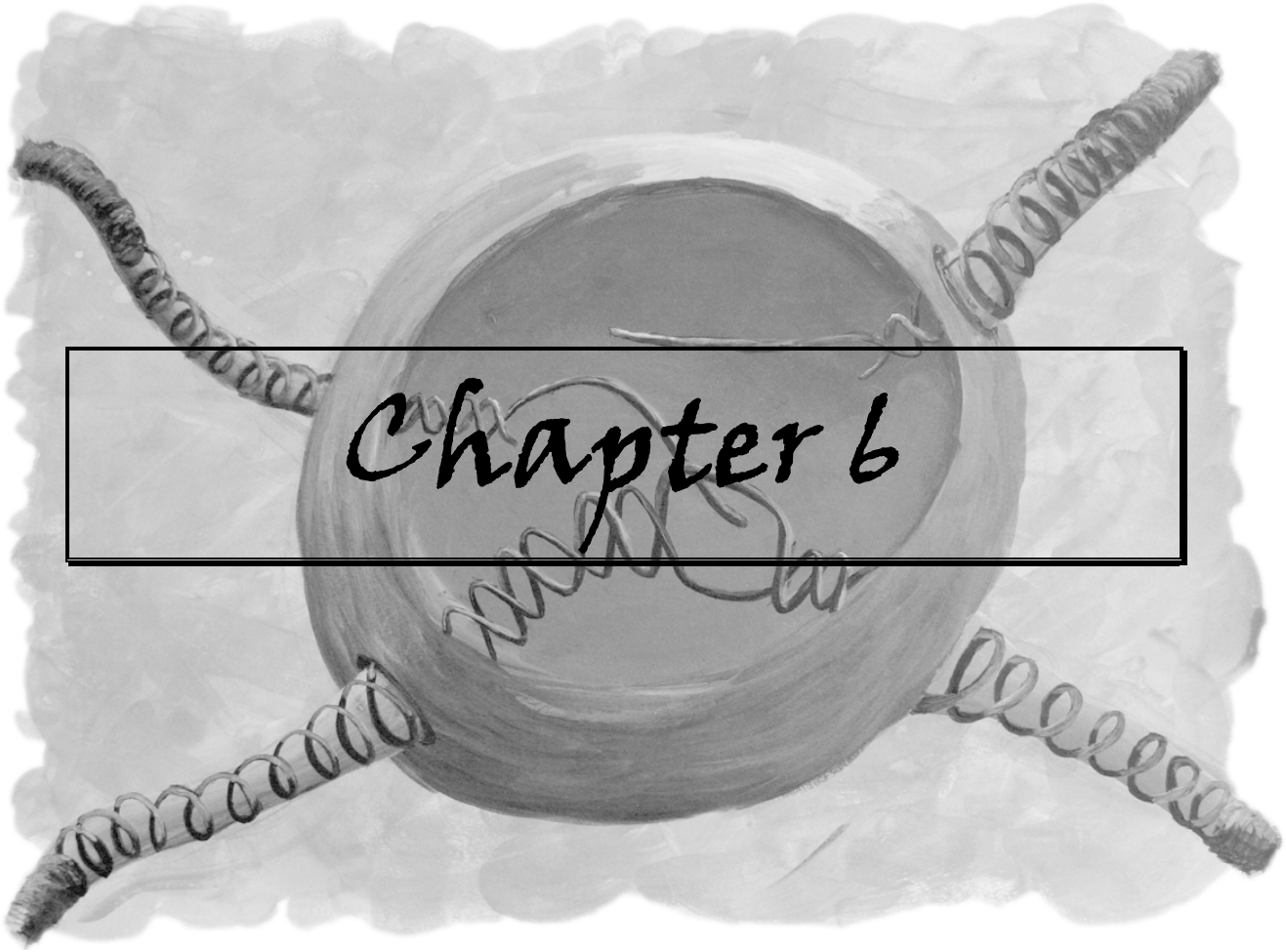

Chapter 6

DNA double-strand break repair and chromosome translocations

Published in:
DNA repair 5 (9 – 10): 1075 – 1081
2006

Everyone makes mistakes. The trick is to make them when nobody's looking.

~Unknown

DNA double-strand break repair and chromosome translocations

Sheba Agarwal[a], Agnieszka A. Tafel[a], Roland Kanaar[a,b,*]

[a]Department of Cell Biology and Genetics, [b]Department of Radiation Oncology, Erasmus MC, PO Box 1738, 3000 DR Rotterdam, The Netherlands

*Corresponding author. Tel.: +31 10 4087168; Fax: +31 10 4089472.
E-mail address: r.kanaar@erasmusmc.nl (Roland Kanaar)

Abstract

Translocations are genetic aberrations that occur when a broken fragment of a chromosome is erroneously rejoined to another chromosome. The initial event in the creation of a translocation is the formation of a DNA double-strand break (DSB), which can be induced both under physiological situations, such as during the development of the immune system, or by exogenous DNA damaging agents. Two major repair pathways exist in cells that repair DSBs as they arise, namely homologous recombination, and non-homologous end-joining. In some situations these pathways can function inappropriately and rejoin ends incorrectly to produce genomic rearrangements, including translocations. Translocations have been implicated in cancer because of their ability to activate oncogenes. Due to selection at the level of the DNA, the cell, and the tissue certain forms of cancer are associated with specific translocations that can be used as a tool for diagnosis and prognosis of these cancers.

Keywords: Translocations; Homologous recombination; Non-homologous end-joining; Fragile sites

1. Introduction

A chromosomal translocation is a genomic aberration involving the rejoining of a broken chromosome fragment to another chromosome. While there need not be a net change in the amount of genetic material following this event, it can result in the disruption of genes or cause the juxtaposition of elements that disturb normal expression of the gene present at the breakpoint. This becomes critical when such translocations result in rearrangements that create genetic elements with oncogenic characteristics. In

this case, it can lead to a selective advantage of cells containing these translocations with the potential for uncontrolled proliferation.

2. Clinical implications

Several documented cases of cancer exist in which translocations play an important role. One of the first described was the Philadelphia chromosome, t(9;22), found in cancer cells of patients suffering from chronic myelogenous leukemia [1]. The proto-oncogene *ABL* (*c-ABL*), a gene encoding a protein tyrosine kinase, was discovered to be located at the breakpoint on chromosome 9 [2]. *c-ABL* is highly regulated in its normal chromosomal environment, but is hyper-activated in the context of the Philadelphia chromosome translocation. Another example is Burkitt's lymphoma, where translocations involving chromosome 8 and chromosomes 2, 14 or 22 have been documented. In this case, the proto-oncogene *c-MYC* and the genes implicated in the production of antibodies (immunoglobulin (*Ig*) light (*L*) and heavy (*H*) chains) have been found at the breakpoints [3-5]. As a result, *MYC* is mis-regulated; it is abnormally overexpressed under the influence of the *Ig* gene promoters. *MYC* could increase DNA damage load by increased production of reactive oxygen species, due to its role in mitochondrial gene expression [6]. Other genes have been implicated in cancers involving translocations, for example, deregulation of the homeobox gene *HOX11* by the t(10;14) translocation is involved in T-cell acute lymphoblastic leukemia [7].

Over the years, many more translocations occurring in leukemias, lymphomas and solid tumors have been identified. While found mostly in hematological cancers, translocations have been implicated in cancers of mesenchymal and epithelial origin as well [8]. An online database that catalogues the occurrence of diseases with specific chromosomal aberration has been compiled (http://cgap.nci.nih.gov/Chromosomes/Mitelman).

The identification of translocations is carried out by classical karyotyping or spectral karyotyping (SKY) analysis [9]. In the clinic, certain types of chromosome translocations are used in classification of primarily haematopoeitic cancers and for the clinical prognosis of patients. For example, in an acute myeloid leukemia patient, a t(8;21) translocation is indicative of a good prognosis, that is, a positive response to treatment and long-term survival, compared to patients with a t(9;22) translocation. This information is then used to identify patients that will benefit from chemotherapy, and to determine the length and dosage of treatment [10].

3. Pathways of DNA double-strand break repair

The mechanism of the formation of translocations has been the focus of intense studies over the years. Chromosome breakage is a first step in the creation of a translocation; in its simplest form, the breakage occurs due to the formation of a DNA double-strand breaks (DSBs) in a chromosome. DSBs can be caused by both exogenous agents, such as ionizing radiation and certain chemicals, as well as by endogenous agents, including the byproducts of cellular metabolism, such as oxygen free radicals [11]. DSBs can also arise spontaneously in each S phase, for example, when a single-strand break in a parental strand is passed by a replication fork, a DSB will result [12]. Besides the pathological DSBs mentioned above, certain cell types undergo processes that require the induction of physiologically important DSBs. For example, nuclease-induced DSBs in germ cells trigger meiotic recombination that results in creation of genetic diversity. In addition, the assembly of active *Ig* and T cell receptor (*TCR*) genes as well as in *IgH* class switch recombination (CSR) occurring in the immune system requires the controlled induction of DSBs.

Repair mechanisms exist in the cell to promote the beneficial effects of the physiologically occurring DSBs and to counteract the deleterious effects of the pathological DSBs. The importance of DSB repair pathways in genome maintenance is underscored by the fact that genomic instability is a characteristic feature of cell lines and animals deficient in DSB repair pathways [13]. Proper functioning of these pathways is important in the deterrence of the illegitimate reattachment of broken chromosomes, preventing the disruption and misregulation of genes in this way. There are two mechanistically distinct methods to rejoin DNA ends, dependent on their requirement for homologous DNA sequences: homology-directed repair and non-homologous end-joining. Both can be divided in a number of subpathways that will be discussed below.

3.1 Homologous recombination

Homologous recombination is generally an error-free pathway of homology-directed repair. A DSB is accurately repaired by using the undamaged sister chromatid as a template for the repair of the broken sister chromatid (Figure 1). Homologous recombination in eukaryotes is carried out by the RAD52 epistasis group of proteins, so called because they were originally identified by the genetic analysis of ionizing radiation hypersensitive *Saccharomyces cerevisiae* mutants [14,15]. In human cells, the proteins in this group include the MRN (RAD50/MRE11/NBS1) complex, RAD51, the RAD51

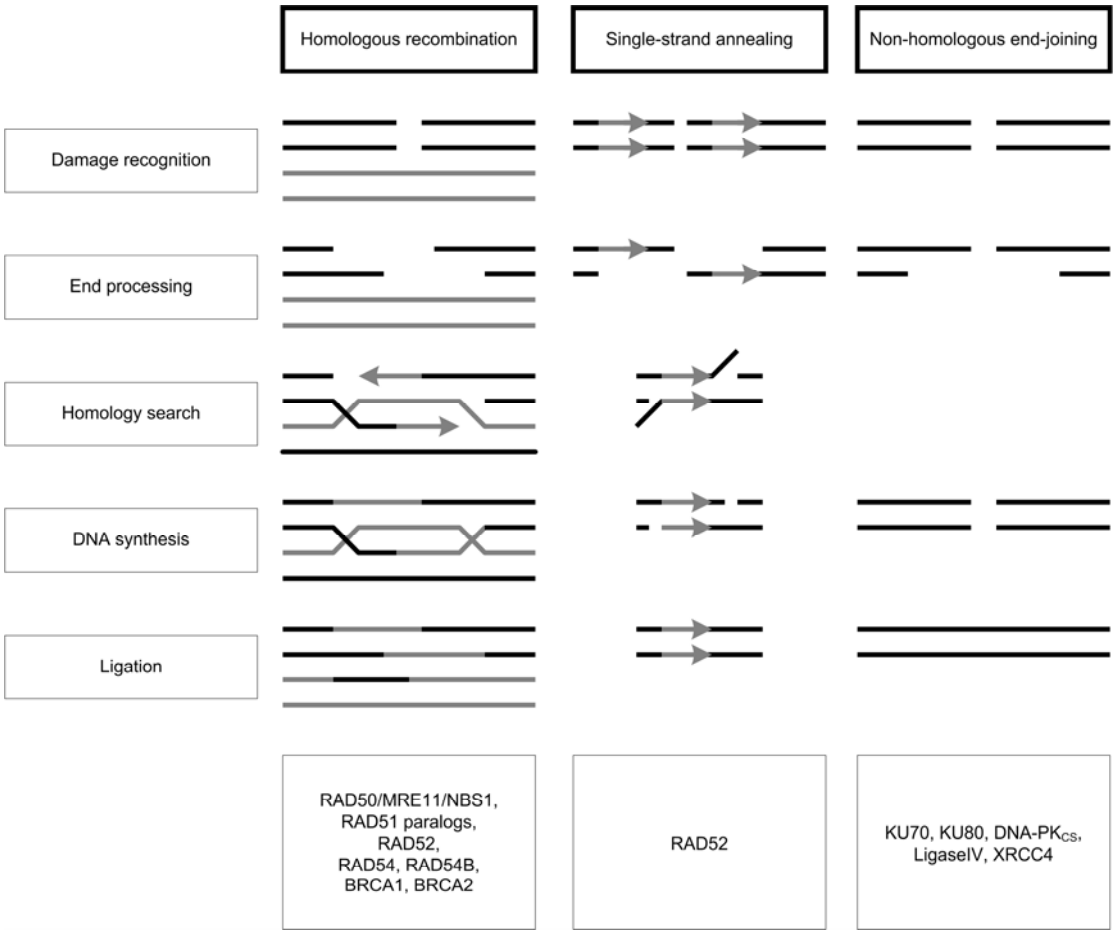

Figure 1. Schematic representation of DNA double-strand break repair pathways. The homology-directed DSB repair pathways, homologous recombination and single-strand annealing, are indicated in the left and middle panels, respectively. Non-homologous end-joining is shown in the panel on the right. The broken DNA molecule is indicated by the black double lines. During homologous recombination, the intact, homologous template DNA, indicated in grey, is essential for an accurate repair. DNA replication is portrayed by the arrowhead. Single-strand annealing can repair breaks occurring between or within repeated DNA sequences (indicated by grey arrows). This repair pathway results in deletion of a repeat sequence and the sequences between the original repeats. Homologous DNA is not required for non-homologous end-joining and nucleotides at the break might be added or lost, resulting in inaccurate repair. All three pathways involve damage recognition, resection of broken DNA ends, DNA resynthesis and ligation. Homology search, although in mechanistically distinct manners, takes place during homologous recombination and single-strand annealing. Subsequent stages taking place in the repair pathways are listed on the left. The proteins involved in each pathway, which are discussed in the text, are indicated below each scheme.

paralogs (RAD51B, RAD51C, RAD51D, XRCC2, XRCC3), RAD54 and RAD54B [16]. The products of the breast cancer susceptibility genes, BRCA1 and BRCA2, are also involved in the modulation of the homologous recombination [17-19].

When a DSB is detected, the initial damage response is mediated through the MRN complex and Ataxia telangiectasia mutated protein (ATM) [20]. The resection of DNA ends is required to generate 3' single-stranded DNA tails, which are the substrate for homologous recombination, because they are utilized for the nucleation of recombination factors on the DNA. RAD51 is an important protein at the core of homologous recombination. With the help of accessory factors, RAD51 polymerizes on the 3' tails to create a nucleoprotein filament. After homology search, the nucleoprotein filament invades the target duplex at the site of homology to create a critical intermediate, the D-loop. This joint molecule between the broken sister chromatid and the intact sister chromatid is used as a template for DNA polymerases such that sequence information that was lost in the initial processing of the DSB end is restored. The reaction is concluded with the ligation of DNA strands and the separation of the joint molecules to yield two intact DNA copies (Fig. 1).

One of the proteins involved in the regulation of homologous recombination is the product of the breast cancer susceptibility gene, BRCA2. BRCA2 has been implicated in a mediator-type function involving multiple interactions with RAD51. BRCA2 binds to and sequesters RAD51, presumably preventing the promiscuous binding of RAD51 to DNA, that could instigate illegitimate homologous recombination within highly repetitive DNA content in the genome. However, upon DNA damage induction, RAD51 accumulates at a high local concentration into foci at the sites of damage with the help of BRCA2 [21,22]. Evidence for the involvement of Brca2 in genome stability has been provided by murine cells that express a truncated form of Brca2. These cells display impaired recombination, accumulate DNA breaks, and spontaneous chromosomal abnormalities, including translocations [23].

3.1.1 Homologous recombination and translocations

Translocations can occur due to an inappropriate use of recombination mechanisms [8]. In mitotic cells, specifically in the late S/G_2 phase, the template for DSB repair through homologous recombination is preferentially the sister chromatid. This guarantees that the original sequence is restored without any changes [24]. In the human genome however, the presence of highly repetitive sequences can lead to ectopic recombination, resulting in DNA rearrangements including translocations. The highly repetitive *Alu* sequences in the genome can undergo homology-promoted replication slippage or homology-mediated illegitimate DSB repair within and between sister

chromatids, homologous or heterologous chromosomes. The *ALL1* (acute lymphoblastic leukemia 1) gene presents an example of how mistakes in homologous recombination can result in oncogenic translocations [25]. *ALL1* is unique among leukemia genes because it can be involved in fusions with a large number of different partner genes located on various chromosomes. Furthermore, *ALL1* can itself be rearranged or duplicated internally by tandem duplication of a portion of the gene [26-28]. In one case of leukemia with a normal karyotype, parts of the duplicated *ALL1* gene have been found fused with *Alu* sequences, such that a chimeric, full-length *Alu* sequence is recreated [29]. This evidence points to homologous recombination between two *Alu* sequences as a molecular mechanism for the partial duplication of *ALL1*.

3.2 Single-strand annealing

Single-strand annealing is another subpathway of homology-directed repair, but in contrast to homologous recombination, it is non-conservative, because it results in loss of genetic material (Fig. 1). Single-strand annealing is limited to operating between directly repeated sequences. The action of an exonuclease or helicase at a DSB between such direct repeats results in the exposure of complementary single strands. In a RAD51 independent fashion, complementary sequences (ranging between 30 – 100 base pairs flanking the breaks) anneal to form an intermediate, facilitated by the DNA binding and annealing properties of RAD52 [30]. Single-stranded non-complementary overhangs are removed by nucleases. The result is the loss of one repeat unit and the intervening sequence, demonstrating the imprecise nature of this mechanism.

3.2.1 Single-strand annealing and translocations

Single-strand annealing within a chromosome can lead to deletions, and between two chromosomes, it can result in translocations. This was demonstrated in an experimental set-up in which the site for the rare cutting endonuclease I-Sce I was incorporated in the context of homologous sequences placed in chromosomes 14 and 17 in mouse embryonic stem cells [31]. Following the induction of breakages of the chromosomes by transient expression of I-Sce I, the status of exchanges between chromosomes was determined. Translocations were only detected when the I-Sce I sites were present on both chromosomes. Sequence analysis revealed that none of the recombinants could have arisen by gene conversion accompanied by crossing-over, and

were therefore the products of single-strand annealing between homologous sequences [32].

3.3 Non-homologous end-joining

Conceptually, non-homologous end-joining is the simplest way of repairing DSBs: the straightforward religation of ends without the requirement for a template (Fig. 1). Non-homologous end-joining plays a major role in the elimination of DSBs during G_1 phases of the cell cycle since homologous recombination is not efficient in this phase due to the lack of sister chromatids. In addition, non-homologous end-joining is the mechanism by which the DSBs that initiate V(D)J-recombination and *Ig* CSR are processed in the immune system.

After DSB formation, the KU70/80 heterodimer binds the DNA ends. This facilitates the recruitment of DNA dependent protein kinase catalytic subunit (DNA-PK_{CS}) to the DSB. This sequential binding of the proteins activates the phosphorylation function of DNA-PK_{CS}, phosphorylating itself, the KU heterodimer, and other proteins involved in cell cycle regulation [33]. It has been speculated that KU70/80 might function as an alignment factor that binds DSB ends, creating easy access for and greatly stimulating the function of the DNA ligase IV-XRCC4 complex, increasing the efficiency and accuracy of non-homologous end-joining [34-36]. The Ligase IV-XRCC4 complex then ligates the juxtaposed DNA ends.

A subpathway of non-homologous end-joining requires the nuclease Artemis. Based on pulsed-field gel electrophoresis and phosporylation of the histone H2 variant H2AX as measures of DSBs, approximately 10% of radiation-induced breaks were shown to require processing by Artemis. This process also requires various other players like NBS1, MRE11 and DNA-PK, as well as mediator proteins like H2AX and p53BP1. This highly error-prone pathway repairs DSBs with slower kinetics compared to the Artemis independent pathway [37,38].

Besides the repair of DNA damage induced pathological DSBs, non-homologous end-joining is essential for processing of programmed DSBs in the lymphocyte, a cell-type specific for Ig and TCR production for a functional immune system. Ig and TCR diversity is created during early B and T cell development. In these cells, the programmed induction of DSBs occurs at specific sites, named recombination signal sequences, in the germline variable (V), diversity (D) and joining (J) gene segments. These DSBs are introduced by recombination activating gene (RAG) 1 and 2 proteins. One of each

region (V, D and J) is brought together and ligated via non-homologous end-joining, which completes V(D)J recombination and leads to the production of functional Igs and TCRs [33]. The programmed generation of DSBs is restricted to the G_1 phase of developing lymphocytes, by the cell cycle dependent expression of the RAG2 protein [39-41].

Mature B cells undergo clonal expansion in response to an antigen. In order to accommodate this, these cells undergo a process called CSR. Here, the preassembled VDJ_H exon is attached to different constant (C_H) region, changing the antibody effector function. DNA lesions are introduced by activation induced deaminase (AID) in the large repetitive switch (S) region, upstream of the C_H genes; these lesions are thought to be processed by mismatch repair or base excision repair proteins. This creates staggered single-strand breaks on both DNA strands, ultimately resulting in DSBs within the S regions. The repair mechanism of these DSBs is still unclear, although it is thought to involve elements of both non-homologous end-joining and homologous recombination, including KU70/80, DNA-PK_{CS}, H2AX, and p53BP1 [41,42].

3.3.1 Non-homologous end-joining and translocations

The process of breakage and rejoining in V(D)J recombination that is utilized in the physiological process of mature receptor generation can be misused to create aberrations. The consequence of this might be the joining of a proto-oncogene locus with the elements of the antigen receptor locus, bringing the oncogene under an active promoter. An example of this is the activation of *c-MYC* in Burkitt's lymphoma [43,44].

Translocations can arise when non-homologous end-joining is not functioning properly. The first non-homologous end-joining defective mouse discovered was the severe combined immunodeficiency (SCID) mouse. The cells from this mouse were found to be defective in DNA-PK_{CS}, and therefore is defective in joining the DSB intermediate in V(D)J recombination [45,46]. As a result, these mice cannot develop a functional immune system, and eventually succumb to lymphoid tumors [13]. The cancer phenotype is exacerbated in mice deficient for both non-homologous end-joining and p53, which develop pro-B cell lymphomas much earlier compared to *scid* mice. A possible explanation for this is that there is reduced apoptosis in cells from *p53*$^{-/-}$ mice, and cells that accumulate genetic aberrations are not efficiently eliminated [47,48]. The RAG-dependent lymphomas in p53-deficient *scid* mice often contain a characteristic translocation between chromosomes 12, containing the *IgH*, and 15 containing *c-MYC*

[41,47,49]. This is also seen in humans, where the *IgH/c-MYC* translocation is frequently seen in lymphomas [41,47,50].

Theoretically, the RAG proteins might make a cut at one true recombination sequence which is at the V(D)J region, and another cryptic recombination sequence at the other chromosome involved, resulting in the aberrant rejoining of ends. Thus the chromosomal loci containing such sequences might be more likely to participate in translocations. For example, the major breakpoint region of the *BCL1* locus, which forms unusual structures that render them RAG targets (see below). It is conceivable that RAG post-cleavage synaptic complexes capture non-specific chromosome ends and join these together with ends generated during V(D)J recombination. It has also been shown that many B lineage tumors, such as sporadic forms of Burkitt's lymphoma, harbor translocations that map within the C region sequences, suggesting aberrant repair of a DSB that was generated through AID during CSR [41,51].

4. Aberrant DNA structures and translocations

As has been discussed above, translocations can be a consequence of inappropriate action of DSB repair pathways. However, another important aspect with regard to the occurrence of translocations is the stability of the genome itself. The genome is not uniformly stable and contains fragile sites, so called because they have been implicated in chromosome breakage and DSB formation [52-54]. Many fragile sites are therefore also recombination "hot spots", i.e., regions where recombination has a higher probability of occurring compared to the overall genome [55]. Fragile sites have been shown to contain expanded repeated sequences [52], specifically purine and pyrimidine repeat regions.

Other aberrant DNA structures might also trigger the DSB repair pathways to act. For example, for the translocation t(14;18), implicated in follicular lymphomas, it was found that the major breakpoint region, about 150 bps on chromosome 18, assumes a non-B-DNA structure with single-stranded characteristics, which appears to be cleaved by the RAG complex [56]. A similar non-B-DNA type region was discovered in the human *PKD1* gene, where breakages were seen in a 2.5 kbp poly(purine/pyrimidine) stretch [57]. Furthermore, DNA with mirror repeat symmetry can form an intra-molecular triplex structure called H-DNA, which was seen to be clustered in *c-MYC*, is also hypothesized to be mutagenic [58]. Another abnormal DNA structure appears in palindronic AT-rich repeats that have been shown to be involved in DSB formation (at

the center of the palindrome) and subsequent translocations, such as t(11;22) [59-61]. The *in vitro* tertiary structure of this palindrome was investigated and revealed to form a cruciform structure under physiological conditions. It was hypothesized that this unstable conformation might be a cause for translocations observed involving this region [62]. These observations indicate that while the translocations are a direct consequence of the dysfunction of DSB repair mechanisms, the DNA itself may exist in abnormal conformations, which are then erroneously recognized as substrates by specific DSB repair proteins. Therefore DNA itself, instead of exogenous DNA damage, can be the causative agent of aberrations.

5. Perspective

The factors that can exacerbate the formation of translocations can be classified into cis- and trans-acting factors. An example of a cis-acting factor is DNA structure. It has been shown in various studies that non-cononical DNA structures can be prone to breakage. Since the central intermediate in the generation of a chromosome translocation is a DSB, loci which contain hotspots for DSB formation have a higher probably of being involved in a translocation. The fact that some of these fragile sites have been shown to be at the breakpoints of documented oncogenic translocations is consistent with this. Exogenous agents that cause DNA damage and/or impede DNA replication can uncover fragile sites [63]. In this regard, an interesting correlation between an increase in the expression of fragile sites involved in breakage resulting in cancer and smoking has been documented [64]. On the other hand, trans-acting factors are the proteins involved in the different types of DSB repair pathways. Cells defective in a DSB repair protein contain a higher frequency of chromosome aberrations compared to cells in which DSB repair pathways function optimally.

A crucial question that still remains to be answered is: what is the actual frequency with which chromosomal translocations occur in normal DSB repair proficient cells in the body? This issue is not an easy one to address due to complications at various levels. First of all, there is the consideration that the genome is not uniformly stable. Because certain DNA structures are more likely to lead to breakage of the DNA backbone, loci containing such structures have a higher probability of being involved in a translocation over loci lacking such sites. Second, there is selection at the cellular level. A critical consideration here is that not all translocations provide the cells with a proliferative advantage. In fact, cells containing gross DNA aberrations are more likely to

undergo apoptosis. Third, the effects of aberrations might be difficult to document at the tissue level, because translocations that are oncogenic in the context of one tissue may not be oncogenic in the context of others.

Although the factors mentioned above conspire against determining the exact frequency with which translocations occur, they do provide an advantage in the context of cancer therapy. The bias at the level of the DNA, the cell, and the tissue eventually result in the occurrence of specific chromosomal translocations in certain cancers, such that they can be used for the diagnosis and prognosis of these cancers.

Acknowledgements

Work in the authors' laboratory is funded by grants from the Dutch Cancer Society (KWF), the Netherlands Organization for Scientific Research (NWO) and the European Commission.

References

[1] P.C. Nowell and D.A. Hungerford, A minute chromosome in human chronic granulocytic leukemia, Science 132 (1960) 1497.

[2] A. de Klein, A.G. van Kessel, G. Grosveld, C.R. Bartram, A. Hagemeijer, D. Bootsma, N.K. Spurr, N. Heisterkamp, J. Groffen and J.R. Stephenson, A cellular oncogene is translocated to the Philadelphia chromosome in chronic myelocytic leukaemia, Nature 300 (1982) 765-767.

[3] I.R. Kirsch, C.C. Morton, K. Nakahara and P. Leder Human, immunoglobulin heavy chain genes map to a region of translocations in malignant B lymphocytes, Science 216 (1982) 301-303.

[4] R. Dalla-Favera, M. Bregni, J. Erikson, D. Patterson, R.C. Gallo and C.M. Croce, Human c-myc onc gene is located on the region of chromosome 8 that is translocated in Burkitt lymphoma cells, Proc Natl Acad Sci U S A 79 (1982) 7824-7827.

[5] G.M. Lenoir, J.L. Preud'homme, A. Bernheim and R. Berger, Correlation between immunoglobulin light chain expression and variant translocation in Burkitt's lymphoma, Nature 298 (1982) 474-476.

[6] C.V. Dang, F. Li and L.A. Lee, Could MYC induction of mitochondrial biogenesis be linked to ROS production and genomic instability?, Cell Cycle 4 (2005) 1465-1466.

[7] M. Hatano, C.W. Roberts, M. Minden, W.M. Crist and S.J. Korsmeyer, Deregulation of a homeobox gene, HOX11, by the t(10;14) in T cell leukemia, Science 253 (1991) 79-82.

[8] J.D. Rowley, Chromosome translocations: dangerous liaisons revisited, Nat Rev Cancer 1 (2001) 245-250.

[9] A. Kolialexi, G.T. Tsangaris, S. Kitsiou, E. Kanavakis and A. Mavrou, Impact of cytogenetic and molecular cytogenetic studies on hematologic malignancies, Anticancer Res 25 (2005) 2979-2983.

[10] L.M. Staudt, Molecular diagnosis of the hematologic cancers, N Engl J Med 348 (2003) 1777-1785.

[11] E.C. Friedberg, L.D. McDaniel and R.A. Schultz, The role of endogenous and exogenous DNA damage and mutagenesis, Curr Opin Genet Dev 14 (2004) 5-10.
[12] J.E. Haber, DNA recombination: the replication connection, Trends Biochem Sci 24 (1999) 271-275.
[13] D.C. van Gent, J.H. Hoeijmakers and R. Kanaar, Chromosomal stability and the DNA double-stranded break connection, Nat Rev Genet 2 (2001) 196-206.
[14] J.C. Game and R.K. Mortimer, A genetic study of x-ray sensitive mutants in yeast, Mutat Res 24 (1974) 281-292.
[15] L.S. Symington, Role of RAD52 epistasis group genes in homologous recombination and double-strand break repair, Microbiol Mol Biol Rev 66 (2002) 630-670, table of contents.
[16] A. Dudas and M. Chovanec, DNA double-strand break repair by homologous recombination, Mutat Res 566 (2004) 131-167.
[17] M.E. Moynahan, J.W. Chiu, B.H. Koller and M. Jasin, Brca1 controls homology-directed DNA repair, Mol Cell 4 (1999) 511-518.
[18] M.E. Moynahan, A.J. Pierce and M. Jasin, BRCA2 is required for homology-directed repair of chromosomal breaks, Mol Cell 7 (2001) 263-272.
[19] A.A. Davies, J.Y. Masson, M.J. McIlwraith, A.Z. Stasiak, A. Stasiak, A.R. Venkitaraman and S.C. West, Role of BRCA2 in control of the RAD51 recombination and DNA repair protein, Mol Cell 7 (2001) 273-282.
[20] M.F. Lavin, The Mre11 complex and ATM: a two-way functional interaction in recognising and signaling DNA double strand breaks, DNA Repair (Amst) 3 (2004) 1515-1520.
[21] M.K. Shivji and A.R. Venkitaraman, DNA recombination, chromosomal stability and carcinogenesis: insights into the role of BRCA2, DNA Repair (Amst) 3 (2004) 835-843.
[22] L. Pellegrini and A.R. Venkitaraman, Emerging functions of BRCA2 in DNA recombination, Trends Biochem Sci 29 (2004) 310-316.
[23] V.P. Yu, M. Koehler, C. Steinlein, M. Schmid, L.A. Hanakahi, A.J. van Gool, S.C. West and A.R. Venkitaraman, Gross chromosomal rearrangements and genetic exchange between nonhomologous chromosomes following BRCA2 inactivation, Genes Dev 14 (2000) 1400-1406.
[24] R.D. Johnson and M. Jasin, Sister chromatid gene conversion is a prominent double-strand break repair pathway in mammalian cells, Embo J 19 (2000) 3398-3407.
[25] S.A. Schichman, E. Canaani and C.M. Croce, Self-fusion of the ALL1 gene. A new genetic mechanism for acute leukemia, Jama 273 (1995) 571-576.
[26] M.A. Caligiuri, M.P. Strout, S.A. Schichman, K. Mrozek, D.C. Arthur, G.P. Herzig, M.R. Baer, C.A. Schiffer, K. Heinonen, S. Knuutila, T. Nousiainen, T. Ruutu, A.W. Block, P. Schulman, J. Pedersen-Bjergaard, C.M. Croce and C.D. Bloomfield, Partial tandem duplication of ALL1 as a recurrent molecular defect in acute myeloid leukemia with trisomy 11, Cancer Res 56 (1996) 1418-1425.
[27] M.A. Caligiuri, M.P. Strout, A.R. Oberkircher, F. Yu, A. de la Chapelle and C.D. Bloomfield, The partial tandem duplication of ALL1 in acute myeloid leukemia with normal cytogenetics or trisomy 11 is restricted to one chromosome, Proc Natl Acad Sci U S A 94 (1997) 3899-3902.
[28] M.P. Strout, G. Marcucci, C.D. Bloomfield and M.A. Caligiuri, The partial tandem duplication of ALL1 (MLL) is consistently generated by Alu-mediated homologous recombination in acute myeloid leukemia, Proc Natl Acad Sci U S A 95 (1998) 2390-2395.

[29] S.A. Schichman, M.A. Caligiuri, M.P. Strout, S.L. Carter, Y. Gu, E. Canaani, C.D. Bloomfield and C.M. Croce, ALL-1 tandem duplication in acute myeloid leukemia with a normal karyotype involves homologous recombination between Alu elements, Cancer Res 54 (1994) 4277-4280.

[30] S.C. West, Molecular views of recombination proteins and their control, Nat Rev Mol Cell Biol 4 (2003) 435-445.

[31] C. Richardson and M. Jasin, Frequent chromosomal translocations induced by DNA double-strand breaks, Nature 405 (2000) 697-700.

[32] C.S. Griffin and J. Thacker, The role of homologous recombination repair in the formation of chromosome aberrations, Cytogenet Genome Res 104 (2004) 21-27.

[33] E. Weterings and D.C. van Gent, The mechanism of non-homologous end-joining: a synopsis of synapsis, DNA Repair (Amst) 3 (2004) 1425-1435.

[34] E. Feldmann, V. Schmiemann, W. Goedecke, S. Reichenberger and P. Pfeiffer, DNA double-strand break repair in cell-free extracts from Ku80-deficient cells: implications for Ku serving as an alignment factor in non-homologous DNA end joining, Nucleic Acids Res 28 (2000) 2585-2596.

[35] P. Pfeiffer, W. Goedecke, S. Kuhfittig-Kulle and G. Obe, Pathways of DNA double-strand break repair and their impact on the prevention and formation of chromosomal aberrations, Cytogenet Genome Res 104 (2004) 7-13.

[36] S. Thode, A. Schafer, P. Pfeiffer and W. Vielmetter, A novel pathway of DNA end-to-end joining, Cell 60 (1990) 921-928.

[37] P.A. Jeggo and M. Lobrich, Artemis links ATM to double strand break rejoining, Cell Cycle 4 (2005) 359-362.

[38] E. Riballo, M. Kuhne, N. Rief, A. Doherty, G.C. Smith, M.J. Recio, C. Reis, K. Dahm, A. Fricke, A. Krempler, A.R. Parker, S.P. Jackson, A. Gennery, P.A. Jeggo and M. Lobrich, A pathway of double-strand break rejoining dependent upon ATM, Artemis, and proteins locating to gamma-H2AX foci, Mol Cell 16 (2004) 715-724.

[39] W.C. Lin and S. Desiderio, Regulation of V(D)J recombination activator protein RAG-2 by phosphorylation, Science 260 (1993) 953-959.

[40] D.O. Ferguson and F.W. Alt, DNA double strand break repair and chromosomal translocation: lessons from animal models, Oncogene 20 (2001) 5572-5579.

[41] C.H. Bassing and F.W. Alt, The cellular response to general and programmed DNA double strand breaks, DNA Repair (Amst) 3 (2004) 781-796.

[42] J.P. Manis, M. Tian and F.W. Alt, Mechanism and control of class-switch recombination, Trends Immunol 23 (2002) 31-39.

[43] F.G. Haluska, S. Finver, Y. Tsujimoto and C.M. Croce, The t(8; 14) chromosomal translocation occurring in B-cell malignancies results from mistakes in V-D-J joining, Nature 324 (1986) 158-161.

[44] L.R. Finger, R.C. Harvey, R.C. Moore, L.C. Showe and C.M. Croce, A common mechanism of chromosomal translocation in T- and B-cell neoplasia, Science 234 (1986) 982-985.

[45] T. Blunt, N.J. Finnie, G.E. Taccioli, G.C. Smith, J. Demengeot, T.M. Gottlieb, R. Mizuta, A.J. Varghese, F.W. Alt, P.A. Jeggo and et al., Defective DNA-dependent protein kinase activity is linked to V(D)J recombination and DNA repair defects associated with the murine scid mutation, Cell 80 (1995) 813-823.

[46] C.U. Kirchgessner, C.K. Patil, J.W. Evans, C.A. Cuomo, L.M. Fried, T. Carter, M.A. Oettinger and J.M. Brown, DNA-dependent kinase (p350) as a candidate gene for the murine SCID defect, Science 267 (1995) 1178-1183.

[47] K.D. Mills, D.O. Ferguson and F.W. Alt, The role of DNA breaks in genomic instability and tumorigenesis, Immunol Rev 194 (2003) 77-95.
[48] L.R. Van Veelen, Kanaar, R. and D.C. van Gent, DNA repair and malignant hematopoiesis., Textbook of Malignant Hematology (2nd Edition), L. Degos, D.C. Linch, and B. Löwenberg, eds., Taylor & Francis Group, London, UK (2005) 155-164.
[49] G.J. Vanasse, J. Halbrook, S. Thomas, A. Burgess, M.F. Hoekstra, C.M. Disteche and D.M. Willerford, Genetic pathway to recurrent chromosome translocations in murine lymphoma involves V(D)J recombinase, J Clin Invest 103 (1999) 1669-1675.
[50] R. Taub, I. Kirsch, C. Morton, G. Lenoir, D. Swan, S. Tronick, S. Aaronson and P. Leder, Translocation of the c-myc gene into the immunoglobulin heavy chain locus in human Burkitt lymphoma and murine plasmacytoma cells, Proc Natl Acad Sci U S A 79 (1982) 7837-7841.
[51] A.R. Ramiro, M. Jankovic, T. Eisenreich, S. Difilippantonio, S. Chen-Kiang, M. Muramatsu, T. Honjo, A. Nussenzweig and M.C. Nussenzweig, AID is required for c-myc/IgH chromosome translocations *in vivo*, Cell 118 (2004) 431-438.
[52] Y.H. Wang, Chromatin structure of human chromosomal fragile sites, Cancer Lett (2005).
[53] J. Surralles, S. Puerto, M.J. Ramirez, A. Creus, R. Marcos, L.H. Mullenders and A.T. Natarajan, Links between chromatin structure, DNA repair and chromosome fragility, Mutat Res 404 (1998) 39-44.
[54] K. Huebner and C.M. Croce, FRA3B and other common fragile sites: the weakest links, Nat Rev Cancer 1 (2001) 214-221.
[55] M. Lichten and A.S. Goldman, Meiotic recombination hotspots, Annu Rev Genet 29 (1995) 423-444.
[56] S.C. Raghavan, P.C. Swanson, X. Wu, C.L. Hsieh and M.R. Lieber, A non-B-DNA structure at the Bcl-2 major breakpoint region is cleaved by the RAG complex, Nature 428 (2004) 88-93.
[57] A. Bacolla, A. Jaworski, J.E. Larson, J.P. Jakupciak, N. Chuzhanova, S.S. Abeysinghe, C.D. O'Connell, D.N. Cooper and R.D. Wells, Breakpoints of gross deletions coincide with non-B DNA conformations, Proc Natl Acad Sci U S A 101 (2004) 14162-14167.
[58] G. Wang and K.M. Vasquez, Naturally occurring H-DNA-forming sequences are mutagenic in mammalian cells, Proc Natl Acad Sci U S A 101 (2004) 13448-13453.
[59] A.L. Gotter, T.H. Shaikh, M.L. Budarf, C.H. Rhodes and B.S. Emanuel, A palindrome-mediated mechanism distinguishes translocations involving LCR-B of chromosome 22q11.2, Hum Mol Genet 13 (2004) 103-115.
[60] N. Chuzhanova, S.S. Abeysinghe, M. Krawczak and D.N. Cooper, Translocation and gross deletion breakpoints in human inherited disease and cancer II: Potential involvement of repetitive sequence elements in secondary structure formation between DNA ends, Hum Mutat 22 (2003) 245-251.
[61] M.A. Nimmakayalu, A.L. Gotter, T.H. Shaikh and B.S. Emanuel, A novel sequence-based approach to localize translocation breakpoints identifies the molecular basis of a t(4;22), Hum Mol Genet 12 (2003) 2817-2825.
[62] H. Kurahashi, H. Inagaki, K. Yamada, T. Ohye, M. Taniguchi, B.S. Emanuel and T. Toda, Cruciform DNA structure underlies the etiology for palindrome-mediated human chromosomal translocations, J Biol Chem 279 (2004) 35377-35383.

[63] T.W. Glover, M.F. Arlt, A.M. Casper and S.G. Durkin, Mechanisms of common fragile site instability, Hum Mol Genet 14 Spec No. 2 (2005) R197-205.

[64] C.S. Kao-Shan, R.L. Fine, J. Whang-Peng, E.C. Lee and B.A. Chabner, Increased fragile sites and sister chromatid exchanges in bone marrow and peripheral blood of young cigarette smokers, Cancer Res 47 (1987) 6278-6282.

Summary

Life is short, art long, opportunity fleeting, experience treacherous, judgment difficult.

~ Hippocrates

Summary

The maintenance of genomic integrity is vital to the dissemination of correct genetic information in living cells. DNA can be modified in many distinct ways due to various endogenous and exogenous sources, all of which can lead to damage and a compromise of its information. Many specialized repair pathways have evolved to circumvent the deleterious effects of DNA damage, underscoring the critical importance of genome maintenance.

A double-strand break (DSB) is a particularly dangerous lesion, as both strands of the double helix are broken. Incorrect rejoining of DSB-ends or unrepaired DSBs can lead to genomic fragmentation, deletion and rearrangements at both the micro and chromosomal level. Homologous recombination is a high fidelity DNA repair process in which a DSB is repaired in an accurate and timely manner, using the intact sister chromatid to replace lost genetic information. RAD51 is the central protein in the pathway, and carries out the important steps of homology recognition and joint molecule formation. RAD51 is assisted in its role by several accessory proteins, one of which is Rad54. Rad54 has been described in literature as the Swiss army knife of recombination, as several integral functions have been described that place the protein in almost every step of the process. Since most evidence for these functions is derived from biochemical studies that involve purified proteins and various DNA structures, our main interest in this thesis has been to elucidate the *in vivo* function of Rad54 and its activity in living cells, and to hypothesize a link between our studies and the biochemical data.

In **Chapter 2**, we list the available tools and methodology used to study cellular behavior of proteins within cells, some of which we have utilized to study our protein of interest in the subsequent chapters. This chapter also describes in detail the specifics of the homologous recombination pathway, as well as the cell biology that is known for the proteins involved in the process.

Chapter 3 describes the development of a model system to study the cellular behavior of the Rad54 protein during mouse development. Mouse embryonic stem (ES) cells have been modified at the endogenous Rad54 locus, where part of the genomic sequence has been targeted and replaced by an artificial Rad54 cDNA construct fused with a DNA sequence encoding green fluorescent protein (GFP). Importantly, the locus expresses the Rad54-GFP fusion protein at physiological and endogenous levels. Using this system we have traced the expression of Rad54-GFP during mouse development as

well as in fetal and adult cells. We conclude that mitotic progenitor cells express Rad54-GFP, indicating a role of Rad54 in accurate repair of DSBs in these cells.

In **Chapter 4**, we investigate the alteration of Rad54 cellular behavior when its ATPase domain has been tampered with. Using a similar knock-in system as described in Chapter 3, we have found that the presence of mutant Rad54 affects the number of spontaneous foci, as well as kinetics of both Rad54 and Rad51 foci. Interestingly, both the protein turnover in the Rad54 focus as well as the time taken in which the focus is disassembled is retarded in the ATPase mutants, indicating a requirement for Rad54 ATPase activity in normal and timely clearance of Rad54 foci.

Chapter 5 documents the biochemical, genetic and cellular characterization of Rad54B, a Rad54 paralog identified in mammals. We have established that Rad54 and Rad54B have overlapping biochemical characteristics. In addition, ES cells that are deficient in either or both proteins show similar sensitivities to DNA-damaging agents, demonstrating a possible functional redundancy. Mice that are deficient in both proteins, however, show an extreme sensitivity to mitomycin C, indicating a potential tissue-specific function of each protein. Finally, the above analysis indicates that Rad54B is not the meiotic counterpart of Rad54 (as suggested by previous studies).

Chapter 6 exemplifies the consequences of improper and inaccurate repair of DSBs. Mistakes in homologous recombination and nonhomologous end joining can result in chromosomal translocations, many of which have been documented in various types of leukemias, lymphomas and solid tumors. The mechanisms by which these mistakes can occur are discussed in this chapter.

Samenvatting

Het onderhouden van de integriteit van het genoom is van levensbelang voor de correctheid van de genetische informatie in de levende cel. Zowel endogene als exogene factoren kunnen DNA op verscheidene manieren aanpassen, wat kan leiden tot beschadiging en verlies van informatie. Het belang van onderhoud aan het genoom blijkt uit de vele gespecialiseerde reparatie mechanismen die zijn geëvolueerd om de nadelige effecten van DNA beschadiging te voorkomen.

Een dubbelstrengs breuk (DSB) is een uitermate gevaarlijke beschadiging, aangezien beide strengen van de dubbele helix structuur beschadigd zijn. Het foutief samenvoegen van de uiteinden van een DSB kan leiden tot genomische fragmentatie, deletie en chromosomale translocaties. Homologe recombinatie (HR) is een proces waarbij met een hoge betrouwbaarheid en coördinatie een DSB gerepareerd wordt, gebruikmakend van het zuster chromatide om de missende genetische informatie weer aan te vullen. Rad51 is het sleuteleiwit in HR, dat de belangrijke stappen van identificatie van het identieke DNA en het uitwisselen van de DNA strengen vervult. Rad51 wordt hierin bijgestaan door verschillende andere eiwitten waaronder Rad54. Rad54 wordt ook wel het "manusje van alles" van de recombinatie genoemd, verscheidene functies zijn beschreven die het eiwit in bijna iedere stap van het HR proces plaatsen. Aangezien het merendeel van het bewijs van deze functies afkomstig is uit biochemische studies die gebruik maken van gezuiverde eiwitten en verschillende DNA structuren, is de nadruk in deze thesis vooral gelegd op de *in vivo* functionaliteit van Rad54 en de activiteit in de levende cel, daarbij een link leggend tussen ons onderzoek en de biochemische data.

In **hoofdstuk 2** worden de beschikbare middelen en methodes beschreven die gebruikt worden om het cellulaire gedrag van eiwitten in de cel te bestuderen, sommige daarvan worden in de latere hoofdstukken gebruikt in het onderzoeken van het eiwit in kwestie. Dit hoofdstuk beschijft tevens in detail de specificaties van het HR proces, zowel als de cel biologie die bekend is voor de eiwitten die in dit proces een rol spelen.

Hoofdstuk 3 beschrijft de ontwikkeling van een model om het cellulaire gedrag van het Rad54 eiwit te bestuderen gedurende de ontwikkeling van een muis. Embryonale stam (ES) cellen van een muis zijn aangepast in het endogene Rad54 gen, waarbij een gedeelte van de genetische code is vervangen door een kunstmatig Rad54 cDNA construct gefuseerd met de DNA code voor het groen fluorescerend eiwit (GFP). Belangrijk is dat het gen het Rad54-GFP eiwit op het endogene niveau tot expressie

brengt. Gebruikmakend van dit systeem hebben we de expressie van Rad54-GFP gedurende de embryonale ontwikkeling van een muis als wel als in foetus en volwassen cellen getraceeerd. We zijn tot de conclusie gekomen dat mitotische stam cellen Rad54-GPF tot expressie brengen, daarmee een rol aangevend voor Rad54 in de accute reparatie van DSBs in deze cellen.

In **hoofdstuk 4** onderzoeken we de afwijking in het cellulaire gedrag van Rad54 wanneer zijn ATPase domein is aangepast. Gebruik makend van een "knock-in" systeem gelijkend aan dat beschreven in hoofdstuk 3 hebben we ontdekt dat de aanwezigheid van gemuteerd Rad54 een effect heeft op het aantal spontane foci als wel als de kinetische eigenschappen van zowel Rad54 als Rad51 foci. Zowel de eiwit omzetting, als de tijd waarin de focus verdwijnt is vertraagd in de ATPase mutanten, wat een indicatie is voor de Rad54 ATPase activiteit tijdens de normale en gecoördineerde opruiming van Rad54 foci.

Hoofdstuk 5 documenteert de biochemische, genetische en cellulaire karakteristieken van Rad54B, een Rad54 paraloog geïdentifiseerd in zoogdieren. We hebben vastgesteld dat Rad54 en Rad54B overlappende biochemische eigenschappen hebben. Bovendien laten cellen met een tekort aan één of beide eiwitten een gelijkwaardige gevoeligheid zien voor DNA beschadiging wat mogelijk duidt op een overlappende functie. Muizen met een tekort aan beide eiwitten laten een extreme gevoeligheid zien voor mitomycine C, identicatief voor een potentiële weefsel specifieke functie van de eiwitten. Bovenstaande analyse geeft aan dat Rad54B geen meiotische tegenhanger is van Rad54 (zoals voorgesteld door voorgaande studies).

Hoofdstuk 6 geeft voorbeelden van de consequenties van incorrecte reparatie van DSBs. Fouten tijdens HR en DNA eind-verbinding kunnen resulteren in chromosomale translocaties, welke gedocumenteerd zijn in verschillende vormen van leukemie, lymphonen en massieve tumoren. De mechanismen die ten grondslag liggen aan deze fouten worden in dit hoofdstuk beschreven.

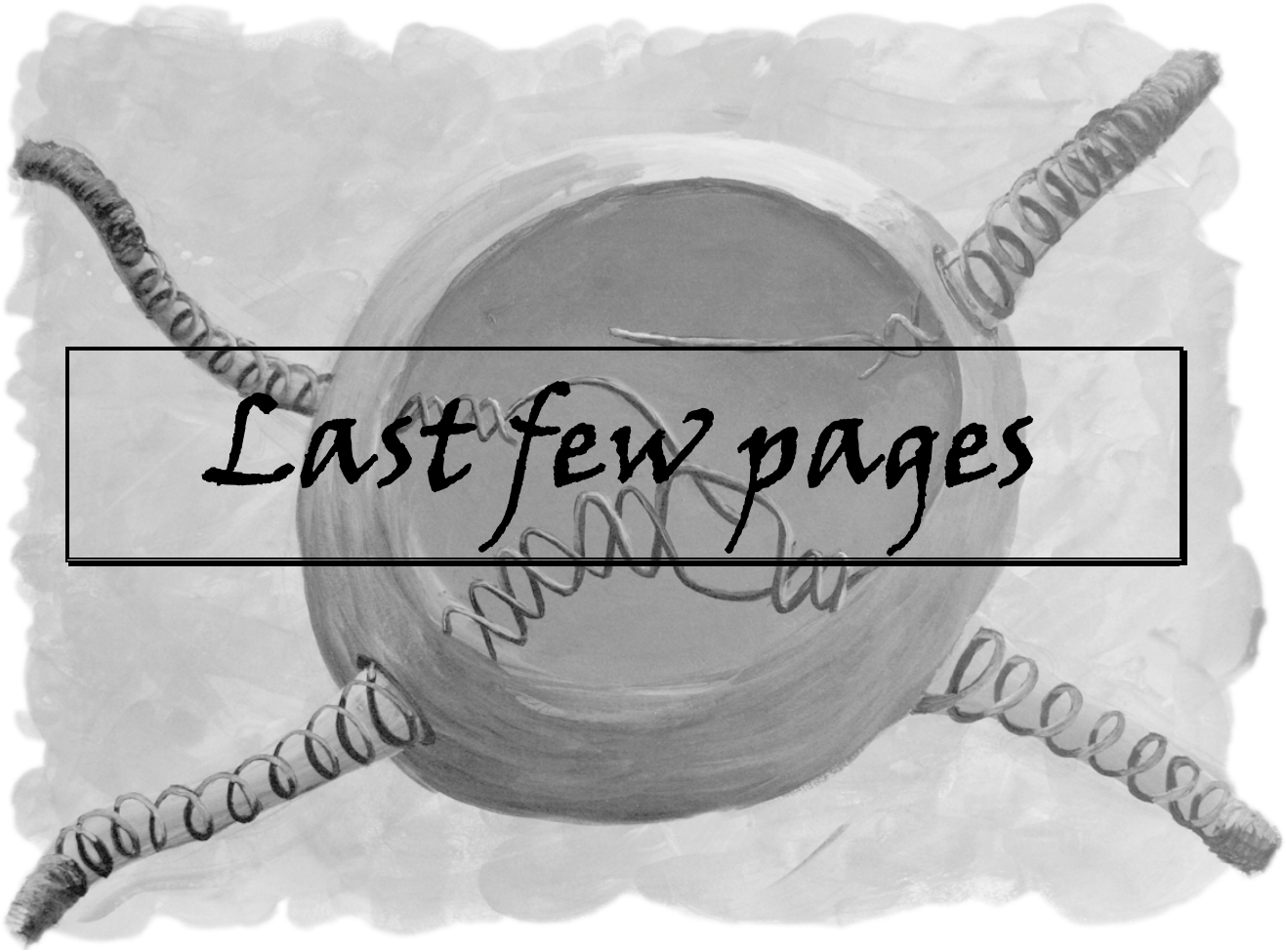
Last few pages

The end of labor is to gain leisure.

~ Aristotle

List of abbreviations

AGM	Aorta-gonad-mesonephros
ATLD	Ataxia telangiectasia-like disease
ATP	Adenosine 5'-triphosphate
cDNA	Complementary DNA
D_{eff}	Diffusion coefficient
D-loop	Displacement loop
DAPI	4',6-diamidino-2-penylindole
DNA	Deoxyribonucleic acid
DNA-PK_{cs}	DNA dependent protein kinase (catalytic subunit)
DSB	Double-strand break
Da	Dalton
dpc	Days post coitum
dsDNA	Double-stranded DNA
E. coli	*Escherichia coli*
eGFP	Enhanced GFP
ES	Embryonic stem
FACS	Fluorescence-activated cell sorting
FLIP	Fluorescence loss in photobleaching
FRAP	Fluorescence recovery after photobleaching
FSC	Forward scatter compartment
GFP	Green fluorescent protein
Gy	Gray
h	Human
γH2AX	Phosphorylated H2AX
IR	Ionizing radiation
IgM	Immunoglobulin M
LIF	Leukemia inhibitory factor
m	Mouse
mRNA	Messenger RNA
MDF	Mouse dermal fibroblast
MEF	Mouse embryonic fibroblast
MLPA	Methylation-specific multiplex ligation dependent probe amplification
MMC	Mitomycin C
MRX	Mre11/Rad50/Xrs2
n	Number
NBS	Nijmegen breakage syndrome
NER	Nucleotide excision repair
NHEJ	Nonhomologous end joining
PBS	Phosphate buffered saline
PCNA	Proliferating cell nuclear antigen
pol	DNA polymerase
polyA	Polyadenylation
RNA	Ribonucleic acid
RPA	Replication protein A
RT-PCR	Reverse transcriptase polymerase chain reaction
S. cerevisiae	*Saccharomyces cerevisiae*
SEM	Standard error of the mean
ssDNA	Single-stranded DNA
$t_{½}$	Half life

List of publications

Agarwal S, Hendriks RW, Lopez J, Peeters M, Maas A, Kanaar R, Essers J (2007) Analysis of mouse fluorescence-tagged Rad54 expression *in vivo*. *(Manuscript in preparation)*

Agarwal S, Guénolé A, Linsen SL,van Cappellen WA, Houtsmuller A, Kanaar R, Essers J (2007) ATP hydrolysis by mammalian Rad54 controls nuclear foci kinetics and is essential for DNA damage repair. *(Manuscript in preparation)*

Agarwal S, Kanaar R, Essers J (2007) The cell biology of double-strand break repair. *Molecular Genetics of Recombination, A. Aguilera & R. Rothstein (Eds.) Topics in Current Genetics (Springer Verlag): 335 - 362*

Agarwal S, Tafel AA, Kanaar R (2006) Double-strand break repair and chromosome translocations. *DNA repair 5 (9 – 10): 1075 – 1081*

Wesoly J, **Agarwal S**, Sigurdsson S, Bussen W, Van Komen S, Qin J, van Steeg H, van Benthem J, Wassenaar E, Baarends WM, Ghazvini M, Tafel AA, Heath H, Galjart N, Essers J, Grootegoed JA, Arnheim N, Bezzubova O, Buerstedde JM, Sung P, Kanaar R. (2006) Differential contributions of mammalian Rad54 paralogs to recombination, DNA damage repair, and meiosis. *Molecular and Cellular Biology 26 (3): 976 – 989*

Agarwal S, Gamper HB, Kmiec EB. (2003) Nucleotide replacement at two sites can be directed by modified single-stranded oligonucleotides *in vitro* and *in vivo*. *Biomolecular Engineering 20 (1): 7 – 20*

Liu H, **Agarwal S**, Kmiec E, Davis BR. (2002) Targeted beta-globin gene conversion in human hematopoietic CD34(+)and Lin(-)CD38(-)cells. *Gene Therapy 9 (2): 118 – 126*

Curriculum Vitae

Name

Sheba Agarwal

Date of Birth

8th December 1975

2006 – present

Department of Clinical Genetics, Section Oncogenetics
Vrije Universiteit Medical Center, Amsterdam, The Netherlands

Postdoctoral research project, under supervision of Prof. dr. Johan de Winter

2002 – 2006

Department of Genetics,
Erasmus Medical Center, Rotterdam, The Netherlands

Ph.D. in Genetics, under supervision of Prof. dr. Roland Kanaar

- Thesis title: "The cell biology of Rad54: Implications for homologous recombination" (2008)

1997 – 2002

Department of Biological Sciences,
University of Delaware, Delaware, U.S.A.

M.Sc. in Molecular Biology & Genetics

- Thesis title: "DNA context dependency and structural parameters of targeted gene repair *in vitro* and *in vivo*" (2002)

1994 – 1997

Department of Biology,
National University of Singapore, Singapore

B.Sc. in Cell & Molecular Biology

- "Cloning of full length fibroblast growth factor receptor 2 gene in Zebrafish" – *Directed research project* (1997)
- "A PCR based protocol for screening cDNA libraries for rare messages" – *National Undergraduate Research Program* (1996)

Acknowledgements

And I say this to you tonight, let us not forget. There is Hope!
~ Keep hope alive (Crystal Method)

I can't freaking believe it, this is unreal. I'm finally writing the last bit, the ultimate lines, the conclusion to my long boring scientific bla-bla. Faced with these final pages, I realize that it's much too easy to declare the end of a long hard trek like this one with such words as "Yes, *I* got it done, *I* did the work, *I* went through hell to get it done." The extended time period during which one is faced with experiments that don't work or make sense, writing that never seems to end, critique that never stops…it all takes quite a fair bit of courage, patience and strength. The truth is, ladies and gents, that one cannot endure the nuances of doing a PhD alone. So the statement that *I* am the one getting a PhD is premature, it is more so that *we* are all getting a PhD. So here I stand before you, in earnest, aflame with gratitude and other such emotions, preparing to lay my appreciation where it is due.

[Nota bene: Being ever so mindful of my tendency for (unintentional) verbal diarrhea, I promise to stop well before I feel the need to thank my (nonexistent) lawyers and personal make-up artist.]

First and foremost, to my promoters, Roland and Jan: thank you for the fantastic opportunity and continuous support. Roland - thanks for taking a chance on me when my confidence level was on a precipitous downward spiral. You have had a large hand in reversing that trend, so thank you for being always available whenever I walked into your room asking for a minute, when you knew very well it was more like half an hour. Jeroen, I have never understood how you can be so different a person outside work. Perhaps one day I will get to know that side of you, rather than what I know from the lab.

It was a revelation to me right from the beginning how eager and willing everyone was to help the poor new kid figure things out, not just once but a few times over. This was definitely not something I was used to. Here's to the 6th floor Genetics collective! Asia, Ellen, Esther, Gusia, Hanny, Iris, Mandy, Claire, Nicole, Berina, Raoul, Eddy, Kris, Jacqueline, Lineke, Bobby, Dejan, Daniel, Edward, Pierre-Olivier: thank you, it was an honor to work with you all! Cecile, I'm sure the volume of our harmonic voices is sorely missed by everyone. Thanks for everything! You know, the "piraatjes" have never been more personal to me. Veronique, it is unfortunate that we got closer when both I and you moved far apart, but it is better late than never, toch? Thanks for all the invaluable help and friendship, including the necessary, vague ultimatums about missed dinners (sorry!). Céline, merci pour tout les coups de pied, parfois bien mérites, à mon auguste popotin. Ton entousiasme pour la science a eu une grande influence sûr ce que je compte faire dans ma carrière. Mauro you brilliant flirt you! I'd gladly kiss your elbow (again) just to be able to say that I have! Maurice-je, I miss our lunches at Sophia, thanks for your friendship and confidence. Katsu, your scientific mind and knowledge of the

facts have always amazed me. Thanks for all the brain-picking sessions; I've always learnt something new whenever we talked. Alex, thank you for being my mental coach (in every sense of the word), and for your patience during the many many FACS sessions. Magdalena! You have always been a great friend, supportive, sympathetic, kind…If not for you and the sometimes "Emergency Cell Splitting Committee", things would have been much more difficult in Rotterdam. Thank you so much! Linda, you are always so positive and happy, it puts me to shame. Thanks for being my companion and roomie during conferences and for helping me out in so many ways in the lab. Eric, Dutch dude in the ten gallon Texas hat, I really enjoyed our endless talks about life, love and The Thesis. You were always sympathetic no matter how pathetic my whinging got, so thank you so much for your patience, advice and kind words. Sam, you were a heck of a Masters' student and a great pleasure to work with. No more jokes about the "good head on your shoulders" I promise. Gert, I appreciate all your kind help with the confocal microscope, as well as the very useful discussions about experiments and data. Adriaan, I have always enjoyed the discourses about the philosophical aspect of science. Listening to you is a fascinating experience and I wish I had a chance to do so without having a deadline to meet. Martijn (Dekkers) my fiercely creative friend! I miss our unique tête-à-tête about everything under the sun. Thank you for being so reassuring during one of the scariest times of my life, and of course, for making me laugh. Marike, thanks for being so superb with all the silly official stuff that we all have to do. You made my Rotterdam stay much easier.

To my paranimfen: Martijn, you should know that you were missed terribly when you left (yes, even the flying ep/tip missiles from the other side of the lab). You have always been the one to give me the most balanced advice and opinion, which I have very much valued, thank you. Jasperina, my friend, my confidant, my Lowlands partner in crime* (LPiC #1)!! How many times have I come over or called you in utter panic over something or the other? Even when I got sick of myself, you kept your temper and patience. Thank you so much for everything, for your help and for your fabulousness.

¡Javier! Mi colega, mi amigo, mi hermano. Gracias por una maravillosa amistad que ha sido probada una y otra vez, y que afortunadamente ha llegado a ser más fuerte que nunca.Eres una fuente de inspiración para mí, y solo espero lo mejor para ti siempre.

Thanks are also definitely due to my current colleagues at the VUMC, including Hans (who said "*An accepted paper does not make it acceptable*"), Johan (thank you for all your advice), Jurgen (totally mad, fellow bass junkie…in other words, absolutely fabulous), Martin (self-proclaimed oude mannetje – I'd add "crazy" in there), Monique on standby, Anneke H (LPiC* #2, you are quite wonderful), Davy (LPiC* #3, who says he sings better than that Aguilera girl), pretty Petra in pearls…Thank you all for the ongoing great time, and for sympathizing with my thesis-related tirades.

Andrea (LPiC* #4), your company is extraordinary, your laughter therapy. Thanks for all the Friday evenings, the shopping trips, and everything in between. You have always shown me a view of life outside of work and worry, which I sometimes

forgot existed. Ivy, someday I will tell you how your beautiful eyes saved your Auntie Sheba from the brinks of outright psychosis. Arne-tje (LPiC* #5 & concert buddy), I still shake my head in disbelief at how interested you are in what I do, when most people just wish I'd shut up. Thanks for your easy camaraderie and encouragement: you are fantastic. Remy and Roos, you guys are the best: Dank jullie wel voor alles.

To my properly British friends…Ian, you constantly amaze me with your absolute laid back attitude to life. What are you on and can I please have some?? Thanks for the cautious questions about the thesis and the matter-of-fact solutions to my frustration. Lee, you fabulous person! Your daily salutations always made me smile and lifted the dark morning cloud, especially at the very time when it was so sorely needed. Thank you, you are a star.

To my Dutch family: Ada, Hans, Sandra and Erik: because of your love and support, I have never felt like a foreigner in this country. Thanks for making the transition and my life here so easy. Mum, dankje voor jouw fantastische adviezen. Ik zou jouw "Sipelsoppen soep" nooit vergeten! Ik hou van jou.

Mom and Dad, how do I begin to thank the ones who gave me life? Papaji, your absolute dedication to mathematics, duty and life has been an inspiration to me since the day I was born. Mom, everything that you have ever taught me, from the alphabet and beyond, has given me the confidence to always aim for the sky. You both have given me the curiosity, passion and dedication that research and life needs. Still, you would agree that, as the legendary Mukesh sang, "Saab kuch seekha hamne na seekhi hoshiyari, Sach hai duniyawaalon ki hum hain anaadi." To my brother Hans, who so kindly agreed to be my paranimf (even thought he had no clue what a "paranimf" is) and also to read my chapters for the sake of proper scientific English: dude you are even more finicky than Mom ever could be. I enjoyed such comments as "Mutant mice! How terrifying!", "My head spinneth" and "What an incredible superscript!" (see Chapter 4). I love and miss you all very much.

And oh to the guy I married, the old ball 'n chain, the one whose socks I've promised to wash forever, etc etc. You walked through every step of PhD-induced hell with me, in spite of your bewilderment at my need for validation and self worth from a mere "piece of paper". It was a long struggle my love, through the ups and downs, the bitter frustration on both our parts, the tears, but it's finally over. Words completely fail me when I try to think of what to say to you, but here's a simple way to put it: none of this could have been possible without you. Jasper, your love is liberation.

And finally, to my precious wee miracle, I realize now that everything I've done up to this point was just a prelude to the symphony of my life. Now, everything begins anew, and with you on one side and Jasper on the other, we will walk the paths of our lives together. My darling, I can't wait!

I'm walking on sunshine! Sheba

• • •

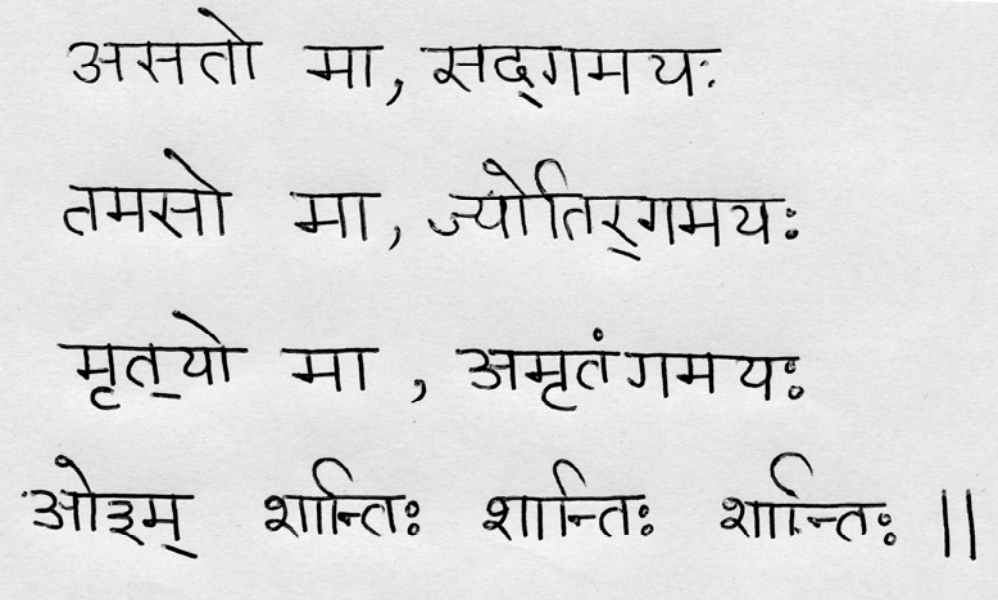

Aum Asato mā sad gamaya
Tamaso mā jyotir gamaya
Mṛtyormā amṛtam gamaya
Aum śānti śānti śāntiḥ

(Bṛhadāraṇyaka Upaniṣad I.iii.28)

"From ignorance, lead me to truth;

From darkness, lead me to light;

From death, lead me into immortality"

Stellingen behorend bij het proefschrift

The Cell Biology of Rad54: Implications for homologous recombination

Sheba Agarwal

1. Cell biology techniques have evolved extensively in the past years to visualize true to life pictures of proteins within cells and organs, and yet making the connection between a particular protein's biochemical properties and its cellular behaviour is still a major challenge. *This thesis*

2. Not all types of mitotic cells in culture express Rad54, possibly due to its S phase specific expression. However, this could also be related to the "stemness" or developmental stage of the particular cell type observed. *This thesis*

3. The Rad54 focus can be interpreted as high local concentration of constantly interchanging proteins that brings together double-stranded DNA for synapsis and branch migration. *This thesis, Bianco P.R. et. al. J Mol. Biol. 374 (3) 618 – 640 (2007), Mazina O.M. et. al. J Biol. Chem. 282 (29) 21068 – 21080 (2007)*

4. The fact that *Rad54*$^{-/-}$ ES cells display a normal number of spontaneous Rad51 foci suggests that a redundant protein takes over Rad54 function with respect to Rad51 foci clearance in these cells. *This thesis*

5. It is dangerous to extrapolate data from cellular assays to the level of the organism, as illustrated by the discrepancy in the MMC sensitivity of *Rad54*$^{-/-}$ *Rad54B* $^{-/-}$ knockout cells and animals. *This thesis*

6. Hailed as the "Swiss army knife" of recombination and a "Jack of all trades", Rad54 nonetheless seems to be the master of none. *Heyer W.D. et al. Nucleic Acids Res. 34 (15) 4115 – 4125 (2006), Tan T.L. et. al. DNA repair 2 (7) 787 – 794 (2003)*

7. Rad51 foci in cells should not be equated to Rad51 nucleoprotein filaments. *Zhao G.Y. et al. Mol. Cell 25 (5) 663 – 675 (2007)*

8. The conclusion that foci of two different proteins colocalize requires more than a single confocal image.

9. Scientific research is no longer a marginalized quest to satisfy curiosity, but a booming mainstream business. Scientists now have to also be businessmen, showmen, salesmen, lawyers, mediators and politicians, but many individuals have compromised their scientific integrity in order to achieve this.

10. It should be an absolute requirement for all scientists to take formal courses in people management skills, just like managers in any company or business.

11. Albert Einstein said "Only two things are infinite, the universe and human stupidity, and I'm not sure about the former." Stupidity by itself is simply a relative condition, not a cardinal sin, but stupidity combined with arrogance will bring about the eventual demise of the human species.